

FEB 25 1989

NAS 1.55: 3003/v. 2

NASA Conference Publication 3003—Vol. 2

# Lewis Structures Technology—1988

## Volume 2—Structural Mechanics

*Proceedings of an exposition and  
symposium of structures technology  
developed under the auspices of  
NASA Lewis Research Center's  
Structures Division  
Cleveland, Ohio  
May 24-25, 1988*

NASA

NASA Conference Publication 3003—Vol. 2

# Lewis Structures Technology—1988

## **Volume 2—Structural Mechanics**

*Proceedings of an exposition and  
symposium of structures technology  
developed under the auspices of  
NASA Lewis Research Center's  
Structures Division  
Cleveland, Ohio  
May 24-25, 1988*



National Aeronautics and  
Space Administration

**Scientific and Technical  
Information Branch**

1988

I



## PREFACE

Aeronautical and space propulsion systems structures technology has been the mission of the Structures Division at the NASA Lewis Research Center for many years. We have carried out both fundamental and applied research projects in pursuit of that mission. We have worked cooperatively with members of the industrial and academic communities in order to strengthen our ties to both the discipline rigors found in university research and the needs of industrial design engineers. It is from this perspective that we have prepared the material for this symposium. And we hope to transfer our technology beyond our usual industrial partners.

The technology required for the reliable, high-performance, lightweight structures needed for aerospace propulsion is among the most complex and challenging facing the design engineer. We provide a comprehensive review of the status of the technology, a review of our recent contributions, and a flavor of the directions for the future. The symposium is meant to be as informative as possible, with the intent to establish new and broader lines for technology transfer. We encourage continued interaction and the chance to exchange information, ideas, and problems with the intention of improving the capability of aerospace propulsion systems.

Our two-day symposium and exposition, LST '88, is expected to attract 300 technologists from all walks of structurally related engineering. The 83 technical contributions have been created by over 100 authors who are respected authorities in their fields. Fifty percent of these are NASA civil servants, and twenty-five percent are on-site contractors and grantees, National Research Council associates, Institute for Computational Mechanics in Propulsion (ICOMP) associates, and U.S. Army Aviation Research and Technology Activity (AVSCOM) personnel. The balance are from industry and academia.

It is a well-rounded symposium, and the proceedings should be a valuable resource for several years to come. The format is easy to access and extract information from. Each topic within a presentation is self-contained on a single page. The topic title appears at the top of the page followed by an extended figure caption, and the figure is located at the bottom of the page. Considerable effort has been expended in streamlining the presentations and freeing them of extraneous information so as to make them clear to the potential user - YOU. References are cited for more detailed followup of a particular topic. On-site personnel are also willing to lend assistance in answering questions and resolving problems that need clarification.

Lester D. Nichols  
Chief, Structures Division  
NASA Lewis Research Center

## CONTENTS TO VOLUME 2

### CONSTITUTIVE MODELS AND EXPERIMENTAL CAPABILITIES

|  |      |
|--|------|
| <b>Session Overview</b> . . . . .  | 2-1  |
| Robert L. Thompson, NASA Lewis Research Center   |      |
| <b>High-Temperature Combustor Liner Tests in Structural Component Response Test Facility</b> . . . . .                           | 2-5  |
| Paul E. Moorhead, NASA Lewis Research Center   |      |
| <b>Life Assessment of Combustor Liner Using Unified Constitutive Models</b> . . . . .  | 2-15 |
| M.T. Tong, Sverdrup Technology, Inc., Lewis Research Center Group, and R.L. Thompson, NASA Lewis Research Center                 |      |
| <b>Experiments Investigating Advanced Materials Under Thermomechanical Loading</b> . . . . .                                     | 2-27 |
| Paul A. Bartolotta, NASA Lewis Research Center   |      |
| <b>Biaxial Experiments Supporting the Development of Constitutive Theories for Advanced High-Temperature Materials</b> . . . . . | 2-37 |
| J.R. Ellis, NASA Lewis Research Center   |      |
| <b>Unified Constitutive Model Development for Metal Matrix Composites at High Temperature</b> . . . . .                          | 2-49 |
| D.N. Robinson, University of Akron   |      |
| <b>Unified Constitutive Model for Single Crystal Deformation Behavior with Applications</b> . . . . .                            | 2-57 |
| K.P. Walker, Engineering Science Software, Inc., T.G. Meyer, Pratt & Whitney, and E.H. Jordan, University of Connecticut         |      |
| <b>Finite Element (MARC) Solution Technologies for Viscoplastic Analyses</b> . . . . .   | 2-73 |
| V.K. Arya, National Research Council, and Robert L. Thompson, NASA Lewis Research Center   |      |

### STRUCTURAL MECHANICS CODES

|  |       |
|--|-------|
| <b>Session Overview</b> . . . . .  | 2-81  |
| Christos C. Chamis, NASA Lewis Research Center   |       |
| <b>The Composite Blade Structural Analyzer (COBSTRAN)</b> . . . . .                          | 2-83  |
| Robert A. Aiello, NASA Lewis Research Center   |       |
| <b>Features and Applications of the Integrated Composites Analyzer (ICAN) Code</b> . . . . . | 2-99  |
| C.A. Ginty, NASA Lewis Research Center   |       |
| <b>Three-Dimensional Inelastic Approximate Analysis Code (MOPM)</b> . . . . .                | 2-113 |
| Jeffrey P. Meister, Sverdrup Technology, Inc., Lewis Research Center Group                   |       |
| <b>Specialty Three-Dimensional Finite Element Analysis Codes</b> . . . . .                   | 2-123 |
| Joseph J. Lackney, Sverdrup Technology, Inc., Lewis Research Center Group                    |       |

|   |              |
|---|--------------|
| <b>MHOST: An Efficient Finite Element Program for Inelastic Analysis of Solids and Structures . . . . .</b> | <b>2-131</b> |
| S. Nakazawa, MARC Analysis Research Corp.   |              |
| <b>METCAN - the Metal Matrix Composite Analyzer . . . . .</b>   | <b>2-141</b> |
| Dale A. Hopkins, NASA Lewis Research Center, and<br>Pappu L.N. Murthy, Cleveland State University           |              |
| <b>Computational Simulation Methods for Composite Fracture Mechanics . . .</b>                              | <b>2-157</b> |
| Pappu L.N. Murthy, Cleveland State University   |              |

## STRUCTURAL OPTIMIZATION

|   |              |
|---|--------------|
| <b>Session Overview . . . . .</b>   | <b>2-171</b> |
| Robert H. Johns, NASA Lewis Research Center   |              |
| <b>Probabilistic Structural Analysis Computer Code (NESSUS) . . . . .</b>   | <b>2-173</b> |
| Michael C. Shiao, Sverdrup Technology, Inc., Lewis Research<br>Center Group   |              |
| <b>Structural Tailoring of High-Speed Turbine Blades(SSME/STAEBL) . . . . .</b>   | <b>2-183</b> |
| Robert Rubinstein, Sverdrup Technology, Inc., Lewis Research<br>Center Group  |              |
| <b>Computational Structural Mechanics for Engine Structures . . . . .</b>   | <b>2-189</b> |
| Christos C. Chamis, NASA Lewis Research Center  |              |
| <b>Structural Tailoring of Advanced Turboprops . . . . .</b>  | <b>2-205</b> |
| K.W. Brown, Pratt & Whitney, and Dale A. Hopkins, NASA Lewis<br>Research Center   |              |
| <b>Advanced Probabilistic Methods for Quantifying the Effects of Various<br/>Uncertainties in Structural Response . . . . .</b> | <b>2-219</b> |
| Vinod K. Nagpal, Sverdrup Technology, Inc.  |              |

## STRUCTURAL MECHANICS CODE APPLICATIONS

|  |              |
|--|--------------|
| <b>Session Overview . . . . .</b>  | <b>2-233</b> |
| Robert H. Johns, NASA Lewis Research Center  |              |
| <b>Impact Damage in Composite Laminates . . . . .</b>  | <b>2-235</b> |
| Joseph E. Grady, NASA Lewis Research Center  |              |
| <b>Thermostructural Analysis of Simulated Cowl Lips . . . . .</b>  | <b>2-245</b> |
| Matthew E. Melis, NASA Lewis Research Center   |              |
| <b>Thermal-Structural Analyses of Space Shuttle Main Engine (SSME)<br/>Hot Section Components . . . . .</b>                              | <b>2-255</b> |
| Ali Abdul-Aziz, Sverdrup Technology, Inc., Lewis Research<br>Center Group, and Robert L. Thompson, NASA Lewis Research<br>Center         |              |
| <b>Structural Analyses of Engine Wall Cooling Concepts and Materials . . .</b>   | <b>2-265</b> |
| Albert Kaufman, Sverdrup Technology, Inc., Lewis Research<br>Center Group  |              |
| <b>Structural Assessment of a Space Station Solar Dynamic Heat Receiver<br/>Thermal Energy Storage Canister . . . . .</b>                | <b>2-281</b> |
| R.L. Thompson and T.W. Kerslake, NASA Lewis Research Center,<br>and M.T. Tong, Sverdrup Technology, Inc., Lewis Research<br>Center Group |              |

|   |              |
|---|--------------|
| <b>An Efficient Mindlin Finite Strip Plate Element Based on Assumed Strain Distribution . . . . .</b>                   | <b>2-295</b> |
| Abhisak Chulya, Institute for Computational Mechanics in Propulsion, and Robert L. Thompson, NASA Lewis Research Center |              |

APPENDIX

|                                       |              |
|---------------------------------------|--------------|
| <b>Contents to Volume 1 . . . . .</b> | <b>1-466</b> |
| <b>Contents to Volume 3 . . . . .</b> | <b>1-468</b> |

## CONSTITUTIVE MODELS AND EXPERIMENTAL CAPABILITIES

### SESSION OVERVIEW

Robert L. Thompson  
Structural Mechanics Branch  
NASA Lewis Research Center

Hot section components of gas turbine engines and aerospace propulsion and power systems are subjected to severe cyclic thermal-structural loading conditions during their mission cycles. The most severe and damaging strains and stresses are those induced during the startup and shutdown transients. The transient as well as steady-state stresses and strains are difficult to predict, in part because the temperature gradients and distributions are not well known or readily predictable and, in part, because the cyclic elastic-viscoplastic behavior of the materials at these extreme temperatures and strain is not well known or readily predictable. Since conventional analytical/experimental capabilities are not adequate to address many of these deficiencies, a broad spectrum of structures related technology programs, basic to applied, including the Hot Section Technology (HOST) and in-house research programs, has been underway at NASA Lewis since 1981. Lewis with participation by industry, universities, and other government agencies has focused the structures research activities on three key technology areas: viscoplastic constitutive model development, experiments to calibrate and validate the models, and the development of nonlinear structural analysis methods and codes. To illustrate the need for doing this critical research shown in the figure are hot section components of various propulsion and power systems which undergo nonlinear structural (stress/strain) response when subjected to severe, but different, environments. Also summarized in the figure are many of the deficiencies that are characterized and modelled with the viscoplastic models and codes developed in this program.

## NONLINEAR STRUCTURAL ANALYSIS APPLICATIONS

SPACE STATION  
SOLAR DYNAMIC POWER MODULE  
THERMAL ENERGY STORAGE CANISTERS



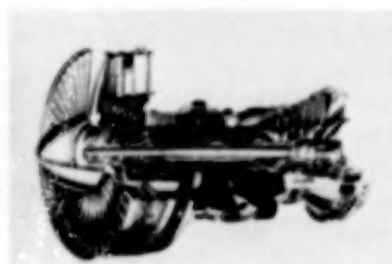
ADVANCED MATERIALS  
AND  
COMPLEX STRUCTURAL  
CONCEPTS

HIGH TEMPERATURE

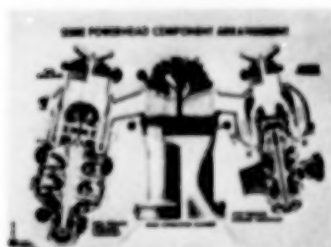
NONISOTHERMAL

THERMOMECHANICAL

GAS TURBINE ENGINES  
HOT SECTION COMPONENTS



SPACE SHUTTLE  
MAIN ENGINES



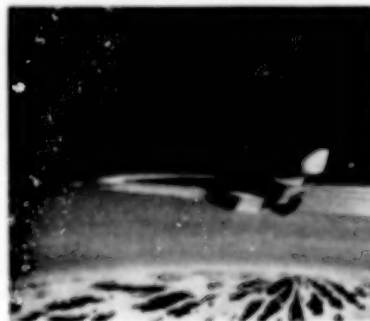
INELASTIC

HISTORY  
TRANSIENTS  
CYCLIC

3-DIMENSIONAL

VISCOPLASTIC CONSTITUTIVE MODELS  
(DEFORMATION/DAMAGE)

HYPERSONIC VEHICLE  
LEADING EDGES/PROPULSION SYSTEM



CD-88-32916

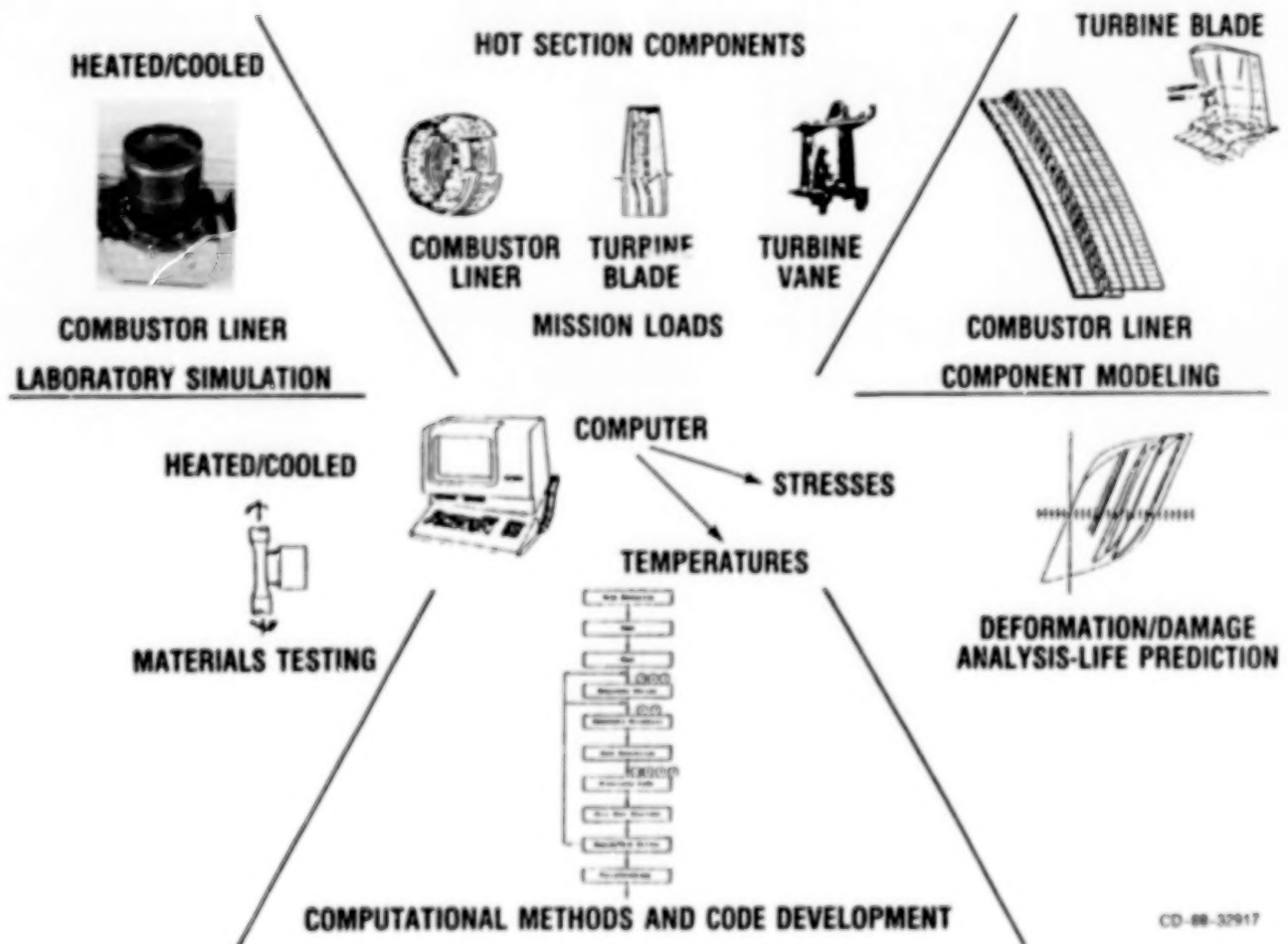


## VISCOPLASTIC CONSTITUTIVE MODEL DEVELOPMENT

The key elements of the structures technology program related to the development of viscoplastic constitutive models for gas turbine engine hot section components are shown in the next figure. Because of the interdisciplinary (thermal/structural/life) nature and integration of complex analyses and experiments necessary for the success of this research effort, several contractors, grantees, and in-house researchers, each with unique technical expertise, participated synergistically in the program. Drawing on this expertise, particularly a select group of model developers, several viscoplastic models were developed, calibrated, and evaluated for a variety of high-temperature materials. The materials characterized ranged from isotropic nickel-base superalloys to single crystal and directionally solidified superalloys to metal matrix composites. Unique high-temperature structures test facilities, both in-house and out-of-house, were implemented to provide the necessary databases for calibration and validation of the models. Versatility, accuracy, and efficiency of the models were demonstrated with the incorporation of the models in several nonlinear finite-element structural analysis codes and the prediction of structural (stress/strain) response of hot section components. Selected presentations are presented in this session to illustrate the many significant results and accomplishments from this program. The presentations are on experimental data obtained from the High Temperature Fatigue and Structures Laboratory and the Structural Component Response Test Facility, two of the many viscoplastic models developed, and implementation of various models in a nonlinear structural analysis code. Other results and applications from this program are presented in Session 11, Structural Mechanics Codes, and Session 16B, Structural Mechanics Code Applications.



# VISCOPLASTIC CONSTITUTIVE MODEL DEVELOPMENT



CD-88-32917

## HIGH-TEMPERATURE COMBUSTOR LINER TESTS IN STRUCTURAL COMPONENT RESPONSE TEST FACILITY

Paul E. Moorhead  
Structural Mechanics Branch  
NASA Lewis Research Center

### ABSTRACT

Jet engine combustor liners were tested in the structural component response facility at NASA Lewis Research Center in a cooperative program with Pratt & Whitney Aircraft, East Hartford, Connecticut. In this facility combustor liners are thermally cycled to simulate a flight envelope of takeoff, cruise, and return to idle. Temperatures were measured with both thermocouples and an infrared thermal imaging system.

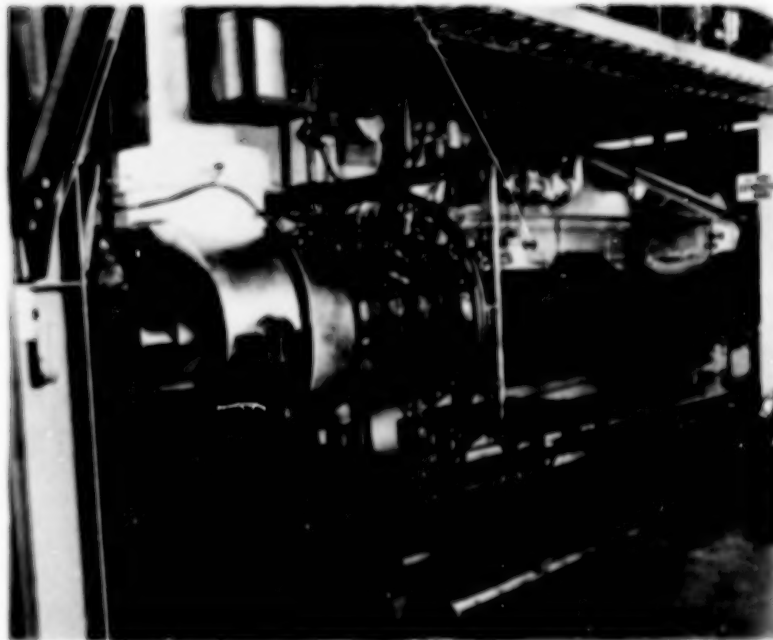
A conventional stacked-ring louvered combustor liner developed a crack at 1603 cycles. This test was discontinued after 1728 cycles because of distortion of the liner.

A segmented or float-wall combustor liner tested at the same heat flux showed no significant change after 1600 cycles. Changes are being made in the facility to allow higher temperatures. Testing is continuing.

## OVERVIEW

### STRUCTURAL COMPONENT RESPONSE TEST FACILITY

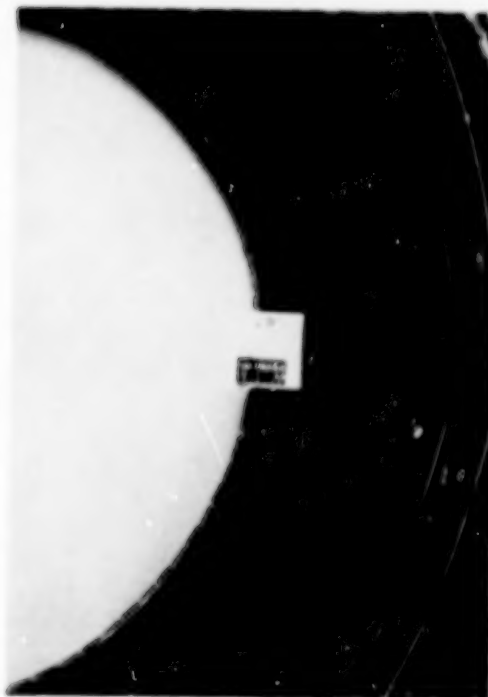
Jet engine combustor liners were tested in the NASA Lewis structural component response test facility to see if damage developed in this testing simulated the damage in actual engine tests. Work was also done on developing methods to measure strain on the liner during testing. In this facility the heat flux to simulate the heat of combustion is supplied by 112 6.5-kW quartz lamps arranged in a cylindrical configuration inside the combustor liner. The lamps are cycled automatically by using a dual-loop programmable controller to simulate takeoff, cruise, and return to idle.



CD-86-32173

### STACKED-RING LOUVERED COMBUSTOR LINER

A conventional stacked-ring louvered combustor liner as instrumented before testing is shown below. After 1603 cycles a crack developed that had increased 2 percent in length at 1728 cycles. The test was discontinued at this point because the distortion caused the liner to interfere with the lamp brackets. The distortion noted was similar to distortion in combustor liners in jet engines.



CD-66-32374

#### SEGMENTED OR FLOAT-WALL COMBUSTOR LINER

A segmented or float-wall combustor liner is currently under test. At 1600 cycles there was little or no distortion in the liner. Changes are being instituted in the facility to allow higher operating temperatures.

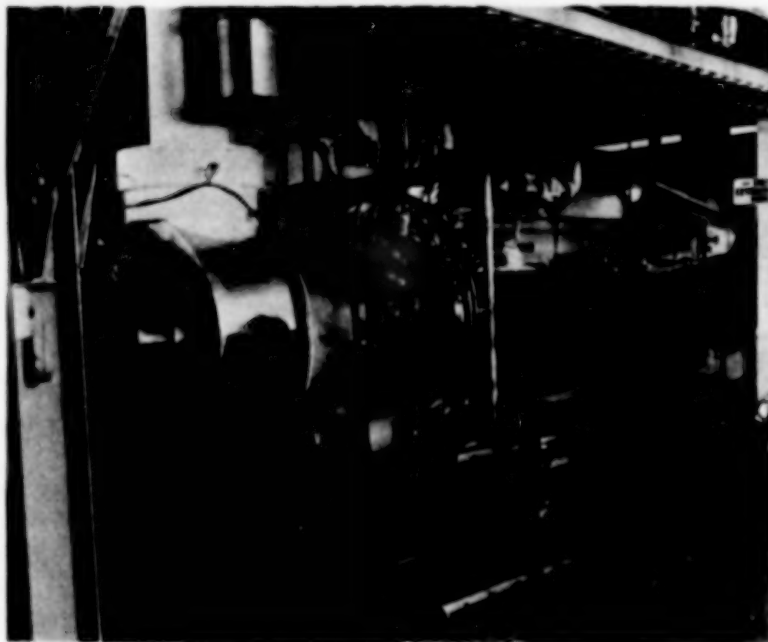


CD-86-32375

## POSTER PRESENTATION

### STRUCTURAL COMPONENT RESPONSE TEST FACILITY

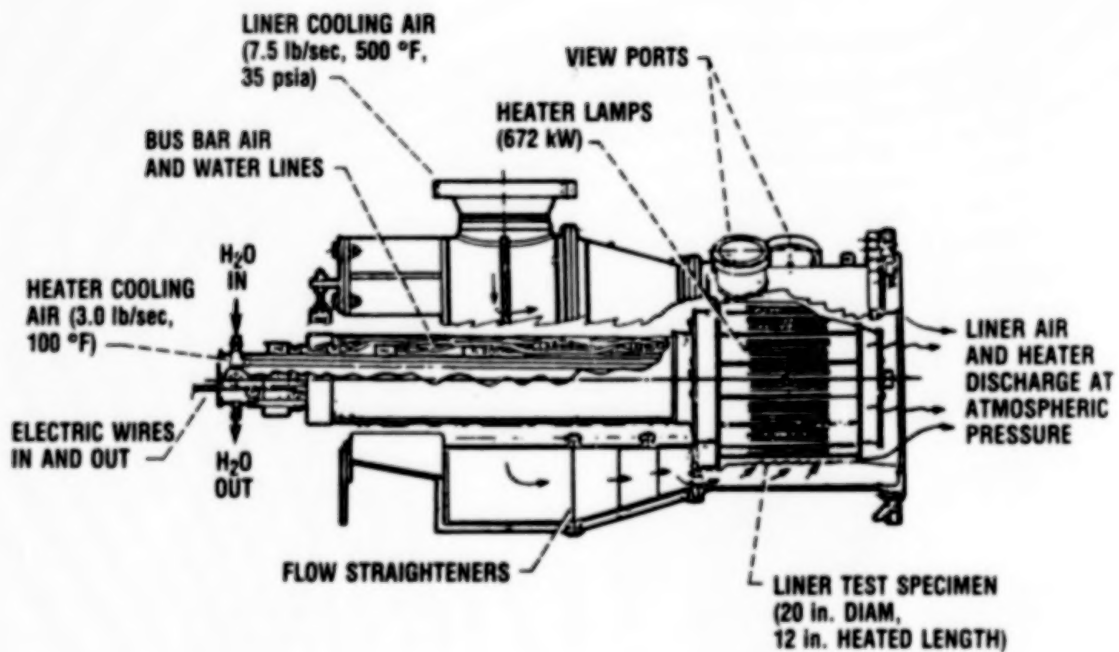
Jet engine combustor liners are being tested in the structural component response test facility. The facility was designed to simulate the thermal cycling encountered by a jet engine combustor liner during takeoff, cruise, and return to idle. The heat flux from combustion is simulated by quartz lamp heaters. The purposes of the tests are (1) to see if damage developed in these tests simulates damage developed in actual jet engine operation and (2) to compare measured strain with calculated strain on liners. The tests would not be relevant unless the damage developed was of the same type that occurs in actual engines. Computer calculations of strain are not relevant unless there is correlation between calculations and measured values. The program is a cooperative program between the NASA Lewis Research Center and Pratt & Whitney Aircraft, East Hartford, Connecticut.



CD-86-32373

## AIRFLOW THROUGH COMBUSTOR LINER TEST FACILITY

Cooling air is preheated to simulate the air from a compressor section and flows through circumferential cooling holes in the liner and out the exhaust. The airflow through the test facility is shown in the line drawing below.



CD-88-32376



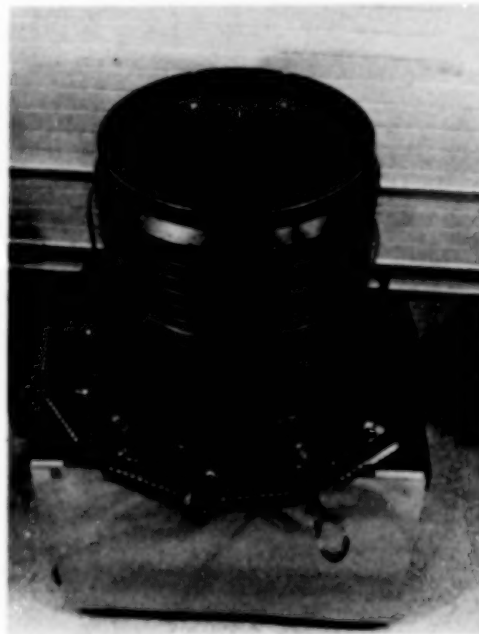
## COMBUSTOR LINER CONFIGURATIONS

One type of combustor liner tested was a conventional stacked-ring louvered liner. A second type under test is the "segmented" or float-wall combustor liner. The water flow and airflow through the test rig are controlled manually. The temperature cycling is controlled by a dual-loop programmable controller.

**STACKED-RING LOUVERED LINER**



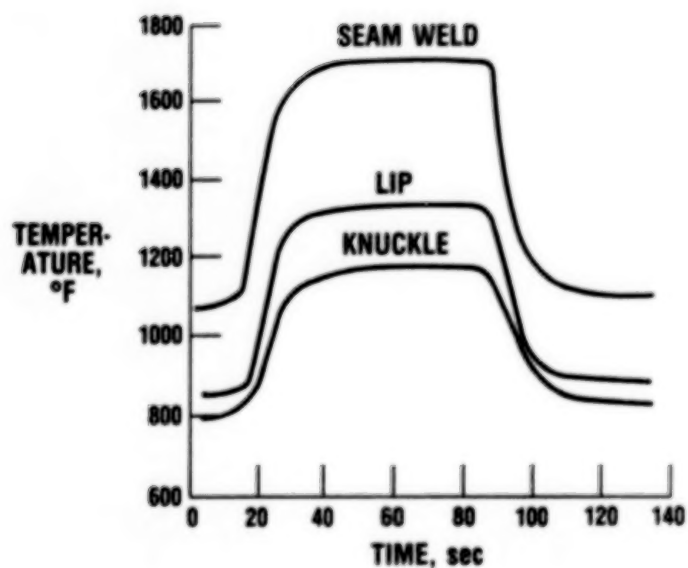
**SEGMENTED LINER**



CD-68-32377

## STACKED-RING LOUVERED COMBUSTOR LINER TEMPERATURE HISTORY

The stacked-ring louvered liner was cycled on a 2.2-minute thermal cycle. Cycling between 25 and 65 percent of nominal power was carried out for 1000 cycles. The temperatures measured at several locations on a louver in the hot zone are shown below.



CD-88-32378

#### THERMAL CYCLING DAMAGE

Although a small amount of distortion occurred, no damage was noted that would lead to failure in a reasonable number of cycles. Therefore the maximum power during the cycle was raised to 70 percent, which resulted in an increase in the maximum temperature of about 60 deg F. Thermal cycling was continued and resulted in more distortion. After 1603 cycles a crack developed. This was actually the result of a hot spot that developed because machining defects blocked cooling holes. The crack showed about 2 percent extension at 1728 cycles. The test was terminated at this point because the combustor liner collapsed on the lamp bracket frame.



CD-88-32379

**BLANK PAGE**

## LIFE ASSESSMENT OF COMBUSTOR LINER USING UNIFIED CONSTITUTIVE MODELS

M.T. Tong\* and R.L. Thompson  
Structural Mechanics Branch  
NASA Lewis Research Center

### ABSTRACT

Hot section components of gas-turbine engines are subject to severe thermo-mechanical loads during each mission cycle. Inelastic deformation can be induced in localized regions leading to eventual fatigue cracking. Assessment of durability requires reasonably accurate calculation of the structural response at the critical location for crack initiation.

In recent years nonlinear finite-element computer codes have become available for calculating inelastic structural response under cyclic loading. Most of these, in keeping with an accepted practice in the elevated-temperature design community, partition nonlinear elevated-temperature material behavior into rate-dependent creep and rate-independent plasticity components. However, analytical studies of hot-section components such as turbine blades (McKnight, 1981) and combustor liners (Moreno, 1981) have demonstrated that the classical creep and plasticity methods do not always predict the cyclic response of the structure accurately because of the lack of the interaction between plasticity and creep behavior. Experimental results have shown that the interaction of elevated temperature is very significant and cannot be ignored (Corum, 1977; Kujawski et al., 1979; Pugh and Robinson, 1978; and Senseny et al., 1978).

Under the Hot Section Technology Project (HOST), NASA Lewis Research Center sponsored the development of unified constitutive material models and their implementation in nonlinear finite-element computer codes for the structural analyses of hot-section components (Ramaswamy et al., 1984 and 1985; and Lindholm et al., 1984 and 1985). These unified constitutive models account for the interaction between the time-dependent and time-independent material behavior. In eliminating the overly simplified assumptions of the classical material model, unified models can more realistically represent the behavior of materials under cyclic loading high-temperature environments. The purpose of this study was to evaluate these unified models with regard to their effect on the life prediction of a hot-section component. The component under consideration was a Pratt & Whitney gas-turbine-engine combustor liner. A typical

---

\*Sverdrup Technology Inc., Lewis Research Center Group. Work performed on-site at the NASA Lewis Research Center under contract NAS3-24105.

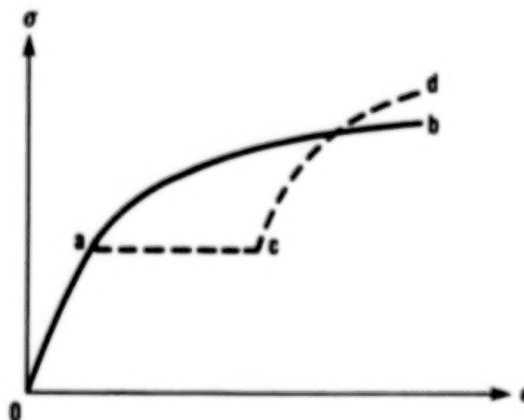
engine mission cycle was used for the thermal and structural analyses. The analyses were performed at Lewis Research Center on a CRAY-XMP computer using the MARC finite-element code. Unified constitutive models of Bodner and Walker were used for the analyses. The results were compared with laboratory test results, in terms of crack initiation lives.

## OVERVIEW

### HARDENING EFFECT OF CREEP ON PLASTICITY

Life assessment of engine hot-section components requires a thorough knowledge of the thermal environment, accurate material characterization, calibrated failure data, and reasonably accurate calculation of the structural response at the critical location for crack initiation. In recent years, nonlinear finite-element computer codes have become available for calculating inelastic structural response under cyclic loading. Most of these computer codes are based on the classical inelastic methods. They partition nonlinear, elevated-temperature material behavior into rate-dependent creep and rate-independent plasticity components. In other words, inelastic strains are decoupled and formulated independently for the creep and plasticity portions, as illustrated in the left figure. However, analytical studies of hot-section components such as turbine blades (McKnight, 1981) and combustor liners (Moreno, 1981) have demonstrated that the classical creep and plasticity methods do not always predict the cyclic response of the structure accurately because of the lack of the interaction between the plasticity and creep behavior. Experimental results have shown that the interaction at high temperature is significant and cannot be ignored (Corum, 1977; Kujawski et al., 1979; Pugh and Robinson, 1978; and Senseny et al., 1978). The interaction is illustrated in the figure, wherein two loading paths are indicated by o-a-b and o-a-c-d. In the second loading path the applied stress is held constant between a and c, which results in creep deformation. As a consequence of the accumulated creep strain, c-d may appear to be stiffer than a-b for a creep hardening alloy. Creep softening alloys would exhibit a less stiff response.

$$\text{INELASTIC STRAIN} = \text{CREEP STRAIN} + \text{PLASTIC STRAIN}$$

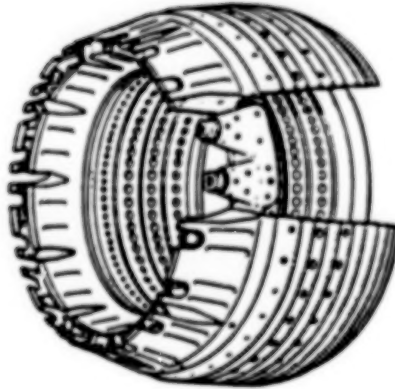


CD-88-32709



## ANNULAR COMBUSTOR LINER

Under the Hot-Section Technology Project (HOST), NASA Lewis sponsored the development of unified constitutive material models and their implementation in nonlinear, finite-element computer codes for the structural analyses of hot-section components. These unified constitutive models account for the interaction between the time-dependent and time-independent material behavior. In eliminating the simplified assumptions of the classical material model, unified models should more realistically represent the behavior of materials under cyclic loading and high-temperature environments. In an application of the unified material constitutive models, life assessment of a Pratt & Whitney gas turbine engine annular combustor liner (as shown below) was conducted. Unified constitutive models of Walker and Bodner were used. The results were compared with laboratory test results, in terms of crack initiation lives.



CD-88-32710

## POSTER PRESENTATION

### CLASSICAL MATERIAL CONSTITUTIVE MODEL - DECOUPLED STRAINS

Conventionally, the most widely used constitutive description of metals at high-temperature employs the time-independent classical theory of plasticity to characterize short-term deformation, while relying upon time-dependent classical theory of creep to characterize long-term deformation. The total strain, or strain increment, then, consists of four additive contributions - elastic, plastic, creep, and thermal components. In other words, constitutive equations are decoupled and formulated independently for the elastic-plastic, creep, and thermal portions. Although the classical theories of plasticity have been used quite extensively to characterize the behavior of metallic structures at room temperature, it does not necessarily justify their applicability to other loading conditions such as high-temperature environment. Analytical studies of engine hot section components such as turbine blades and combustor liners have demonstrated that the classical theories do not always predict the cyclic response of the structure accurately. For high-temperature applications the most severe shortcoming of classical theories is that the interaction between creep and plasticity is not adequately taken into account. Experimental results have shown that the interaction at elevated temperature is significant and cannot be ignored.

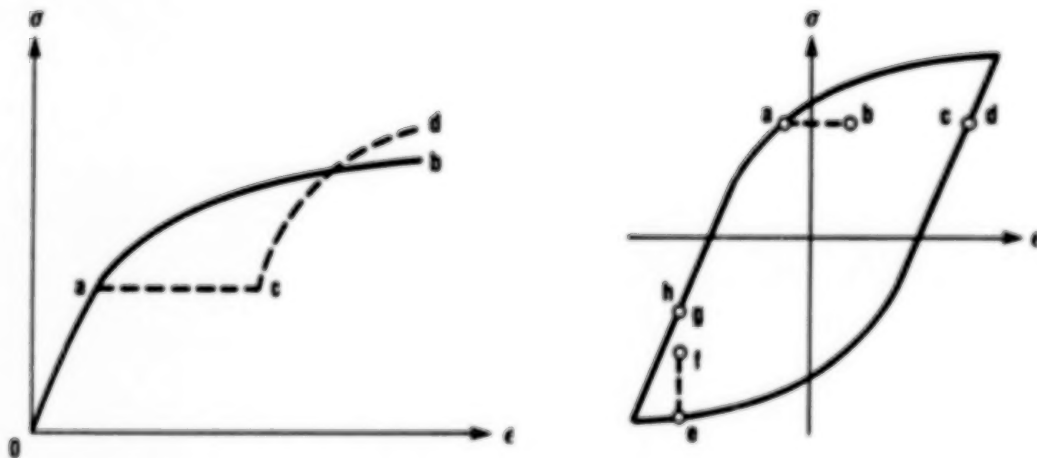
$$\text{INELASTIC STRAIN} = \text{CREEP STRAIN} + \text{PLASTIC STRAIN}$$



CLASSICAL UNCOUPLED

# CREEP-PLASTICITY INTERACTION

Two types of creep-plasticity interactions are generally observed. First, accumulated creep strain has a hardening effect on subsequent plastic response. This phenomenon is shown in the left figure, wherein two loading paths are indicated by o-a-b and o-a-c-d. In the second loading path the applied stress is held constant between a and c, which results in creep deformation. As a consequence of the accumulated creep strain, c-d appears to be stiffer than a-b. Second, recent history of plastic strain has significant influence on subsequent time-dependent behaviors. In the right figure, a-b and c-d represent creep strains corresponding to creep tests performed at loading and unloading branches, respectively, but at the same stress level. While the former undergoes a significant amount of creep deformation, the latter shows virtually no creep. The same kind of phenomenon is also observed when relaxation tests are conducted as designed by e-f and g-h in the right figure.



CD-68-32712

# UNIFIED MATERIAL CONSTITUTIVE MODELS

In light of the previous discussion, it is apparent that effort must be made to improve the prediction of inelastic behavior of metals at high temperatures. The new theories toward characterization of material behavior at high temperatures are known as unified theories in the sense that plastic and creep strains are represented and treated by a single kinetic equation and a discrete set of internal variables. They are also known as viscoplastic theories because they are capable of modeling both rate-dependent and rate-independent behaviors.

$$\begin{aligned}\dot{\sigma} &= E(\dot{\epsilon} - \dot{\epsilon}^I - \dot{\epsilon}^{TH}) & \dot{\alpha} &= h_{\alpha} \dot{\epsilon}^I - r_{\alpha} \\ \dot{\epsilon}^I &= \left[ \frac{\sigma - \alpha}{K} \right] & \dot{K} &= h_K |\dot{\epsilon}^I| - r_K\end{aligned}$$

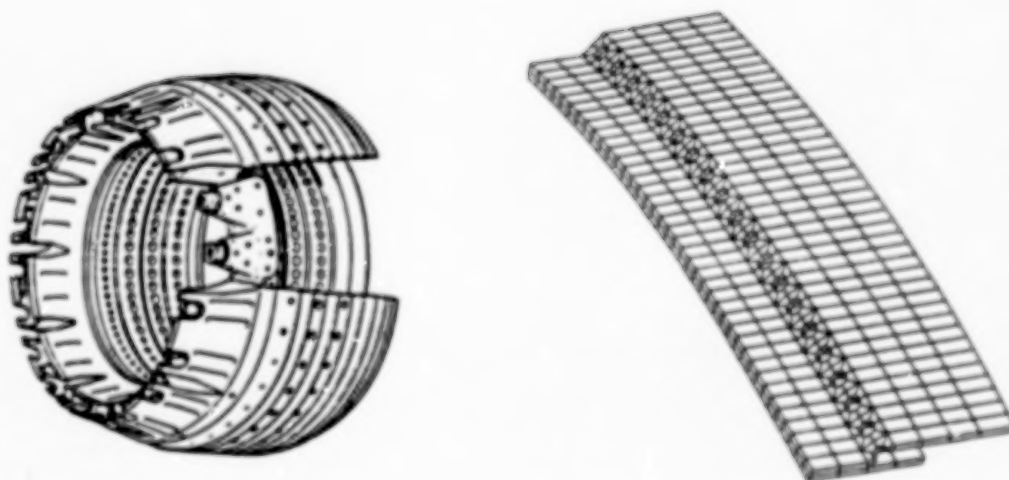
## WHERE

|                   |                            |
|-------------------|----------------------------|
| $h_{\alpha}, h_K$ | STRAIN HARDENING FUNCTIONS |
| $r_{\alpha}, r_K$ | RECOVERY FUNCTIONS         |
| $\alpha, K$       | STATE VARIABLES            |
| $\epsilon^I$      | INELASTIC STRAIN           |
| $\epsilon^{TH}$   | THERMAL STRAIN             |
| $\sigma$          | STRESS                     |

CD-88-32713

## COMBUSTOR LINER AND ITS FINITE ELEMENT MODEL

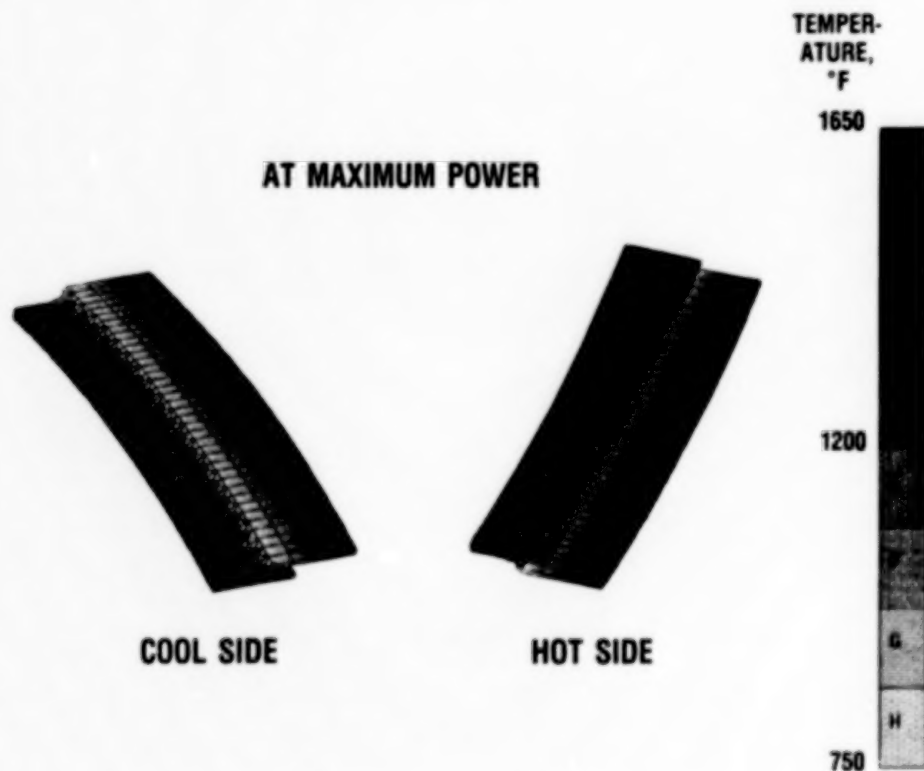
In an application of the unified material constitutive models, life assessment of a Pratt & Whitney gas-turbine-engine annular combustor liner was conducted. The liner is air-cooled and is made of Hastelloy-X alloy. The finite-element model has 546 elements and 1274 nodes. Eight-node solid elements were used. Because of symmetry only a section of the liner was modeled.



CO-88-32714

## THERMAL ANALYSIS OF ANNULAR COMBUSTOR LINER

Thermal analysis was first conducted to determine the temperature distribution of the combustor liner. These temperatures were later used for the structural analysis of the liner. A typical engine mission cycle was used for the analysis. Temperature histories at the combustor liner critical locations were also determined.



CD-88-32715

## COMPARISON WITH TEST RESULTS

Subsequent nonlinear structural analysis of the combustor liner was performed. The analysis was conducted with the unified constitutive models of Walker and Bodner (Lindholm et al., 1984 and 1985). Both models were implemented into the MARC finite-element code. Stress and strain ranges at the liner critical locations were determined.

The total strain and inelastic strain ranges were used for the life assessment of the combustor liner, based on the experimental results by Jablonski (1978). In conjunction with the analyses, laboratory tests were performed on the combustor liner. Comparisons were made of crack initiation lives. Good agreement between predicted and measured life was obtained.

| ANALYTICAL METHOD | MECHANICAL STRAIN RANGE, % |           | PREDICTED LIFE, CYCLES |
|-------------------|----------------------------|-----------|------------------------|
|                   | TOTAL                      | INELASTIC |                        |
| UNIFIED (WALKER)  | 0.587                      | 0.315     | 1000 TO 1500           |
| UNIFIED (BODNER)  | .580                       | .270      | 1000 TO 1500           |

OBSERVED LIFE = 1603 CYCLES

CD-88-32716



## REFERENCES

- Corum, J.M., 1977, "Evaluation of Inelastic Analysis Methods," Transactions of the 4th SMIRT Conference, San Francisco, Vol. L, Paper L.
- Jablonski, D.A., 1978, Fatigue Behavior of Hastelloy-X Elevated Temperatures in Air, Vacuum, and Oxygen Environments. Ph.D. Thesis, University of Connecticut.
- Kujawski, D., Kallianpur, V., and Krempl, E., 1979, "Uniaxial Creep, Cyclic Creep and Relaxation of AISI Type 304 Stainless Steel at Room Temperature, An Experimental Study," RPI Report CS 79-4.
- Lindholm, U.S., Chan, K.S., Bodner, S.R., Weber, R.M., Walker, K.P., and Cassenti, B.N., 1984, "Constitutive Modeling for Isotropic Materials," NASA CR-174718.
- Lindholm, U.S., Chan, K.S., Bodner, S.R., Weber R.M., Walker, K.P., and Cassenti, B.N., 1985, "Constitutive Modeling for Isotropic Materials," NASA CR-174980, 1985.
- McKnight, R.L., Laflen, J.H., and Spamer, G.T., 1981, "Turbine Blade Tip Durability Analysis," NASA CR-165268.
- Moreno, V., 1981, "Combustor Liner Durability Analysis," NASA CR-165250.
- Pugh, C.E., and Robinson, D.N., 1978, "Some Trends in Constitutive Equation Model Development for High-Temperature Behavior of Fast-Reactor Structural Alloys," Journal of Nuclear Engineering and Design, Vol. 48, pp. 269-276.
- Ramaswamy, V.G., Van Stone, R.H., Dame, L.T., and Laflen, J.H., 1984, "Constitutive Modeling for Isotropic Materials," NASA CR-17485.
- Ramaswamy, V.G., Van Stone, R.H., Dame, L.T., and Laflen, J.H., 1985, "Constitutive Modeling for Isotropic Materials," NASA CR-175004.
- Senseny, P.E., Duffy, J., and Hawley, R.H., 1978, "Experiments on Strain Rate History and Temperature Effect During the Plastic Deformation of Closed-Packed Metals," ASME Journal of Applied Mechanics, Vol. 45, pp. 60-66.

**BLANK PAGE**

**EXPERIMENTS INVESTIGATING ADVANCED MATERIALS UNDER  
THERMOMECHANICAL LOADING**

**Paul A. Bartolotta  
Structural Mechanics Branch  
NASA Lewis Research Center**

**ABSTRACT**

Many high-temperature aircraft and rocket engine components experience large mechanical loads as well as severe thermal gradients and transients. These nonisothermal conditions are often large enough to cause inelastic (thermomechanical) deformations, which are the ultimate cause for failure in those components. A way to alleviate this problem is through improved designs based on better predictions of thermomechanical material behavior. Ongoing work at the NASA Lewis Research Center is dedicated to observing the effects of thermomechanical deformation on material behavior and evaluating and incorporating these effects into constitutive models for better prediction capabilities.

To address this concern, an experimental effort was recently initiated within the Hot Section Technology (HOST) program at Lewis. As part of this effort, two new test systems were added to the Fatigue and Structures Laboratory, which allowed thermomechanical tests to be conducted under closely controlled conditions. These systems are now being used for thermomechanical testing for the Space Station Solar Receiver program, and will be used to support development of metal matrix composites.

## OVERVIEW

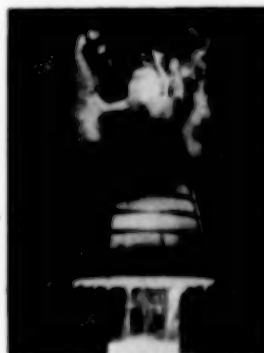
### PRACTICAL OCCURRENCES OF THERMOMECHANICAL LOADING

Under operating conditions, components in high-temperature applications (i.e., hot sections of aircraft and rocket engines, energy systems, etc.) are subjected to thermomechanical deformations. It is believed that such deformations are the ultimate cause of structural failure in these components. To improve life and performance, the material's thermomechanical behavior must be incorporated into the component's design. The High Temperature Fatigue and Structures Laboratory is dedicated to observing the effects of thermomechanical deformation on material behavior and integrating these effects into constitutive models to improve high-temperature component design.

**GAS TURBINE ENGINE**



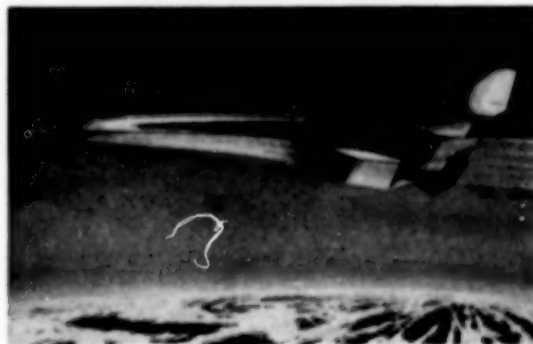
**SPACE SHUTTLE MAIN ENGINE**



**SPACE STATION**



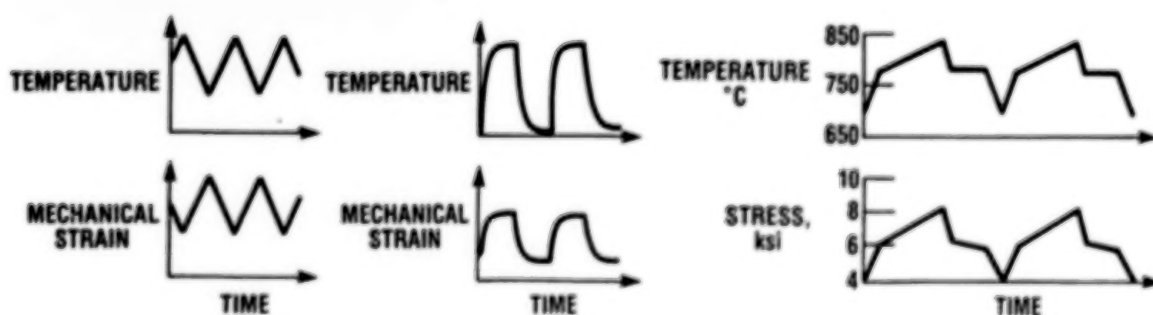
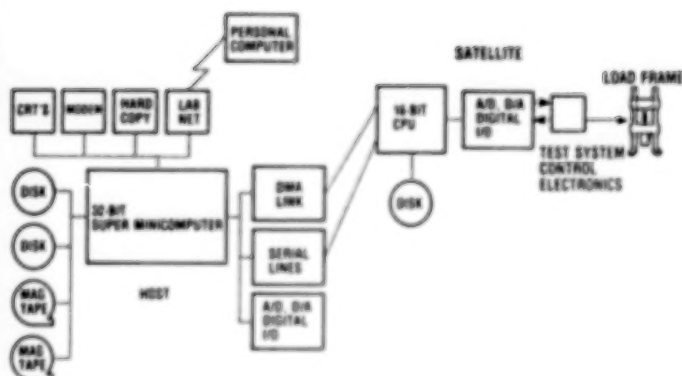
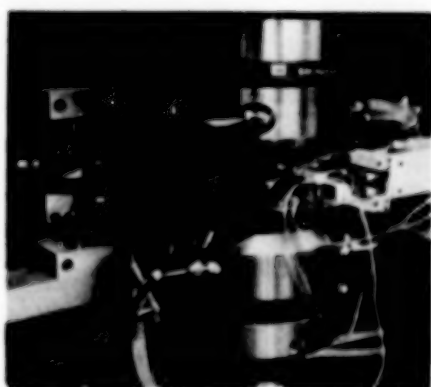
**HYPERSONIC AIRCRAFT**



CD-88-31763

## THERMOMECHANICAL TEST CAPABILITIES

An experimental effort was initiated within the HOST Program at the NASA Lewis Research Center to enhance the thermomechanical testing capability of the High Temperature Fatigue and Structures Laboratory. As part of this effort, new test systems were obtained, and a computer testing system was developed. By utilizing this new capacity, we can subject test specimens to prototypical loading conditions and record the material response.



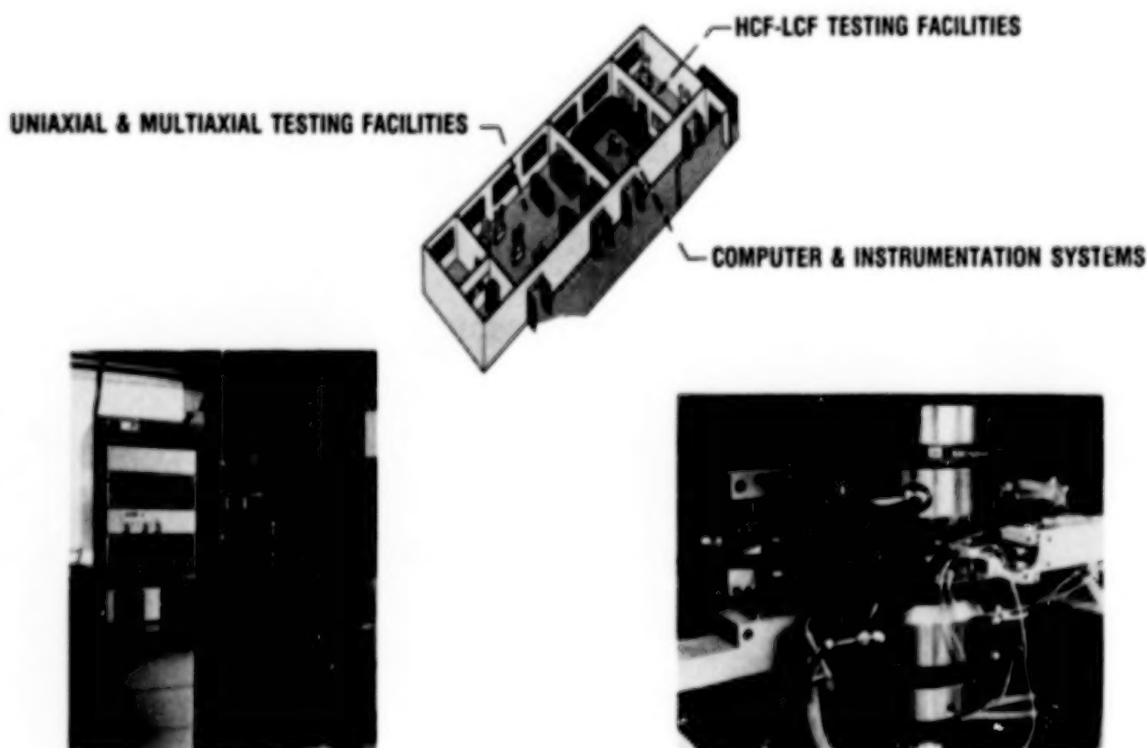
CD-88-31764

## POSTER PRESENTATION

### THERMOMECHANICAL TEST SYSTEMS

The High Temperature Fatigue and Structures Laboratory at the NASA Lewis Research Center has improved its testing capability in order to investigate advanced materials under complex thermomechanical loadings. These improvements include the acquisition of new test systems, and the development of a locally distributed digital computer system for experimental control, data acquisition, and data manipulation. Two of the newly obtained test systems are dedicated to high-precision thermomechanical deformation testing. Special features of these systems include the following:

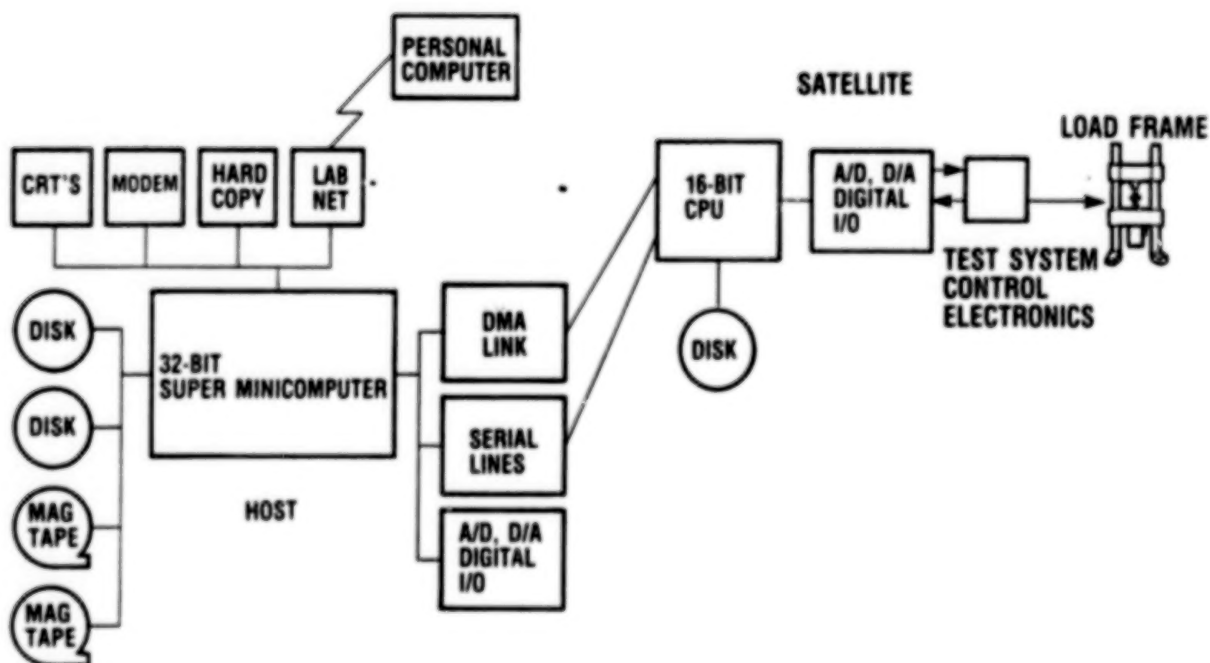
- (1) Hydraulic actuator bearings for maintaining alignment throughout the length of the stroke
- (2) Hydraulic grips for assured specimen alignment, ease of specimen installation, and specimen geometry adaptability. The grips are water cooled for protection during high-temperature testing
- (3) Dual servovalves for high system fidelity
- (4) Induction coil heating fixture for uniform temperature profile



CD-88-31765

## ARCHITECTURE OF LABORATORY'S COMPUTER TEST SYSTEM

One of the most important enhancements of the laboratory's thermomechanical capabilities is its digital computer test system. The system is composed of a host 32-bit super minicomputer, fourteen 16-bit satellite microcomputers, and four personal computers. All 19 processors are linked together by a high-speed multiprocessor communication system. The host processor is used for program development work and data storage. Each test system has a satellite processor dedicated to experimental control and data acquisition. The personal computers provide data display and plotting capabilities in addition to data analysis.



CD-88-31766

## HOT SECTION GAS TURBINE PROGRAM

Recent experimental efforts towards understanding thermomechanical material behavior have been focused on the area of gas turbine engines. This effort was supported by the Hot Section Technology (HOST) program at Lewis. Utilizing the laboratory's new thermomechanical capabilities, materials for hot section components (i.e., turbine blades, combustor liners, etc.) are easily subjected to prototypical mission cycles. In this figure, we see examples of mechanical and thermal loading histories for turbine blades and combustor liners.

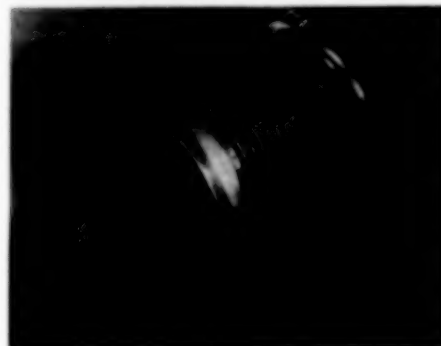
### GAS TURBINE ENGINE



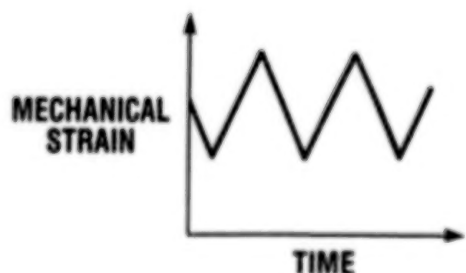
**TURBINE BLADES**



**COMBUSTOR LINER**



CD-88-32020



CD-88-31767



## SPACE STATION SOLAR RECEIVER

Initially the electrical power for the NASA space station will be provided by several sets of photovoltaic solar arrays, which will provide a 75-kW power source. Eventually, as electrical power requirements increase, the station will add two solar dynamic power systems. This upgrade will increase the electric power supply from 75 kW to 125 kW.

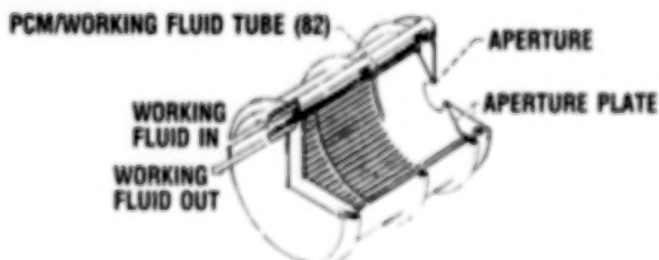
As the space station orbits the earth, the sun's energy is directed into the solar receiver's aperture via a set of parabolic mirrors. In the receiver the energy is used to heat 82 working fluid tubes. Once heated, this working fluid will drive a series of turbines, compressors, and generators to produce a continuous flow of electrical power. To provide a heat source during the eclipse of the station's orbit, the working fluid tubes will utilize the solar energy stored in containment canisters filled with a liquid/solid phase change material.

### SPACE STATION



### SOLAR RECEIVER

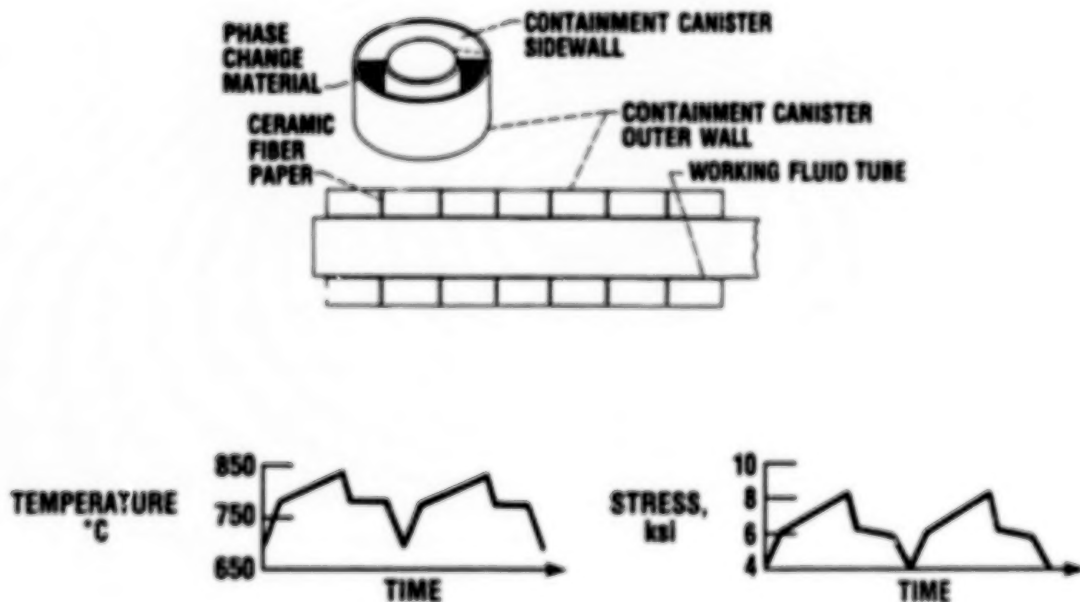
DIAMETER, 6.1 ft; LENGTH, 9.8 ft



CD-86-31768

STRUCTURAL ANALYSIS AND EXPERIMENTAL RESPONSE OF  
SOLAR RECEIVER CONTAINMENT CANISTERS

Initial structural analysis of a proposed canister design determined that during its design life (30 years) the canister material (Haynes 188) will experience relatively low cyclic stresses and high service temperatures. Based upon isothermal, monotonic steady-state creep and creep rupture data, it was concluded that creep would not be a significant design factor. However, after the completion of a series of creep "threshold" and thermomechanical experiments, it was shown that there was a significant accumulation of creep strains in a matter of 90 min at stress levels as low as 4 ksi for the predicted service temperatures. Also it was observed that as the material was subjected to prototypical service cycles it exhibited creep ratcheting behavior. It is important to note that with the laboratory's new thermomechanical testing capabilities, we can easily simulate complex service loadings and measure the material response rather than having to rely on irrelevant data to calculate what might happen. Further goals of this program will aim towards the development of a constitutive model for Haynes 188 that will be incorporated into a finite element code and used to improve the overall canister design.



LST '88

CO-88-31789

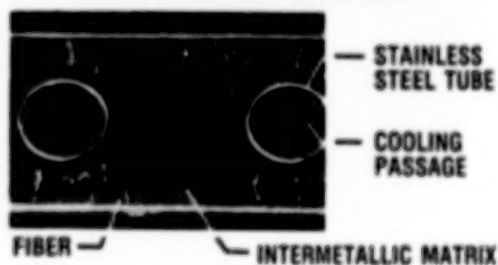
## FUTURE PROGRAMS FOR THERMOMECHANICAL DEFORMATION TESTING

Design concepts for hypersonic airframes and propulsion system components dictate the use of advanced lightweight, high-strength, high-temperature materials such as metal and ceramic matrix composites. These materials will be subjected to high heat flux and thermomechanical loads induced by aerodynamic friction and complex engine operating conditions. A major obstacle (aside from material fabrication methods) for advanced composite materials to overcome is that of the mismatch of the coefficient of thermal expansion between fiber and matrix. It has been shown that this mismatch can produce large amounts of internal residual stresses within the composite system, which could lead to premature component failure. It is believed that thermomechanical testing would be an ideal method of screening candidate composite systems before the material is characterized for constitutive models. Subsequent presentations in this symposium will address the issues of thermal/structural analysis of these systems.

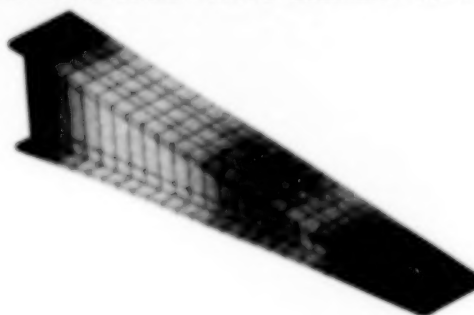
### HYPERSONIC AIRCRAFT



### METAL MATRIX COMPOSITE



### LEADING-EDGE FINITE ELEMENT ANALYSIS



CD-88-31770

BLANK PAGE

# **BIAXIAL EXPERIMENTS SUPPORTING THE DEVELOPMENT OF CONSTITUTIVE THEORIES FOR ADVANCED HIGH-TEMPERATURE MATERIALS**

**J.R. Ellis**  
Structural Mechanics Branch  
NASA Lewis Research Center

## **ABSTRACT**

In most engineering applications, complex states of stress and strain are introduced into components during service. It follows that analysis of such components requires material descriptions, or constitutive theories, which reflect the tensorial nature of stress and strain. In most applications involving low homologous temperatures and stress levels below yield, material response is linear and elastic. These material characteristics lead to simple constitutive relationships involving two material constants.

For applications involving stress levels above yield, the situation is more complex in that material response is both nonlinear and history dependent. Plasticity theories have been developed to model these features by using flow laws and evolutionary laws expressed in differential form. At elevated temperatures, the situation is more complicated still in that material response is time dependent. This has led to the development of viscoplastic constitutive theories which introduce time by expressing the flow and evolutionary equation in the form of time derivatives. Most recently, attempts have been made to extend viscoplastic theories to transversely isotropic materials. The intent here is to develop models which can be used to analyze high-temperature components manufactured from advanced composite materials.

In parallel with the theoretical studies, considerable effort has been directed at developing multiaxial testing techniques to verify the various theories. This work faces two technical challenges. The first is identifying the type of experiment best suited to verifying particular theories. In the case of plasticity, yield surface testing techniques were developed and used successfully to support the theoretical effort. A similar approach has recently been proposed to support development of viscoplastic theories. In this case, the time-dependent characteristics of elevated temperature response are captured by using inelastic strain rate as a measure of inelastic state and by determining flow surfaces. It is interesting to note that this approach can be extended without difficulty to experimental studies of composite materials.

The second challenge is being able to make stress and strain measurements to high levels of precision under biaxial loading conditions. Presently,

tension-torsion load cells are fully developed, and so stress measurements do not present much difficulty. In contrast, the systems available for measuring biaxial strains need further development. At room and intermediate temperatures, foil strain gage rosettes have been used with some success in yield surface studies. Attempts to extend this approach to elevated temperatures have proved less successful because of the unreliability of high-temperature strain gages when used in biaxial stress fields. This has led to the development of a number of mechanical extensometers designed specifically for use in flow surface determinations at elevated temperature. Again, this instrumentation can be used to characterize advanced composite materials provided these materials can be fabricated in the form of thin-walled tubes.

The primary aim of this paper is to outline recent progress in the development of constitutive theories both from the theoretical and experimental viewpoints. One important aspect of this work is that it is leading to verified material descriptions for advanced composite materials which can be implemented in general purpose finite element codes and used for practical design.

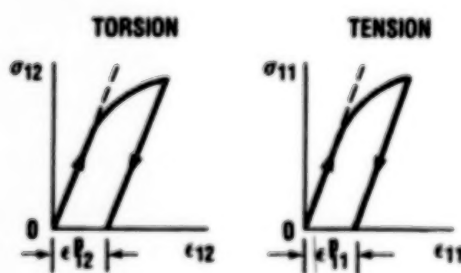


## POSTER PRESENTATION

### BIAXIAL EXPERIMENTS SUPPORTING DEVELOPMENT OF PLASTICITY THEORIES

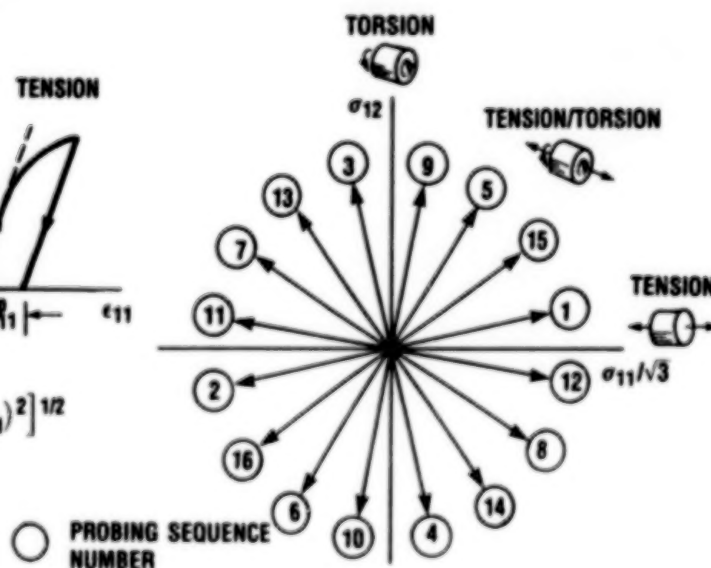
Yield surface experiments have been used extensively to investigate multiaxial deformation behavior at room and intermediate temperatures. In these experiments, tubular specimens are loaded under computer control at fixed ratios of torsional stress and axial stress. The specimens are instrumented with strain gage rosettes which provide decoupled measures of axial strain and tensorial shear strain. During the initial stages of loading, straight line relationships are established between stress and strain for both components of loading. The stress levels are increased proportionately until the stress-strain response deviates a predetermined amount from linear. These deviations, or small offset definitions of yield, are kept small, 25  $\mu\epsilon$  or less, to avoid changing the material's state significantly. After achieving the target offset, the specimen is unloaded, and the procedure is repeated for stress ratios in all quadrants of tension-torsion stress space. The combinations of torsional stress and axial stress giving the required yield condition are noted at the termination of each probe and used to construct yield surfaces.

INDIVIDUAL LOADING PROBES ARE TERMINATED WHEN A TARGET VALUE OF EQUIVALENT INELASTIC STRAIN  $\bar{\epsilon}^P$  IS REACHED



$$\bar{\epsilon}^P = \left[ (\epsilon_2^P)^2 + 3/4 (\epsilon_1^P)^2 \right]^{1/2}$$

PROBING SEQUENCE USED TO DETERMINE YIELD SURFACES IN TENSION/TORSION STRESS SPACE



CD-88-33305

## PLASTICITY THEORIES FOR INITIALLY ISOTROPIC MATERIALS

The aim of plasticity theories is to provide mathematical descriptions of material response at stress levels above yield. Here, material response is both nonlinear and history dependent. In the case of initially isotropic materials, material descriptions should not be directional. This requirement can be met by using as many as three invariants to introduce stress into the theory. Classically, the single invariant used for this purpose is the  $J_2$ , or Von Mises, form of equivalent stress. One approach adopted in treating history-dependent material response is to use an internal state variable  $\alpha_{ij}$  which provides a measure of inelastic state. Evolutionary equations are used to relate changes in  $\alpha_{ij}$  to incremental changes of inelastic strain (Prager) or effective deviatoric stress (Ziegler). It is important to note that these theories can only be verified through careful experimentation.

$$\text{FLOW LAW:} \quad d\epsilon_{ij}^p = \lambda \frac{\partial f}{\partial \sigma_{ij}} \frac{\partial f}{\partial \sigma_{kl}} d\sigma_{kl} \quad (\text{DRUCKER})$$

$$\text{POSSIBLE EVOLUTIONARY EQUATIONS:} \quad d\alpha_{ij} = c \, d\epsilon_{ij}^p \quad (\text{PRAGER})$$

$$d\alpha_{ij} = (S_{ij} - \alpha_{ij}) \, d\mu \quad (\text{ZIEGLER})$$

$$\text{POSSIBLE YIELD FUNCTIONS:} \quad f(J_2) = J_2 - K \quad (\text{VON MISES})$$

$$f(J_2, J_3) = J_2 + \beta J_3^{2/3} - K \quad (\text{DRUCKER})$$

WHERE

$$J_2 = 1/2 S_{ij} S_{ij}; \quad J_3 = 1/3 S_{ij} S_{jk} S_{ki}$$

$$S_{ij} = \sigma_{ij} - 1/3 \sigma_{kk} \delta_{ij}; \quad \alpha_{ij} - \text{INTERNAL STATE VARIABLE}$$

AND  $c$ ,  $\lambda$ , AND  $\mu$  ARE MATERIAL CONSTANTS.

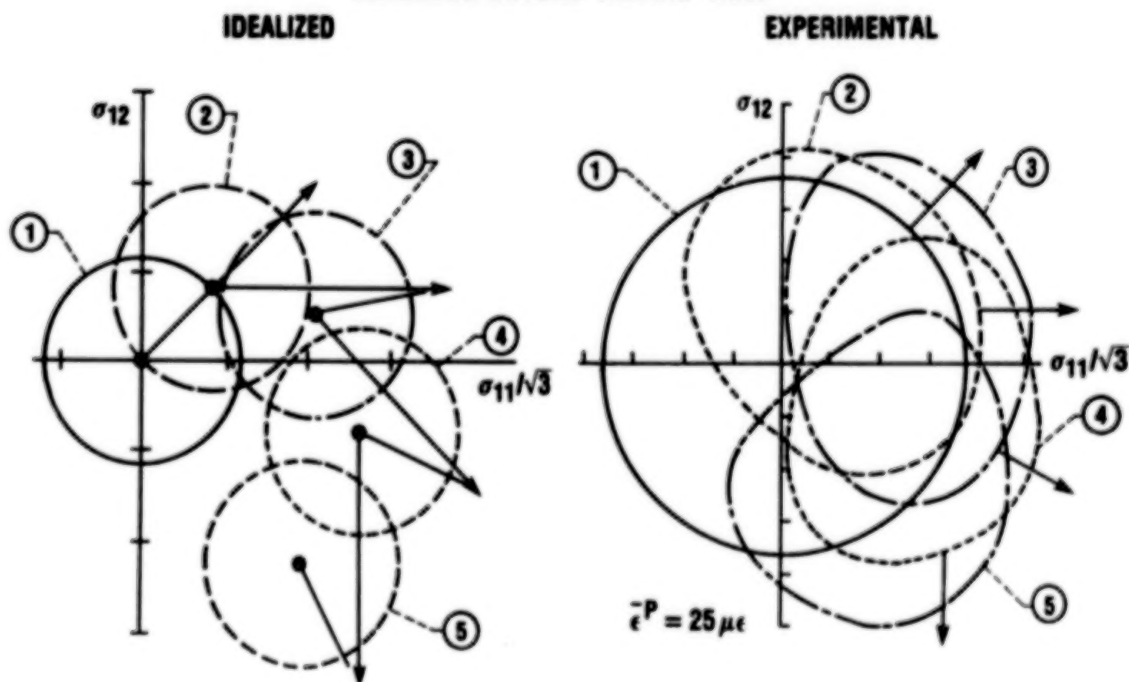
CD-88-33306



## COMPARISON OF EXPERIMENTAL YIELD SURFACES WITH THEORETICAL PREDICTIONS

The yield surface concept described earlier provides a convenient means of interpreting plasticity theories. Adopting this approach, the yield function describes the shape of the yield surface, and the evolutionary equation describes the translation of the yield surface in stress space. Interpretation of the data can be simplified further by using modified stress space  $\sigma_{12}$  versus  $\sigma_{11}/\sqrt{3}$ . This is because the Von Mises yield function plots as a circle in this stress space. Theoretical and experimental yield surfaces for a series of nonproportional loadings beyond initial yield are shown here. The experiments were conducted at 20 °C on 9Cr-1Mo steel and used a 25- $\mu\epsilon$ -offset definition of yield (Ellis, 1985). As is typical for most structural alloys, the Von Mises yield function gives a close representation of initial yield behavior and a poor representation of subsequent yield behavior. Also, Prager and Ziegler forms of evolutionary equation provide reasonable approximations of yield surface translation in stress space.

### TRANSLATION OF YIELD SURFACES RESULTING FROM NONPROPORTIONAL LOADINGS BEYOND INITIAL YIELD

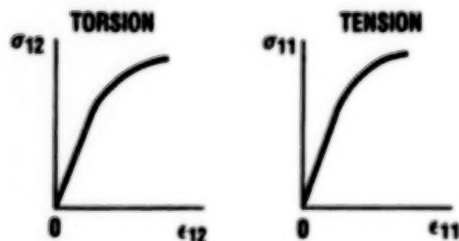


CD-88-33307

# ELEVATED-TEMPERATURE BIAXIAL TESTING SUPPORTING THE DEVELOPMENT OF VISCOPLASTIC CONSTITUTIVE THEORIES

Attempts to extend yield surface testing techniques to elevated temperatures have proved less than successful. One major difficulty has been the unreliability of high-temperature strain gages when used in biaxial stress fields. This led to the development of a number of biaxial extensometers which have recently shown promise in probing-type experiments (Ellis, 1983). Another difficulty is that the traditional concept of yield breaks down at elevated temperatures when material response becomes time dependent. One experimental approach developed to resolve this difficulty is to use inelastic strain rate  $\dot{\epsilon}^P$  as a measure of change in inelastic state. By adopting this approach, flow surfaces can be determined for particular values of  $\dot{\epsilon}^P$  and used to guide the development of viscoplastic constitutive theories.

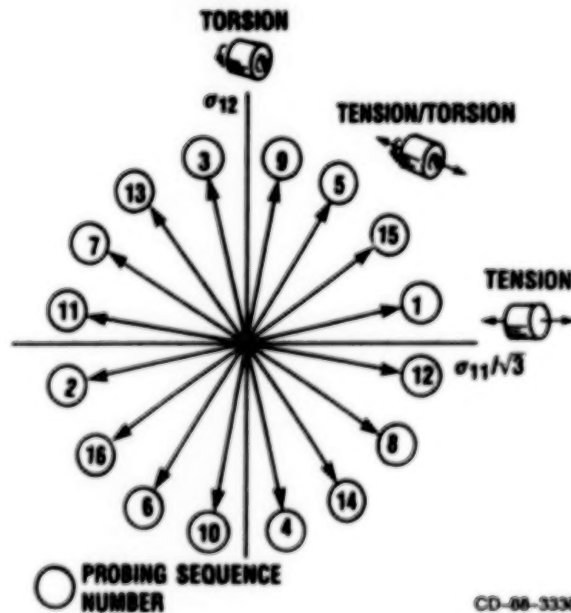
INDIVIDUAL LOADING PROBES ARE  
TERMINATED WHEN A TARGET VALUE OF  
EQUIVALENT INELASTIC STRAIN RATE  $\dot{\epsilon}^P$   
IS REACHED



$$\dot{\epsilon}_{12}^P = \dot{\epsilon}_{12} - \dot{\sigma}_{12}/2G \quad \dot{\epsilon}_{11}^P = \dot{\epsilon}_{11} - \dot{\sigma}_{11}/E$$

$$\text{AND } \dot{\epsilon}^P = [(\dot{\epsilon}_{12}^P)^2 + 3/4 (\dot{\epsilon}_{11}^P)^2]^{1/2}$$

PROBING SEQUENCE USED TO DETERMINE  
FLOW SURFACES IN TENSION/TORSION  
STRESS SPACE



# A VISCOPLASTIC CONSTITUTIVE THEORY FOR INITIALLY ISOTROPIC MATERIALS

In addition to treating the complexities of plasticity, viscoplastic constitutive theories attempt to model the time-dependent features of material response at elevated temperature. These features include creep, relaxation, recovery, and rate dependence. A convenient method of introducing time into the material description is to express the flow and evolutionary equations in the form of time derivatives. The majority of viscoplastic theories use two internal state variables,  $\alpha_{ij}$  and  $K$ , to treat the complexities of elevated temperature behavior (Freed, 1988). As in the case of plasticity, stress is introduced into the material description by means of invariants. Again, the Von Mises form of equivalent stress is used in the majority of these models for initially isotropic materials. The validity of this approach remains to be verified experimentally.

$$\text{FLOW LAW:} \quad \dot{\epsilon}_{ij}^p = \theta(T) Z\left(\frac{\Sigma_2}{K}\right) \frac{\Sigma_{ij}}{\Sigma_2}$$

$$\begin{aligned} \text{EVOLUTIONARY LAWS:} \quad \frac{\dot{\alpha}_{ij}}{H} &= \dot{\epsilon}_{ij}^p - \frac{\alpha_{ij}}{K} \dot{\epsilon}_2^p \\ \frac{\dot{K}}{h} &= \frac{1}{K} \Sigma_{ij} \dot{\epsilon}_{ij}^p - \theta(T) r(K) \end{aligned}$$

WHERE  $Z(\Sigma_2)$ ,  $r(K)$ , AND  $\theta(T)$  ARE MATERIAL FUNCTIONS;  $H$  AND  $h$  ARE MATERIAL PARAMETERS; AND

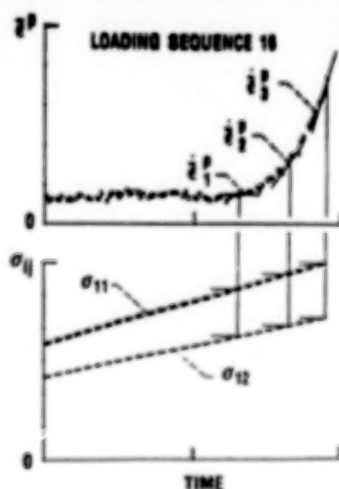
$$\begin{aligned} \Sigma_{ij} &= S_{ij} - \alpha_{ij} & S_{ij} &= \frac{3}{2} \sigma_{ij} - \frac{1}{2} \sigma_{kk} \delta_{ij} \\ \Sigma_2 &= \left[ \frac{2}{3} \Sigma_{ij} \Sigma_{ij} \right]^{1/2} & \dot{\epsilon}_2^p &= \left[ \frac{2}{3} \dot{\epsilon}_{ij}^p \dot{\epsilon}_{ij}^p \right]^{1/2} \end{aligned}$$

CD-88-33309

## DETERMINATION OF FLOW SURFACES AT ELEVATED TEMPERATURES

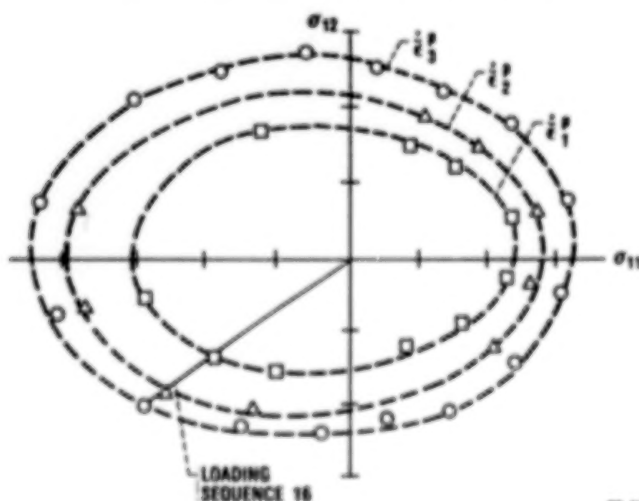
The feasibility of using flow surfaces to investigate multiaxial response at elevated temperatures has been demonstrated in a series of experiments conducted on type-316 stainless steel at 20 and 650 °C (Battiste and Ball, 1986). As indicated earlier, the main challenge in conducting these experiments is strain measurement. Obvious requirements in probing-type experiments are linearity and high resolution. A requirement for minimum crosstalk is unique to biaxial testing. This problem arises when loading in the axial sense produces apparent torsional strains and vice versa. Further complications arise in conducting these experiments at elevated temperatures. The problem here is that the electrical noise produced by most heating systems causes problems with test system control and resolution. As demonstrated by the results shown here, mechanical extensometers have been developed which meet most of the requirements discussed previously. Further improvements are necessary, however, before some of the more fundamental theoretical assumptions can be tested with a high degree of confidence.

FLOW SURFACES FOR SMALL VALUES OF EQUIVALENT INELASTIC STRAIN RATE  
CAN BE DETERMINED IN POST-TEST ANALYSIS OF THE EXPERIMENTAL DATA



CD-86-33310

PRELIMINARY FLOW SURFACES DETERMINED FOR TYPE-316 STAINLESS STEEL AT 20 °C

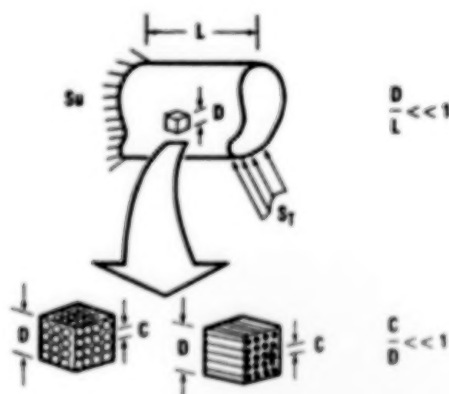


CD-86-33311

## EXTENSION OF BIAxIAL TESTING AND CONTINUUM THEORIES TO ADVANCED COMPOSITE MATERIALS

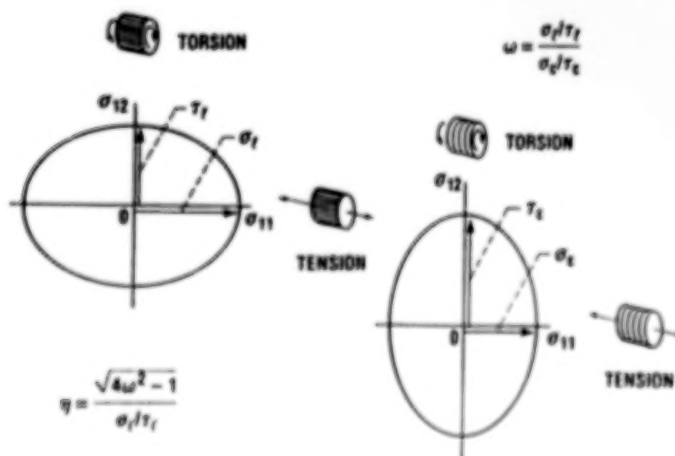
It has been recognized for some time that the thin-walled tube and tension-torsion loading provide an ideal means of investigating deformation behavior in composite materials. One advantage of this approach is that properties can be determined for compressive loadings without too much difficulty. Further, shear properties can be obtained with minimum ambiguity by using the torsional component of loading. Thus, it appears that the high-temperature instrumentation and experimental techniques developed for isotropic materials can be used to advantage in developing deformation theories for advanced composite materials.

APPLICATION OF CONTINUUM THEORIES TO STRUCTURED MATERIALS REQUIRES IDENTIFICATION OF A CONTINUUM ELEMENT (D) THAT IS SMALL COMPARED TO CHARACTERISTIC STRUCTURAL DIMENSIONS BUT LARGE COMPARED TO CELL SIZE DIMENSIONS



CD-88-32012

MEASURES OF ANISOTROPY,  $\omega$  AND  $\eta$ , CAN BE OBTAINED BY DETERMINING FLOW SURFACES FOR TUBES REINFORCED IN THE LONGITUDINAL AND TRANSVERSE SENSES



CD-88-32013

# VISCOPLASTIC CONSTITUTIVE THEORY FOR TRANSVERSELY ISOTROPIC MATERIALS

Procedures are well established for extending continuum mechanics concepts to composite materials. Here, the challenge is to incorporate directionality into the material description without violating the laws of mechanics. A viscoplastic constitutive theory developed by using this approach is shown below for the case of transversely isotropic materials (Robinson et al., 1987). This form of directionality was incorporated into the theory by specifying a strong direction,  $d_i$ . This increased the number of invariants initially involved in the theoretical development to seven. This number subsequently, was reduced to three by tailoring the theory to match assumed material response. The strength of the continuum mechanics approach is that it makes use of more than three decades of progress in the field of viscoplasticity. This almost assures that the theory will prove successful in predicting time dependence and history dependence in composite structures involving a single strong direction. Whether the theory can be extended to predict the response of complex composite structures is open to question.

$$\text{FLOW LAW: } \dot{\epsilon}_{ij}^p = f(F) \Gamma_{ij}$$

$$\text{EVOLUTIONARY LAW: } \dot{\alpha}_{ij} = h(G) \dot{\epsilon}_{ij}^p - \gamma(G) \pi_{ij}$$

WHERE

$f(F)$ ,  $h(G)$ , AND  $\gamma(G)$  ARE MATERIAL FUNCTIONS, AND

$$F = \frac{1}{K_T^2} \left[ I_1 + \frac{I_2}{\eta^2} + \frac{9}{4(4\omega^2 - 1)} I_3 \right] - 1$$

$$\Gamma_{ij} = \Sigma_{ij} - \xi [d_k d_j \Sigma_{jk} + d_j d_k \Sigma_{ki} - 2I_0 d_i d_j] - \frac{1}{2} \zeta I_0 (3d_i d_j - \delta_{ij})$$

$$G = \frac{1}{K_T^2} \left[ I_1' + \frac{I_2'}{\eta'^2} + \frac{9}{4(4\omega'^2 - 1)} I_3' \right]$$

CD-88-33314

$$\pi_{ij} = a_{ij} - \xi [d_k d_j a_{jk} + d_j d_k a_{ki} - 2I_0' d_i d_j] - \frac{1}{2} \zeta I_0' (3d_i d_j - \delta_{ij})$$

$$\xi = \frac{\eta^2 - 1}{\eta^2} \quad \zeta = \frac{4(\omega^2 - 1)}{4\omega^2 - 1}$$

$$\eta = K_L/K_T \quad \omega = Y_L/Y_T$$

$$I_1 = J_2 - I + \frac{1}{4} I_3 \quad I_2 = I - I_3$$

$$I_3 = (I_0)^2 \quad J_2 = \frac{1}{2} \Sigma_{ij} \Sigma_{ij}$$

$$I = d_i d_j \Sigma_{jk} \Sigma_{ki} \quad I_0 = d_i d_j \Sigma_{ij}$$

NOTE THAT THE PRIMED INVARIANTS IN  $G$  AND  $\pi_{ij}$  ARE OBTAINED BY REPLACING  $\Sigma_{ij}$  BY  $a_{ij}$  IN THE ABOVE EXPRESSIONS.

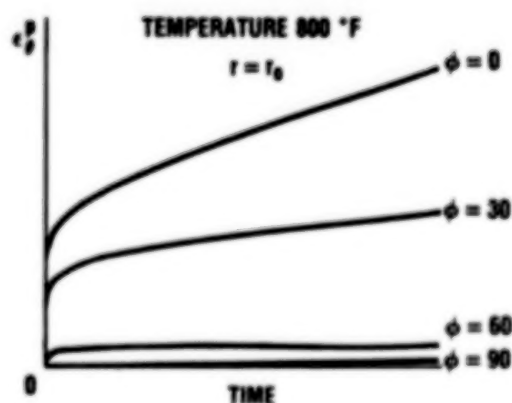
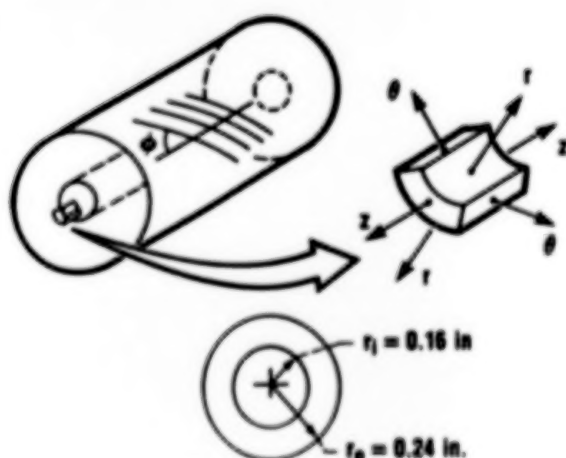
CD-88-33315

# IMPLEMENTATION OF THE VISCOPLASTIC CONSTITUTIVE THEORY FOR TRANSVERSELY ISOTROPIC MATERIALS IN THE MARC FINITE ELEMENT CODE

The subject viscoplastic model has been implemented in the MARC finite element code and exercised in a number of trial calculations (Arya, 1987). The material properties used in these calculations were similar to those of a metal matrix composite material, tungsten-copper, at about 800 °F. Initially, the analyses were limited to uniaxial stress states. Under these conditions, it was shown that the model can treat cyclic plasticity, rate dependence, and creep for a range of fiber orientations. More recently, a thick-walled cylinder was analyzed to determine performance in calculations involving multiaxial stress states. As indicated below, the theory was successful in predicting creep-like behavior which was highly dependent on fiber orientation. For example, creep in the hoop direction can be seen to be negligible for the case of  $\phi = 90^\circ$ .

THE SUBJECT CONSTITUTIVE THEORY HAS BEEN IMPLEMENTED IN THE MARC FINITE ELEMENT CODE AND USED TO ANALYZE A THICK-WALLED CYLINDER WITH A RANGE OF FIBER ORIENTATIONS ( $\phi$ )

WHEN LOADED UNDER INTERNAL PRESSURE,  $\approx 4000$  psi, THE MATERIAL EXHIBED CREEP-LIKE BEHAVIOR WHICH WAS HIGHLY DEPENDENT ON FIBER ORIENTATION



CD-88-33316



#### REFERENCES

- Arya, V.K., 1987, "Finite Element Implementation of Viscoplastic Models," Turbine Engine Hot Section Technology 1987, NASA CP-2493, pp. 335-348.
- Battiste, R.L., and Ball S.J., 1986, "Determination of Surfaces of Constant Inelastic Strain Rate at Elevated Temperature," Turbine Engine Hot Section Technology 1986, NASA CP-2444, pp. 307-325.
- Ellis, J.R., 1985, "An Experimental Study of Biaxial Yield in Modified 9Cr-1Mo Steel at Room Temperature," NASA CR-175012.
- Ellis, J.R., 1983, "A Multiaxial Extensometer for Measuring Axial, Torsional, and Diametral Strains at Elevated Temperature," ORNL- TM-8760.
- Freed, A.D., 1988, "Structure of a Viscoplastic Theory," NASA TM-100794.
- Robinson, D.N., Duffy, S.F., and Ellis, J.R., 1987, "A Viscoplastic Constitutive Theory for Metal Matrix Composites at High Temperature," Thermal Stress, Material Deformation and Thermo-Mechanical Fatigue, ASME PVP 123, H. Sehitoglu and S.Y. Zamrik, eds., ASME, pp. 49-56.



# UNIFIED CONSTITUTIVE MODEL DEVELOPMENT FOR METAL MATRIX COMPOSITES AT HIGH TEMPERATURE

D.N. Robinson\*  
University of Akron  
Akron, Ohio

## INTRODUCTION

Structural alloys used in high temperature applications exhibit complex thermo-mechanical behavior that is time-dependent and hereditary. Recent attention is being focused on metal-matrix composite materials for high-temperature applications (e.g., in aerospace) where they exhibit all the complexities of conventional alloys (creep, relaxation, recovery, rate sensitivity, etc.) and their strong anisotropy adds further complexities.

A unified continuum theory is being developed for representing the high-temperature deformation behavior of metallic composites that can be idealized as pseudohomogeneous continua with locally definable directional characteristics. Treatment of textured materials (molecular, granular, and fibrous) as pseudohomogeneous and the applicability of continuum mechanics depend relatively upon characteristic structural dimensions, the severity of gradients (stress, temperature, etc.), and the size of the internal structure (cell size) of the material. The appropriate conditions are met in a sufficiently large class of anticipated aerospace applications of metallic composites to justify research into the formulation of continuum based theories.

The point of view taken in this research is that the composite is a material in its own right, with its own properties, and that these properties can be measured and specified. Experiments for this purpose are discussed by Robinson et al. (1987). This viewpoint is aimed at satisfying the design engineer who needs reasonably simple methods of structural analysis to predict deformation behavior, particularly at high temperatures where material response is enormously complex. Indeed, the prediction of component lifetime depends critically on the accurate prediction of deformation behavior.

Here, a proven constitutive model for isotropic materials in which the inelastic strain rate and internal state are expressible as gradients of a dissipation potential is taken to depend on invariants that reflect local transverse isotropy. Applications (Arya, 1988; and Arya and Robinson, 1988) illustrate the capability of the theory of representing the time-dependent, hereditary, anisotropic behavior typical of these materials at high temperature.

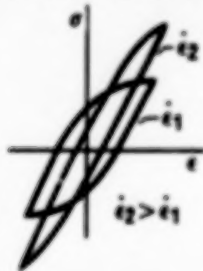
---

\*Work performed on-site at for the Structural Mechanics Branch under NASA grant NAG3-379 (monitor: R.L. Thompson).

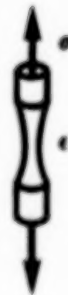
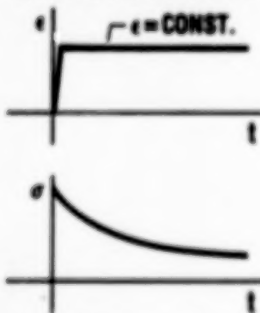
## HIGH-TEMPERATURE BEHAVIOR OF COMPOSITE CONSTITUENTS

Metals used as constituents of composite materials exhibit all of the high-temperature behavioral complexities of metals used conventionally. Intense effort has been devoted over the past decade (e.g., NASA's HOST Project) in understanding and representing such behavior.

### STRAIN-RATE DEPENDENCE

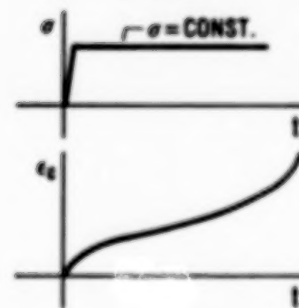


### STRESS RELAXATION

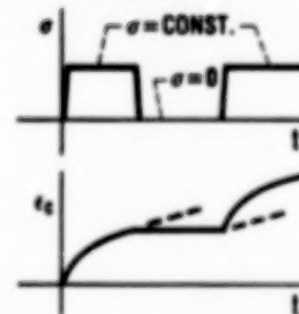


ETC.

### CREEP



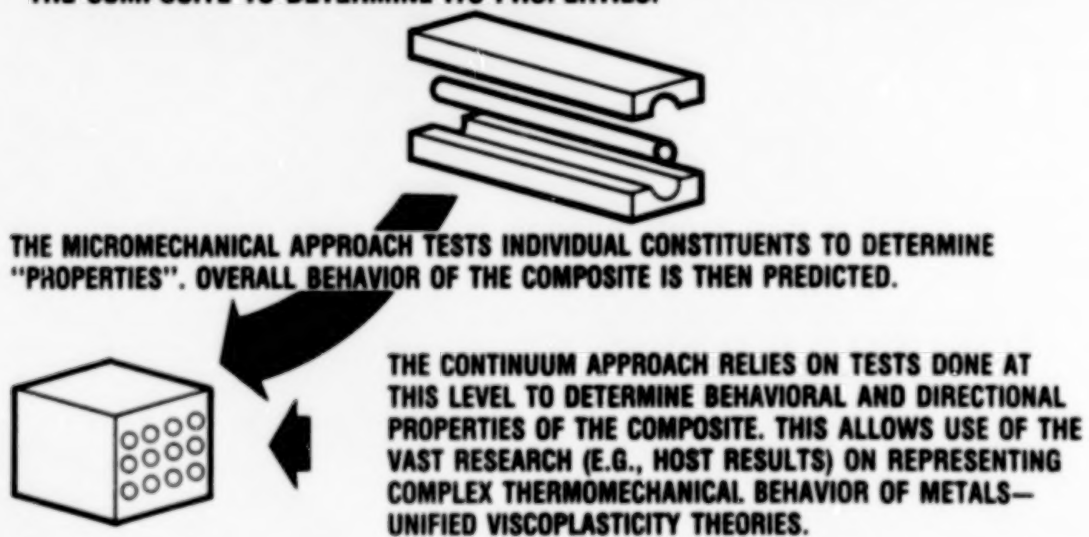
### RECOVERY



CD-88-32718

## MICROMECHANICS AND MACROMECHANICS APPROACHES TO COMPOSITES

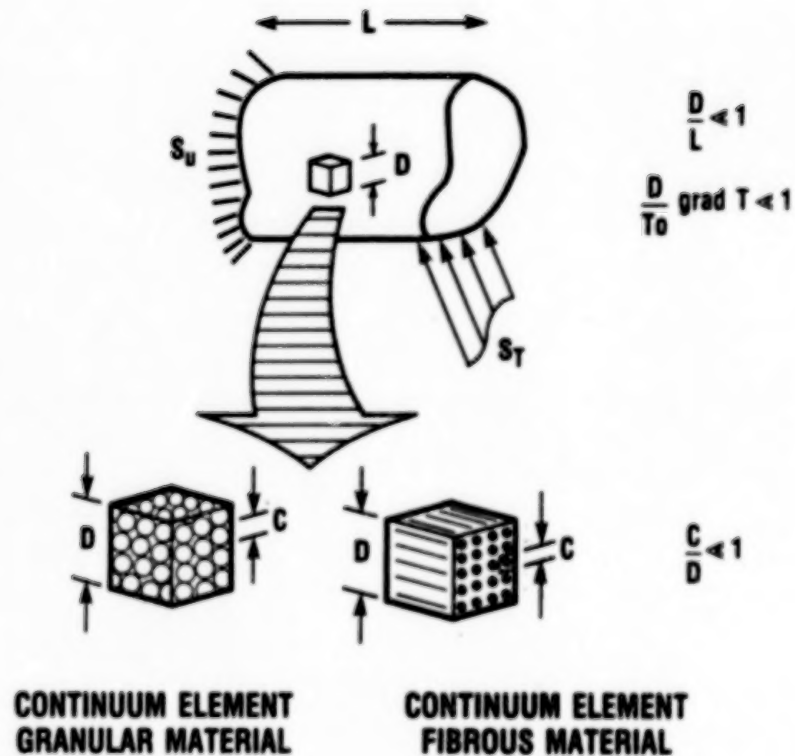
WITH ONE OR BOTH CONSTITUENTS OF THE COMPOSITE BEHAVING AS IN FIG. 1, MICROMECHANICS HAS DIFFICULTY PREDICTING OVERALL BEHAVIOR. THE MACROMECHANICS OR CONTINUUM APPROACH VIEWS THE COMPOSITE AS A MATERIAL (PSEUDOHOMOGENEOUS, ANISOTROPIC). TESTS ARE CONDUCTED ON THE COMPOSITE TO DETERMINE ITS PROPERTIES.



CD-88-32719

# APPLICABILITY OF CONTINUUM CONCEPTS

The application of continuum theories to structured materials requires identification of a continuum element  $D$  that is small compared with characteristic structural dimensions and gradients, but large compared with cell size dimensions.



CO-88-32720

## EXTENSION OF UNIFIED THEORIES TO COMPOSITES

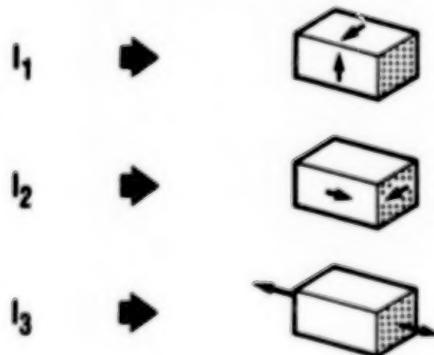
Unified viscoplasticity theories appropriate for isotropic metals are modified for metallic composites by taking advantage of well-established disciplines (mathematical invariant theory) and the wealth of research conducted over the past decade (e.g., HOST, etc.).

Familiar quantities in isotropic representations such as effective stress get replaced by effective stress measures involving other invariants that reflect the appropriate directional properties of the composite.

$$\bar{\sigma} = \sqrt{J_2}$$

WHERE  $J_2$  = SECOND PRINCIPAL INVARIANT OF DEVIATORIC STRESS.

$$\bar{\sigma} = \sqrt{I_1 + \alpha I_2 + \beta I_3}$$

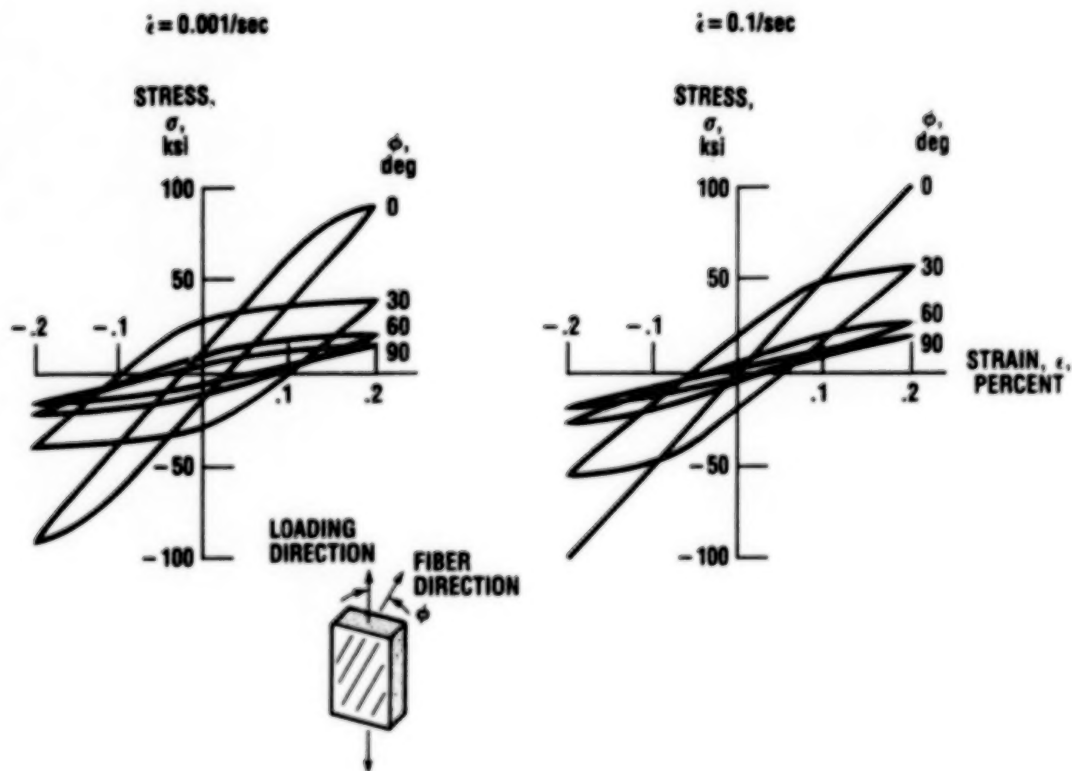


CD-88-32721

## STRAIN RATE DEPENDENCE IN METALLIC COMPOSITES

Continuum deformation theories for metallic composites are readily implemented into existing structural analysis codes. The present theory has been implemented into MARC (Arya, 1988) and several uniaxial and multiaxial structural analyses have been performed.

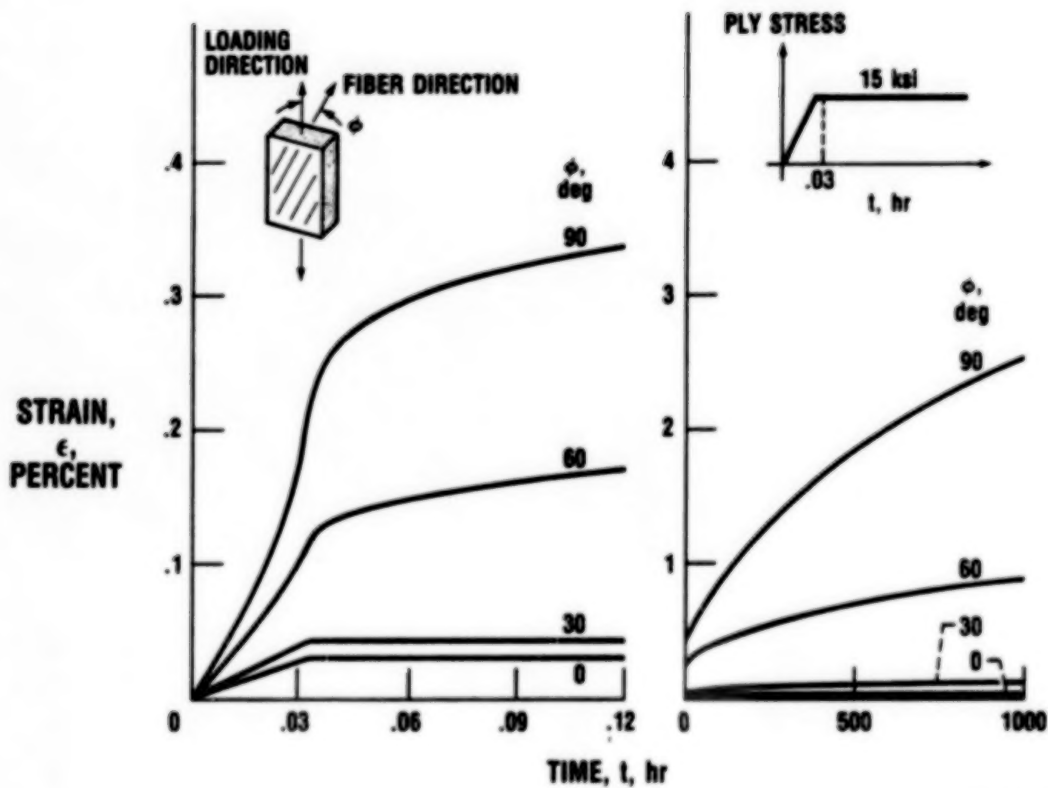
Predictions of uniaxial constant-strain-range - constant-strain-rate cycling show the expected directional features and the appropriate strain-rate dependence.



CD-88-32722

## CREEP OF METALLIC COMPOSITES

The same model (no change in material constants) predicts the correct qualitative features of creep and relaxation observed in metallic composites. See Arya (1988) for other uniaxial and multiaxial predictions.



CD-88-32723

#### REFERENCES

- Arya, V.K., 1988, "Finite Element (MARC) Solution Technologies For Viscoplastic Analyses," Lewis Structures Technology '88, NASA Lewis Research Center, May 24-25.
- Robinson, D.N., Duffy, S.F., and Ellis, J.R., 1987, "A Viscoplastic Constitutive Theory for Metal Matrix Composites at High Temperature," Thermal Stress. Material Deformation and Thermo-Mechanical Fatigue, ed. Sehitoglu, Zamrik, ASME, Vol. 123.
- Robinson, D.N., and Duffy, S.F., 1988, "A Continuum Deformation Theory for Metal-Matrix Composites at High Temperature," submitted to J. of Mech. and Physics of Solids.



# UNIFIED CONSTITUTIVE MODEL FOR SINGLE CRYSTAL DEFORMATION BEHAVIOR WITH APPLICATIONS

K.P. Walker      Engineering Science Software, Inc. (Smithfield, RI)  
T.G. Meyer      Pratt & Whitney (East Hartford, CT)  
E.H. Jordan      University of Connecticut (Storrs, CT)

Single crystal materials are being used extensively in gas turbine airfoils and are candidates for other hot section components because of their increased temperature capabilities and resistance to thermal fatigue. Under many operating conditions, the thermal and mechanical loads are sufficiently severe to cause inelastic material behavior. It is widely recognized that design of such components for long fatigue life requires an accurate assessment of that inelastic behavior. However, no convenient inelastic material models are currently available for structural analysis of these anisotropic components.

Development of such a constitutive model for single crystal material has been undertaken recently in two NASA sponsored programs: Life Prediction and Constitutive Models for Engine Hot Section Anisotropic Materials (NAS3-23939) and Biaxial Constitutive Equation Development for Single Crystals (NAG3-512). A slip system based constitutive model for single crystal materials is now in its final stages of development. The model has been fit to a large body of constitutive data for single crystal PWA 1480 material and will also be tested against data for a second single crystal material. The model uses a unified approach for computing total inelastic strains (creep plus plasticity) on crystallographic slip systems reproducing observed directional and strain rate effects as a natural consequence of the summed slip system quantities. The model includes several of the effects that have been reported to influence deformation in single crystal materials. These include the contributions from slip system stresses other than the Schmid shear stress, latent hardening due to simultaneous straining on all slip systems, and cross-slip from the octahedral to the cube slip systems. The model is operational in a commercial Finite Element code and is being installed in a Boundary Element Method code.

---

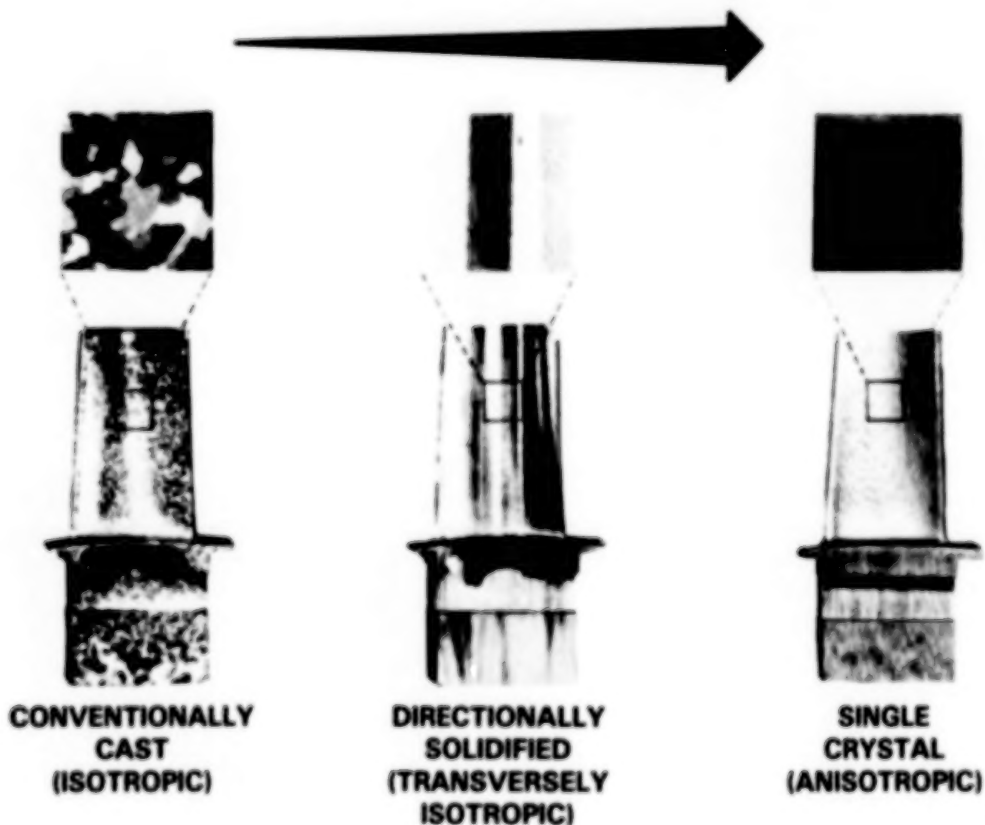
Contract: NAS3-23939

Grant: NAG3-512

NASA LeRC Technical Monitors: Drs. G.R. Halford and R.L. Thompson

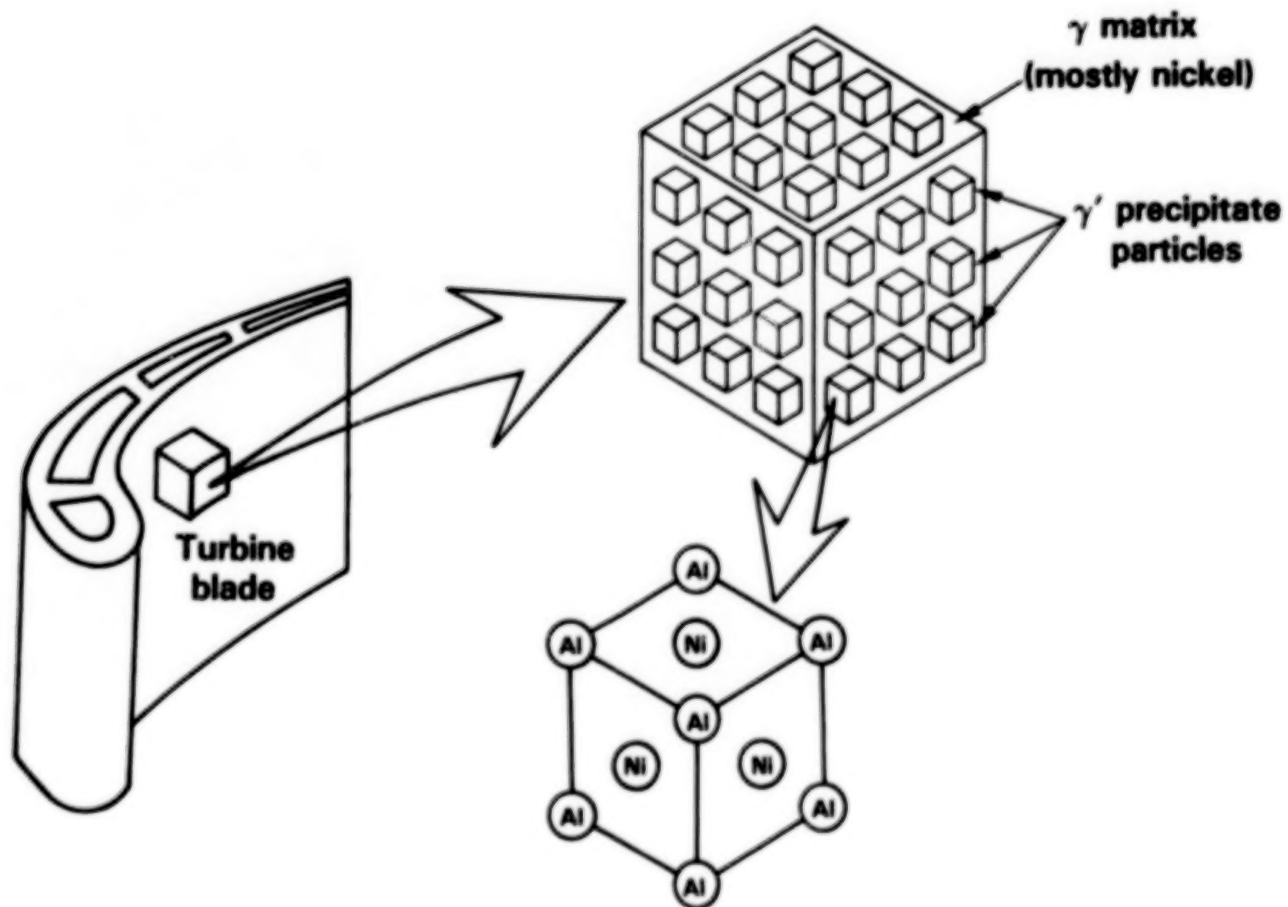
## **ADVANCES IN TURBINE AIRFOIL MATERIALS HAVE RESULTED IN HIGHER STRENGTH AND INCREASED DURABILITY**

One of the more important recent developments in gas turbine blade materials has been the introduction of directionally solidified and single crystal castings. Among the advantages of these new materials is an increased creep and oxidation resistance which results from the elimination of grain boundaries. In addition, the elimination of grain boundary strengthening elements in single crystal material results in higher melting temperature and permits greater flexibility in achieving optimum heat treatments. The low elastic modulus in the growth direction also improves the fatigue life by reducing the thermally induced stresses.



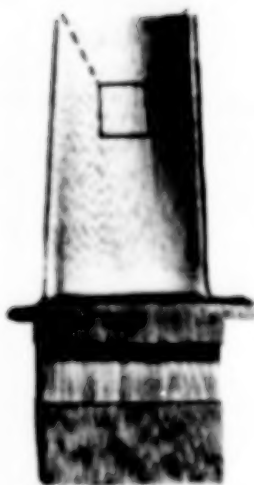
## NICKEL BASE SINGLE CRYSTAL SUPERALLOYS HAVE A FACE CENTERED CUBIC CRYSTALLINE STRUCTURE

The single crystal material being used in the current effort is PWA 1480. It is a two phase Nickel based superalloy having a Face Centered Cubic atomic arrangement in both the  $\gamma$  matrix (mostly Nickel) and the  $\gamma'$  strengthening phase. The cuboidal  $\gamma'$  is arranged in a regular array in the matrix material. It is well known that this material deforms by slip on specific crystallographic planes. This fact has been used in developing a constitutive model for PWA 1480.

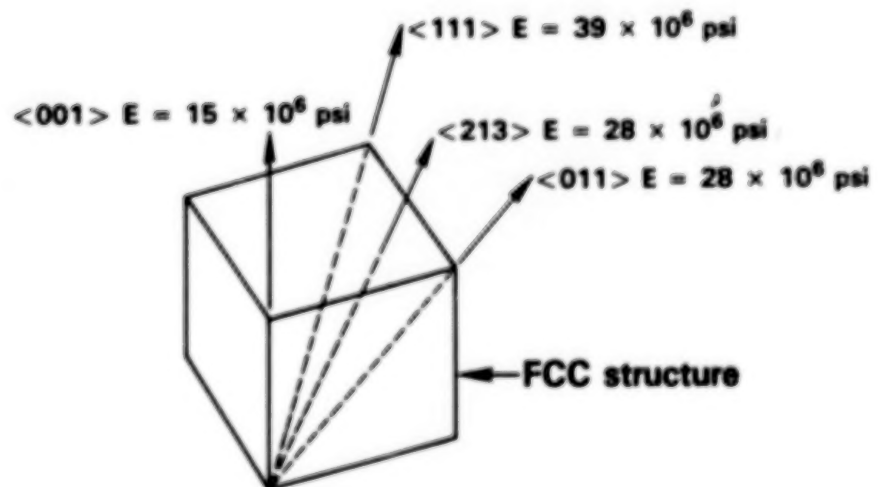


## SINGLE CRYSTAL COMPONENT PROPERTIES ARE HIGHLY DIRECTIONAL (ANISOTROPIC)

A key factor in the design and behavior of columnar grained and single crystal material is the variation of material properties with respect to the natural material axes. For example, in PWA 1480 at 1200F, Young's Modulus obtained from a tensile bar oriented along one of the material's cubic axes ( $\langle 001 \rangle$  Miller index) is approximately 15 Msi while the value in the cube diagonal direction ( $\langle 111 \rangle$  Miller index) is approximately 39 Msi.



Single crystal

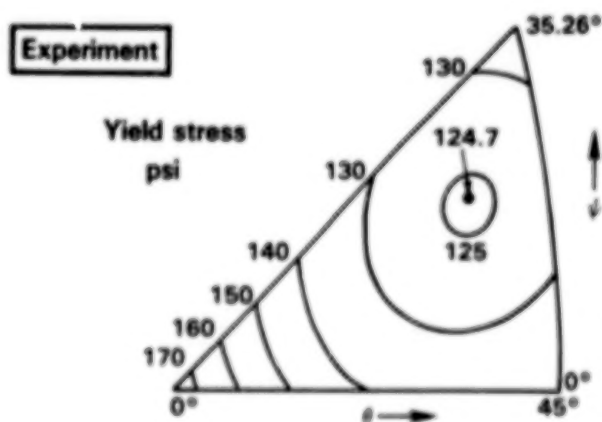
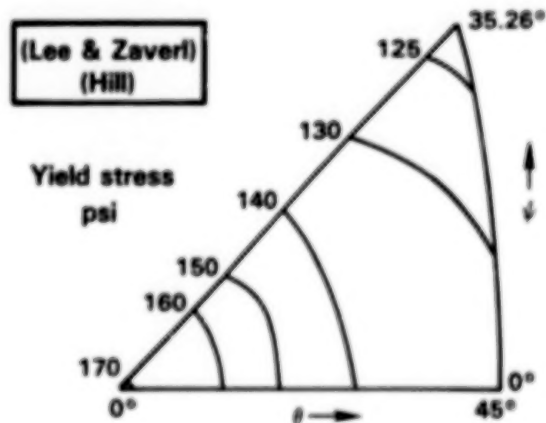
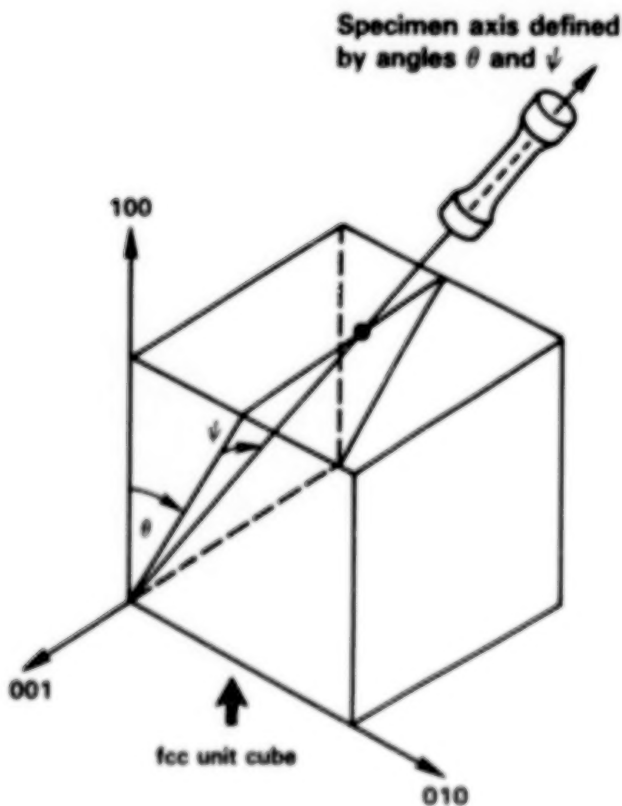


Young's modulus varies by almost a  
factor of 3 with direction

## CLASSICAL MODELS GIVE POOR PREDICTIONS OF YIELD STRESS VARIATION WITH ORIENTATION

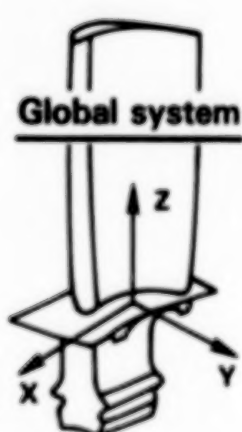
While these elastic property variations are correctly predicted with most current structural analysis tools, the prediction of creep and plastic behavior, which is often required for durability assessment, is not easily accomplished. For example, the classical yield models of Lee & Zaverl (1978) and Hill (1948) would predict the yield stress to decrease continually from a maximum along the  $\langle 001 \rangle$  axis to a minimum along the  $\langle 111 \rangle$  direction. But experiment has shown that the yield strength has a minimum for an orientation in the middle of the stereographic projection. Furthermore, it is now recognized that the classical approach of separately calculating creep and plastic strains is difficult to apply in the structural analysis of components that operate in transient thermal and mechanical environments.

The constitutive model developed in the current effort attempts to incorporate metallurgical observations regarding the deformation of single crystals in a unified viscoplastic formulation. Inelastic strains (accounting for "plasticity" and "creep" simultaneously) are computed on crystallographic slip systems. The model thus achieves the required directional properties as a natural consequence of summing the slip system stresses and strains.

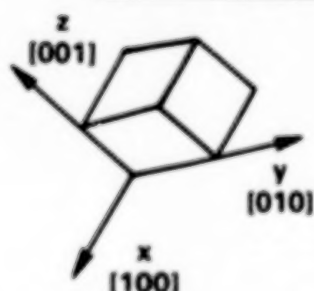


# CRYSTALLOGRAPHIC SLIP FORMULATION

The model has been formulated to use stresses and strains referred to any geometric or "global" coordinate system which may be convenient for the structural analysis of a component. As with any analysis involving an anisotropic material, the relative orientation of the global and material axes are also required. The model then transforms the global stresses and strains onto a crystal coordinate system. These crystal system quantities are subsequently resolved onto each of twelve octahedral and six cube slip systems. The Schmid shear stress on each system is used to calculate the inelastic shear stress on that system. Provision has been made in the model to include the effect of all six components of slip system stress.

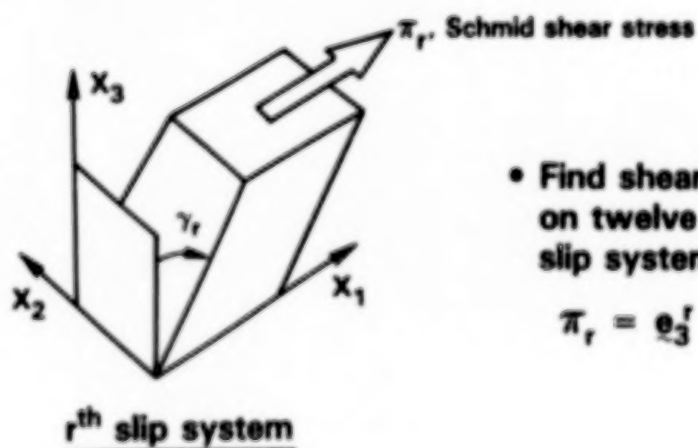
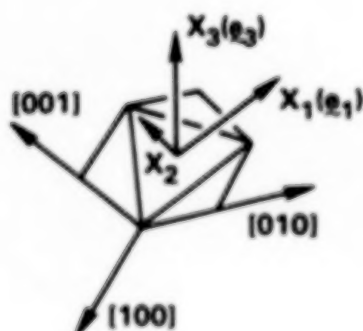


## Crystal system



- Find stress in crystal system,  $x, y, z$

$$[\underline{\sigma}] = \begin{pmatrix} \sigma_{xx} & \sigma_{xy} & \sigma_{xz} \\ \sigma_{xy} & \sigma_{yy} & \sigma_{yz} \\ \sigma_{xz} & \sigma_{yz} & \sigma_{zz} \end{pmatrix}$$



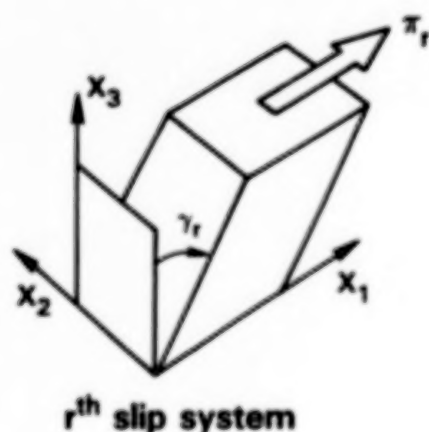
- Find shear stress on twelve octahedral slip system

$$\pi_r = \underline{e}_3^r \cdot \underline{\sigma} \cdot \underline{e}_1^r$$



## CRYSTALLOGRAPHIC SLIP FORMULATION

The general form of the equations governing the inelastic strain on each slip system is shown below. The form is the familiar viscoplastic equation employing two state variables (Walker 1981). The rate of change of the slip system inelastic shear strain is a function of the applied slip system shear stress, an internal back stress, and a drag stress. The back stress and the drag stress each evolve with inelastic strains. An inelastic shear strain rate is calculated in each slip system's coordinate axes and transformed to the common crystal coordinate system where they are summed to obtain a combined inelastic strain rate. Once this inelastic strain rate is known, the rate of change of stress is easily obtained using the known total strain rate and the stiffness matrix. Finally, the stress rate is transformed onto the global coordinate system.



$$\dot{\gamma}_r = \left| \frac{\pi_r - \omega_r}{K_r} \right|^{p-1} \left( \frac{\pi_r - \omega_r}{K_r} \right)$$

Equilibrium stress  
 Drag stress

$\Rightarrow$  Evolution equations for  $\dot{\omega}_r$  and  $K_r$

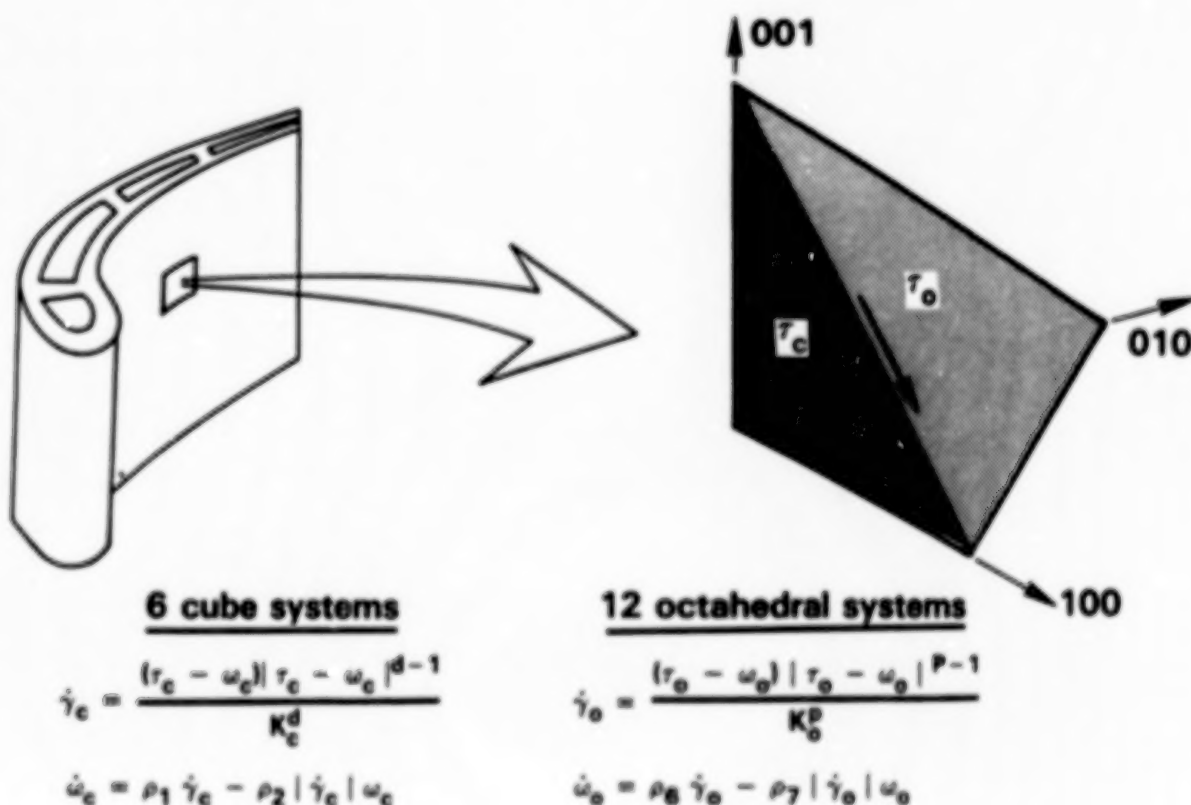
$$\dot{\epsilon}_{ij}^{(p)} = \begin{pmatrix} 0 & 0 & \dot{\gamma}_{r/2} \\ 0 & 0 & 0 \\ \dot{\gamma}_{r/2} & 0 & 0 \end{pmatrix} \Rightarrow \text{Crystal system} \Rightarrow \dot{\epsilon}_{kl}^{(p)} = (Q_{kl}^T)_r \dot{\epsilon}_{ij}^{(p)} (Q_{jl})_r$$

$$\dot{\sigma}_{ij} = D_{ijkl} \left\{ \dot{\epsilon}_{kl} - \sum_{r=1}^{12} (\dot{\epsilon}_{kl}^{(p)})_r^{\text{oct}} - \sum_{r=1}^6 (\dot{\epsilon}_{kl}^{(p)})_r^{\text{cube}} \right\}$$

$$\text{Global system } \dot{\sigma}_{ij} = R_{ik}^T \dot{\sigma}_{kl} R_{lj}$$

## CONSTITUTIVE MODEL EMPLOYS VISCOPLASTIC EQUATIONS ON OBSERVED MATERIAL SLIP PLANES

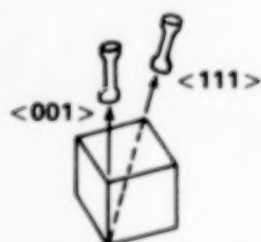
The viscoplastic model constants for the octahedral and cube slip systems are not the same. The figure below shows the terms in the evolution equation that were found to be active for the PWA1480 data base. The full model however includes thermal recovery terms in the back stress rate equation and an evolutionary equation for the drag stress which includes latent hardening among like slip systems and cross hardening between the cube and octahedral systems. Details of the mathematical formulation can be found in the reports by Walker and Jordan (1985) and Swanson et. al. (1987).



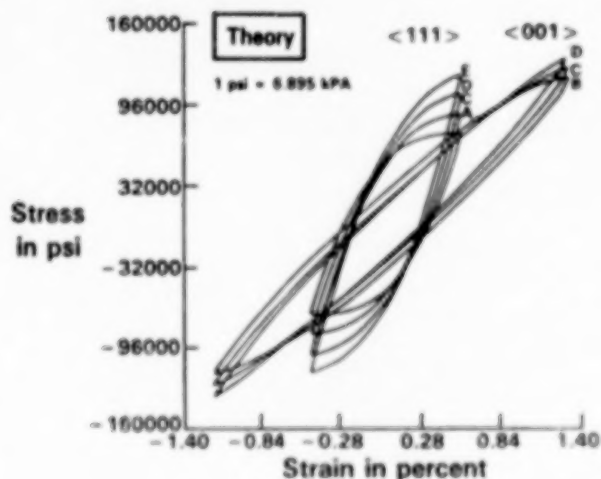
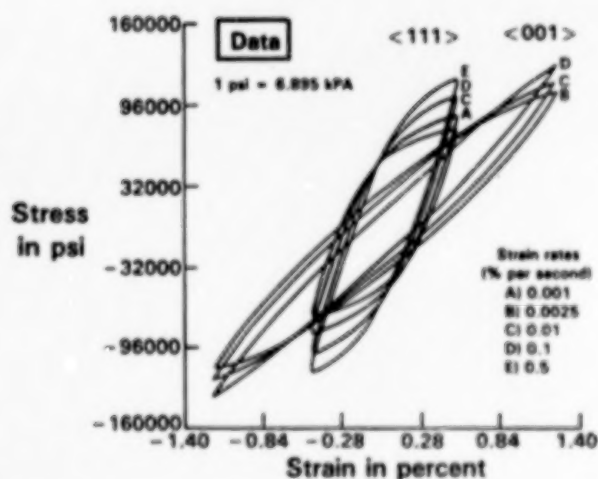


# SINGLE CRYSTAL CONSTITUTIVE MODEL BASED ON CRYSTALLOGRAPHIC SLIP THEORY CAPTURES THE OBSERVED ORIENTATION AND RATE DEPENDENT DEFORMATION BEHAVIOR

A large body of uniaxial cyclic stress - strain data has been obtained from temperatures of 800F to 2100F using specimens oriented in the  $\langle 001 \rangle$ ,  $\langle 111 \rangle$ ,  $\langle 011 \rangle$  and  $\langle 123 \rangle$  directions (Swanson et. al. 1978). Additional torsional stress - strain data has also been obtained (Jordan and Walker, 1985). Strain rates were varied over four orders of magnitude from 1% per sec. to .0001% per sec. The figure below is typical of the correlation with experiment. The slip system based model captures the orientation and rate dependence quite well.

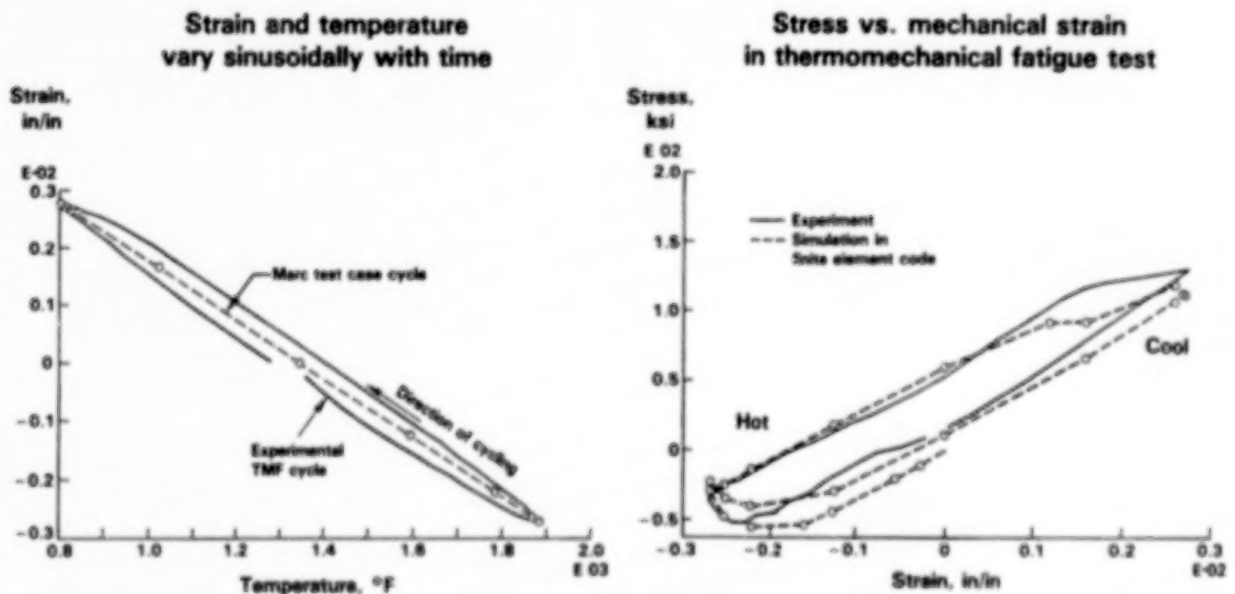


1600°F steady state cyclic hysteresis loops



# SLIP BASED CRYSTALLOGRAPHIC CONSTITUTIVE MODEL IS NOW BEING TESTED UNDER THERMOMECHANICAL LOADING CONDITIONS SIMILAR TO THOSE ENCOUNTERED IN SERVICE

The constitutive model has been formulated for use in non-isothermal analyses and is currently being evaluated against a body of thermomechanical loading tests as illustrated in the figure below. In this test cycle, the temperature and imposed strain are varied simultaneously while the stress is monitored. Good correlation has been achieved in the high temperature portion of the cycle. However too much inelasticity is predicted in the low temperature portion. Final adjustments to the model are now being undertaken to address the low temperature response.



# SINGLE CRYSTAL MODEL CAN EASILY BE INSTALLED AS A SUBROUTINE IN ANY NONLINEAR FINITE ELEMENT PROGRAM

The single crystal model is now operational in the MARC finite element code and is being installed in the "BEST3D" boundary element code under NASA LeRC contract "Inelastic Analysis Methods for Hot Section Components", NAS3-23697. It is also operational in a nonlinear structural analysis code on the IBM PC-XT and is being installed on a 80386-WEITEK desktop/lap personal computer. As part of the current contract effort, the code will be demonstrated in a finite element analysis of a gas turbine hot section component. The constitutive model has been written to be compatible with any finite element code that uses the initial load vector approach for material nonlinearity.

- Start increment N; obtain  $\Delta u$  from previous increment; compute  $\Delta \epsilon = B \Delta u$  } Performed in FE program
- Enter constitutive subroutine and compute D and  $\Delta \zeta$  } Pass D and  $\Delta \zeta$  to FE program

$$\Delta \sigma = D(\Delta \epsilon - \alpha \Delta T) - \Delta \zeta(\Delta u)$$

Anisotropic elasticity matrix
Inelastic stress increment from single crystal model depends on  $\Delta u$

$$\left( \sum_V B^T D B dV \right) \Delta u = \Delta P + \sum_V B_T \left( \alpha \Delta T + \Delta \zeta(\Delta u) \right) dV$$

K = stiffness matrix
Applied load vector
Initial load vector

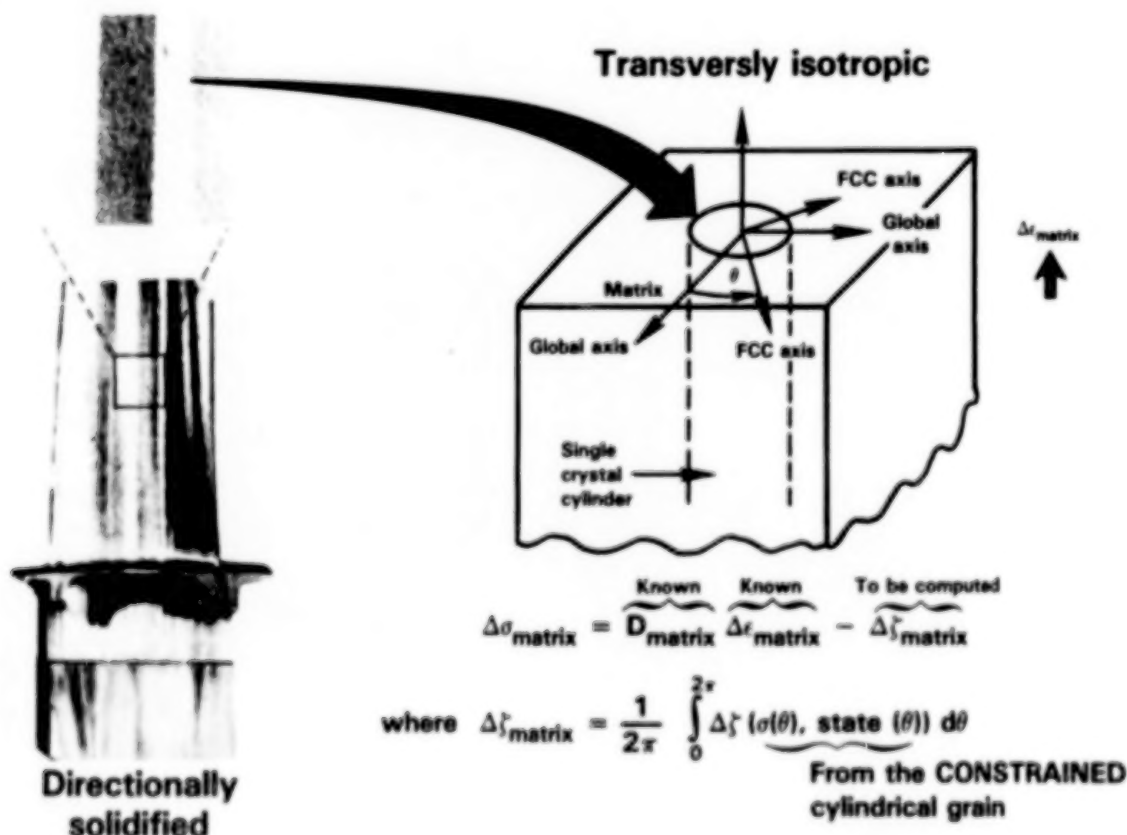
} FE program solves FE equilibrium equation for displacement increment  $\Delta u$

Iterate until solution  $\Delta u$  has converged

- Update solution and proceed to next increment, N + 1 } Performed in FE program

# THE SINGLE CRYSTAL CONSTITUTIVE RELATIONS CAN BE EXTENDED TO OTHER CLASSES OF MATERIAL BY MEANS OF SELF-CONSISTENT MODELS

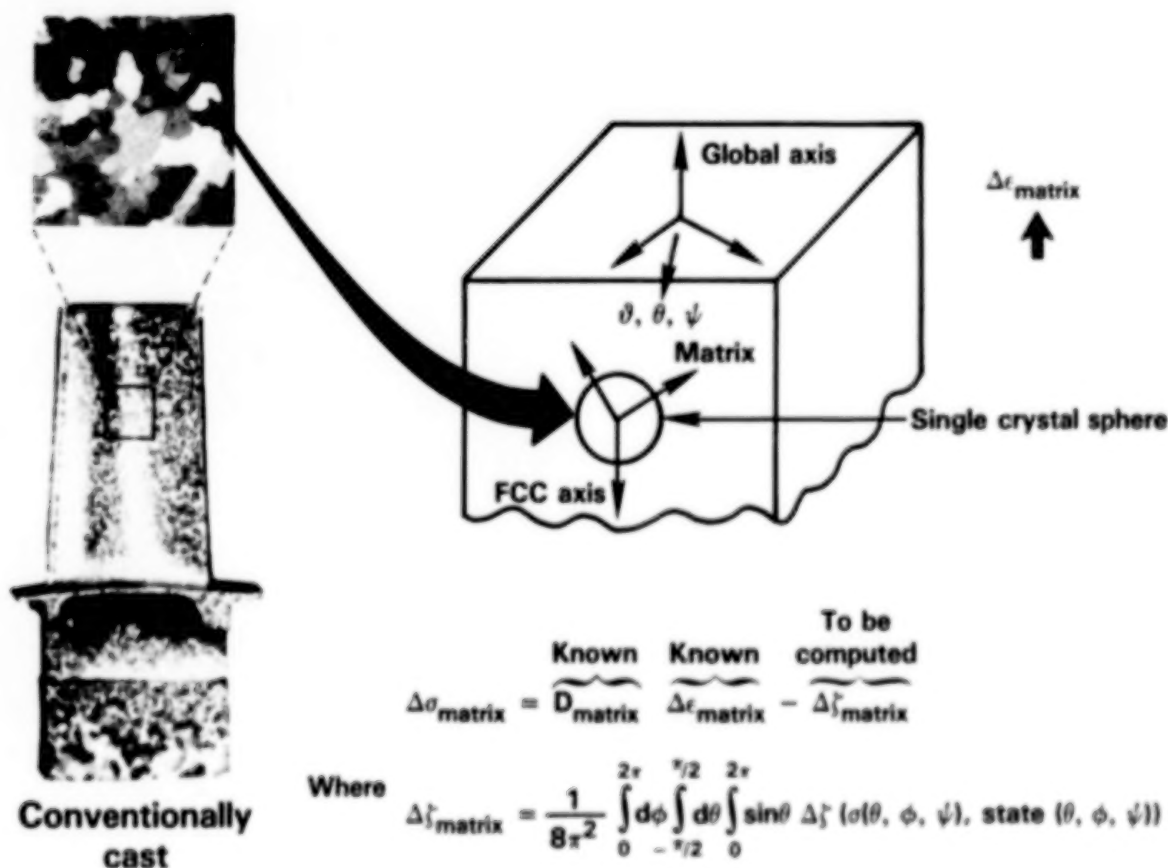
This slip system based model for single crystal material offers the opportunity to develop constitutive models for other classes of materials by means of self-consistent methods (Walker, 1984). Directionally solidified materials consist of aligned columnar single crystal grains which are oriented at random in the basal plane perpendicular to the solidification direction. This random orientation of grains produces a material with transversely isotropic properties. A self consistent method for modeling this material is achieved by surrounding a particular single crystal columnar grain with a transversely isotropic material. Using methods proposed by Eshelby (1957), the properties of the surrounding transversely isotropic material are found by averaging the properties of the single crystal grain which has been constrained by the surrounding material. The averaging is done about the axis of the columnar grain.



# EXTENSION OF THE SINGLE CRYSTAL CONSTITUTIVE RELATIONS TO ISOTROPIC MATERIALS BY MEANS OF A SELF CONSISTENT MODEL

Using a similar self consistent approach, it is possible to develop a constitutive model for isotropic materials. In this case the averaging in the constrained grain must be done with respect to all directions.

In both of these cases, transversely isotropic and isotropic, the slip system formulation developed in this effort can serve as the base model for the grains. Appropriate model constants for the particular material would of course be required and the influence of grain boundary sliding may require additional modeling.

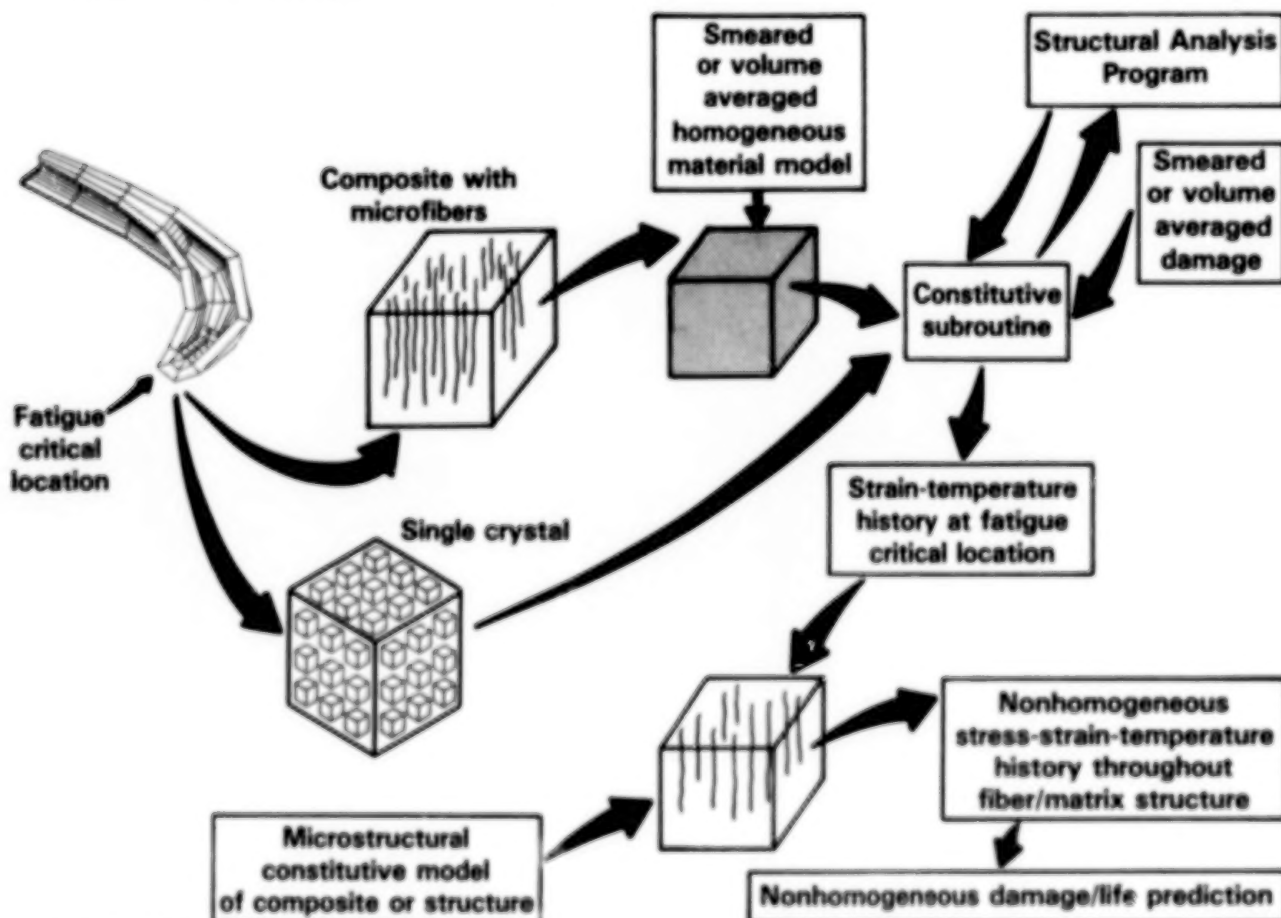




## WHAT IS THE CURRENT STATE OF OUR TECHNOLOGY?

The single crystal constitutive model developed in this effort represents an advance in the state of our technology for durability prediction. A structural analysis using the single crystal constitutive model can now be used to obtain a more accurate stress - strain response at the fatigue critical location of a component. These more accurate results can now be used to develop more accurate life models. Global stress and strain quantities as well as slip systems quantities are available from the model for life prediction.

A similar, although more complicated, approach is envisioned for composite materials. In these materials, the size scale of the material constituents relative to the overall composite structure prohibits modeling individual fibers and their surrounding matrix explicitly throughout the entire structure. Instead, a homogenized or "smeared" material model could be constructed for the bulk properties of the composite by assuming some periodicity of the fibers in the matrix and then volume averaging the constituent responses. This homogenized material model can then be used in the structural analysis program to obtain the overall composite structure's response. Damage models can be developed based on these "smeared" results directly or these results can be used as boundary conditions on a composite sub-element. The same constituent material models that were used to obtain the smeared material model can now be used to obtain local fiber/matrix stresses and strains in the sub-element.



LeRC LST'88

### References

Eshelby, J. D., "The Determination of the Elastic Field of an Ellipsoid Inclusion, and Related Problems," Proc. Royal Society of London, A241, p376, 1957.

Hill, R., "A Theory of the Yielding and Plastic Flow of Anisotropic Metals," Proc. Royal Society of London, Ser. A Vol. 193, pp. 281-297, 1948.

Jordan, E. H. and Walker, K. P., "Biaxial Constitutive Modeling and Testing of a Single Crystal Superalloy at Elevated Temperature," presented at the Second International Conference on Biaxial/Multiaxial Fatigue, Sheffield, England, December 1985. To appear in Fatigue and Fracture of Engineering Materials and Structures.

Lee, D., Zaverl, F. Jr., Shih, C. F., and German, M. D., "Plasticity Theories and Structural Analysis of Anisotropic Metals," Report No. 77CRD285, General Electric Corporate Research and Development Center, Schenectady, New York, 1977.

Swanson, G. A., I. Linask, D. M. Nissley, P. P. Norris, T. G. Meyer, and K. P. Walker, "Life Prediction and Constitutive Models for Engine Hot Section Anisotropic Materials Program, Annual Status Report, " Nasa CR-174952, February, 1986.

Walker, K. P., "Research and Development for Nonlinear Structural Modeling with Advanced Time-Temperature Dependent Constitutive Relationships," NASA CR-165533, November 1981.

Walker, K. P. and Jordan, E. H., "Constitutive Modeling of Superalloy Single Crystal and Directionally Solidified Materials," NASA CP-2369, pp 63 - 81, 1984.

Walker, K. P. and Jordan, E. H., "First Annual Report on NASA Grant NAG3-512," 1985.



BLANK PAGE

## **FINITE ELEMENT (MARC) SOLUTION TECHNOLOGIES FOR VISCOPLASTIC ANALYSES**

**V.K. Arya\* and Robert L. Thompson  
Structural Mechanics Branch  
NASA Lewis Research Center**

### **INTRODUCTION**

The drive for enhanced and improved performances of structural components operating at high temperatures, such as in aerospace and nuclear industries, has made a need for development of realistic constitutive models, accompanied by appropriate solution technologies for stress/life analyses of these components. The observed interaction between creep and plastic deformation at high temperatures has led to the development of a number of viscoplastic models. These models treat all inelastic strain as a single time-dependent quantity, and thus, automatically include creep, relaxation, and plasticity interactions.

Viscoplastic models provide a better description of inelastic behavior of materials, but their mathematical structure is very complex. The highly nonlinear and "stiff" nature of the constitutive equations makes analytical solutions difficult. It is, therefore, of the utmost importance that suitable solution (finite element or other numerical) technologies be developed to make these models adaptable for better and rational designs of components.

NASA Lewis has undertaken this important and challenging task. As a result of concerted efforts at Lewis during the last few years, several such solution technologies (in conjunction with the finite-element program, MARC, and other nonlinear structural analysis codes) have been developed and successfully applied to the solution of a number of uniaxial and multiaxial problems.

This paper describes some of these solution technologies and the models and presents representative results. The solution technologies developed and presented encompass a wide range of models, for example, isotropic, anisotropic, metal-matrix composites (with or without damage), and single-crystal (micromechanics) models.

It is believed that the solution technologies described herein will aid the designers and structural analysts in the stress/life analyses of components and will be exploited for better and rational component designs.

---

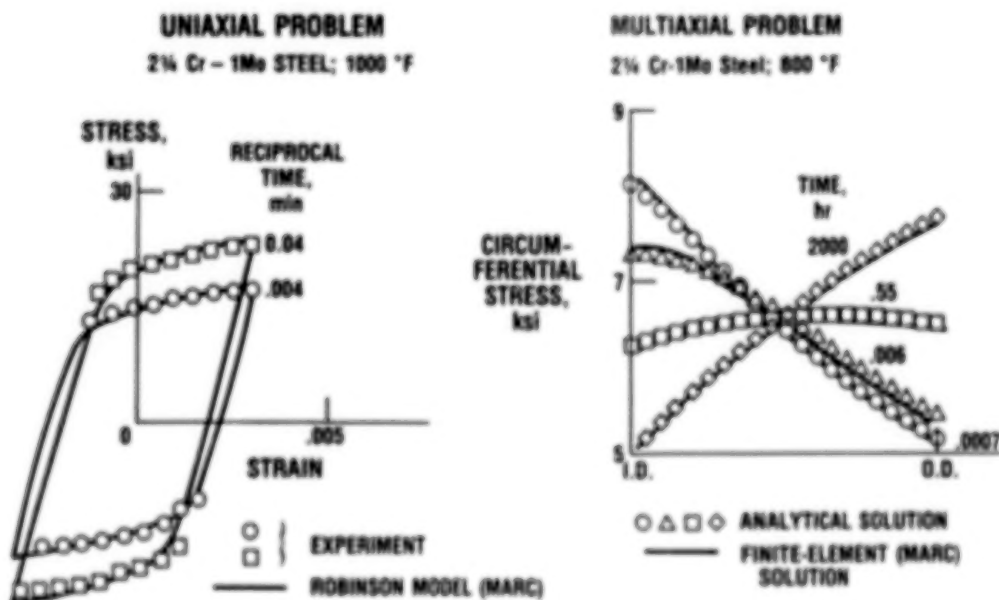
\*National Research Council - NASA Resident Associate.

## ROBINSON'S ISOTROPIC MODEL

The viscoplastic model developed by Robinson (Robinson and Swindeman, 1982) was implemented in the MARC general purpose, finite-element code (MARC Analysis Research Corp., 1983). Several uniaxial and multiaxial problems were solved to demonstrate the feasibility and applicability of the implementation as a useful structural analysis tool. Details of implementation are given by Cassenti (1983) and by Arya and Kaufman (1987). Two representative results are shown below.

A comparison of MARC and experimental hysteresis loops for the alloy 2½Cr-1Mo steel at two strain rates is presented in the left plot. Excellent agreement between the MARC and experimental loops confirms the correct finite-element implementation of the model.

The right side of the figure provides an example of application of the implementation to the multiaxial problem of a thick-walled cylinder of 2½Cr-1Mo steel under constant internal pressure at 800 °F. The circumferential stress redistribution in the cylinder after various periods of time is shown. The stresses were obtained using the finite-element implementation and a classical analytical solution. The good agreement between the two solutions indicates that the implementation can beneficially be utilized for other problems involving complex geometries and severe thermomechanical loadings.



CD-88-21897

CD-88-21892

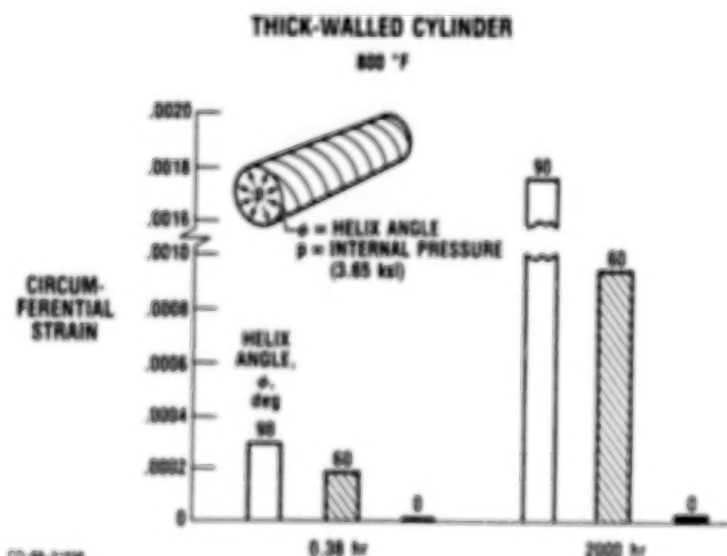
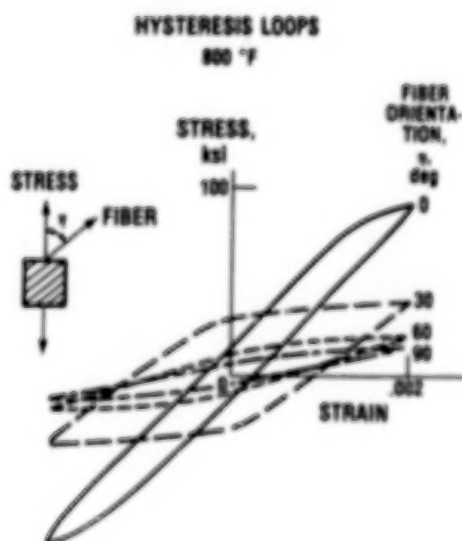
## ROBINSON'S METAL-MATRIX COMPOSITE (ANISOTROPIC) CONSTITUTIVE MODEL

Because of their lightweight and enhanced strength, the metal-matrix composite materials are attracting considerable attention for high-temperature applications. As a result of concerted and leading efforts in this direction at Lewis, a metal-matrix composite viscoplastic model has been developed by Robinson and Duffy (1988).

To provide the designers and structural analysts with a complete finite-element package for the stress-life analyses, the above-mentioned model was implemented in MARC by Arya (1987). Several uniaxial and multiaxial problems were analyzed.

The stress-strain hysteresis loops shown below for different fiber orientations of tungsten fiber in a copper matrix are at a strain rate of 0.001/min at 800 °F. The loops reveal a considerable strength dependence on the fiber-loading angle.

The circumferential strains at the inner radius of a thick-walled metal-matrix composite cylinder at different times and fiber orientations are shown below. The cylinder is subjected to an internal pressure. As expected, the creep (inelastic) resistance of the cylinder can be greatly increased by placing the fibers in the circumferential direction, perpendicular to its axis.



CD-88-2188

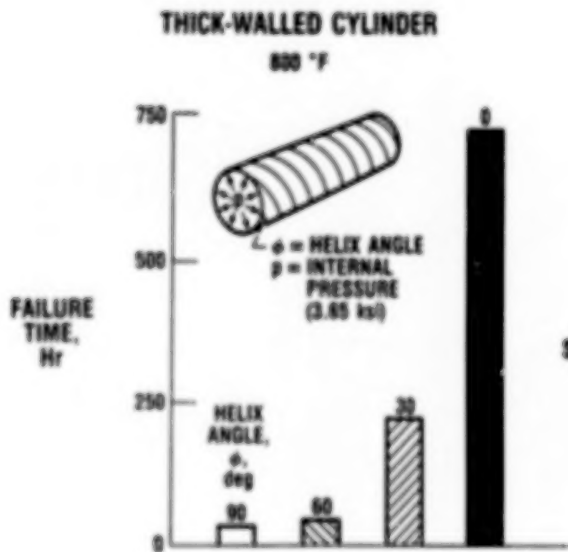
CD-88-2188

# ROBINSON'S METAL-MATRIX COMPOSITE VISCOPLASTIC DAMAGE MODEL

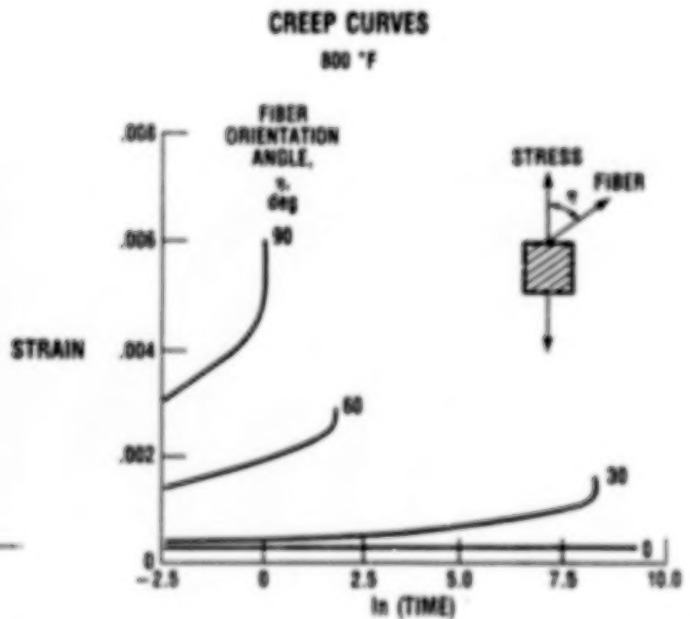
The concept of damage evolution has recently been included by Robinson (personal communication, 1988) in the metal-matrix composite model described in the preceding section. This unique model has been implemented successfully in the MARC code. Two representative solutions have been obtained using the implementation as shown below.

The creep curves for constant axial stress including damage are shown for four fiber orientations. As expected, the minimum creep occurs when the load is applied in a direction parallel to the fibers.

Also shown is the time-to-failure for a thick-walled, internally pressurized cylinder for the same fiber orientation angles. As expected, the life of the cylinder can substantially be increased by orientating the fibers in the circumferential direction.



CD-66-01024



CD-66-01025

## STOUFFER'S SINGLE-CRYSTAL CONSTITUTIVE MODEL

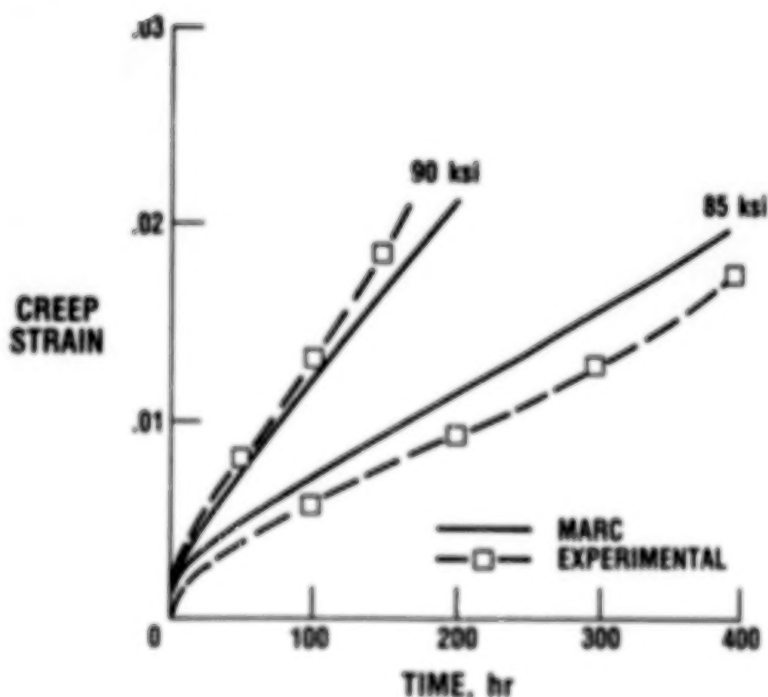
Conventionally cast polycrystalline superalloys, owing to the presence of grain boundaries, are susceptible to transverse grain boundary oxidation, corrosion and creep deformation, and subsequent cracking. The absence of grain boundaries in single-crystal alloys such as René-N4, MAR-M247, PWA 1480, has made them useful in gas turbine engines. A time-dependent, micromechanics, crystallographic viscoplastic model was developed by Stouffer (Dame and Stouffer, 1986) to characterize the inelastic behavior of single-crystal alloys.

To make the model applicable in the analysis and design of single-crystal components, it was implemented in the MARC code. Several uniaxial problems, including creep, relaxation, tensile, and cyclic loadings were analyzed.

A comparison is shown of MARC calculations and experimental creep curves at 1400 °F for the single-crystal alloy René-N4 in the direction [110]. The experimental values were taken from Stouffer (Dame and Stouffer, 1986). Good agreement is observed, which indicates the successful MARC implementation of the model.

A comparison of predictions and experimental uniaxial stress-strain hysteresis loops is also presented. The experimental values are again taken from Stouffer (Dame and Stouffer, 1986). Good agreement between MARC and experimental results encourages the use of this finite-element implementation for more complex loading conditions of more complex geometries.

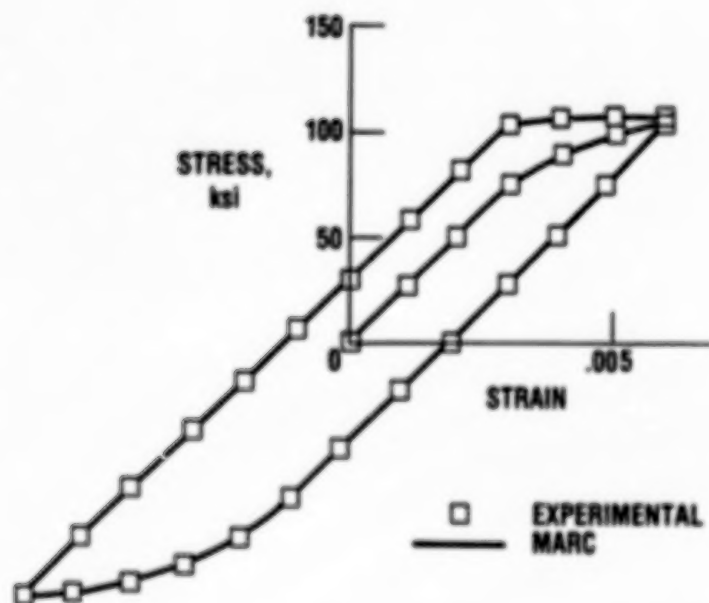
**CREEP CURVES**  
RENÉ-N4, [110], AT 1400 °F



CD-88-31796

# HYSTERESIS LOOP

RENÉ-N4, [110], AT 1400 °F



CD-68-31835



#### REFERENCES

- Arya, V.K., 1987, "Finite Element Implementation of Viscoplastic Models," Turbine Engine Hot Section Technology - 1987, NASA CP-2493.
- Arya, V.K., and Kaufman, A., 1987, "Finite Element Implementation of Robinson's Unified Viscoplastic Model and Its Application to Some Uniaxial and Multiaxial Problems," NASA TM 89891.
- Cassenti, B.N., 1983, "Research and Development Program for the Development of Advanced Time-Temperature Dependent Constitutive Relationships", (R830956077-1, -2, United Technologies Research Center; NASA Contract NAS3-23273), NASA CR-168191.
- Dame, L.T., and Stouffer, D.C., 1986, "Anisotropic Constitutive Model for Nickel Base Single Crystal Alloys, Development and Finite Element Implementation," NASA CR-175015.
- MARC Analysis Research Corp., 1983, "MARC General Purpose Finite Element Program," MARC Analysis Research Corp., Palo Alto, CA.
- Robinson, D.N., and Duffy, S.F., 1988, "A Continuum Deformation Theory for Metal-Matrix Composites at High Temperature," Journal of Mechanics and Physics of Solids.
- Robinson, D.N., and Swindeman, R.W., 1982, "Unified Creep-Plasticity Constitutive Equations for 2%Cr-1Mo Steel at Elevated Temperature," ORNL/TM-8444.

BLANK PAGE

## STRUCTURAL MECHANICS COMPUTER CODES

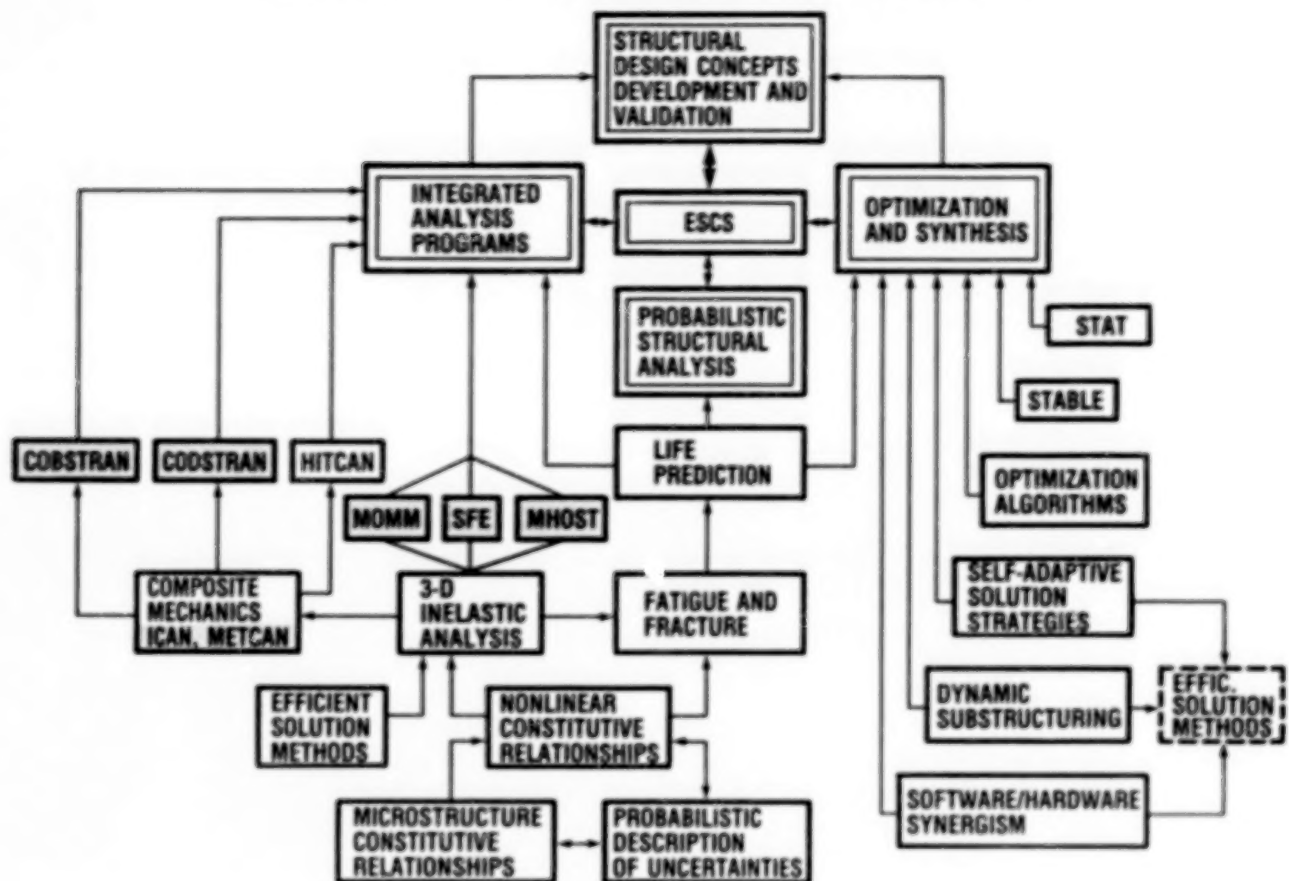
### SESSION OVERVIEW

Christos C. Chamis  
Structures Division  
NASA Lewis Research Center

The need for light, durable, fuel efficient, cost effective aircraft requires the development of engine structures which are flexible and are made from advanced materials (including composites). These engine structures must resist higher temperatures, maintain tighter clearances, and have lower maintenance costs. The formal quantification of any or several of these requires integrated computer programs (multilevel, multidiscipline analysis programs) for engine structural analysis/design. Several integrated analysis computer programs have been developed at Lewis Research Center over the past 10 years. These programs encompass four major disciplines: (1) composite mechanics and structures, (2) 3-D inelastic analyses, (3) probabilistic structural analysis, and (4) structural tailoring. In addition, the computer programs from these major disciplines are further integrated to form the engine structures computational simulator (ESCS) as is depicted near the top in the schematic.

The computer programs to be described in this session include (1) COBSTRAN - Composite Blade Structural Analysis, (2) ICAN - Integrated Composite Analyzer, (3) the MOMM code for approximate 3-D inelastic analysis, (4) speciality finite elements for 3-D inelastic analysis, (5) the MHOST mixed element code for 3-D inelastic analysis, (6) METCAN - Metal Matrix Composite Analyzer, and (7) CODSTRAN - Composite Durability Structural Analysis, which deals mainly with the computational simulation of composites fracture mechanics. The codes to be described are shaded in the schematic. Six of the codes (1 and 3 to 7) are described by full presentation, while one (2), ICAN, is described by an executive summary and the visual aids used in the poster presentation.

## STRUCTURAL MECHANICS COMPUTER CODES



CD-88-32624

## STRUCTURAL MECHANICS COMPUTER PROGRAMS

1. COBSTRAN—COMPOSITE BLADE STRUCTURAL ANALYSIS
2. ICAN—INTEGRATED COMPOSITE ANALYZER
3. MOMM CODE FOR APPROXIMATE 3-D INELASTIC ANALYSIS
4. SPECIALITY FINITE ELEMENTS FOR 3-D INELASTIC ANALYSIS
5. MHOST MIXED ELEMENT CODE FOR 3-D INELASTIC ANALYSIS
6. METCAN—METAL MATRIX COMPOSITE ANALYZER
7. CODSTRAN—COMPOSITE DURABILITY STRUCTURAL ANALYSIS

CD-88-32625

## THE COMPOSITE BLADE STRUCTURAL ANALYZER (COBSTRAN)

Robert A. Aiello  
Structural Mechanics Branch  
NASA Lewis Research Center

### ABSTRACT

The use and application of the COBSTRAN (COmposite Blade STRuctural ANalyzer) computer code is presented. COBSTRAN was developed at the NASA Lewis Research Center and is currently being used for the design and analysis of aircraft engine ducted and unducted fan blades. The features of COBSTRAN are demonstrated for the modeling and analysis of a scaled-down wind tunnel model propfan blade made from fiber composites. Comparison of analytical and experimental mode shapes and frequencies are shown, verifying the model development and analysis techniques used. The methodologies and programs developed for this analysis are directly applicable to other propfan blades.

#### TURBOPROP INSTALLATION IN LEWIS RESEARCH CENTER WIND TUNNEL

An advanced turboprop is shown installed for testing in the NASA Lewis Research Center 8 Foot by 6 Foot Transonic Wind Tunnel. This turboprop is 2 ft in diameter with blades swept back at an angle of  $60^\circ$  measured tangent to the leading edge at three-quarter span. The individual blades are twisted about the spanwise axis, swept aft, and curved about the axis of rotation. The blades shown are made of titanium and were tested at speeds up to approximately 8000 rpm.

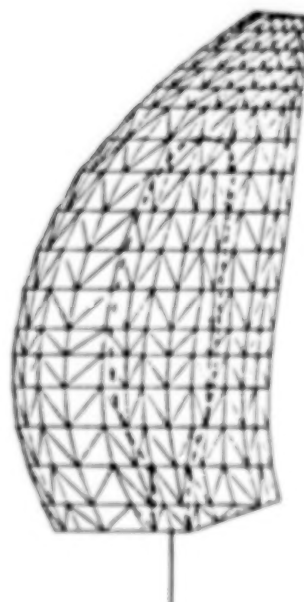
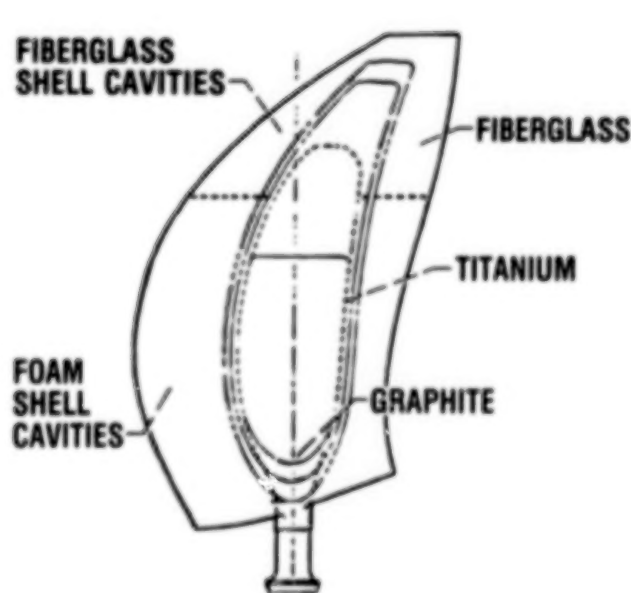


CD-88-31974

## COBSTRAN MODELING OF A SPAR/SHELL COMPOSITE TURBOPROP BLADE

This scaled-down version of a large advanced turboprop blade (Hirschbein et al., 1985) is designed with an internal solid titanium spar which is extended to form the blade shank. Layers of unidirectional graphite/epoxy plies are attached directly over the spar. The airfoil shell surrounding the spar is made of fiberglass/epoxy cross-weave plies. The shell cavity in the lower two-thirds of the blade is filled with foam and the cavity in the upper-third is filled with fiberglass/epoxy cross-weave plies. The finite element model of this blade was generated by using the COBSTRAN (COmposite Blade STRuctural ANalyzer) code. The model consists of 449 two-dimensional triangular elements and a bar element representing the shank. COBSTRAN calculates the anisotropic material properties at each grid point using laminate theory, and the individual ply properties are calculated by the COBSTRAN composite micromechanics module. Grid point properties are then averaged for each element.

(256 NODES, 449 ELEMENTS)

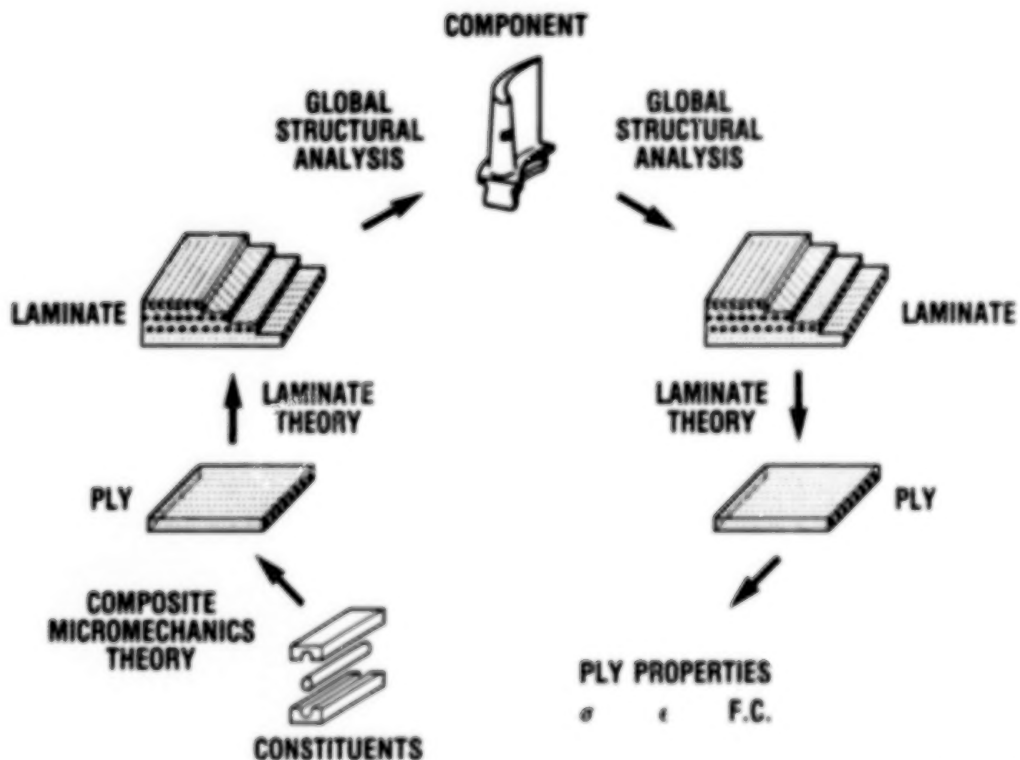


CD-88-31975



## COBSTRAN ANALYTICAL PROCESS

The COBSTRAN code contains an internal databank of constitutive properties for 21 fiber types and 17 matrix types. Starting with these properties the composite ply properties are calculated for each fiber/matrix layer used in the design of the blade (Chamis, 1971). The ply layup at each grid point is determined by COBSTRAN, and the grid point properties are calculated using laminate theory. A global structural finite element analysis model is generated, and the applicable structural analysis is performed. Stress results from this analysis are evaluated and corresponding membrane forces and moments are calculated for each grid point. From these forces and moments, using laminate theory, individual ply stresses, strains, and failure criteria are calculated for each ply layer at each grid point.



CD-88-21978

# COBSTRAN GENERATED PLY PROPERTIES VERSUS MANUFACTURER'S TEST VALUES

The COBSTRAN code is designed to generate individual ply properties from the constitutive properties of the fiber and matrix. A unique feature of COBSTRAN, in addition to its internal databank, is that an external user-supplied databank will override the internal databank. This feature is utilized to generate ply properties compatible with a particular manufacturer's test results. The external databank is modified and the COBSTRAN preprocessor is used iteratively to generate the desired properties. The table below shows the results of COBSTRAN generated values versus manufacturer's test values. There exist some discrepancies when isotropic material properties are calculated from fiber and matrix micromechanics equations. However, this representation is necessary because COBSTRAN, internally, requires more ply properties than can be obtained from tests.

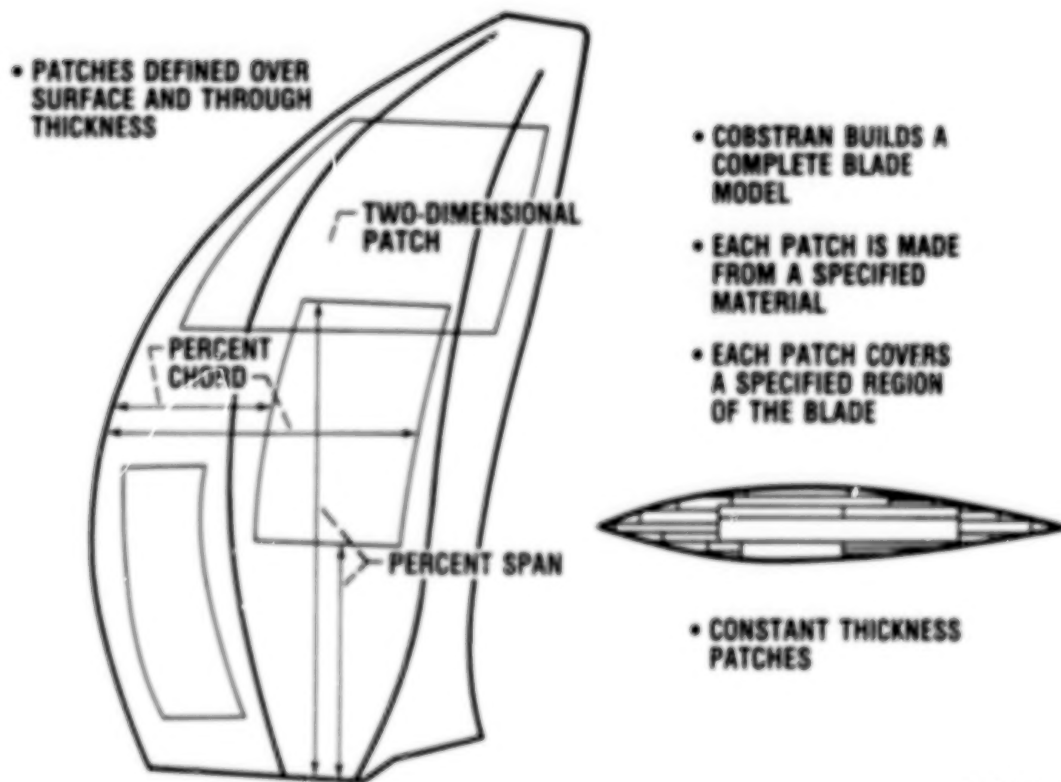
| UNITS,<br>ksi   | SOURCE   | FIBERGLASS<br>(0°/90° CROSS-WEAVE<br>0.0055-IN. THICK) | PAINT<br>(0°/90° CROSS-WEAVE<br>0.002-IN. THICK) | GRAPHITE<br>(0°/0° LAY-UP<br>0.007-IN. THICK) | TITANIUM | FOAM  |
|-----------------|----------|--|--|---|----------|-------|
| E <sub>1</sub>  | COBSTRAN | 3 516  | 2 370  | 13 730  | 16 000   | 9.800 |
|                 | MFG      | 3 510  | 2 370  | 13 800  | 16 000   | 9.800 |
| E <sub>2</sub>  | COBSTRAN | 3 500  | 2 340  | 1 010   | 16 000   | 9.889 |
|                 | MFG      | 3 510  | 2 370  | 1 090   | 16 000   | 9.800 |
| E <sub>12</sub> | COBSTRAN | 737  | 511  | 480   | 6 190    | 4.944 |
|                 | MFG      | 767  | 517  | 580   | 6 100    | 3.630 |

CD-88-31977

## COBSTRAN PLY INPUT REPRESENTATION

The COBSTRAN code produces an integrated lamination model of an entire blade from user-defined constant thickness patches over the surface of the blade and through the thickness. Each patch is made from a specified material system (fiber, matrix, thickness, orientation angle, fiber volume ratio, etc.) and covers a specified region of the blade defined by percent span and percent chord. The integration of these patches for each grid point is determined by COBSTRAN from a user-supplied global layup order.

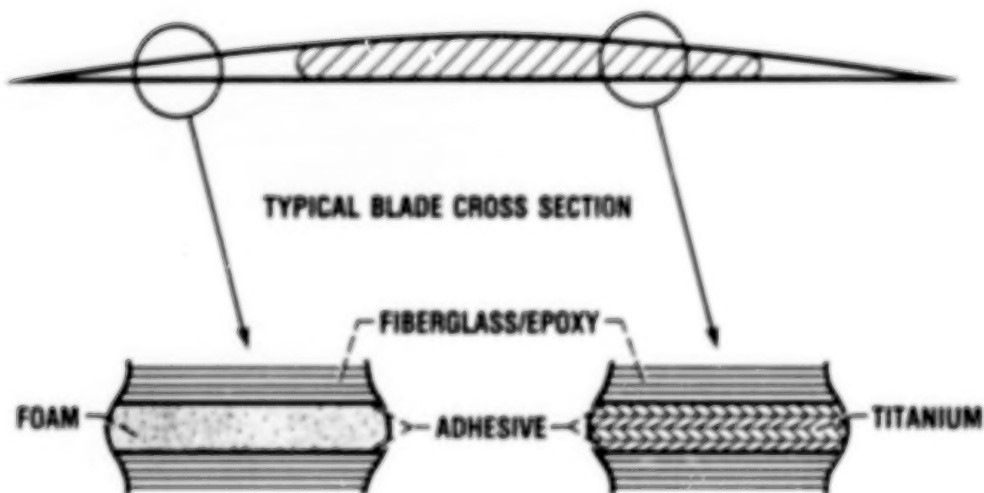
## COBSTRAN PLY INPUT REPRESENTATION



CO-88-31878

## COBSTRAN TWO-DIMENSIONAL LAMINATED BLADE MODELING

The typical advanced composite turboprop blade cross-section shown is designed utilizing a solid internal metal spar and a composite airfoil shell. Shell cavities in the leading and trailing edges are foam filled. This complex blade structure can be simulated effectively by two-dimensional finite elements with one element through the thickness. By modeling the metal, foam, and adhesive as ply layers and utilizing the COBSTRAN code, the two-dimensional anisotropic material properties are calculated for each grid point by laminate analysis. Grid point properties are then averaged for each element.



CO-88-21979

# EFFECTS OF MATERIAL PROPERTY COMBINATIONS ON FREE FREQUENCIES

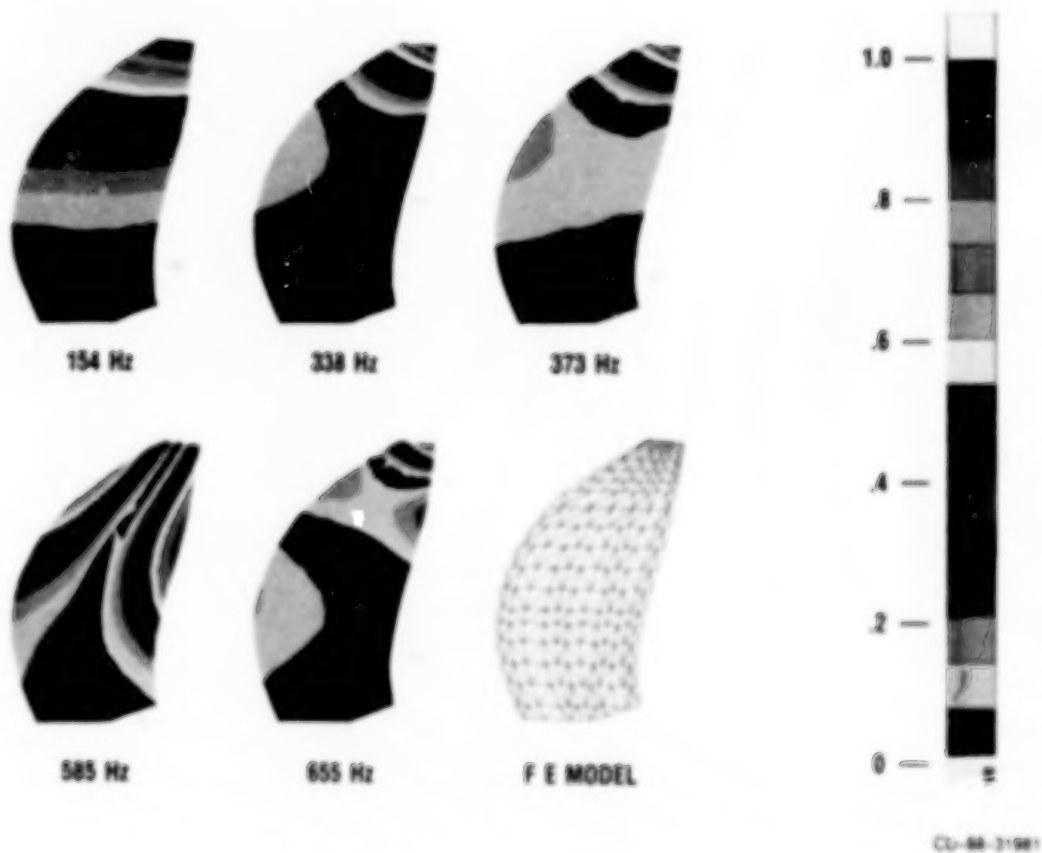
The COBSTRAN code calculates the bending, membrane, transverse shear properties, and the membrane-bending coupling relationship for all elements of the composite turboprop blade. These properties may be selectively used in the finite element analysis. The contribution of a particular material property to the frequency is a function of the blade activity indicated by the mode shape of vibration. Three different material combinations were considered for this study. Coupling was not a factor because of symmetry in the blade layup. Results are compared with holographic test frequencies (Mehmed, 1983). For the column labeled "Bending" bending properties were used to represent bending and membrane properties. Transverse shear effects were considered negligible. For the column labeled "Membrane and Bending" both properties were used separately in the analysis. Transverse shear effects were considered negligible. For the third column, all three properties were used in the analysis.

| MODE | ELEMENT PROPERTIES USED IN ANALYSIS |                             |   | HOLOGRAPHIC<br>TEST RESULTS, Hz |
|------|-------------------------------------|-----------------------------|---|---------------------------------|
|      | BENDING,<br>Hz                      | MEMBRANE AND<br>BENDING, Hz | MEMBRANE, BENDING AND<br>TRANSVERSE SHEAR, Hz |                                 |
| 1    | 154                                 | 158                         | 147   | 155                             |
| 2    | 338                                 | 339                         | 334   | 326                             |
| 3    | 373                                 | 369                         | 364   | 377                             |
| 4    | 585                                 | 571                         | 561   | 545                             |
| 5    | 655                                 | 650                         | 635   | 638                             |
| 6    | 1011                                | 1005                        | 986   | 921                             |

CO-88-31980

## PREDICTED NATURAL FREQUENCIES AND MODE SHAPES

The first five calculated frequencies and mode shapes are represented for a composite turboprop blade. The finite element model used for this analysis was generated by utilizing the COBSTRAN code. Eigenvectors were normalized to the maximum tip displacement. The solid black surfaces (see arrows) indicate areas of zero or negligible motion during each natural vibration mode. Predicting these mode shapes is important to understanding and analyzing blade flutter characteristics.



## MEASURED NATURAL FREQUENCIES AND MODE SHAPES

The first seven frequencies and mode shapes shown were experimentally determined. The composite blade was acoustically excited and photographed with a holographic technique (Mehmed, 1983). The solid bright surfaces (see arrows) indicate areas of zero or negligible motion during each natural vibration mode. These frequencies and mode shapes are comparable to those calculated with a finite element model generated by the COBSTRAN code.

## MEASURED NATURAL FREQUENCIES AND MODE SHAPES



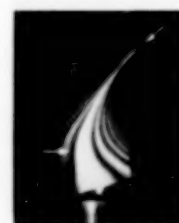
**1F**  
155 Hz



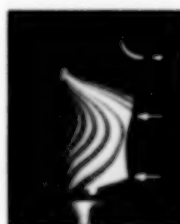
**1E**  
326 Hz



**2F**  
377 Hz



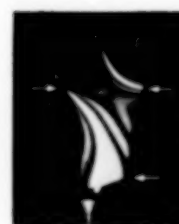
**1T**  
545 Hz



**3F**  
638 Hz



**2T**  
921 Hz



**4F**  
996 Hz

CD-86-31982



## FREQUENCY SENSITIVITY TO STRUCTURAL AND LOAD CONSIDERATIONS

The ability to predict frequencies and mode shapes early in the design phase is important to the development of composite turboprop blades. The effects of airloads, protective paint, and a shank (instrumentation) hole on frequencies have been studied. Airloads and shank hole effects were not significant considerations in the analysis of this turboprop blade. However, the protective paint layer, 0.002-in. thick, did affect the frequency calculations. The paint on the blade surface tended to reduce the calculated frequencies enough to be included in all analyses. The last column shows results from an independent finite element analysis (Nagle et al., 1986).

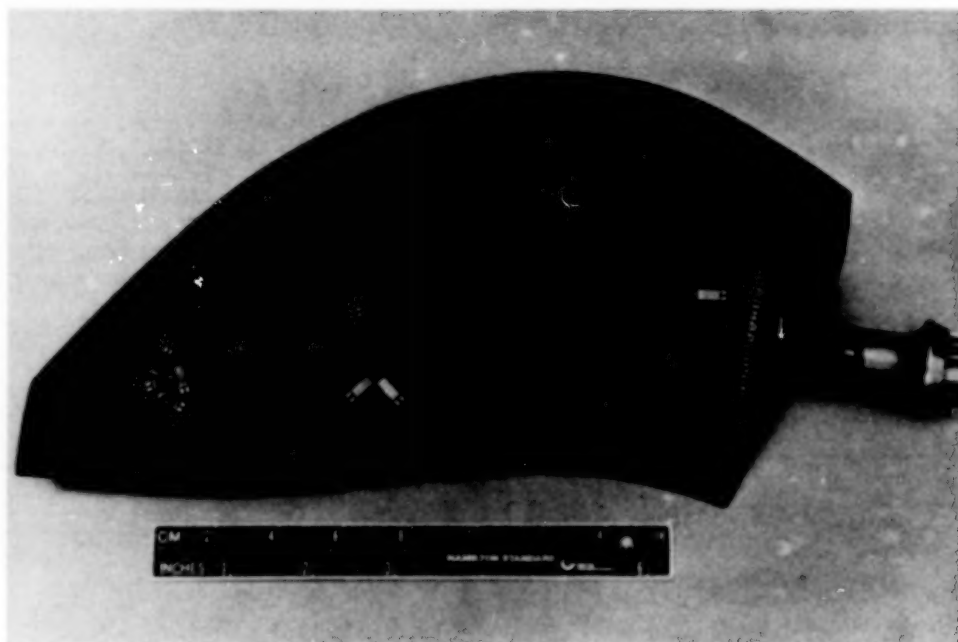
[NATURAL FREQUENCIES (Hz) AT 7484 rpm, AIRLOADS AT 35 000-ft ALTITUDE.]

| MODE | FREQUENCY, Hz                                       |   |  |  |  |
|------|---|---|--|--|--|
|      | WITH AIRLOADS,<br>WITH PAINT,<br>WITH SHANK<br>HOLE | WITHOUT AIRLOADS,<br>WITH PAINT,<br>WITH SHANK HOLE | WITH AIRLOADS,<br>WITHOUT PAINT,<br>WITH SHANK<br>HOLE | WITH AIRLOADS,<br>WITH PAINT,<br>WITHOUT SHANK<br>HOLE | WITH AIRLOADS,<br>WITHOUT PAINT,<br>WITHOUT SHANK<br>HOLE<br>(F.E. ANALYSIS) |
| 1    | 202.30  | 202.04  | 205.13   | 202.15   | 207.5  |
| 2    | 366.28  | 366.34  | 374.16   | 367.07   | 376.0  |
| 3    | 461.41  | 459.83  | 462.08   | 460.07   | 468.6  |
| 4    | 623.32  | 626.27  | 634.05   | 626.40   | 642.5  |
| 5    | -----   | 780.39  | 786.05   | 780.67   | 782.3  |

CD-88-31983

## TURBOPROP BLADE INSTRUMENTED FOR STRAIN MEASUREMENT

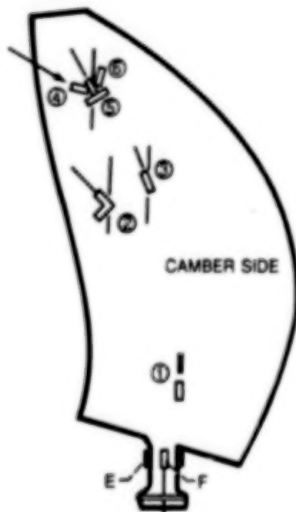
This instrumented turboprop blade was used to evaluate strain results during vibration testing. The COBSTRAN code was used to determine strain gage placement prior to testing. COBSTRAN calculates the strains in all ply layers at each grid point. Relative strain values were calculated by using the normalized eigenvectors as displacements. This identified the areas of largest strain for each vibration mode. During rotational tests the critical strain conditions were flagged by knowing the relation between the measured strains and high strain areas.



CD-88-31984

# PREDICTED VERSUS MEASURED NORMALIZED SURFACE STRAINS

The first figure shows the position of six strain gages on the camber surface of a composite turboprop blade. Gage positions were determined with the COBSTRAN code. The blade was excited in the third mode of vibration. The table shows the results of measured (Mehmed, 1983) and calculated strains for this vibration mode. The actual strains were very small and difficult to measure. Both sets of data were normalized to gage number 4. Gage number 2 failed and therefore is not shown in the table. Comparison was good overall, with gage number 1 showing the largest discrepancy. This gage was located on the thickest part of the blade, the most difficult area to measure strain.



STRAINS NORMALIZED TO GAGE NUMBER 4  
(THIRD MODE OF VIBRATION)

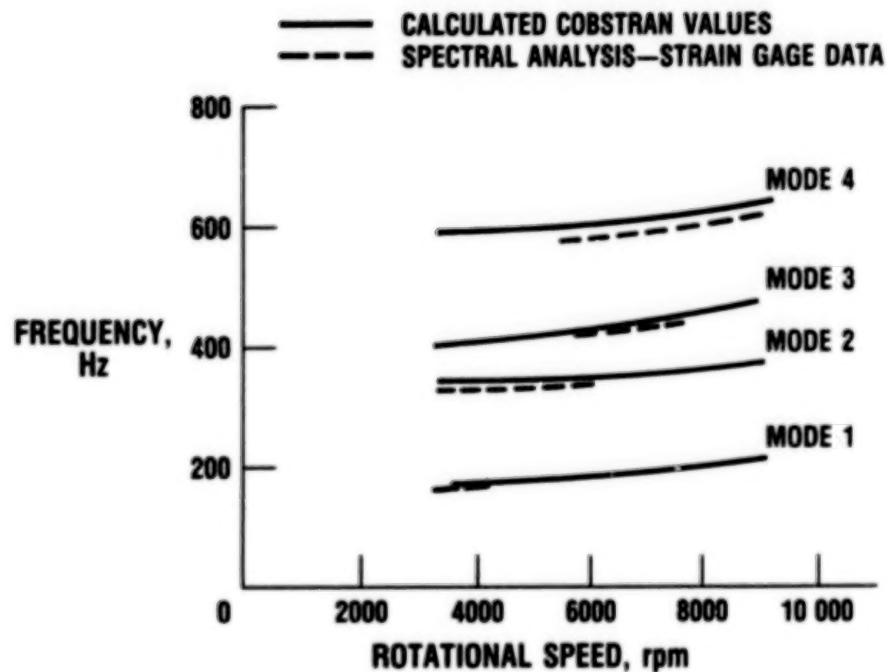
| GAGE NUMBER | MEASURED DATA | COBSTRAN ANALYSIS |
|-------------|---------------|-------------------|
| 1           | 0.152         | 0.106             |
| 3           | .386          | .340              |
| 4           | 1.000         | 1.000             |
| 5           | .519          | .650              |
| 6           | .122          | .144              |
| E           | .377          | .440              |
| F           | .152          | .138              |

NOTE: GAGES E AND F SHOWN OUT OF  
TRUE CIRCUMFERENTIAL POSITION  
LOCATION AND ORIENTATION OF  
STRAIN GAGES ON CAMBER/  
CONVEX SURFACE

CD-88-31985

## CALCULATED AND TEST FREQUENCIES VERSUS ROTATIONAL SPEED

The ability to predict blade frequencies when a blade is subjected to centrifugal forces is important in the design of composite turboprop blades (Aiello and Chamis, 1982). The calculated frequencies were generated by using a finite element model that was generated by the COBSTRAN code. These are indicated by the solid lines. The measured frequencies were obtained by spectral analysis of strain gage data resulting from tests in the NASA Lewis 9 Foot by 15 Foot Wind Tunnel (Mehmed, 1983) and are indicated by the dashed lines.



CD-88-31987

#### REFERENCES

- Aiello, R.A. and Chamis, C.C., 1982, "Large Displacement and Stability Analysis of Nonlinear Propeller Structures, NASA TM-82850.
- Chamis, C.C., 1971, "Computer Code for the Analysis of Multilayered Fiber Composites - Users Manual," NASA TN D-7013.
- Hirschbein, M. et al., 1985, "Structural and Aeroelastic Analysis of SR-7L Propfan," NASA TM-86877.
- Mehmed, O., 1983, "SR7A Propfan Model Blade S/N 16: Vibration Test Results and Blade Strain Gage Limits for SR7A."
- Nagle, D., et al., 1986, "SR7A Aeroelastic Model Blade Design Report," NASA CR-174791 Hamilton Standard Div. of United Tech. Corp., NASA Lewis Research Center, Contract NAS3-23051.

BLANK PAGE

## FEATURES AND APPLICATIONS OF THE INTEGRATED COMPOSITES ANALYZER (ICAN) CODE

Carol A. Ginty  
Structural Mechanics Branch  
NASA Lewis Research Center

### ABSTRACT

ICAN (Integrated Composites Analyzer), a stand-alone computer code, was developed to analyze and design multilayered fiber composite structures using micromechanics equations and laminate theory (Murthy and Chamis, 1984). Input parameters of this user-friendly program include material system, fiber volume ratio, laminate configuration, fabrication factors, and environmental conditions. Output features include practically all composite hygral, thermal, and mechanical properties that are needed to perform structural/stress analyses in service environments. As such, ICAN is an effective tool for the preliminary design of composite structures (Ginty and Endres, 1986). In addition, ICAN has a resident data bank which houses the properties of a variety of constituent (fiber and matrix) materials with provisions to add new constituent materials as they become available. The objective herein is to discuss the input and output parameters of the ICAN code as well as to describe procedures for both the implementation of new data in the data bank and modeling techniques which enable ICAN to analyze composite woven fabric/cloth structures (Ginty and Chamis, 1986). Finally, new features recently incorporated in the code which yield life predictions and analyses based on cyclic temperatures (Ginty and Chamis, 1988) will be presented.

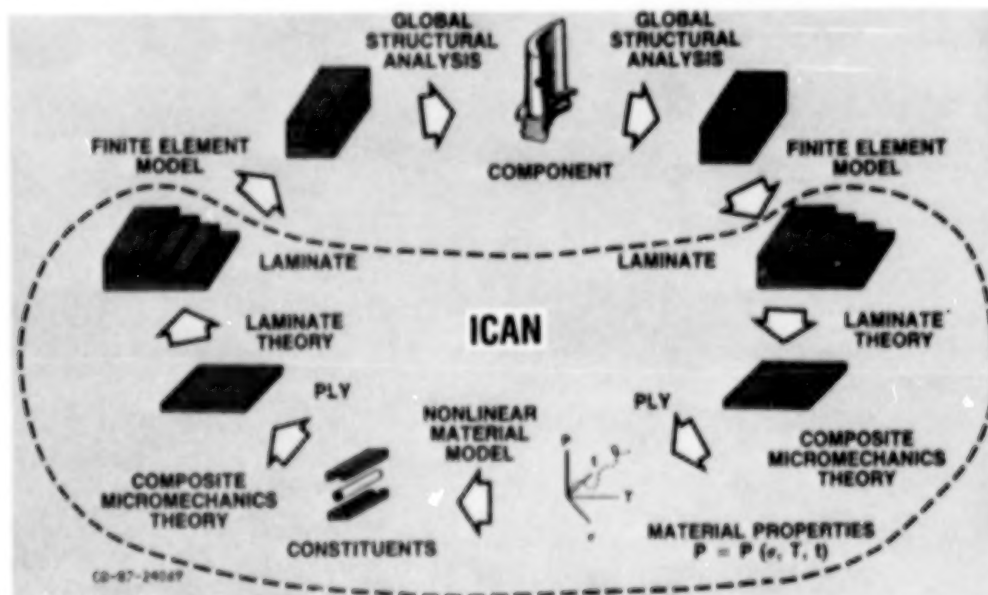


## OVERVIEW

### THEORIES EMBODIED IN ICAN CODE

The most cost effective way to analyze or design fiber composite structures is through the use of computer codes. Over the past 15 years, extensive research has been conducted at NASA Lewis to develop composite mechanics theories and analysis methods from micromechanics to new finite elements. These theories and analysis methods account for environmental effects and are applicable to intraply hybrid composites, interply hybrid composites, and combinations thereof. Most of these theories are presented by simplified equations which have been corroborated by experimental results and finite element analysis. The composite mechanics theories with their respective simplified equations constitute a structures theory which is (1) upward integrated from material behavior space to structural analysis, and (2) top-down traced from structural response to material behavior space. This structured theory has been incorporated into a computer code called ICAN (integrated composites analyzer). ICAN is a synergistic combination of two other Lewis developed codes: MFCA (multi-layered fiber composites analysis) and INHYD (intraply hybrid composite design).

MFCA (Chamis, 1971) is efficient in predicting the structural response of multi-layered fiber composites given the constituent material properties, fabrication process, and composite geometry. INHYD (Chamis and Sinclair, 1983) incorporates several composite micromechanics theories, intraply hybrid composite theories, and a hygrothermomechanical theory to predict the mechanical, thermal and hygral properties of intraply hybrid composites. ICAN uses the micromechanics design of INHYD and the laminate theory of MFCA to build a comprehensive analysis and design capability for structural composites. Features unique to ICAN include microstresses, predictions of probable delamination locations around a circular hole, material cards for finite element analysis for NASTRAN (COSMIC and MSC) and MARC, and laminate failure stresses based on first ply failure and fiber fracture criteria, with and without hygrothermal degradation. In addition, ICAN possesses another unique feature in its resident data bank which houses the constituent (fiber/matrix) properties.



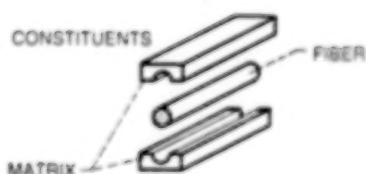
CD-88-32919

## POSTER PRESENTATION

### ICAN UNIQUE FEATURE - RESIDENT DATA BANK

One of the unique features of ICAN is its resident data bank which houses the constituent (fiber and matrix) properties. Its primary function is in reducing the burden on the user in preparing properly formatted data for the program. The simplified equations which determine the composite properties require that the user supply 16 fiber properties and 15 matrix properties. Years of literature searches and in-house experimental programs on materials characterization have resulted in the compilation of the existing data bank.

The fiber and matrix are identified with a four-character coded name. Following the fiber entry are four material cards, FP, FF, FT, and FS, representing the fiber's (F), physical, elastic, thermal, and strength properties (P, E, T, and S, respectively). Likewise, the matrix entry is followed by five material cards, MP, ME, MT, MS, and MV, where the matrix (M) properties are represented, as described above, with one additional card (MV), which contains various (V) properties of the matrix. The data bank is designed to be open-ended, allowing the user the ability to add new constituent materials as they appear on the market. In light of the proprietary nature of many new material systems, it is often difficult to obtain constituent properties from the suppliers. As a result, the user may have to resort to approximating these unknown values.



| CARD | ICAN FIBER ENTRY  |
|------|---|
| 1    | FOUR CHARACTER CODED NAME FOR FIBER   |
| 2    | FP: $N_f, \phi_f, \rho_f$   |
| 3    | FE: $E_{f11}, E_{f22}, \gamma_{f12}, \gamma_{f23}, G_{f12}, G_{f23}$            |
| 4    | FT: $\alpha_{f11}, \alpha_{f22}, K_{f11}, K_{f22}, C_f$                         |
| 5    | FS: $S_{fT}, S_{fC}$ (THE REMAINING ENTRIES ARE OPEN FOR FUTURE MODIFICATIONS.) |

| CARD | ICAN MATRIX ENTRY  |
|------|--|
| 1    | FOUR CHARACTER CODED NAME FOR MATRIX   |
| 2    | MP: $\rho_m$   |
| 3    | ME: $E_m, \nu_m, \alpha_m$   |
| 4    | MT: $K_m, C_m$   |
| 5    | MS: $S_{mT}, S_{mC}, S_{mS}, \epsilon_{mT}, \epsilon_{mC}, \epsilon_{mS}, \epsilon_{mTOR}$ |
| 6    | MV: $K_p, T_{gdr}$   |

### PORTION OF EXISTING DATA BANK

```

T300
FP 3000 0.300E-03 0.840E-01
FE 0.320E 08 0.200E 07 0.200E 00 0.250E 00 0.130E 07 0.700E 06
FT -0.550E-06 0.560E-05 0.580E 03 0.580E 02 0.170E 00
FS 0.350E 06 0.300E 06 0.000 0.000 0.000 0.000

AS-
FP 1000 0.300E-03 0.630E-01
FE 0.310E 08 0.200E 07 0.200E 00 0.250E 00 0.290E 07 0.100E 07
FT -0.550E-06 0.560E-05 0.580E 03 0.580E 02 0.170E 00
FS 0.400E 06 0.400E 06 0.000 0.000 0.000 0.000

SGLA
FP 204 0.360E-03 0.900E-01
FE 0.124E 08 0.124E 08 0.200E 00 0.200E 00 0.517E 07 0.517E 07
FT 0.280E-05 0.280E-05 0.750E 01 0.750E 01 0.170E 00
FS 0.350E 06 0.300E 06 0.000 0.000 0.000 0.000

HMSF HIGH MODULUS SURFACE TREATED FIBER
FP 10000 0.300E-03 0.703E-01
FE 0.550E 08 0.900E 06 0.200E 00 0.250E 00 0.110E 07 0.700E 06
FT -0.550E-06 0.560E-05 0.580E 03 0.580E 02 0.170E 00
FS 0.280E 06 0.200E 06 0.000 0.000 0.000 0.000

OVER END OF FIBER PROPERTIES.

IMSL INTERMEDIATE MODULUS LOW STRENGTH MATRIX
MP 0.460E-01
ME 0.500E 06 0.410E 00 0.570E-04
MT 0.125E 01 0.250E 00
MS 0.700E 04 0.210E 05 0.700E 04 0.140E-01 0.420E-01 0.320E-01 0.320E-01
MV 0.225E 00 0.420E 03

IMHS INTERMEDIATE MODULUS HIGH STRENGTH MATRIX
MP 0.440E-01
ME 0.500E 06 0.350E 00 0.360E-04
MT 0.125E 01 0.250E 00
MS 0.150E 05 0.350E 05 0.130E 05 0.200E-01 0.500E-01 0.350E-01 0.350E-01
MV 0.225E 00 0.420E 03

HMSH HIGH MODULUS HIGH STRENGTH MATRIX
MP 0.450E-01
ME 0.750E 06 0.350E 00 0.400E-04
MT 0.125E 01 0.250E 00
MS 0.200E 05 0.500E 05 0.150E 05 0.200E-01 0.500E-01 0.400E-01 0.400E-01
MV 0.225E 00 0.420E 03

OVER END OF MATRIX PROPERTIES.

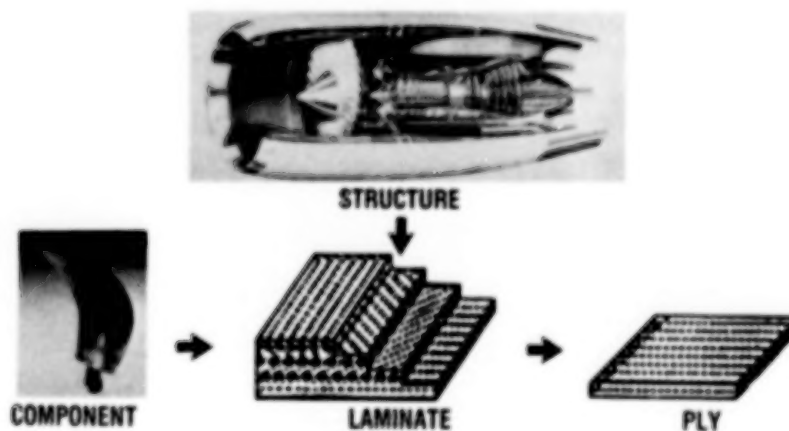
```

CD-88-3290

CD-88-32901

## ICAN SIMULATION OF COMPOSITE STRUCTURES

ICAN has always been labeled user-friendly. The primary reason being the straightforward format used for data entry. Herein, the item referred to as a data set is actually the simulation of the composite structure to be analyzed. In order to accurately simulate a structure for analysis, the user must provide the following information: material system, fiber volume ratio, laminate configuration, fabrication factors, environmental conditions, and loading states. To demonstrate, an engine blade with a configuration of  $[0/90]_S$  has been chosen for simulation.



CD-68-32952

# ICAN SIMULATION OF COMPOSITE STRUCTURES

The first line of the data set is reserved for user comments. The next five cards constitute the Booleans, which are discussed in detail in Murthy and Chamis (1984). Now the actual simulation begins as the structure is modeled ply-by-ply. The columns from left to right contain the following information: ply 1 is made from material 1. The analysis is to be conducted at room temperature (70 °F). The cure temperature for the resin is 350 °F. The ply contains 1.8 percent moisture by weight. The fibers in this ply are aligned in the longitudinal (0) direction, and the ply is 0.010 in. thick. The remaining lines are completed in the same fashion. Next, the composite material system must be identified. Here, material 1 is an AS-- fiber (graphite) and IMLS matrix (epoxy resin). The fiber volume ratio is 0.55, and the void volume ratio is 0.02. As was previously mentioned, ICAN analyzes hybrid structures as well. Material 2 in this example is a hybrid consisting of the SGLA fiber and HMHS resin and the AS -- fiber and IMHS resin. In this line the 0.4 indicates that in this particular ply, 40 percent of the material is AS--/IMHS, leaving the remaining 60 percent to be fabricated from SGLA/HMHS, each with its own specified volume ratio. Finally, an axial load of 1000 lb is being applied in the longitudinal direction. Thus, a very complex structure is simulated with ease using this format.

## ICAN INPUT DATA SET FOR COMPOSITE BLADE

|                 |   |     |       |          |        |      |      |                   |
|-----------------|---|-----|-------|----------|--------|------|------|-------------------|
| T               |   |     |       |          | COMSAT |      |      |                   |
| F               |   |     |       |          | CSANB  |      |      |                   |
| F               |   |     |       |          | BIDE   |      |      |                   |
| F               |   |     |       |          | RINDV  |      |      |                   |
| T               |   |     |       |          | NONUDF |      |      |                   |
| PLY             | 1 | 1   | 70.00 | 350.0    | 1.8    | 0.0  | .010 |                   |
| PLY             | 2 | 2   | 70.00 | 350.0    | 1.8    | 90.0 | .005 |                   |
| PLY             | 3 | 2   | 70.00 | 350.0    | 1.8    | 90.0 | .005 |                   |
| PLY             | 4 | 1   | 70.00 | 350.0    | 1.8    | 0.0  | .010 |                   |
| 1MATCHAS--IMLS  |   | .55 | .02   | AS--IMLS | 0.0    | .57  | .03  |                   |
| 2MATCHOSGLAHMHS |   | .55 | .01   | AS--IMHS | 0.4    | .57  | .01  |                   |
| PLOAD 1000.     |   | 0.0 | 0.0   | 0.0      |        |      |      | NX,NY,NXY,THCS    |
| PLOAD 0.0       |   | 0.0 | 0.0   | 0.0      |        |      |      | MX,MV,MXY         |
| PLOAD 0.0       |   | 0.0 |       |          |        |      |      | MX/QX,DNY/QY,PRSS |
| OPTION          | 0 |     |       |          |        |      |      |                   |

CO-68-33284

## ICAN OUTPUT OPTIONS

Another user-friendly feature of the ICAN code is the compartmentalization of output and the user's ability to retrieve only the information that pertains to his/her analysis. This facet of the program is controlled by the last line of input in the data set which is referred to as the option card. For discussion purposes, the output is contained in 20 categories that range from the ICAN logo to a detailed table which lists the stress concentration factors around a circular hole. In actuality, the features in options 1 to 5 are always printed automatically as output. The remaining 15 features are controlled by the option card. Entering a zero will cause all 20 of the features to be printed. If only two or three features are desired, then the user must add a separate option card for each feature at the end of the data set.

The most frequently used options are shown below. Because of the neat arrangement of the data for finite element analysis in option 10, many users employ ICAN as a preprocessor for more complex structural analyses codes such as NAS-TRAN and MARC. The data in option 10 is read directly as a material (MAT) card into the other codes. For in-house experimental programs, ICAN is often used to simulate the composite specimen and testing environment. The data in option 20 yield a fracture stress that is then used to aid researchers in developing their test plans. Finally, the table of composite properties in option 7 enables researchers to understand the behavior of certain composite materials, particularly when little information has been published in the literature.

## SUMMARY

| ICAN<br>OPTION | ICAN OUTPUT FEATURE   |
|----------------|---|
| 1              | ICAN LOGO   |
| 2              | ICAN COORDINATE SYSTEMS   |
| 3              | ICAN INPUT DATA ECHO  |
| 4              | THE INPUT DATA SUMMARY  |
| 5              | THE FIBER AND THE MATRIX (CONSTITUENT MATERIALS) PROPERTIES OF PRIMARY AND SECONDARY COMPOSITES; THE PLY LEVEL PROPERTIES       |
| 6              | THE COMPOSITE 3-D STRAIN-STRESS AND STRESS-STRAIN RELATIONS ABOUT THE STRUCTURAL AXES; MAT9 CARD FOR MSC/NASTRAN SOLID ELEMENTS |
| 7              | THE COMPOSITE PROPERTIES  |
| 8              | THE COMPOSITE CONSTITUTIVE EQUATIONS ABOUT THE STRUCTURAL AXES  |
| 9              | THE REDUCED BENDING AND AXIAL STIFFNESSES   |
| 10             | SOME USEFUL DATA FOR FINITE-ELEMENT ANALYSIS  |
| 11             | THE DISPLACEMENT-FORCE RELATIONS FOR THE CURRENT LOAD CONDITION   |
| 12             | THE PLY HYGROTHERMOMECHANICAL PROPERTIES/RESPONSE   |
| 13             | THE DETAILS OF POISSON'S RATIO MISMATCH AMONG THE PLIES   |
| 14             | FREE EDGE STRESSES  |
| 15             | THE MICROSTRESSES AND MICROSTRESS INFLUENCE COEFFICIENTS FOR EACH COMPOSITE MATERIAL SYSTEM                                     |
| 16             | STRESS CONCENTRATION FACTORS AROUND A CIRCULAR HOLE   |
| 17             | LOCATIONS OF PROBABLE DELAMINATION AROUND CIRCULAR HOLES  |
| 18             | PLY STRESS AND STRAIN INFLUENCE COEFFICIENTS  |
| 19             | LAMINATE FAILURE STRESSES BASED ON THE FIRST PLY FAILURE/MAXIMUM STRESS CRITERIA  |
| 20             | A SUMMARY OF THE LAMINATE FAILURE STRESSES BASED UPON TWO ALTERNATIVES, THE FIRST PLY FAILURE AND THE FIBER BREAKAGE            |

CO-88-32963

# OPTION 7

COMPOSITE PROPERTIES - VALID ONLY FOR CONSTANT TEMPERATURE THROUGH THICKNESS  
 LINES 1 TO 31 3-D COMPOSITE PROPERTIES ABOUT MATERIAL AXES  
 LINES 32 TO 62 2-D COMPOSITE PROPERTIES ABOUT STRUCTURAL AXES

|    |       |             |    |        |             |
|----|-------|-------------|----|--------|-------------|
| 1  | RHOC  | 0.5552E-01  | 32 | B2DEC  | 0.0000      |
| 2  | TC    | 0.2000E-01  | 33 | CC11   | 0.1858E 08  |
| 3  | CC11  | 0.2148E 08  | 34 | CC12   | 0.3716E 06  |
| 4  | CC12  | 0.6147E 06  | 35 | CC13   | 0.0000      |
| 5  | CC13  | 0.6147E 06  | 36 | CC22   | 0.1198E 07  |
| 6  | CC22  | 0.1549E 07  | 37 | CC23   | 0.0000      |
| 7  | CC23  | 0.7103E 06  | 38 | CC33   | 0.6233E 06  |
| 8  | CC33  | 0.1854E 07  | 39 | EC11   | 0.1880E 08  |
| 9  | CC44  | 0.3623E 08  | 40 | EC22   | 0.1193E 07  |
| 10 | CC55  | 0.6237E 06  | 41 | EC12   | 0.8233E 06  |
| 11 | CC66  | 0.6237E 06  | 42 | NUC12  | 0.3800E 00  |
| 12 | CTE11 | -0.8883E-07 | 43 | NUC21  | 0.1850E-01  |
| 13 | CTE22 | 0.1733E-04  | 44 | CSN13  | 0.0000      |
| 14 | CTE33 | 0.1733E-04  | 45 | CSN31  | 0.0000      |
| 15 | HK11  | 0.3485E 03  | 46 | CSN32  | 0.0000      |
| 16 | HK22  | 0.4281E 01  | 47 | CSN33  | 0.0000      |
| 17 | HK33  | 0.4281E 01  | 48 | CTE11  | -0.8883E-07 |
| 18 | HMC   | 0.1955E 00  | 49 | CTE22  | 0.1733E-04  |
| 19 | EC11  | 0.2115E 08  | 50 | CTE12  | 0.0000      |
| 20 | EC22  | 0.1238E 07  | 51 | HK11   | 0.3475E 03  |
| 21 | EC33  | 0.1323E 07  | 52 | HK22   | 0.4281E 01  |
| 22 | EC23  | 0.3623E 06  | 53 | HK12   | 0.0000      |
| 23 | EC31  | 0.6233E 06  | 54 | HMC    | 0.1955E 00  |
| 24 | EC12  | 0.8233E 06  | 55 | DPC11  | 0.8100E-04  |
| 25 | NUC12 | 0.3800E 00  | 56 | DPC22  | 0.9198E-02  |
| 26 | NUC21 | 0.1850E-01  | 57 | DPC33  | 0.2263E 05  |
| 27 | NUC13 | 0.2506E 00  | 58 | DPC12  | 0.0000      |
| 28 | NUC31 | 0.1967E-01  | 59 | BTAC11 | 0.4255E-04  |
| 29 | NUC23 | 0.4234E 00  | 60 | BTAC22 | 0.1214E-02  |
| 30 | NUC32 | 0.4525E 00  | 61 | BTAC33 | 0.1214E-02  |
| 31 | ZCOC  | 0.1000E-01  | 62 | BTAC12 | 0.0000      |

CD-88-32985

# OPTION 10

SOME USEFUL DATA FOR F.E. ANALYSIS

COMPOSITE THICKNESS FOR F.E. ANALYSIS = 0.2000E-01

PROPERTIES FOR F.E. ANALYSIS E11,E12,E13,E23,E33 PROPERTIES SCALED BY 10\*\*6  
 0.21240E 00 -0.29921E 00 0.00000 0.94820E 00 0.00000 0.34877E 00

BENDING EQUIVALENT PROPERTIES NUCXY, NCYX, ECXX, ECVY, GCXY  
 0.14200E 01 0.31629E 00 0.47058E 07 0.10571E 07 0.28672E 07

NASTRAN MEMBRANE EQUIVALENT ELASTIC COEFFICIENTS G11,G12,G13,G22,G23,G33  
 0.84841E 07 0.28834E 07 0.00000 0.19158E 07 0.00000 0.28672E 07

NASTRAN BENDING EQUIVALENT ELASTIC COEFFICIENTS G11,G12,G13,G22,G23,G33  
 0.84841E 07 0.28834E 07 -0.14205E 01 0.19058E 07 0.17881E 00 0.28672E 07

CD-88-32984

# OPTION 20

## SUMMARY

LAMINATE FAILURE STRESS ANALYSIS -(WITH TEMPERATURE/MOISTURE STRESSES)  
 (BASED UPON FIRST PLY FAILURE)

| (Moisture Content by weight 1.0%)<br>(Uniform Temperature 200.0F) |              |              |         |       |                    |
|---|--------------|--------------|---------|-------|--------------------|
| LOAD TYPE   | STRESS (ksi) | FAILURE MODE | PLY NO. | THETA | MATERIAL SYSTEM    |
| SCKXT   | 18.002       | SL22C        | 4       | -30.0 | AS--10MHS SOLAHHMS |
| SCKXC   | 25.387       | SL221        | 4       | -30.0 | AS--10MHS SOLAHHMS |
| SCVYT   | 8.885        | SL12S        | 1       | 30.0  | AS--10MHS SOLAHHMS |
| SCVYC   | 8.885        | SL12S        | 1       | 30.0  | AS--10MHS SOLAHHMS |
| SCKYS   | 22.638       | SL22C        | 4       | -30.0 | AS--10MHS SOLAHHMS |

LAMINATE FAILURE STRESS ANALYSIS -(WITH TEMPERATURE/MOISTURE STRESSES)  
 (BASED UPON FIBER FAILURE)

| (Moisture Content by weight 1.0%)<br>(Uniform Temperature 200.0F) |              |              |         |       |                    |
|---|--------------|--------------|---------|-------|--------------------|
| LOAD TYPE   | STRESS (ksi) | FAILURE MODE | PLY NO. | THETA | MATERIAL SYSTEM    |
| SCKXT   | 100.918      | SL11T        | 1       | 30.0  | AS--10MHS SOLAHHMS |
| SCKXC   | 55.721       | SL11C        | 1       | 30.0  | AS--10MHS SOLAHHMS |
| SCVYT   | 385.355      | SL11T        | 1       | 30.0  | AS--10MHS SOLAHHMS |
| SCVYC   | 212.773      | SL11C        | 1       | 30.0  | AS--10MHS SOLAHHMS |
| SCKYS   | 28.480       | SL11C        | 4       | -30.0 | AS--10MHS SOLAHHMS |

NOTE: IF THERE IS NO ANGLE PLY "SCKYS" BASED UPON FIBER FAILURE IS NOT PREDICTED

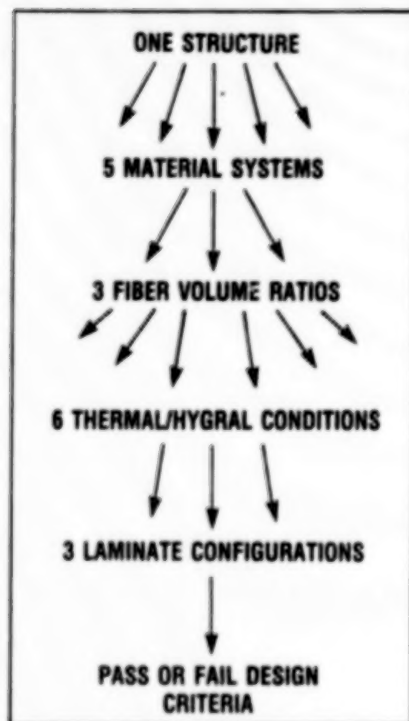
CD-88-32986



## THE POWER OF ICAN IN PARAMETRIC ANALYSES

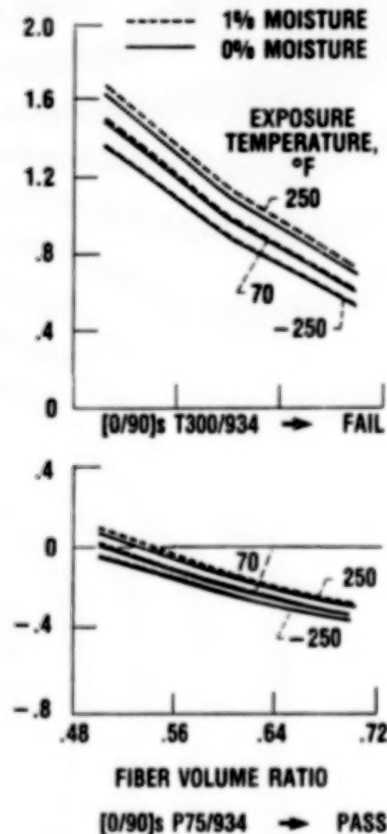
When considering composites for critical component structures, designers often have difficulty in selecting a material system since handbooks simply do not exist. In addition, composite properties, which they require for detailed structural analysis, are difficult to acquire. One alternative is an experimental characterization program whereby behavior would be monitored and properties would be determined. This route, unfortunately, has a long start up time, is quite costly, and requires a great deal of time for completion. There is an alternative, and that is the use of the ICAN code to conduct the parametric analysis. This will be demonstrated by an example of an in-house program in which ICAN was used effectively.

A communication satellite was to be designed using thin face sheets with a honeycomb interior. The designers had five material system candidates for the faces but were uncertain as to which would be the most suitable for the harsh space environment. They established a design criteria of zero, or negative coefficient of thermal expansion (CTE) of the composite. An experimental test matrix, accounting for all parameters, would require at the minimum, 270 specimens. ICAN was used to model the face sheets with various materials, fiber volume ratios, environmental conditions and laminate configurations. On completion, the predicted composite CTE was compared with the design criteria. In 6 months time and 300 cases later, a design was proposed based on the ICAN parametric studies and results. The contractor proposed the same design 1½ years later based on limited experimental data. Hence, ICAN can be used effectively as a preliminary design tool saving time and money in a project.



ISSUES: —TIMELINESS  
—COST-EFFECTIVENESS

COEFFICIENT  
OF THERMAL  
EXPANSION,  
CTEXX  
 $\mu\text{m./in.}$   
 $^{\circ}\text{F}$

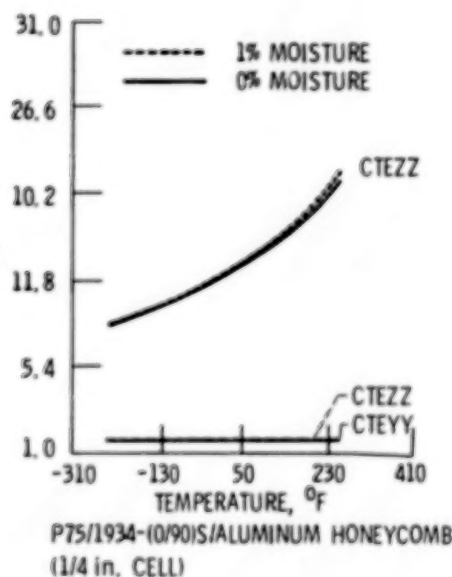
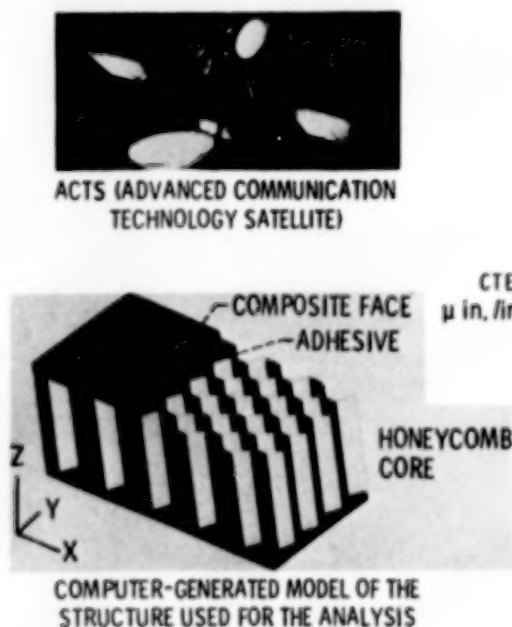




# ICAN SANDWICH COMPUTATIONAL SIMULATION (SCS)

Due in part to ICAN's success with the parametric analysis of the composite face sheets, another version of the code was created for the analysis of the entire sandwich structure, which includes composite face sheets, adhesive, and a honeycomb core. The sandwich structure represents one of the antenna on the Lewis Advanced Communication and Technology Satellite (ACTS), which is scheduled for launch in 1990.

The evolution of ICAN to ICAN/SCS was an arduous procedure requiring four steps: (1) three-dimensional finite element modeling of the entire sandwich, (2) three-dimensional finite element modeling of the sandwich assuming an equivalent homogeneous medium for a core, (3) laminate theory simulation of the honeycomb assumed to be constructed of plies with equivalent properties, and (4) approximate simplified equations for simulating the honeycomb thermal and mechanical properties with an equivalent homogeneous medium. With this version of ICAN, a parametric study was conducted on the sandwich structure, concentrating on the compatibility of CTE's of the various components. Once again, a suitable design was proposed based on ICAN/SCS results.



CD-88-32969

## ICAN SIMULATION OF CLOTH/WOVEN FABRIC COMPOSITES

ICAN was designed to analyze aligned continuous-fiber ply composites. However, the applications of woven fabric (cloth) composite prepregs are increasing for aerospace structural parts; therefore, a technique was developed to simulate woven fabric using the existing parameters in the input data set. The technique involves manipulation of the plies and fiber volume ratios. Each cloth ply is modeled as two plies in ICAN. One ply is oriented in the 0, or warp direction of the cloth, and the second ply is oriented in the 90°, or fill direction of the cloth. Equations have been generated that allow the cloth thickness  $t$  and fiber volume ratio (FVR) to be accurately simulated using this technique. The thickness  $t$  of each ICAN ply is equal to a percentage of the total cloth ply thickness as shown in the equations. The thickness of these two ICAN plies equals the thickness of one cloth ply. Likewise, the FVR is altered in a similar manner. Two material systems corresponding to the 0 and 90° plies are used in ICAN to model the cloth. Each ICAN material system has a different FVR which is a percentage of the given cloth FVR, as shown by the equations. Although this procedure appears cumbersome, it is, in fact, quite easy to implement.

To demonstrate, ICAN was used to simulate various structures fabricated from an E-glass cloth. A comparison experimental program existed enabling us to validate this technique by comparing the predicted results with the measured data. For discussion purposes the most complex laminate in the study is chosen and labeled the representative laminate since it was fabricated from two other glass cloths: 7576 and 7781. The representative laminate consisted of 19 plies in the configuration  $[A/B/D/C/A/D/C/B_2/A/B_2/C/D/A/C/D/B/A]$  where  $A = 7576$  at 0 ply,  $B = 7781$  at 0 ply,  $C = 7781$  at +30° ply and  $D = 7781$  at -30° ply. Total thickness for the representative laminate was 0.181 in. The laminates were cured at 340 °F and the specimens were tested at -300 °F and 200 °F.

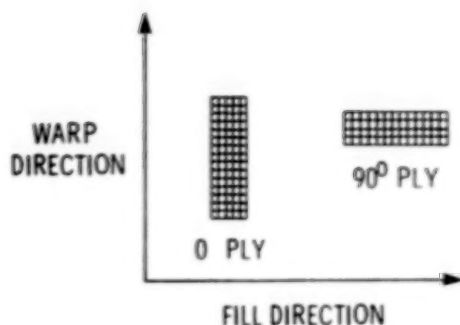
The ICAN results for longitudinal elastic modulus compare well with the experimental data in all thermal regimes. Thus, another modeling technique enables ICAN to serve as a preliminary design tool for cloth/woven fabric structures.

LAMINATE  
CONFIGURATION  
[A/B/D/C/A/D/C/B<sub>2</sub>/A/B<sub>2</sub>/C/D/A/C/D/B<sub>1</sub>A]



19 PLIES OF E GLASS

A — 7576E GLASS 0 PLY  
B — 7781E GLASS 0 PLY  
C — 7781E GLASS +30° PLY  
D — 7781E GLASS -30° PLY



$$FVR_{0 \text{ ply}} = FVR_{\text{cloth}}$$

(FIBERS IN WARP DIRECTION  
LARGEST AMOUNT OF FIBERS  
IN ANY DIRECTION)

$$FVR_{90^\circ \text{ ply}} = FVR_{\text{cloth}}$$

(FIBERS IN FILL DIRECTION  
LARGEST AMOUNT OF FIBERS  
IN ANY DIRECTION)

$$t_{0 \text{ ply}} = t_{\text{cloth ply}} \times$$

(FIBERS IN WARP DIRECTION  
TOTAL FIBERS IN CLOTH PLY)

$$t_{90^\circ \text{ ply}} = t_{\text{cloth ply}} \times$$

(FIBERS IN FILL DIRECTION  
TOTAL FIBERS IN CLOTH PLY)

CD-88-32970

### COMPARISON OF RESULTS

| LAMINATE MATERIAL                 | EXPERIMENTAL |       |        | ICAN PREDICTIONS |       |        |
|-----------------------------------|--------------|-------|--------|------------------|-------|--------|
|                                   | -300 °F      | 70 °F | 200 °F | -300 °F          | 70 °F | 200 °F |
| LONGITUDINAL ELASTIC MODULUS, ksi |              |       |        |                  |       |        |
| 7781E-GLASS CLOTH                 | 4600         | 4370  | 3970   | 4589             | 4251  | 4076   |
| 7576E-GLASS CLOTH                 | 6540         | 6020  | 6050   | 5587             | 5395  | 5457   |
| REPRESENTATIVE                    | 5320         | 4370  | 4150   | 4440             | 4114  | 3948   |

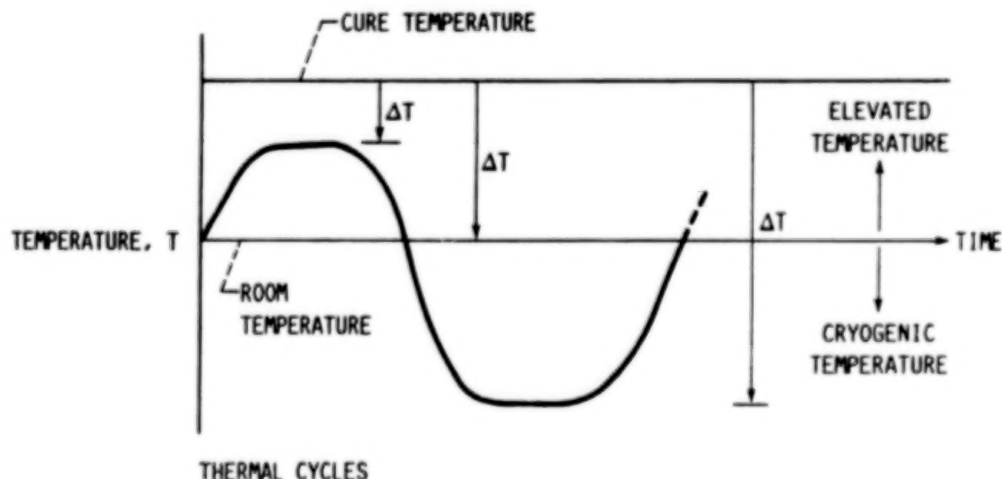
CD-88-33283

## ICAN SIMULATION OF THERMAL FATIGUE

As composites are incorporated in the designs of more complex structures, a major and continuing concern is the accurate prediction of the structural durability and damage tolerance of these structures in service environments. Of major concern is temperature, moisture, and mechanical loads, both static and cyclic. Prior to any service environment, a composite usually has endured one thermal cycle resulting from the fabrication process in which the room-temperature resin composite is cured at a rather high temperature of 350 °F. Then the extreme service environment can consist of either high temperatures or cryogenic temperatures, or both, as is the case of an orbiting satellite which encounters high temperatures when facing the sun and low temperatures when behind the Earth. The resin (matrix) is most susceptible to damage from the thermal cycling. This damage takes the form of transply cracks (referred to as microcracking in the literature) which degrade the properties, thereby affecting the structural durability.

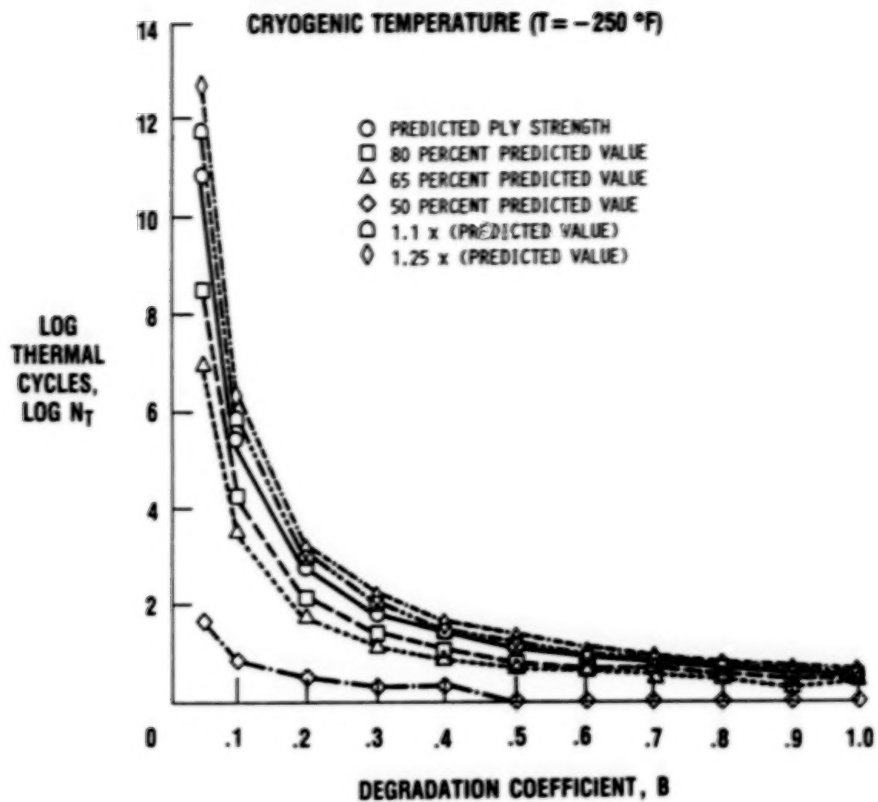
To address these critical issues, a predictive model has been formulated that yields the number of thermal cycles (N) to initial transply cracking. The model requires material properties, service conditions, and an empirical value B which is discussed in detail in Chamis and Sinclair (1982). The useful information from the model, as plotted below, will aid designers in making a life assessment for composite structures. In addition, one can also conduct a sensitivity analysis wherein the number of thermal cycles N is based on various composite strengths. As discussed earlier, accurate properties are often not available; therefore, with this analysis, designers can plan their designs within an acceptable range.

This is one of the most recently added features to the ICAN program and although it has not been validated by experimental data, there are plans to do so.

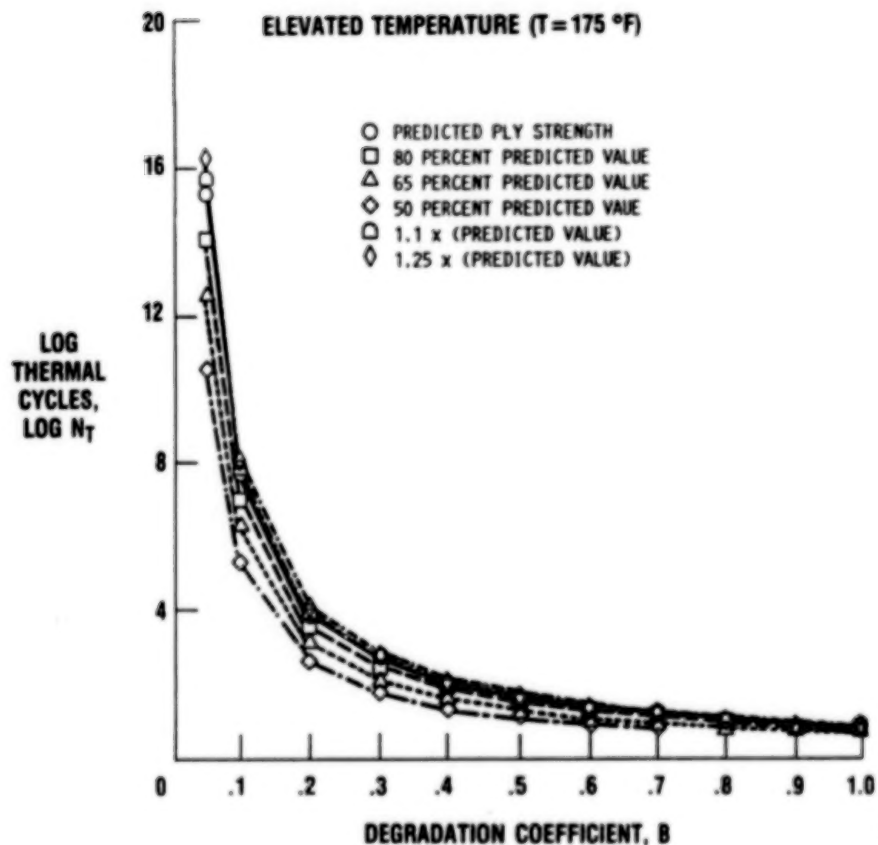


$$\log N_T = \frac{1}{B} \left[ \left( \frac{T_{GW} - T}{T_{GD} - T_0} \right)^{1/2} - \frac{\sigma_{L22CYC}}{S_{LYY0}} \right]$$

$\sigma_{L22CYC}$  = MAXIMUM TRANSVERSE PLY STRESS AT  $\Delta T$  TO YIELD  
MAXIMUM ( $\sigma_{L22CYC}/S_{LYY0}$ ) RATIO



CD-86-33377



CD-86-33378

## REFERENCES

- Chamis, C.C., 1971, "Computer Code for the Analysis of Multilayered Fiber Composites - User's Manual." NASA TN D-7013.
- Chamis, C.C., and Sinclair, J.H., 1982 "Composite Materials: Testing and Design." I.M. Daniel, ed., ASTM-STP-787, ASTM, Philadelphia, pp. 498-512.
- Chamis, C.C., and Sinclair, J.H., 1983, "INHYD: Computer Code for Intraply Hybrid Composite Design." NASA TP-2239.
- Ginty, C.A., and Chamis, C.C., 1986, "ICAN: A Versatile Code for Predicting Composite Properties." NASA TM-87334.
- Ginty, C.A., and Chamis, C.C., 1988, "Hygrothermomechanical Fiber Composite Fatigue: Computational Simulation." NASA TM-100840.
- Ginty, C.A., and Endres, N.M., 1986, "Composite Space Antenna Structures: Properties and Environmental Effects." NASA TM-88859.
- Murthy, P.L.N., and Chamis, C.C., 1984 "ICAN: Integrated Composites Analyzer." NASA TM-83700.

## THREE-DIMENSIONAL INELASTIC APPROXIMATE ANALYSIS CODE (MOMM)

Jeffrey P. Meister\*  
Sverdrup Technology, Inc.  
Lewis Research Center Group  
NASA Lewis Research Center

### ABSTRACT

The Mechanics of Materials Model (MOMM) is one of a series of new stand-alone three-dimensional nonlinear structural analysis codes developed under the Three-Dimensional Inelastic Analysis Methods Program. The primary goal of the program was to address the need for more efficient and accurate three-dimensional structural analysis procedures for hot-section engine components. General-purpose finite element computer codes containing a variety of inelastic material models have been available for more than a decade. Incorporation of such codes into the hot-section design process has been severely limited by the high costs associated with such analyses and the difficulties encountered in properly defining the nature of the problem under consideration by using such codes.

The initial development of the Mechanics of Materials Model was conducted by United Technologies Research Center under the direction of NASA Lewis Research Center as a part of the Hot Section Technology Program. MOMM is a stiffness-method finite element code that uses an internally generated network of beams to characterize hot-section component behavior. The method was proposed as a fast, easy to use, computationally efficient tool for approximate analyses. The code is intended for applications during early phases of component design. MOMM incorporates a wide variety of analysis capabilities, material models, and load type specifiers instrumental for the analysis of hot-section components.

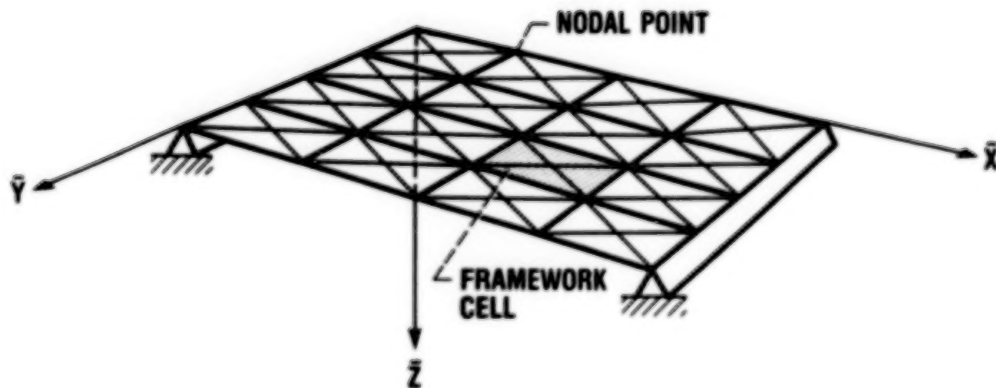
---

\*Work performed on-site at the Lewis Research Center for the Structural Mechanics Branch.



## FRAMEWORK REPRESENTATION OF A CONTINUOUS SURFACE

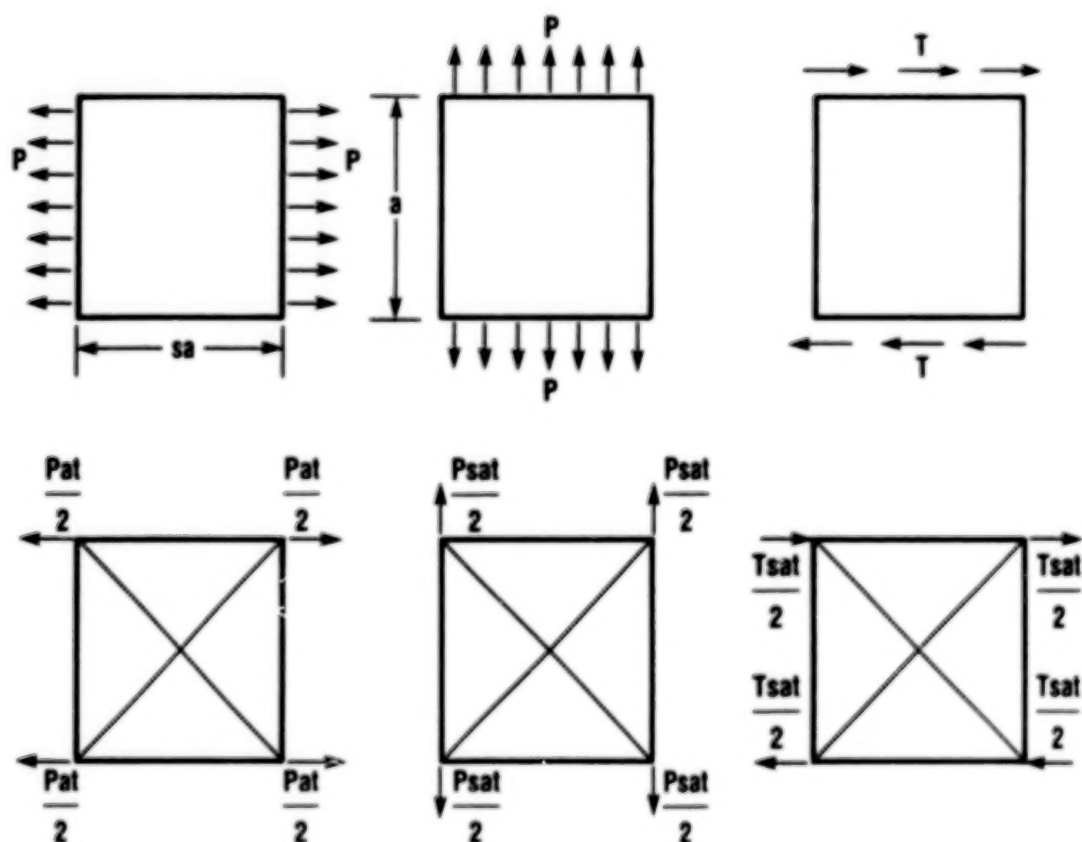
The Mechanics of Materials Model represents a continuous surface structure by a network of beams, thus reducing the elastomechanics of a continuous surface structure to the analysis of a beam or grid network. The substitute beam network is internally generated by using concepts derived from the framework method. A six-beam structure, called a framework cell, is the basic building block of the framework method. The user inputs the four nodes defining the framework cell, the thickness of the continuum, and the material properties of the continuum, and MOMM generates the appropriate substitute beam network.



CD-88-31911

# SIMULATION OF IN-PLANE DEFORMATION

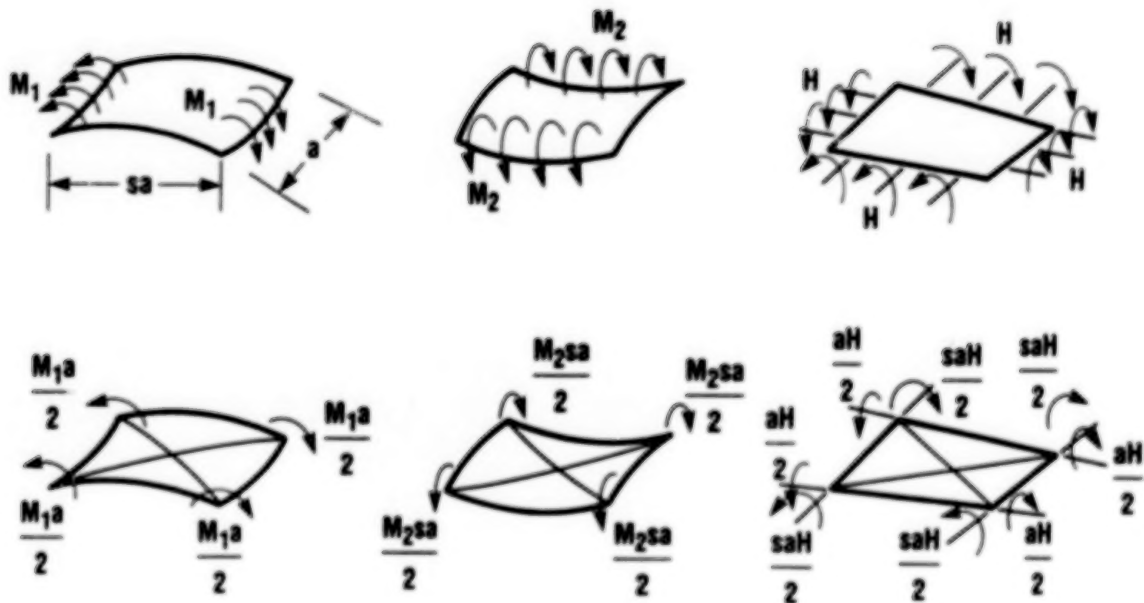
The in-plane deformation of the framework cell is controlled by the cross-sectional area of the beam members composing the framework cell. The cross-sectional areas of the beam members are determined by equivalencing the nodal displacements of a plate subject to states of constant stress and a framework cell subject to statically equivalent nodal forces. Thus the framework method solution will converge upon the exact solution for the generalized load case as the mesh is refined and the stress acting upon the individual cells approaches a state of constant stress.



CD-88-31912

# SIMULATION OF PLATE BENDING

The bending behavior of the framework cell is controlled by the cross-sectional moments of inertia of the cells' beam members. These moments are determined by equivalancing the nodal displacements of a plate subject to constant edge moments and a framework cell subject to statically equivalent nodal forces. Thus the framework method solution will converge upon the exact solution for the generalized load case as the mesh is refined and as the edge moments acting upon the individual framework cells converge to a constant state.



CD-88-31913

## ANALYSIS CAPABILITIES AND LOAD TYPES

The Mechanics of Materials Model contains a variety of useful analysis capabilities; these include static analysis capabilities, transient analysis capabilities using Newmark's integration scheme, and buckling and frequency analysis capabilities using eigenvalue extraction techniques on either the initial or the tangent stiffness matrix. A wide variety of load types may also be prescribed by using MOMM; these include applied loads (concentrated loads, line loads, pressure loads, centrifugal loads), enforced displacements, and thermal loads.

### ANALYSIS CAPABILITIES

- **STATIC**
- **TRANSIENT—NEWMARK INTEGRATION SCHEME**
- **FREQUENCY—EIGENVALUE EXTRACTION USING INITIAL OR TANGENT STIFFNESS**
- **BUCKLING—EIGENVALUE EXTRACTION USING INITIAL OR TANGENT STIFFNESS**

### LOAD TYPES

- **APPLIED LOADS**
  - **CONCENTRATED LOADS**
  - **LINE LOADS**
  - **PRESSURE LOADS**
  - **CENTRIFUGAL LOADS**
- **ENFORCED DISPLACEMENTS**
- **THERMAL LOADS**

CD-88-31914

## CONSTITUTIVE MODELS

The Mechanics of Materials Model contains three material models with varying levels of sophistication. The first model, called the Simplified Material Model, assumes a bilinear stress-strain response and generally glosses over the complications associated with strain rate effects. The second model, called the State-of-the-Art Material Model, partitions time-independent (plasticity) and time-dependent (creep) phenomena in the conventional manner, invoking Mises yield criteria and standard (isotropic, kinematic, combined) hardening rules for plasticity and a steady-state power law for creep. The third and most sophisticated model, called the Modified Walker's Model, is a modified version of Walker's viscoplastic model. This model accounts for the interaction between creep and plasticity that occurs under cyclic loading conditions.

- **SIMPLIFIED MATERIAL MODEL**

- **USES BILINEAR STRESS-STRAIN CURVE BASED UPON ELASTIC MODULUS AND HARDENING SLOPE**

- **STATE-OF-THE-ART MATERIAL MODEL**

- **ELASTIC-PLASTIC-CREEP STRAIN DECOMPOSITION**
- **STEADY-STATE POWER LAW CREEP MODEL**
- **PLASTICITY MODEL CONTAINS ISOTROPIC AND KINEMATIC HARDENING**

- **MODIFIED WALKER'S MODEL**

- **UNIFIED VISCOPLASTIC MODEL**
- **ACCOUNTS FOR INTERACTION OF CREEP AND PLASTICITY UNDER CYCLIC LOADING**

CD-88-31915

## NONLINEAR SOLUTION ALGORITHM

The Mechanics of Materials Model contains an efficient solution algorithm. The stiffness matrix is constructed only once and all stiffness changes and inelastic strains are incorporated in a residual load vector. Convergence is satisfied if the relative difference between the internal stress resultant and the externally applied load is within the user-specified tolerance.

- **STIFFNESS MATRIX CONSTRUCTED ONCE—STIFFNESS CHANGES AND INELASTIC STRAINS INCORPORATED IN RESIDUAL-LOAD VECTOR**

$$K \Delta u = \Delta P + P - F + I$$

**K** GLOBAL STIFFNESS MATRIX  
 **$\Delta u$**  INCREMENTAL DISPLACEMENT  
 **$\Delta P$**  INCREMENTAL LOAD  
**P** CUMULATIVE LOAD, INCLUDING  $\Delta P$   
**F** INTERNAL STRESS RESULTANT DUE TO **P**  
**I** RESIDUAL LOAD DUE TO INELASTIC STRAINS

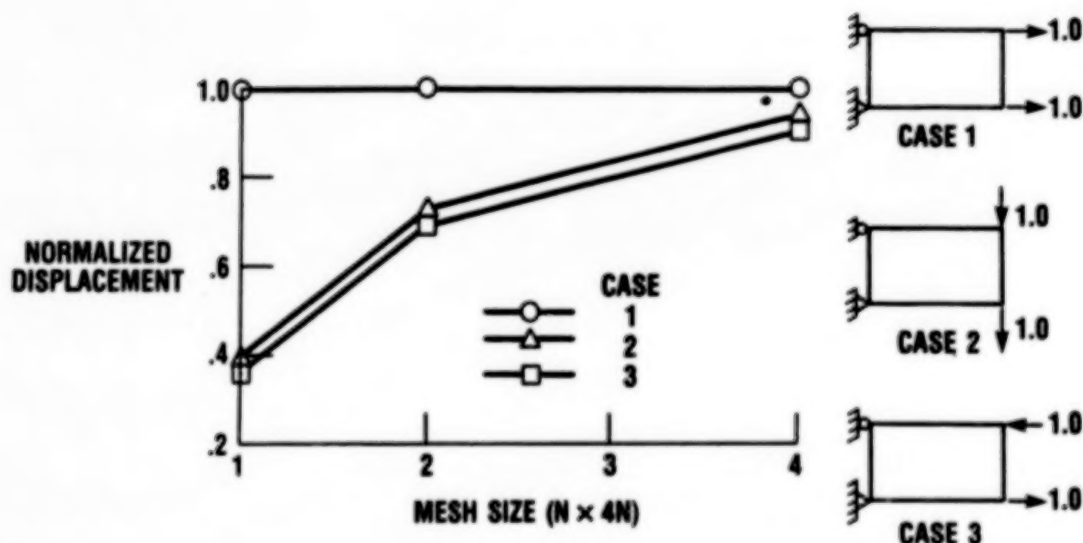
- **CONVERGENCE SATISFIED IF INTERNAL STRESS RESULTANT BALANCES EXTERNALLY APPLIED LOADS**

$$\frac{|P| - |F|}{|P|} < \text{TOLERANCE}$$

CD-88-31916

# MESH SIZE SENSITIVITY - CANTILEVERED PLATE

A cantilevered plate subject to three in-plane load cases was analyzed by using the Mechanics of Materials Model in order to investigate the codes ability to model in-plane deformation. In load case 1 the plate was subjected to an axial load, which induces a state of constant stress. As illustrated in the results shown below, the MOMM solution was equal to the exact solution for all mesh sizes analyzed. The high accuracy of these results should be expected since the framework method was formulated to characterize the behavior of a plate subjected to a constant stress state. In load cases 2 and 3 the plate was subjected to a vertical shear force and a force couple. As illustrated below, the MOMM solution approached the exact solution as the mesh was refined.

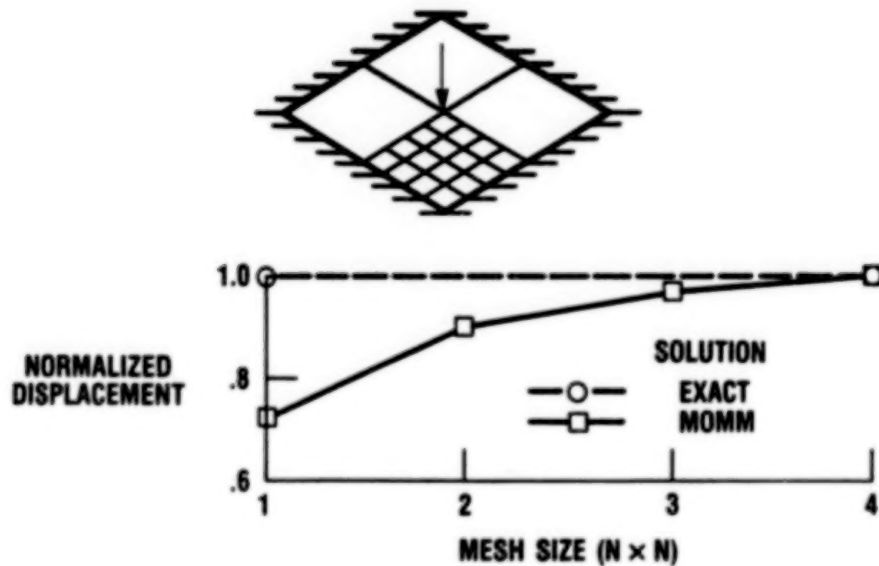


CD-88-31917



### MESH SIZE SENSITIVITY - CLAMPED PLATE

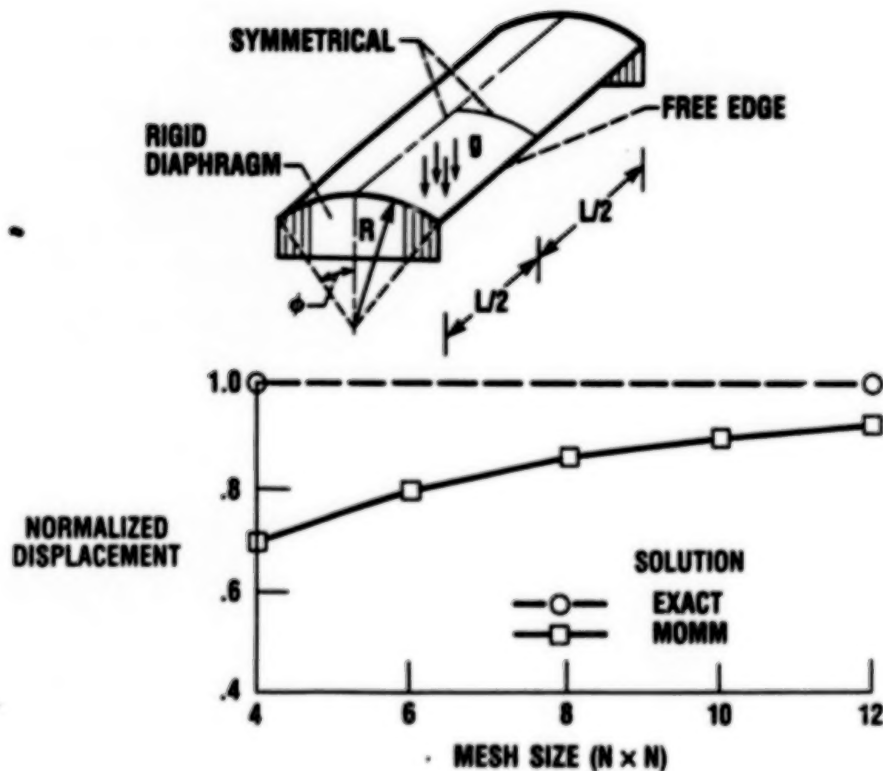
A clamped plate subjected to a transverse load was analyzed by using the Mechanics of Materials Model in order to investigate its ability to model bending. A concentrated load was applied at the plate's center, and because of symmetry only one-quarter of the plate was modeled. As illustrated in the graph shown below, the MOMM solution converged upon the exact solution with minimal mesh refinement.



CD-88-31918

# MESH SIZE SENSITIVITY - CYLINDRICAL SHELL ROOF

A cylindrical shell roof loaded by its own weight was analyzed in order to investigate the ability of the Mechanics of Materials Model to model combined in-plane deformation and bending. The shell roof was supported by rigid diaphragms, and only one-quarter of the structure was modeled because of symmetry. Membrane and bending deformations both contribute significantly to this problem. As shown below, the Mechanics of Materials Model Solution approaches the exact solution at a slow rate of convergence, reflecting the framework cells' weakness in modeling in-plane bending.



CD-88-31919

## **SPECIALTY THREE-DIMENSIONAL FINITE ELEMENT ANALYSIS CODES**

Joseph J. Lackney\*  
Sverdrup Technology, Inc.  
(Lewis Research Center Group)  
NASA Lewis Research Center

### **ABSTRACT**

General-purpose finite element computer codes that can model inelastic material behavior have been available for more than a decade. However, these codes have not been accurate enough for use in analyzing hot-section engine components. To correct this problem, General Electric developed a series of nine new stand-alone computer codes for NASA. Because of the large temperature excursions associated with hot-section engine components, these codes have been designed to accommodate broad variations in material behavior, including plasticity and creep. The capabilities of these computer codes are summarized here.

---

\*Work performed on-site at the Lewis Research Center for the Structural Mechanics Branch.

## OBJECTIVE

Under a two-year program at the General Electric Company, a series of three-dimensional inelastic structural analysis computer codes were developed and delivered to NASA. The objective of this program was to develop analytical methods capable of evaluating the cyclic time-dependent inelasticity that occurs in hot-section engine components. Because of the large temperature excursions associated with hot-section engine components, the techniques developed had to be able to accommodate broad variations in material behavior, including plasticity and creep (McKnight et al., 1986). To meet this objective, a matrix consisting of three constitutive models and three element formulations was developed. A separate program for each combination of constitutive model and element formulation was written, making a total of nine programs. The source codes of the nine programs range in size from 7300 lines for the Bodner 20-node code to 19 000 lines for the Haisler-Allen nine-node code. The table below shows the length of each source code. All of the codes were given a stand-alone capability of performing cyclic nonlinear analysis.

| Constitutive models | Element formulation |        |        |
|---------------------|---------------------|--------|--------|
|                     | 20-Node             | 8-Node | 9-Node |
| Simple              | 8300                | 13,800 | 17,900 |
| Classical           | 9200                | 16,300 | 19,000 |
| Unified             | 7300                | 13,800 | 17,600 |

## CONSTITUTIVE MODELS

The three constitutive models are a simple model, a classical model, and a unified model. In an inelastic analysis the simple model uses a bilinear stress-strain curve to determine the plastic strain and a power law equation to obtain the creep strain. The second model is the classical model of Allen and Haisler (1981). The third model is the unified model of Bodner, et al. (1979). The attributes of the three constitutive models are shown below. All of the models were programmed for a linear variation of loads and temperatures, with the material properties being temperature dependent.

| Simple   | Classical  | Unified   |
|--|--|---|
| <ul style="list-style-type: none"><li>• Uncoupled plasticity and creep</li><li>• Plasticity<ul style="list-style-type: none"><li>Isotropic hardening</li><li>Piecewise linear stress-strain curves</li><li>Prandtl-Reuss flow rule</li></ul></li><li>• Creep<ul style="list-style-type: none"><li>Steady state</li><li>Isotropic hardening</li><li>Prandtl-Reuss flow rule</li><li>Nonisothermal</li></ul></li></ul> | <ul style="list-style-type: none"><li>• Uncoupled plasticity and creep</li><li>• Plasticity<ul style="list-style-type: none"><li>Combined isotropic and kinematic hardening</li><li>Piecewise linear stress-strain curves</li><li>Modified Prandtl-Reuss flow rule</li></ul></li><li>• Creep<ul style="list-style-type: none"><li>Steady state</li><li>Isotropic hardening</li><li>Prandtl-Reuss flow rule</li><li>Nonisothermal</li></ul></li></ul> | <ul style="list-style-type: none"><li>• Coupled plasticity and creep</li><li>Isotropic hardening</li><li>No yield surface</li></ul> |

CD-88-31663

## ELEMENT FORMULATIONS

The three element formulations available are an 8-node isoparametric shell element, a 9-node shell element, and a 20-node solid element. Both of the shell elements are obtained by degenerating three-dimensional isoparametric solid elements and then imposing the necessary kinematic assumptions in connection with a thin shell. The eight-node element uses serendipity shape functions for interpolation and Gaussian quadrature for numerical integration. The nine-node element uses Lagrange shape functions and Simpson's rule for numerical integration. The 20-node solid element uses Gaussian quadrature for integration. The attributes of these elements are listed below.

| 8-Node shell  | 9-Node shell   | 20-Node solid   |
|---|--|---|
| <ul style="list-style-type: none"><li>• Five DOF<br/>3 displacements<br/>2 rotations</li><li>• Serendipity shape functions</li><li>• No rotational stiffness about normal to midsurface. Deleted before assembly</li><li>• Isotropic or orthotropic elastic properties</li><li>• Surface, line, nodal, rotational, thermal, and gravity loads</li><li>• Prescribed displacements</li><li>• Gaussian quadrature used for numerical integration</li></ul> | <ul style="list-style-type: none"><li>• Five DOF<br/>3 displacements<br/>2 rotations</li><li>• Lagrange shape functions</li><li>• Rotation about normal to midsurface treated as a prescribed displacement</li><li>• Isotropic or orthotropic elastic properties</li><li>• Surface, line, nodal, rotational, thermal, and gravity loads</li><li>• Prescribed displacements</li><li>• Simpson's rule used for numerical integration</li></ul> | <ul style="list-style-type: none"><li>• Three DOF<br/>(3 displacements)</li><li>• Isotropic or orthotropic elastic properties</li><li>• Surface, nodal, rotational, thermal, and acceleration loads</li><li>• Prescribed displacements</li><li>• Gaussian quadrature used for numerical integration</li></ul> |

CD-88-31664

## INPUT FEATURES AND ANALYSIS TECHNIQUES

To analyze structures with linear material behavior, the nine codes use a blocked-column-skyline, out-of-core equation solver. To analyze structures with nonlinear material behavior, the codes use an initial stress iterative scheme. To increase the convergence rate of the iterative scheme, Aitken's acceleration scheme was incorporated into the codes.

The ability to model piecewise linear load histories was written into the codes. Since the inelastic strain rate can change dramatically during a linear load history, a dynamic time-incrementing procedure was included. The maximum inelastic strain increment, the maximum stress increment, and the maximum rate of change of the inelastic strain rate are the criteria that control the size of the time step. The minimum time step calculated from the three criteria is the value that is used.

In dynamic analysis the eigenvectors and eigenvalues can be extracted by using either the determinant search technique or the subspace iteration method. These methods are only included with those finite element codes containing the eight-node shell element. The table below lists the features of the nine codes.

| Feature <sup>a</sup>                           | Model           |    |    |           |    |    |         |    |    |
|--|-----------------|----|----|-----------|----|----|---------|----|----|
|  | Simple          |    |    | Classical |    |    | Unified |    |    |
|  | Number of nodes |    |    |           |    |    |         |    |    |
|  | 8               | 9  | 20 | 8         | 9  | 20 | 8       | 9  | 20 |
| Free format data input                         | x               | x  | x  | x         | x  | x  | x       | x  | x  |
| Global coordinate system                       |                 |    |    |           |    |    |         |    |    |
| Cartesian                                      | x               | x  | x  | x         | x  | x  | x       | x  | x  |
| Spherical                                      | x               | x  | na | x         | x  | na | x       | x  | na |
| Cylindrical                                    | x               | x  | na | x         | x  | na | x       | x  | na |
| Local coordinate system                        |                 |    |    |           |    |    |         |    |    |
| Cartesian                                      | x               | x  | x  | x         | x  | x  | x       | x  | x  |
| Spherical                                      | x               | x  | na | x         | x  | na | x       | x  | na |
| Cylindrical                                    | x               | x  | na | x         | x  | na | x       | x  | na |
| Automatic generation of nodal coordinates      | x               | x  | na | x         | x  | na | x       | x  | na |
| Automatic generation of element connectivities | x               | x  | na | x         | x  | na | x       | x  | na |
| Restart capability                             | x               | x  | x  | x         | x  | x  | x       | x  | x  |
| Dynamic allocation                             | x               | x  | x  | x         | x  | x  | x       | x  | x  |
| Blocked-column-skyline equation solver         | x               | x  | x  | x         | x  | x  | x       | x  | x  |
| Initial stress iterative scheme                | x               | x  | x  | x         | x  | x  | x       | x  | x  |
| Aitken's acceleration scheme                   | x               | x  | x  | x         | x  | x  | x       | x  | x  |
| Dynamic time incrementing                      | x               | x  | x  | x         | x  | x  | x       | x  | x  |
| Dynamic analysis                               | x               | na | na | x         | na | na | x       | na | na |
| Material change option                         | x               | x  | x  | x         | x  | x  | x       | x  | x  |
| Element removal option                         | x               | x  | na | x         | x  | na | x       | x  | na |
| Midside node generation                        | x               | x  | na | x         | x  | na | x       | x  | na |
| Skewed coordinate system                       | x               | x  | x  | x         | x  | x  | x       | x  | x  |
| Orthotropic orientation definition             | x               | x  | x  | x         | x  | x  | x       | x  | x  |

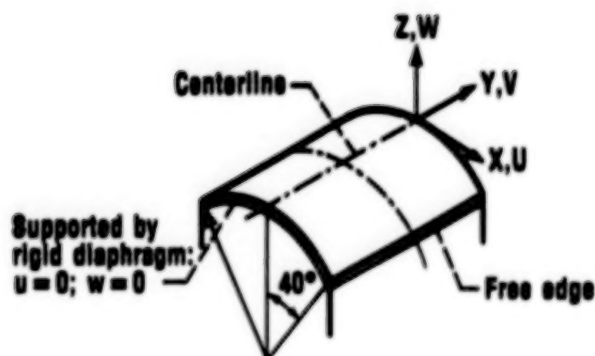
<sup>a</sup>x denotes "feature of the code"; na denotes "feature not yet available."

CD-88-31665



# CYLINDRICAL SHELL ROOF

The cylindrical shell roof shown below has frequently been used to test the behavior of shell elements. The eight-node element is compared with the four-node and eight-node elements of both MARC and NASTRAN. As can be seen from the graph the specialty eight-node finite element compares very favorably with the other elements.



CD-88-31666

#### REFERENCES

- Allen, D.H., and Haisler, W.E., 1981, "A Theory of Thermoplastic Materials, Computers and Structures," vol. 13, pp. 129-135.
- Bodner, S.A., Partom, I., and Partom, Y., 1979, "Uniaxial Cyclic Loading of Elastic-Viscoplastic Material," ASME J. Appl. Mech., vol. 46, p. 805.
- McKnight, R.L., Chen, P.C., Dame, L.T., Holt, R.V., Huang, Ho, Hortle, M., Gellin, S., Allen, D.H., and Haisler, W.E., 1986, "3-D Inelastic Analysis Methods for Hot Section Components," Turbine Engine Hot Section Technology, NASA CP-2444, pp. 257-268.

BLANK PAGE

**MHOST: AN EFFICIENT FINITE ELEMENT PROGRAM FOR INELASTIC  
ANALYSIS OF SOLIDS AND STRUCTURES**

S. Nakazawa  
Marc Analysis Research Corp.  
Palo Alto, California

**ABSTRACT**

The main objective of this development is to construct and validate an efficient finite element program for 3-D inelastic analysis of gas turbine hot section components. A novel mixed-iterative solution strategy is derived from the *augmented* Hu-Washizu variational principle in order to nodally interpolate coordinates, displacements, deformations, strains, stresses and material properties. A series of increasingly sophisticated material models incorporated in MHOST include elasticity, secant plasticity, infinitesimal and finite deformation plasticity, creep and unified viscoplastic constitutive model proposed by Walker. To detect the effects of embedded discontinuities, such as cooling channels in turbine blades, the local-global analysis procedure called *subelement iteration* is developed in the framework of mixed-iterative formulation. The performance of this numerical procedure is demonstrated in the elastic and elastic-plastic computations.

A library of high performance elements is built into this computer program utilizing the concepts of selective reduced integrations and independent strain interpolations. A strain filtering scheme based on the polar decomposition of isoparametric coordinate transformation is devised to improve the accuracy of highly distorted element shapes. The MHOST linear isoparametric elements exhibit high coarse mesh accuracy even when the element bending mode is predominant. Also included are 6 dof/node linear beam and shell elements. For Shells, a simple and efficient hourglass control mechanism is built in.

A family of efficient solution algorithms is implemented in MHOST for linear and nonlinear equation solution including the classical Newton-Raphson, modified-, quasi- and secant Newton methods with optional line search and the conjugate gradient method. Also automatic load increment control in the spirit of arc length is incorporated in the mixed-iterative solution framework. The eigenvalue extraction for the vibration mode and buckling analysis utilizes the subspace iteration method driven by the profile solution for the matrix factorizations. In addition to the conventional feature, MHOST allow users to dig into the analysis of deformation modes for the finite element model looking at the eigenstructure of stiffness matrix itself. The transient dynamic calculations are driven by the Newmark method recast in the mixed-iterative form.

The compact computer program consists of about 47,000 *Fortran 77* statements including extensive comments. To provide a comfortable user interface, a free format data reader and an industry standard formatted post processing data writer are included in the package. The portability of this program has been demonstrated on various computer systems from small engineering workstations to supercomputers.

The robustness of numerical and computational technology built in the MHOST program has served as an ideal software platform for further research and development in finite elements such as the probabilistic structural analysis methods.

---

\*Work performed under NASA Lewis Research Center Contract NAS3-23698 as a subcontractor to United Technologies Pratt and Whitney Aircrafts. Technical monitor: D. Hopkins.

## MIXED ITERATIVE FINITE ELEMENT METHOD

The new mixed finite element formulation and its iterative solution algorithms are developed in this project. This strategy enabled us to boost the performance of elements and computer programs by taking advantages of nodal stress and strain interpolations. The conventional displacement solution is used as the *preconditioner* and independent nodal interpolations for stresses and strains are introduced *iteratively* to improve the quality of numerical solution inexpensively.

The structural model is fed into the numerical computation in a usual way by constructing the stiffness matrix. The nodal strain is then calculated by a projection process which eliminates the numerical instability in strain/stress approximations such as spurious oscillations. The inelastic material models are incorporated in the nodal stress integration in a modular fashion. The resulting nodally interpolated stress field is more accurate in comparison with the conventional displacement method. This improvement is brought back into the displacement field through the equilibrium iteration loop.

The resulting control structure for linear and nonlinear computations as schematically presented in Figure 1 is similar to what is used for the nonlinear finite element analysis derived from the displacement formulation. Indeed the mixed iterative solution concept is used as an framework to derive and analyze the solution strategies for nonlinear finite element analysis.

Additional computer cost of mixed solution for linear problems is insignificant performing only a few re-solution for the same stiffness matrix with modified residual vector. The nodal strain projection is carried out utilizing the diagonalized projection operator not requiring extra matrix manipulations. No additional computation is needed when the method is used for nonlinear computations. The modern iterative solution technology based on the quasi-Newton update is incorporated to further improve the performance of this solution method.

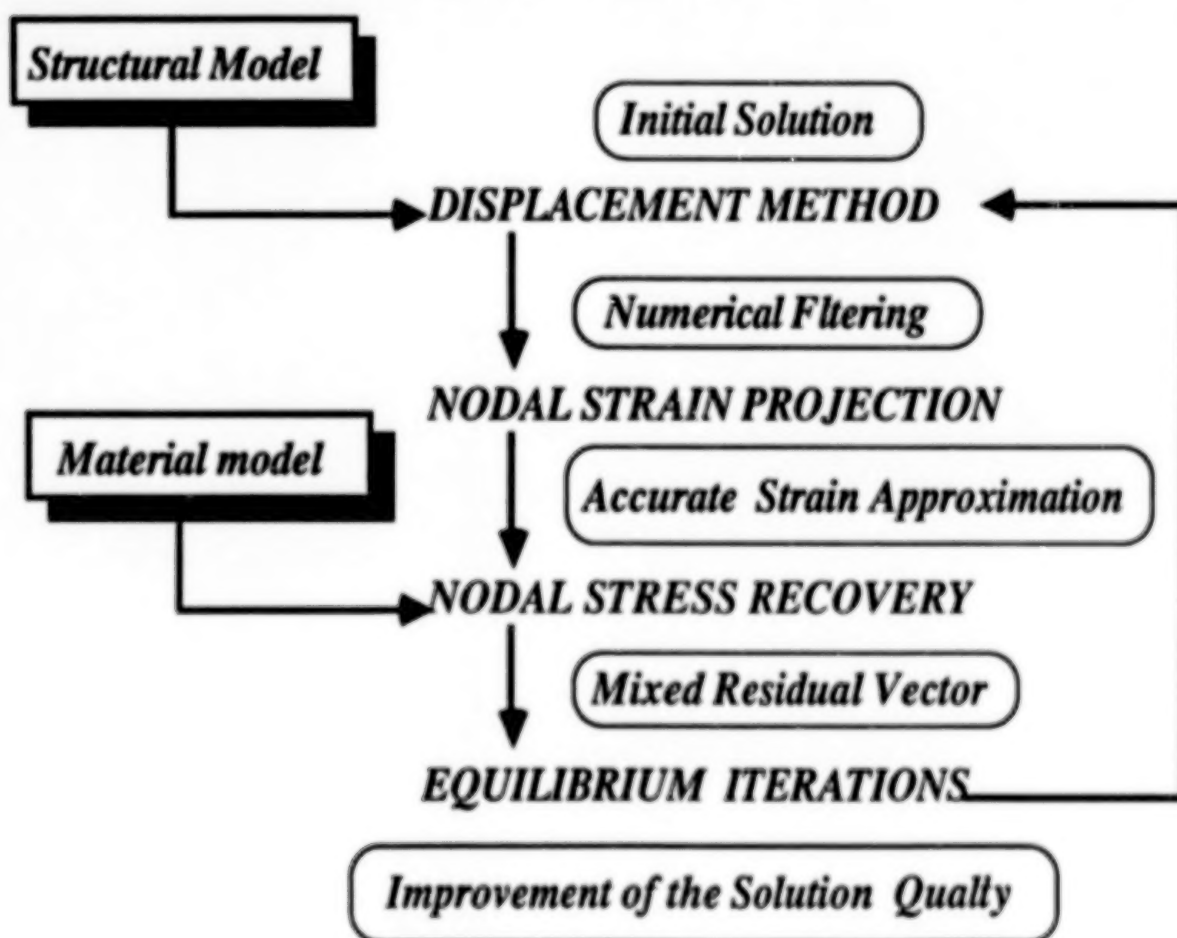


Figure 1 The Concept of Mixed-Iterative Finite Element Solution

## THE ITERATIVE SOLUTION ALGORITHMS

The system of finite element equations solved in the MHOST program is symbolically shown in Figure 2 with the equivalent mixed stiffness equations derived by direct elimination. Computationally the construction and inversion of mixed finite element equation is prohibitively expensive in terms of both computing time and the memory requirement. Hence the iterative solution algorithms are used to overcome this difficulty and make the mixed solution feasible.

The linear convergence of basic mixed iterative method is illustrated in Figure 3a. The difference of displacement and mixed stiffness matrices generates the driving residual vector for the iterations even for linear elastic problems. The quasi-Newton type update algorithms, an example illustrated in Figure 3b, improve the convergence rate of the iterative solution significantly.

In the MHOST program, other than the constant metric iteration scheme, the optional line search, the conjugate gradient, the secant implementation of Davidson rank-one quasi-Newton, BFGS rank-two quasi-Newton update algorithms are implemented. It is observed that the displacement stiffness gives steeper gradient in the load-deflection relation than the exact one whereas the mixed stiffness lies in the flexible side. Therefore the iterative solution algorithm starting from the displacement method gradually recovering the mixed solution is almost always stable and convergent.

### The Augmented Hu-Washizu Finite Element Equations

$$\begin{bmatrix} K & 0 & B^t \\ 0 & D & -C \\ B & -C^t & 0 \end{bmatrix} \begin{bmatrix} U^{n+1} \\ E \\ S \end{bmatrix} = \begin{bmatrix} F - K U^n \\ E_0 \\ 0 \end{bmatrix}$$

### Equivalent Mixed Stiffness Equations

$$(B^t C^{-1} D C^t B) U = F - D E_0$$

Figure 2 Mixed Finite Element Equations and Equivalent Stiffness Matrix

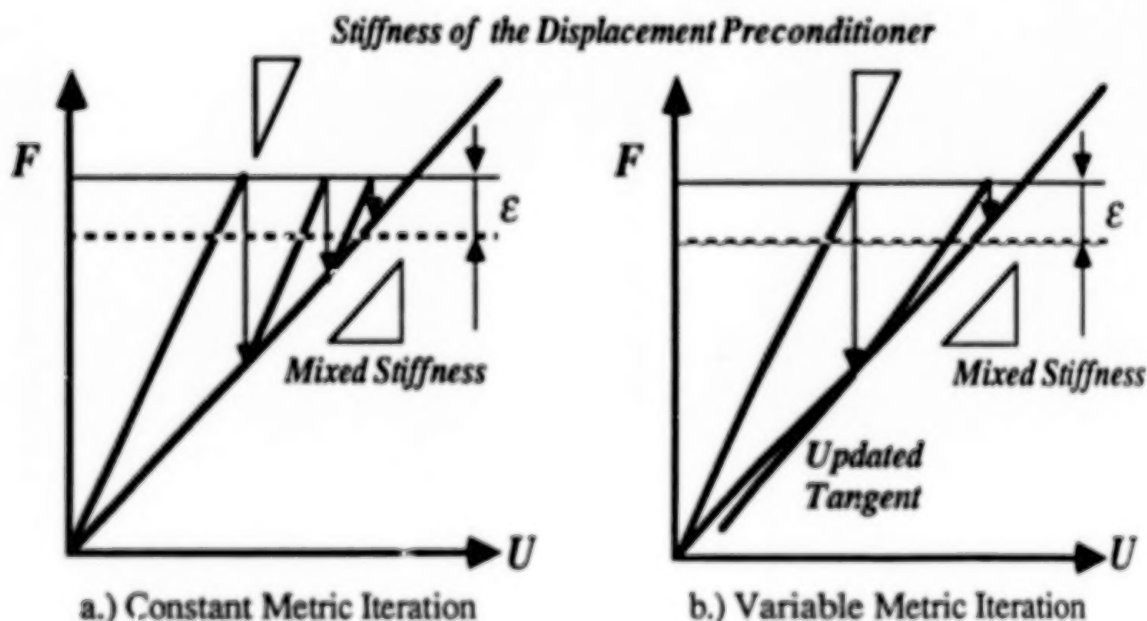


Figure 3 Convergence of Mixed Iterative Solution for a Linear Problem

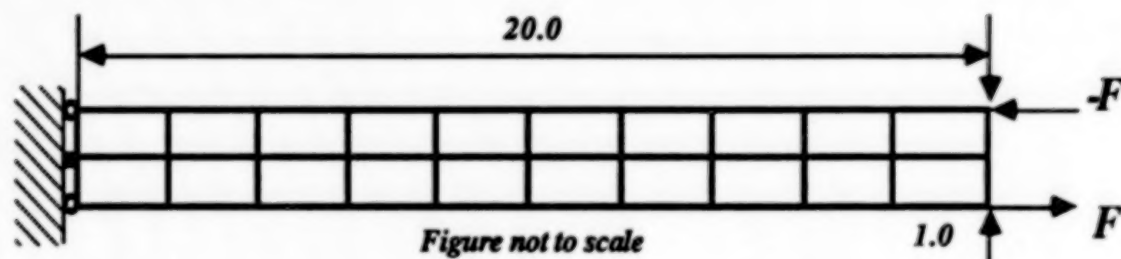


## HIGHLY ACCURATE LINEAR FINITE ELEMENTS

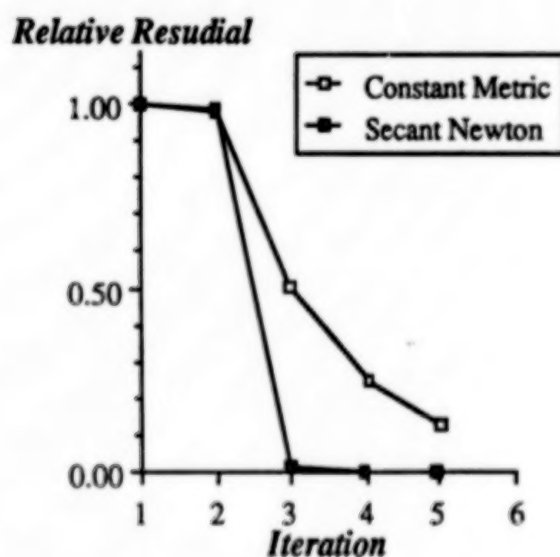
The MHOST program consists of a library of highly accurate linear quadrilateral and hexahedral elements. The selective reduced integration and assumed stress interpolation are used to improve the element responses under bending load. To take the full advantage of these formulations, a rational local coordinate transformation derived from the polar decomposition of the Jacobian matrix is developed and implemented in the code. This highly sophisticated algorithm makes the response of element insensitive to the isoparametric distortion.

For the sampling and nodal projection of element strain components, the trapezoidal integration rule is utilized for the maximum accuracy and stability. The oscillation of strain/stress fields often observed at the element integration points are filtered out by this procedure. The resulting mixed iterative finite element method is capable of producing very accurate displacement, strain and stress simultaneously.

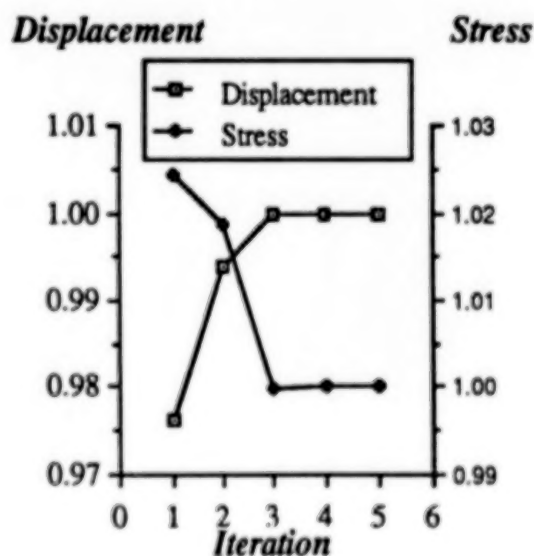
A cantilever beam modelled by the MHOST plane stress elements is used as an example to demonstrate the performance of both the methodology and the element formulation. For this simple problem, the nodally exact values are obtained for the displacement, strain and stress after a few iterations as shown in Figure 4 c). The optional acceleration algorithms such as the Davidson rank-one secant update procedure improve the convergence rate significantly over the standard constant metric scheme as typical result shown in Figure 4 b) in terms of the reduction of normalized mixed residual vector.



a) A Cantilever Beam. Plane Stress Finite Element Model.



b) Convergence of iterative Solution



c) Convergence of Nodal Solution

Figure 4 High Accuracy of MHOST Linear Quadrilateral Element



## GLOBAL-LOCAL SOLUTION BY SUBELEMENT ITERATIONS

In order to include the effects of the embedded singularities such as cooling holes and cracks without excessive mesh refinement, the subelement concept is developed in the framework of mixed-iterative solution strategy and implemented in the MHOST program. The basic idea is to set up a coarse global mesh without considering embedded singularities, but to use locally refined mesh to recover these effects in the mixed residual force calculation process. An example shown in Figure 5 illustrates the concept of this methodology. Instead of using the global mesh with the local effect (top left), a simple mesh without the local singularity is built (top right). The local effect is embedded in the regular grid (shaded area in the top right mesh) and used for the calculation of the residual force. Note that the mixed-iterative process is used in the subelement region for the given initial stress field obtained as the global solution. Under uniform traction loading, the stress at the bottom edge of the circular hole is expected to be three times larger than the uniform uniaxial stress value. In the subelement regions, the linear and quadratic elements are made available in MHOST and, in this particular example, the quadratic subelements produce significantly more accurate stress results (2.708) than the linear subelement solution (2.504). The stress calculated from the linear subelement model is slightly more accurate than the global finite element solution with a hole (2.349). In these analyses, the iterations are carried out until the relative residual value becomes below 10%.

The solution of each subelement can be performed independently and, for a multiple number of subelements, the operation can be fully parallelizable. The subelement meshes for individual global elements can be introduced based on *a posteriori* error estimate and incorporated with the adaptive refinement strategies.

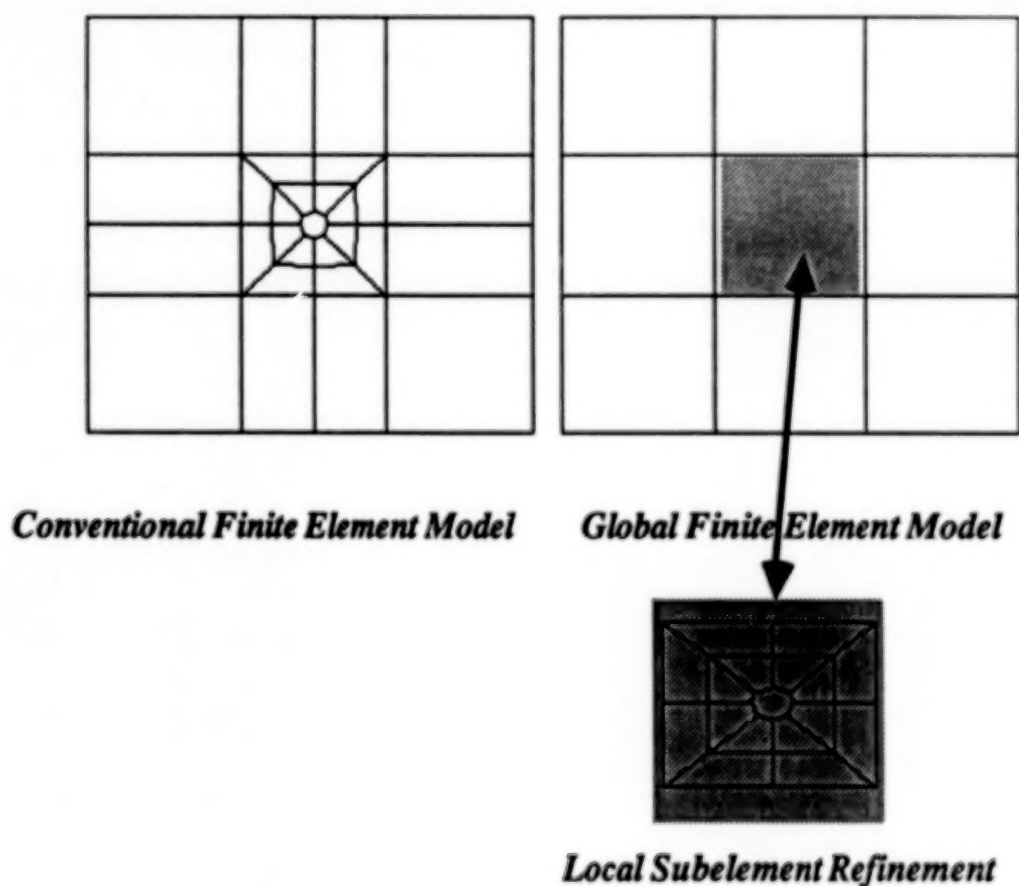


Figure 5 A Square Plate with a Circular Hole.

Global-Local Analysis by Subelement Iteration.

## THE THREE DIMENSIONAL SHELL ELEMENT

The nodally continuous stress assumption used in the beams and shells improves the accuracy of MHOST solution considerably in comparison with the conventional displacement strategies. For example, the nodally exact displacement and moment solution is obtained for a cantilever beam problem modelled by the MHOST shell element subjected to a point load in the transverse direction at the tip. This shows the capability of the mixed iterative shell formulation to capture the linear moment field exactly by using only the linear finite element basis functions.

To avoid numerical instabilities commonly observed for the four node shell elements such as the *numerical locking* and *hourglass* displacement modes, the stiffness matrix for the shell element uses the selective integration for the transverse shear terms and a simple and efficient hourglass control scheme proposed by Belytschko, Tsay and Liu (1981).

Difficulties are encountered when the intersecting shell problems are modelled by the mixed iterative finite element method, in which the continuity of stress at the intersection is no longer a valid assumption. The MHOST program provides a user with the **DUPLICATE NODE** option which allow the stress to be discontinuous at the specified interelement boundaries whereas the displacement field is kept continuous as the concept illustrated in Figure 6 (top).

An hollow shell structure, the MHOST finite element model for the wind turbine blade with an internal stiffener, is shown at the bottom of Figure 6. In this example, the **COMPOSITE** material option is also invoked, which allows the users to directly input the constitutive resultant array (D matrix defined in terms of curvature and bending moment) for anisotropic material responses.

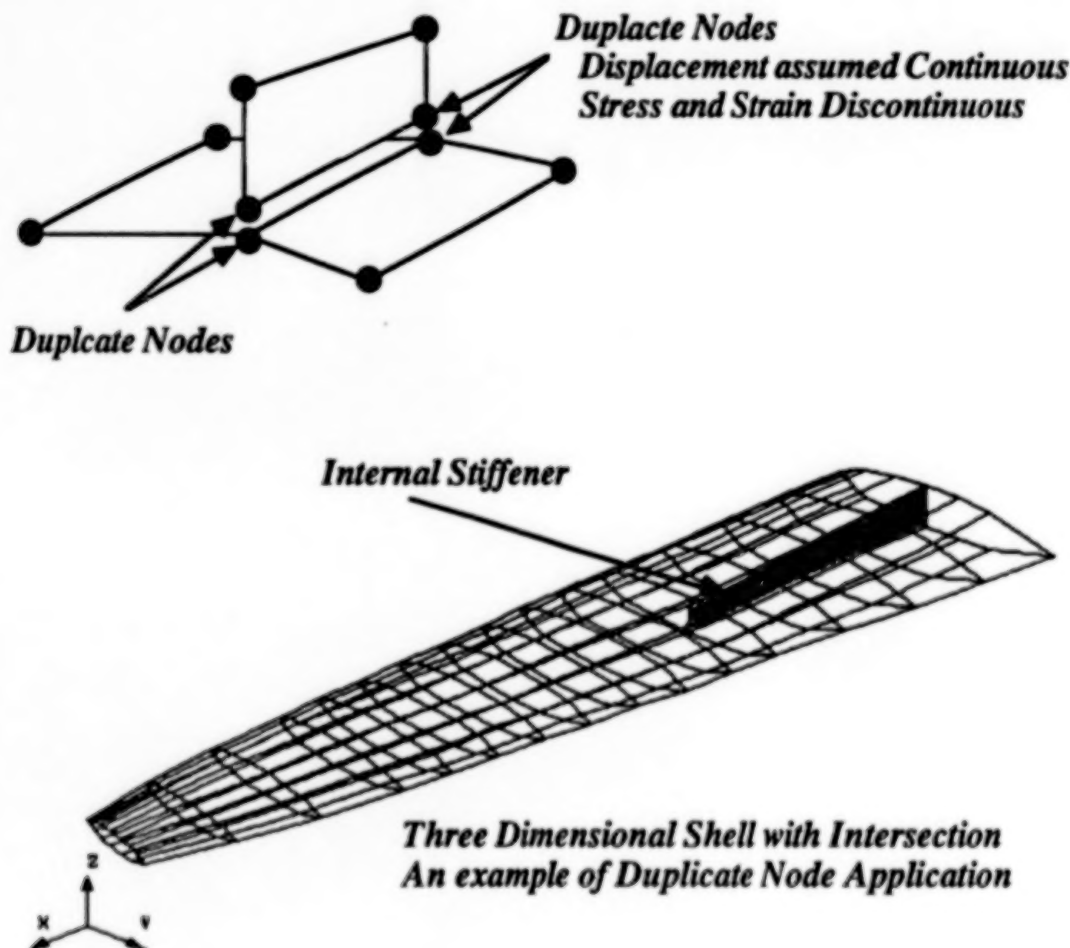


Figure 6 Treatment of Intersecting Shells in the MHOST Mixed Formulation

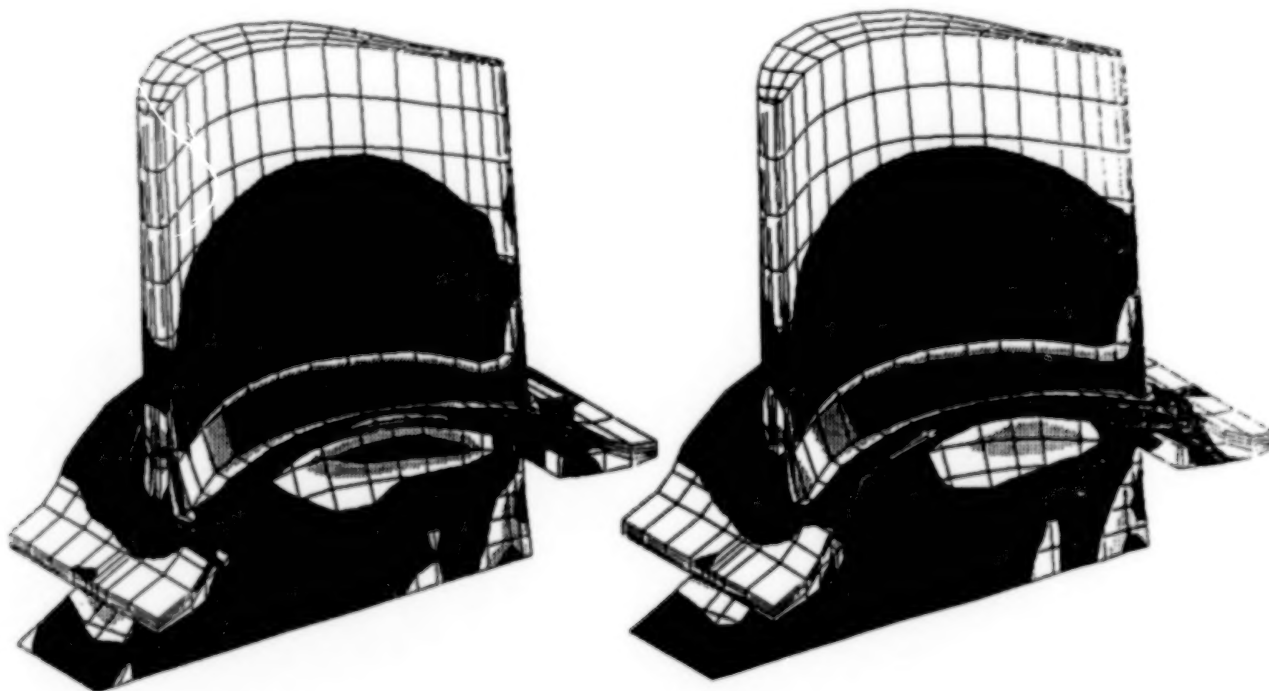
## AN EXAMPLE OF THREE DIMENSIONAL ANALYSIS

The sophisticated three dimensional element implemented in the MHOST program exhibits superior accuracy in comparison with the conventional isoparametric 8 node brick element derived directly from the displacement method formulation. The selective shear integration/assumed stress formulation in conjunction with the local coordinate transformation based on the isoparametric mapping results in a highly accurate displacement field even at the initial displacement preconditioning phase without iterative improvement. The iterative process drives the solution further toward the direction of high accuracy for the given mesh.

The three dimensional brick element implemented in the MHOST program controls the effects of parasitic shear strains when it is subjected to the bending load. When this element is used for the solution to problems in which local bending behavior is predominant (such as the burner blister specimen - a thick circular plate subjected to a intensive thermal loading from one side at the center - a typical three dimensional model uses two layers of elements through the thickness), the conventional displacement element results in a displacement 25% of the *exact solution* (obtained from extremely fine axisymmetric model) whereas the MHOST element manages to reproduce more than 90% of displacement using the same mesh.

An example shown below is a three dimensional model of the SSME HPFTP blade subjected to the thermal and centrifugal loading. This example demonstrates the improvement of the stress field by the mixed iterative process in practical applications. The stress concentrations occurring below the platform and at the leading edge of the blade are captured by the mixed-iterative solution (left), which is not so clearly visible in the displacement solution included in the same figure (right). The additional computational effort by the mixed iterations is insignificant (40% of full displacement solution for 5 extra iterations for this linear elastic problem) involving a few re-solution with the updated mixed residual vectors.

An additional advantage of the present mixed iterative formulation is that the stress is calculated, stored and reported at nodes which makes the interpretation of results and graphic post processing simple and straightforward. The MHOST program produces an industry standard post processing file which can be dealt with by most of the commercially available softwares.



a) Mixed Finite Element Solution.    b) Displacement Solution By MHOST Element

Figure 7 Three Dimensional Solid Finite Element Model of the SSME HPFTP Blade. Equivalent Mises Stress Under Thermal and Centrifugal Loading.

## MHOST ANALYSIS CAPABILITIES

As summarized in the table below, MHOST has become a versatile tool for the linear and nonlinear solid and structural analysis. Similar to the commercially available nonlinear finite element packages such as MARC and ABAQUS, the code consists of the solution algorithm library, the element library (both of which has been discussed extensively in this paper) and the constitutive equation library. The MHOST constitutive equation library consists of: (i) linear elasticity with optional temperature dependency and anisotropy definitions; (ii) simplified secant plasticity; (iii) the infinitesimal and finite deformation versions of J2 plasticity with isotropic and anisotropic yield conditions, and isotropic and kinematic hardening rules with optional temperature dependency and creep; and (iv) the unified viscoplasticity law proposed by Walker. For experienced users to be able to modify/enhance the constitutive equation library, the open ended architecture concept is implemented via user definable subroutines.

The MHOST program is written in the standard *Fortran 77* and highly portable. Currently versions are available on CRAY (COS/CFT), PRIME (PRIMOS/F77), VAX (VMS/FOR), IBM (MVS/VS- FORTRAN) and Alliant (CONCENTRIX/fortran).

Table 1 MHOST Analysis Capability

| Analysis Option                             | Beam | Plane Stress | <u>ELEMENT LIBRARY</u> |           |           |
|---|------|--------------|------------------------|-----------|-----------|
|   |      |              | Plane Strain           | 3-D Solid | 3-D Shell |
| Quasi-Static Analysis* <sup>1</sup>         | X    | X            | X                      | X         | X         |
| Buckling Analysis* <sup>1</sup>             | X    | X            | X                      | X         | X         |
| Deformation Mode Extraction* <sup>1,2</sup> | X    | X            | X                      | X         | X         |
| Modal Analysis* <sup>1</sup>                | X    | X            | X                      | X         | X         |
| Linear Dynamics                             | X    | X            | X                      | X         | X         |
| Transient Dynamics                          | X    | X            | X                      | X         | X         |

\*<sup>1</sup>The effects of the stress stiffening and the centrifugal mass may optionally included in these calculations.

\*<sup>2</sup>This option extracts the eigenvalues and eigenvectors of the stiffness matrix. The facility is particularly useful to test the element formulations and implementations. Often excessive kinematic modes are detected by this option. It may be considered as a tool complementary to the *patch test*.



## CONCLUDING REMARKS

As briefly discussed in this paper, the finite element package MHOST developed under the HOST project consists of an innovative numerical method which has turned out to be highly accurate and efficient. The implementation of the state-of-the-art numerical processes for the advanced element formulations and the constitutive integrations in this program package extends its functionality from a mere research code to an attractive alternative to the commercially available finite element programs for the serious engineering development. The heavy usage of the code indeed indicates its capability as a versatile numerical tool in the research and development environment. Also the fact that the extension of this methodology and computer program to the probabilistic structural analysis demonstrates its potential for a wide range of applications not limited to the straightforward structural analyses but as a reliable engine to extend the usage of finite elements in design environments where the nonlinear responses of the objects have started to play important roles in assessing the reliability.

The advantages of the new method has not yet been fully exploited and the drawbacks need to be identified and circumvented. The mathematics of this method has not yet fully understood. The establishment of the formal error estimates and stability criteria would help increasing the level of confidence in this class of methodology. Further utilization and users' feedback of MHOST would motivate further research and development to make this technology really fly as a robust computational mechanics method.

The iterative solution strategy implemented for the solution of the mixed finite element method has a control structure suitable for the further efficiency improvement in the vector and parallel processing environments. In the initial development of the MHOST program, the emphasis was placed on the demonstration of the concept rather than the refinement in the program development. It is now clear that the method is more suitable structured for the modern computing machineries than the traditional finite element procedures. The use of displacement stiffness matrix as a preconditioner to the mixed solution in the current implementation is the most time and memory consuming part in the entire computations, and needs critically reviewed. Modern preconditioning techniques such as the element-by-element algorithm would increase the efficiency of the mixed solution processes considerably. Also the use of relaxation techniques in the framework of mixed finite element method could potentially economize the overall solution time and memory requirement.

The coding strategy used in the MHOST program is rather traditional consisting of multiply nested loops and numerous subroutine calls. Recent programming experiments demonstrate that the unrolled short loops and the inline expansion of subroutines cuts down the redundant computing time, which had not been visible until the new high performance floating point processors emerged. To take advantages of the simplicity of the mixed iterative solution, in particular the constitutive integration operations looped over the nodes, the stress recovery subroutines would be the first one to be rewritten for the performance gain on those machines.

Also the memory allocation schemes to minimize the data transfer between cache, main memory and disk drives need to be reviewed and streamlined. The compactness of the code with full inline documentation makes the MHOST code as an ideal starting point to explore this avenue. The internal nodal database unique to the mixed-iterative code makes the memory management operations far simpler and more compact than the element database used in the displacement type codes. Indeed this was one of the major motivation behind the extension of mixed strategy to the probabilistic analysis, in which multiple number of the perturbed finite element solutions with respect to the random variables are calculated and stored in an accessible manner from the interactive probability analysis packages.

## ACKNOWLEDGEMENT

During the formulation and the computer program development carried out at MARC Analysis Research Corporation from 1983 to 1987, contributions were made by: J.C.Nagtegaal, Hibbitt, Karlsson & Sorensen, Inc.; J.B.Dias, Division of Applied Mechanics, Stanford University; M.S. Spigel, Lockheed Missile and Space, Sunnyvale. The verification effort was performed at United Technologies Pratt and Whitney Aircraft by: S.Lionberger and A.D.Fine.

## REFERENCES

- Belytschko, T., C.S. Tsay and W.K. Liu (1981), A Stabilization Matrix for Bilinear Mindlin Plate Element, *Comp. Meth. Appl. Mech. Eng.*, **29**, 313-327.
- Crisfield, M. (1986), *Finite Elements and Solution Procedures for Structural Analysis, Vol. 1: Linear Analysis*, Pineridge Press, Swansea.
- Dias, J.B. and S. Nakazawa (1988), *An Approach to Probabilistic Finite Element Analysis Using a Mixed Iterative Formulation*, Paper to be presented at ASME/SES Summer Meeting, University of California, Berkeley.
- Fortin, M. and R. Glowinski (eds.) (1982), *Methodes de Lagrangian Augmente*, Dunod, Paris.
- Nakazawa, S. (1987), *3-D Inelastic Analysis Method for Hot Section Components, Fourth Annual Status Report: Volume 1: Special Finite Element Models*, Pratt & Whitney PWA-5940-62.
- Nakazawa, S. (1986), *3-D Inelastic Analysis Method for Hot Section Components, Third Annual Status Report: Volume 1: Special Finite Element Models*, NASA CR-179694, Pratt & Whitney PWA-5940-46.
- Nakazawa, S., J.C. Nagtegaal and O.C. Zienkiewicz (1985), Iterative Methods for Mixed Finite Element Equations, (R.L. Spilker and K.W. Reed, eds.) *Hybrid and Mixed Finite Element Methods*, ASME AMD Vol. 73, pp57-67.
- Washizu, K. (1974), *Variational Methods in Elasticity and Plasticity*, Pergamon Press, Oxford.
- Wilson, R.B., M.J. Bak, S. Nakazawa and P.K. Banerjee (1984), *3-D Inelastic Analysis Methods for Hot Section Components (Base Program), First Annual Status Report*, NASA CR-174700.
- Wilson, R.B., M.J. Bak, S. Nakazawa and P.K. Banerjee (1986), *3-D Inelastic Analysis Methods for Hot Section Components (Base Program), Second Annual Status Report*, NASA CR-175060.
- Zienkiewicz, O.C., X.K. Li and S. Nakazawa (1984), Iterative Solution of Mixed Problems and the Stress Recovery Procedures, *Comm. Appl. Numer. Anal.*, **1**, 3-10.
- Zienkiewicz, O.C., X.K. Li and S. Nakazawa (1986), Dynamic Transient Analysis by Mixed, Iterative Method, *Int. J. num. Meth. Eng.*, **23**, 1343-1353.
- Zienkiewicz, O.C. and S. Nakazawa (1984), On Variational Formulation and Its Modifications for Numerical Solution, *Computer & Struct.*, **19**, 303-313.
- Zienkiewicz, O.C., J.P. Vilotte, S. Toyoshima and S. Nakazawa (1984), Iterative Methods for Constrained and Mixed Approximation. An Inexpensive Improvement of FEM Performance, *Comp. Meth. Appl. Mech. Eng.*, **51**, 3-29.

## METCAN - THE METAL MATRIX COMPOSITE ANALYZER

Dale A. Hopkins and Pappu L.N. Murthy\*  
Structural Mechanics Branch  
NASA Lewis Research Center

### ABSTRACT

Metal matrix composites (MMC) have recently been the subject of intensive study and are receiving serious consideration for critical structural applications in advanced aerospace systems. The routine application of MMC in aerospace structures will evolve as concurrent developments progress in related areas of processing and fabrication, experimental mechanics, and computational structural analysis and design methodologies. This presentation concerns recent research efforts related to the latter aspect, namely, MMC analysis and design.

Predicting the mechanical and thermal behavior and the structural response of components fabricated from MMC requires the use of a variety of mathematical models. These models, for example, relate stresses to applied forces, stress intensities at the tips of cracks to nominal stresses, buckling resistance to applied force, or vibration response to excitation forces. The models just mentioned require initial tangent and strain-dependent stress-strain relationships. Experimental data indicate that the stress-strain responses of unidirectional MMC are (1) slightly nonlinear in the longitudinal direction, (2) mildly nonlinear in the transverse direction, and (3) highly nonlinear in intralaminar shear. In-service loads on MMC structures can generally be expected to strain the metal matrix nonlinearly. The stress-strain relationships for a laminate may then become load-path dependent, and hence it is important to be able to track the composite behavior throughout its load history. Moreover, the mechanical performance and structural integrity of MMC are ultimately governed by the behavior of the constituents at a local level. In general this behavior is dynamic because of various nonlinearities associated with, for example, (1) large local stress excursions, (2) temperature-dependent material properties, (3) time-dependent effects, and (4) constituent chemical reactions. It is important also then to be able to track behavior at the local level.

This presentation describes the extensive research in computational mechanics methods for predicting the nonlinear behavior of MMC. This research has culminated in the development of the METCAN (metal matrix composite analyzer) computer code.

---

\*Cleveland State University, Civil Engineering Department, Cleveland, Ohio 44115 (work funded under NASA Grant NAG3-550; monitor, Christos C. Chamis) and NASA Resident Research Associate.



## OVERVIEW OF STRUCTURAL ANALYSIS

The process of structural analysis can be viewed simplistically as the solution of pertinent governing equations to arrive at estimates of important response variables that are usually of interest in comparison with some limiting values. This is summarized below, where the matrix notation implies solution by a discrete numerical technique such as the finite element method. Nonlinear problems are commonly approached by using a piecewise linear approximation in which the solution becomes an incremental or iterative process. Unique aspects associated with the analysis of a composite structure derive from the additional models required (1) to arrive at a description of the structure characteristics and (2) to determine the localized response, which becomes important for these systems. The additional models are collectively referred to as composite mechanics.

### SYSTEM EQUATIONS OF MOTION

$$[M] \ddot{[u]} + [C] \dot{[u]} + [K][u] = [F(t)]$$

$$\rightarrow [u] \leq [u_A]$$

### CONSTITUTIVE EQUATION

$$[\sigma] = [D][B][u]$$

$$\rightarrow [\sigma] \leq [S_A]$$

### NATURAL FREQUENCY EIGENPROBLEM

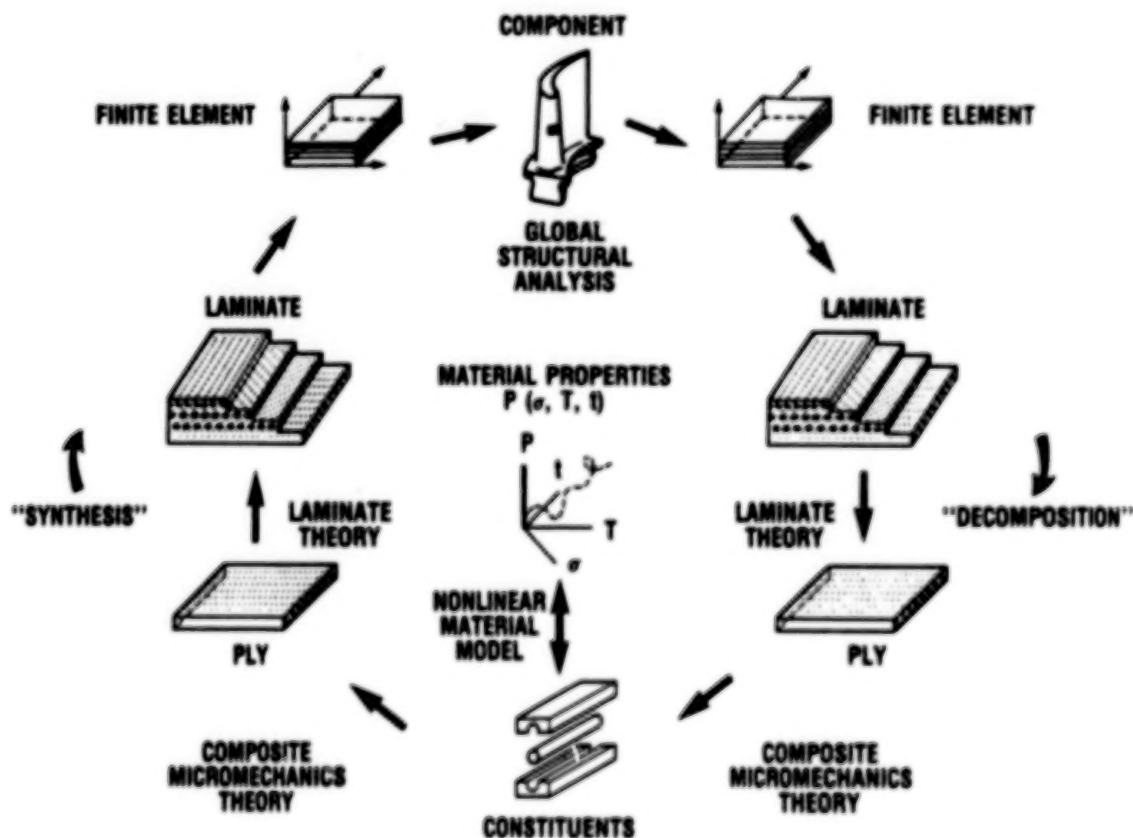
$$([K] - \omega^2[M])[u] = [0]$$

$$\rightarrow \omega \leq \omega_A$$

CD-88-32579

## INTEGRATED APPROACH TO METAL MATRIX COMPOSITE ANALYSIS

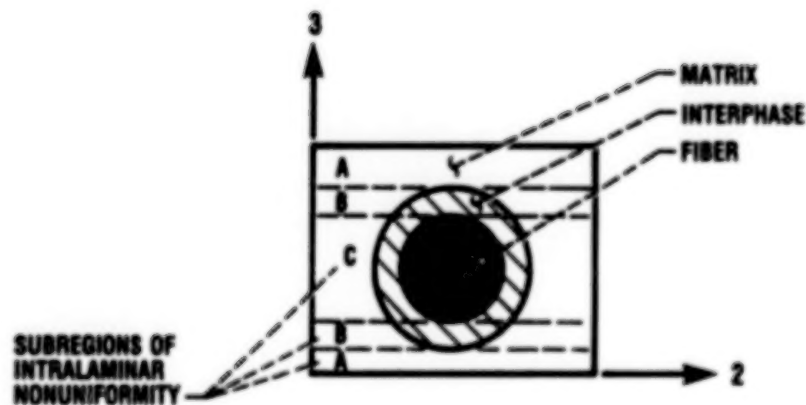
The integrated approach implemented in the METCAN computer code is illustrated in the figure. The cyclic arrangement defines the computational effort for each load increment. Material nonlinearity is treated at the constituent (fiber, matrix, interphase) level, where the current material model describes a time-temperature-stress dependence of a constituent's mechanical and thermal properties at any instant in its "material history space." Characteristic properties of the composite, at the various levels of simulation, are approximated from the instantaneous constituent properties by composite mechanics. This process, termed "synthesis" here, results in a point description of "equivalent pseudo-homogeneous" properties for the composite. These properties could be used, for example, to specify elemental properties for a subsequent global structural analysis by the finite element method. In the reverse or "decomposition" process, global response variables are "decomposed" into localized response, again at the various levels of simulation. The METCAN code, at this point, does not incorporate the global structural analysis capability, and hence "a priori" load histories are specified as part of the input to the code.



CD-88-32580

### COMPOSITE LOCAL BEHAVIOR AND RESPONSE

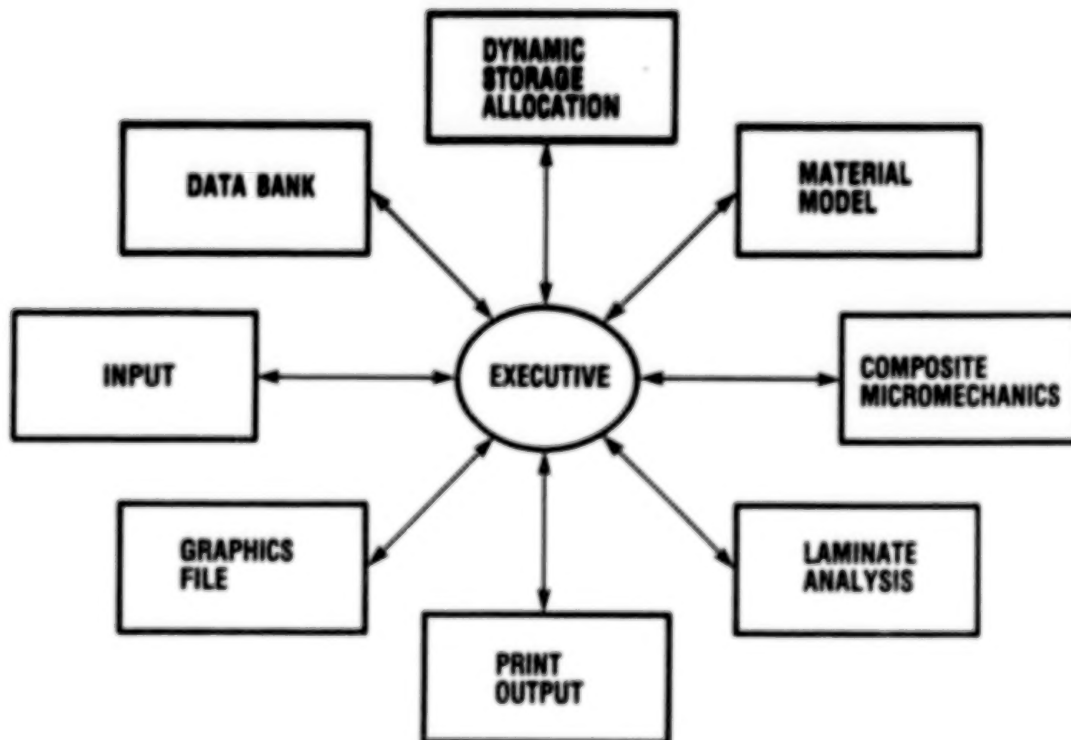
A unique feature of the METCAN computer code is its treatment of the interphase as a separate constituent. This is an important consideration for metal matrix composites in high-temperature applications where the fiber and the matrix may chemically react, forming an interphase. At the most local level constituent behavior and response variables are tracked in the three intralaminar subregions illustrated in the figure.



CD-88-32581

## MODULAR STRUCTURE OF METCAN

In developing the METCAN computer code priority has been placed on maintaining a modular software structure and providing a user-friendly interface. The code features include (1) a dynamic storage allocation scheme for efficient use of computer resources, (2) a resident data bank of constituent material properties, (3) user-selective control of primary (printed) output, (4) generation of a secondary output file for subsequent graphics postprocessing, and (5) both interactive and batch modes of operation.



CD-88-32582

## METCAN CURRENT AND FUTURE CAPABILITIES

The current capabilities of the METCAN computer code provide for most of the essential aspects of metal matrix composite analysis and design. The code also serves as a framework within which future capabilities will be developed. The current and planned future capabilities are summarized below.

- **SIMULATED BEHAVIOR AND RESPONSE**
  - MECHANICAL PROPERTIES**
  - THERMAL PROPERTIES**
  - STRESSES AND STRAINS**
  - MICROSTRESSES**
  - FRACTURE STRESSES**
  - FINITE ELEMENT COMPATIBILITY**
- **LOAD AND EFFECT**
  - MONOTONIC LOAD HISTORIES**
  - CYCLIC LOAD HISTORIES**
  - **INTERPHASE PROPERTIES AND GROWTH**
  - **STEADY-STATE CREEP**
  - **THERMAL RATCHETTING**
  - **CREEP RUPTURE**
  - **DAMAGE**
  - **THERMAL SHOCK**
  - **IMPACT LOADING**

CO-88-32583

# UNIDIRECTIONAL GRAPHITE/COPPER MMC PROPERTY PREDICTIONS

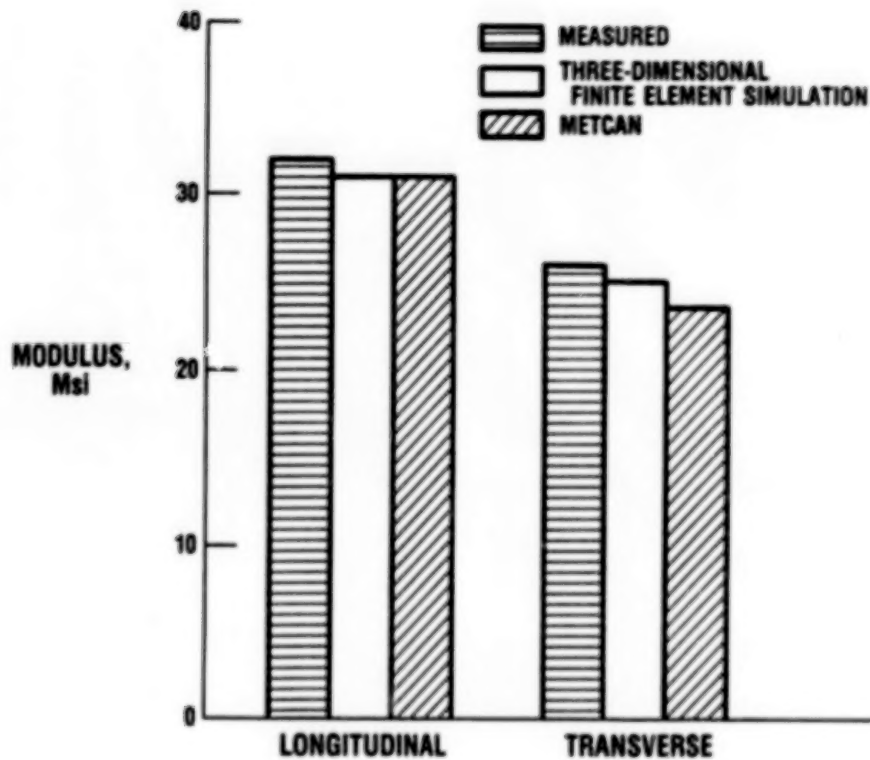
A fairly comprehensive summary of the mechanical and thermal properties for a unidirectional graphite/copper metal matrix composite at several fiber volume fractions is given in the table. The properties were determined (1) by using the METCAN computer code and (2) from a detailed three-dimensional finite element analysis in which both the fiber and the matrix were modeled discretely. The METCAN-predicted properties, based on the simplified composite mechanics equations, show excellent agreement overall with the finite-element-simulated properties.

| PROPERTY                                  | FIBER VOLUME FRACTION, PERCENT |                |        |                |        |                |
|---|--------------------------------|----------------|--------|----------------|--------|----------------|
|   | 22.3                           |                | 46.6   |                | 62.2   |                |
|   | METCAN                         | FINITE ELEMENT | METCAN | FINITE ELEMENT | METCAN | FINITE ELEMENT |
| $E_{11}$ , Msi                            | 37.3                           | 36.7           | 58.4   | 58.0           | 72.0   | 71.8           |
| $E_{22}$ , Msi                            | 10.2                           | ---            | 6.5    | ---            | 4.6    | ---            |
| $E_{33}$ , Msi                            | 10.2                           | 11.0           | 6.5    | 6.9            | 4.6    | 5.0            |
| $G_{12}$ , Msi                            | 4.5                            | 4.8            | 3.2    | 3.4            | 2.5    | 2.6            |
| $G_{23}$ , Msi                            | 4.2                            | 4.5            | 2.8    | 2.7            | 2.1    | 1.8            |
| $G_{13}$ , Msi                            | 4.5                            | ---            | 3.2    | ---            | 2.5    | ---            |
| $\nu_{12}$ , in./in.                      | 0.28                           | 0.30           | 0.25   | 0.29           | 0.24   | 0.28           |
| $\nu_{23}$ , in./in.                      | 0.30                           | 0.28           | 0.30   | 0.22           | 0.30   | 0.19           |
| $\nu_{13}$ , in./in.                      | 0.30                           | ---            | 0.30   | ---            | 0.24   | ---            |
| $\alpha_{11}$ , ppm                       | 3.8                            | 3.7            | 0.63   | 1.40           | 0.09   | 0.42           |
| $\alpha_{22}$ , ppm                       | 9.8                            | 10.9           | 9.4    | 11.1           | 9.2    | 10.9           |
| $\alpha_{33}$ , ppm                       | 9.8                            | ---            | 9.4    | ---            | 9.2    | ---            |
| $K_{11}$ , Btu in./°F hr in. <sup>2</sup> | 20.8                           | ---            | 22.0   | ---            | 22.8   | ---            |
| $K_{22}$ , Btu in./°F hr in. <sup>2</sup> | 20.4                           | ---            | 21.7   | ---            | 22.6   | ---            |
| $K_{33}$ , Btu in./°F hr in. <sup>2</sup> | 20.4                           | ---            | 21.7   | ---            | 22.6   | ---            |

CD-66-32584

# UNDIRECTIONAL BORSIC/TITANIUM MMC PREDICTED MODULI

An example of the METCAN computer code's capability for predicting composite material properties is illustrated in the figure. The results shown are the longitudinal and transverse moduli for a unidirectional borsic/titanium metal matrix composite. The results demonstrate an excellent agreement between METCAN predictions, detailed three-dimensional finite element simulations, and experimentally measured values.

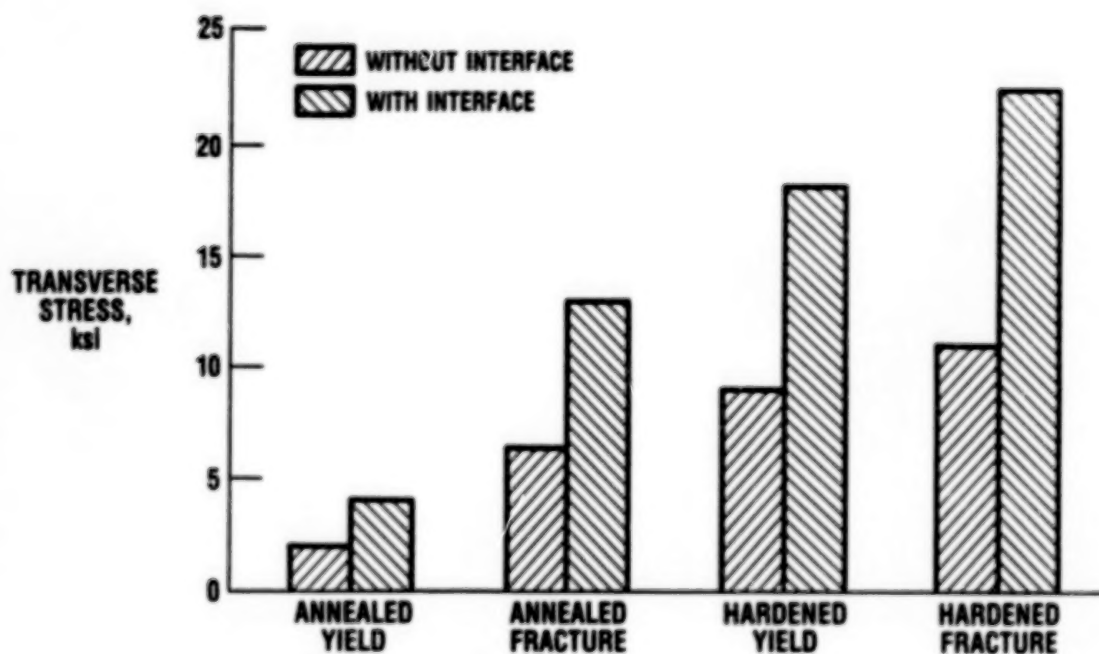


CD-86-32585



# UNIDIRECTIONAL GRAPHITE/COPPER MMC TRANSVERSE STRENGTH BOUNDS

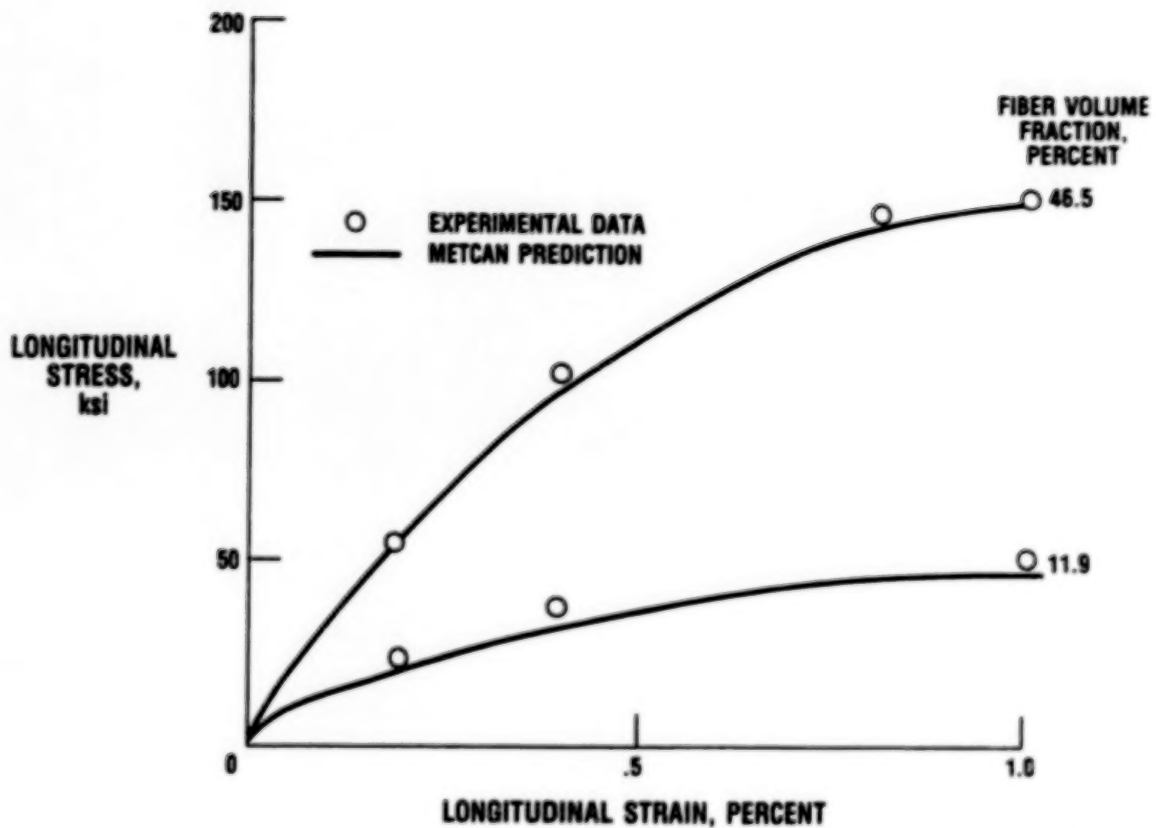
A result of a study of fiber/matrix interface effects (bond quality) on composite transverse strength that used the METCAN computer code is shown in the figure. The yield and fracture stress are presented for a unidirectional graphite/copper metal matrix composite with two different copper matrix treatments (annealed and hardened). Shown are the predicted stress levels without an interface (no bond) and with an interface (perfect bond). The two conditions can be viewed as extremes, or bounds, on the bond quality achieved in actual fabrication. Indeed, experimental data for transverse strength exhibit significant scatter and, although not shown in the figure, generally fall within the bounds predicted by METCAN.



CD-88-32586

# UNDIRECTIONAL TUNGSTEN/COPPER MMC STRESS-STRAIN RESPONSE

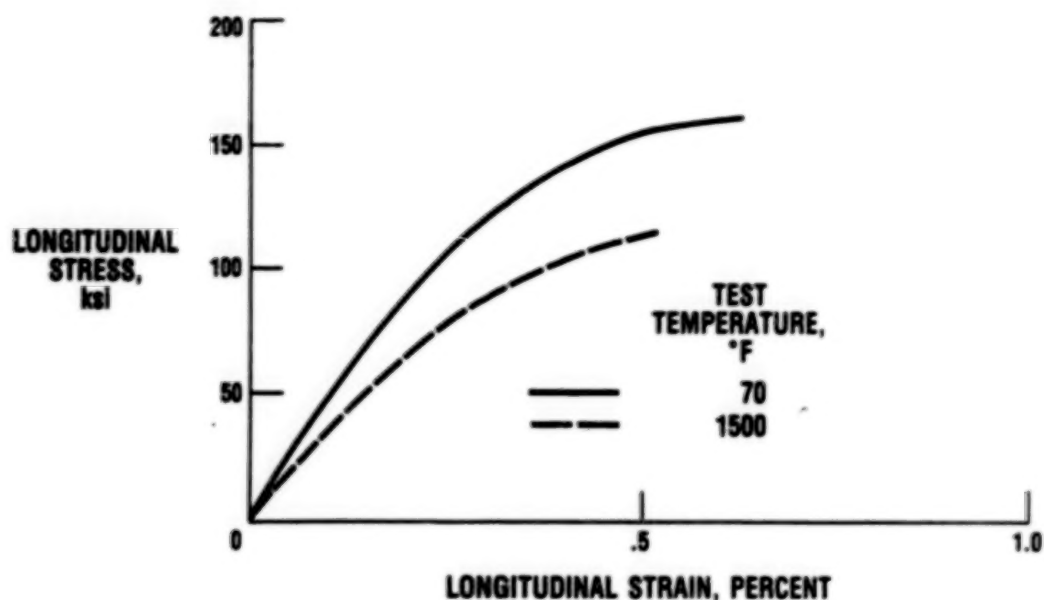
An example of the type of information obtained from the METCAN computer code is given in the figure, which shows the nonlinear stress-strain response due to monotonic loading at room temperature for unidirectional tungsten/copper metal matrix composites with two different fiber volume fractions. Evident from the figure is the excellent agreement between the METCAN-predicted and experimentally measured responses.



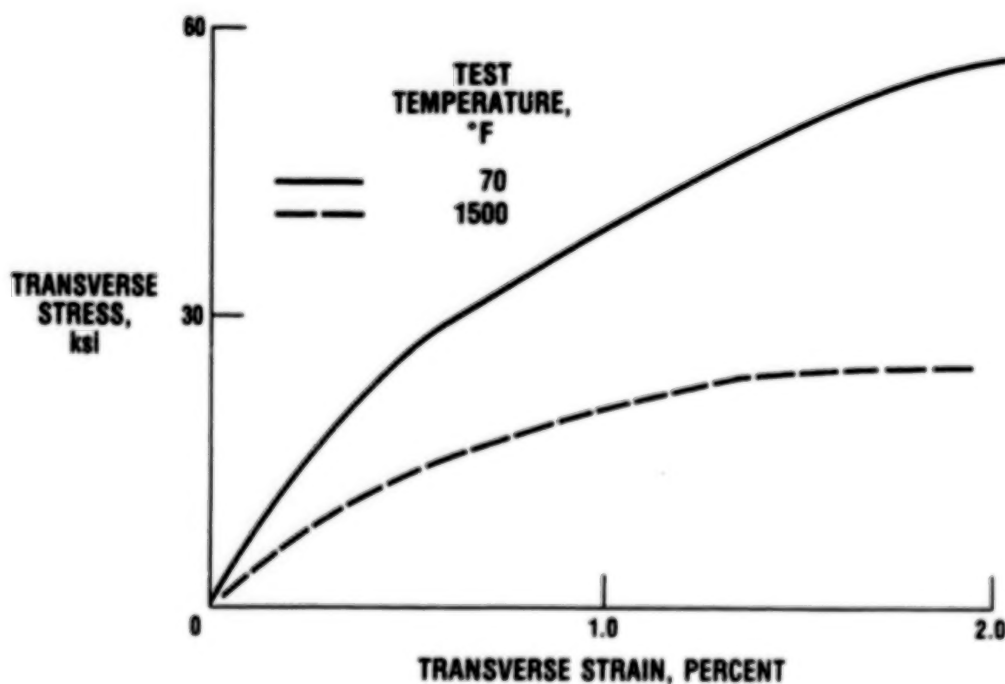
CD-86-32587

# UNDIRECTIONAL GRAPHITE/COPPER MMC STRESS-STRAIN RESPONSE

Another example of METCAN computer code predictive capability is shown here. The results shown in the figure are the nonlinear stress-strain response to monotonic loading for a unidirectional graphite/copper metal matrix composite at elevated as well as room temperature, and for transverse as well as longitudinal loading direction.



CD-88-32588

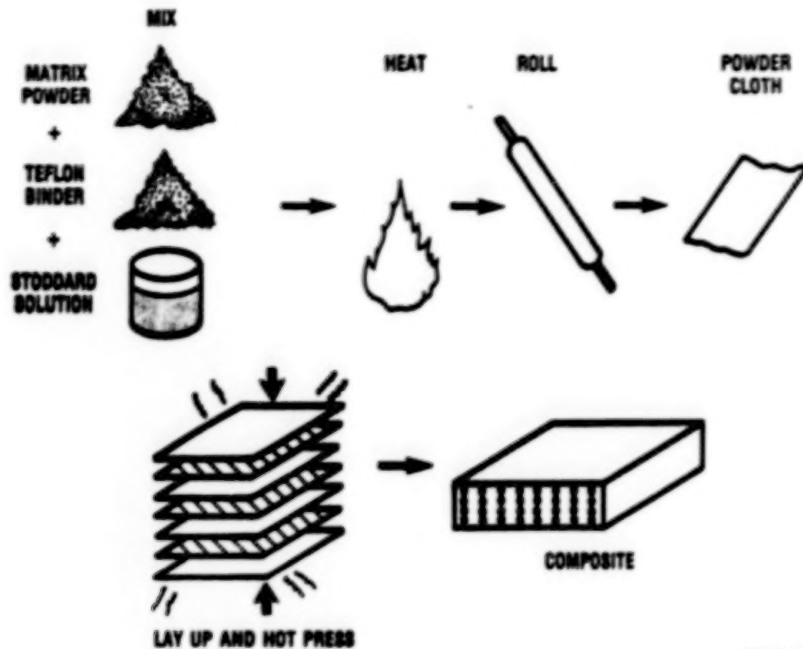


CD-88-32589

## METAL MATRIX COMPOSITE FABRICATION PROCESS

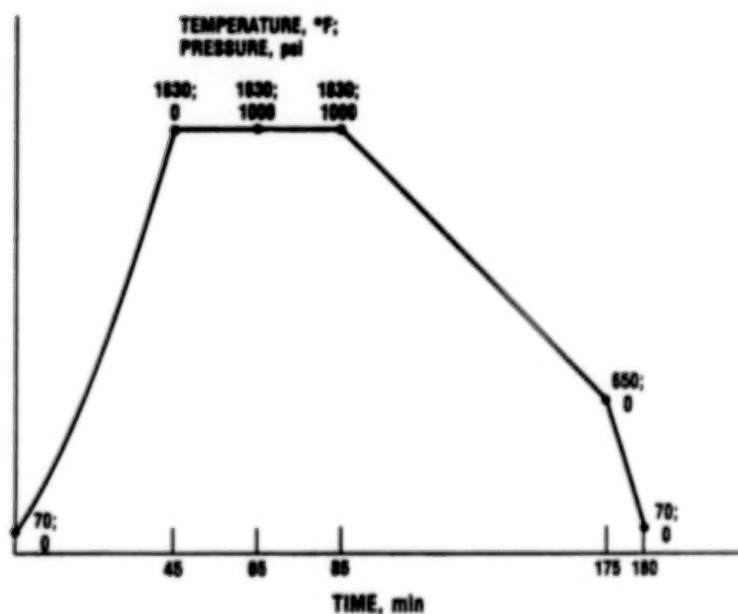
The METCAN computer code has recently been used to investigate the development of residual stresses in a typical fabrication process, as illustrated in the figure. The effect of fabrication residual stresses on subsequent in-service performance of aerospace propulsion structures has also been investigated by using METCAN in conjunction with other global structural analysis computer codes.

## METAL-MATRIX COMPOSITE FABRICATION PROCESS



CD-88-32590

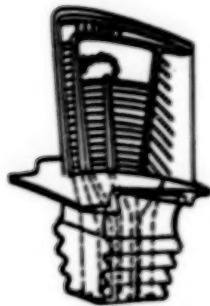
## MMC PROCESSING CONDITIONS



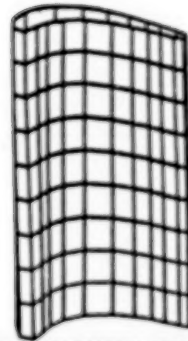
CD-88-32591

## TUNGSTEN/SUPERALLOY MMC TURBINE BLADE

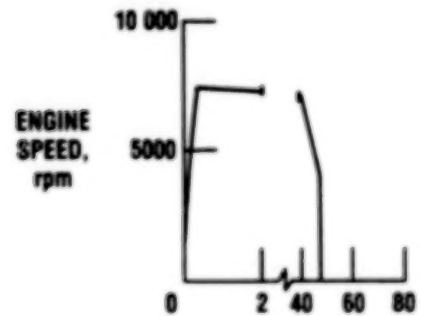
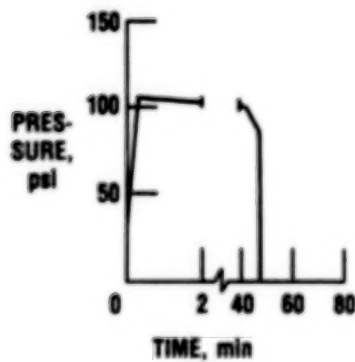
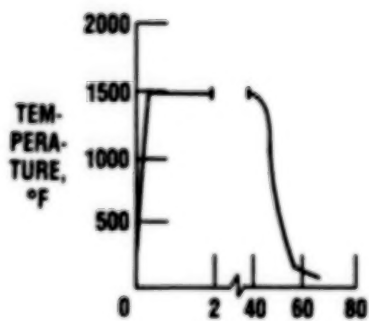
The figure shows a turbine airfoil fabricated from an angle-plyed  $[+45^\circ/-45^\circ]_s$  tungsten/superalloy composite and subjected to hypothetical aircraft engine flight mission conditions.



TURBINE AIRFOIL



FINITE ELEMENT MODEL



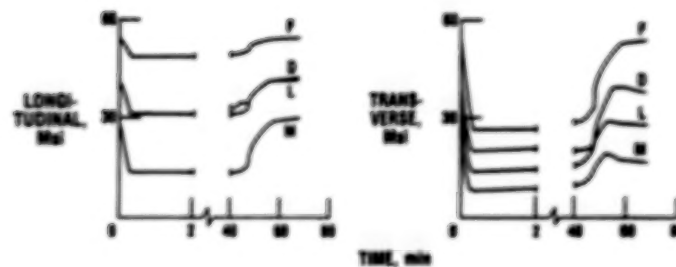
CD-88-32592

# TUNGSTEN/SUPERALLOY MMC TURBINE AIRFOIL ANALYSIS

The results from a quasi-static incremental analysis of the airfoil model show a variety of behavior and response quantities corresponding to the outermost (exterior surface) ply at the midchord root location on the airfoil (identified by arrow in previous figure). These results were obtained by interfacing the METCAN computer code with the familiar NASTRAN finite element structural analysis computer code.

## MODULUS

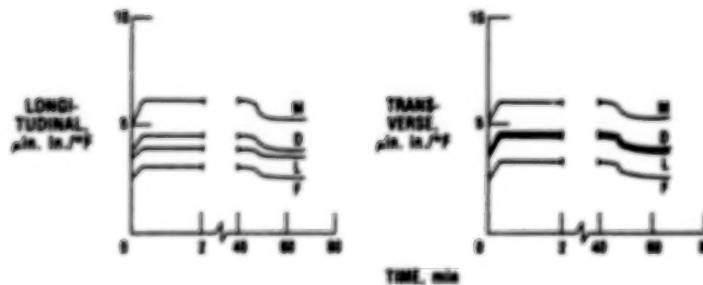
F FIBER  
M MATRIX  
D INTERPHASE  
L PLY



CS-44-10000

## THERMAL EXPANSION COEFFICIENT

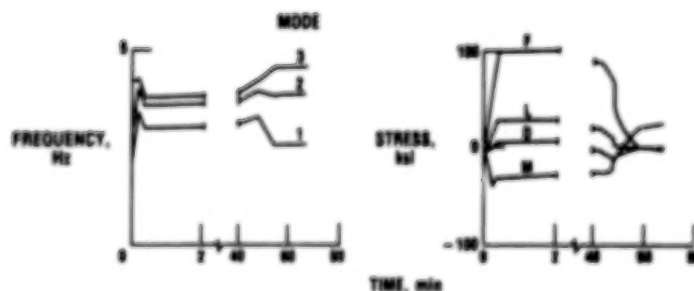
F FIBER  
M MATRIX  
D INTERPHASE  
L PLY



CS-44-10000

## NATURAL FREQUENCY AND LONGITUDINAL STRESS

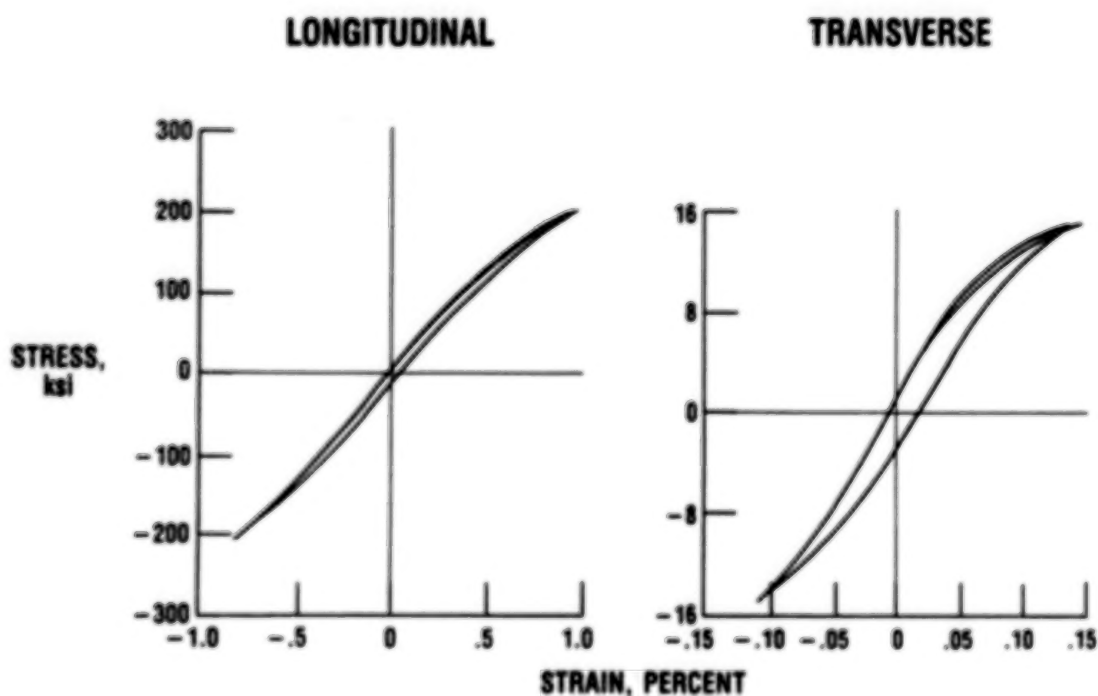
F FIBER  
M MATRIX  
D INTERPHASE  
L PLY



CS-44-10000

## UNIDIRECTIONAL BORON/ALUMINUM MMC CYCLIC STRESS-STRAIN RESPONSE

An example of planned future capability for the METCAN computer code, which is currently under development, is shown in the figure and represents the predicted nonlinear stress-strain response to cyclic loading for a unidirectional boron/aluminum metal matrix composite, for both longitudinal and transverse loading directions. Further investigation of the nature of unloading at the constituent level is needed before this feature can become a permanent capability of the METCAN computer code.



CD-88-32596



## SUMMARY

- METCAN PERFORMS MOST ESSENTIAL ASPECTS OF MECHANICS, ANALYSIS, AND DESIGN OF METAL-MATRIX COMPOSITES
- METCAN IS MODULAR, OPEN ENDED, AND USER FRIENDLY
- STANDARD METAL-MATRIX COMPOSITES AS WELL AS INTERPLY HYBRID METAL-MATRIX COMPOSITES CAN BE ANALYZED
- RESPONSE DUE TO DIFFERENT TYPES OF THERMAL AND MECHANICAL LOAD HISTORIES ACCOUNTING FOR THERMOMECHANICAL DEGRADATION CAN BE OBTAINED ROUTINELY
- KEY FEATURES OF METCAN INCLUDE
  - LINEAR AND NONLINEAR ANALYSIS
  - ROOM- AND HIGH-TEMPERATURE PROPERTIES
  - STRESS AND STRAIN INFLUENCE COEFFICIENTS
  - RESIDENT DATA BANK

CD-88-32587

## COMPUTATIONAL SIMULATION METHODS FOR COMPOSITE FRACTURE MECHANICS

Pappu L.N. Murthy\*  
Cleveland State University  
Cleveland, Ohio 44115

### ABSTRACT

The task of assessing the structural integrity, durability, and damage tolerance of advanced composites from a design viewpoint is twofold. First, damage initiation at various scales (micro, macro, and global) and accumulation and growth leading to global failure must be qualitatively as well as quantitatively assessed. Second, various fracture toughness parameters associated with a typical damage and its growth must be determined. These two points have been the subjects of ongoing research at the NASA Lewis Research Center over the past 10 years. The objective of this research has been to develop computational structural analysis codes to aid the composites design engineer in routinely performing these tasks. The computational simulation methods involved in this research effort are described in this presentation.

The first part of the effort concerns the qualitative as well as quantitative assessment of progressive damage occurring in composite structures due to mechanical and environmental loads. A computer code, CODSTRAN, and an experimental setup to verify the predictions of the code have been under development (Chamis and Smith, 1978; Chamis, 1986; and Ginty, 1985). CODSTRAN stands for composite durability structural analysis. Some of the salient features of CODSTRAN are presented with an illustrative example and results.

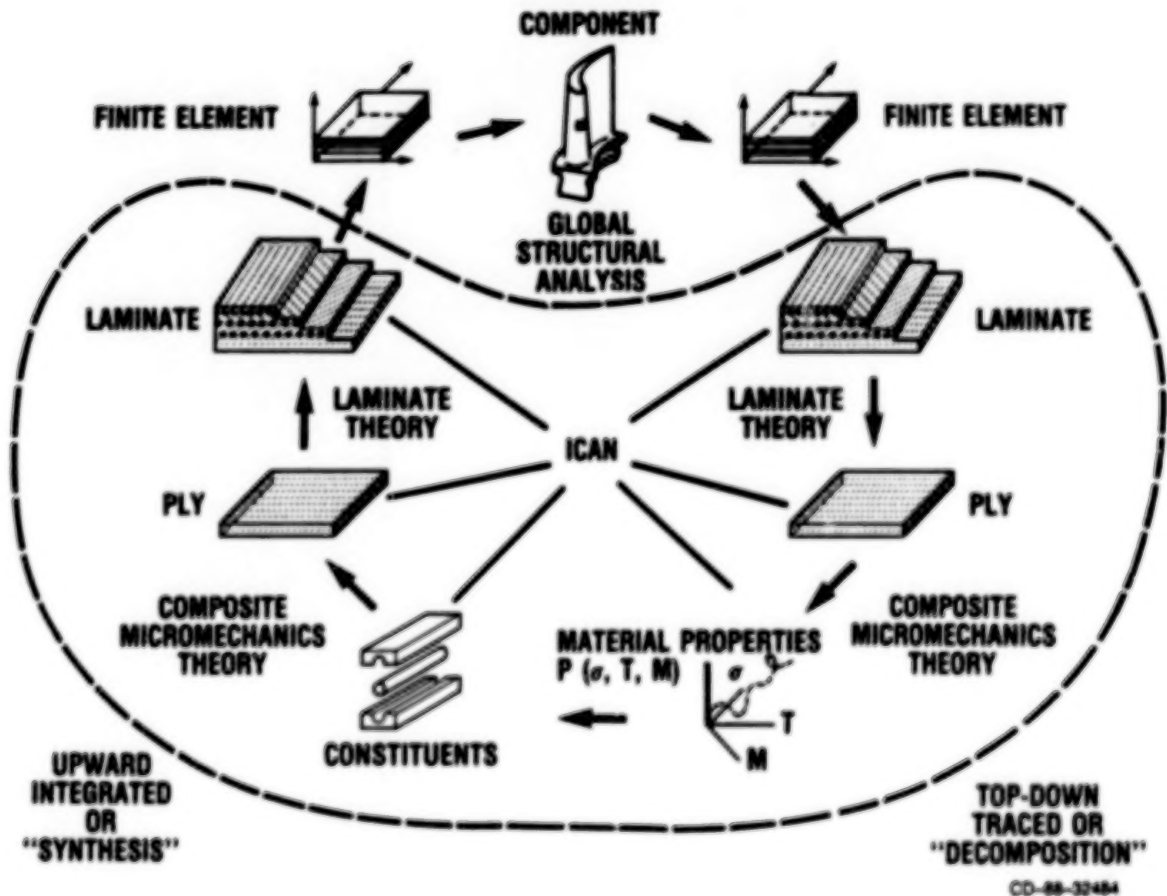
The second part of the presentation covers methods that are currently being developed and used at Lewis to predict interlaminar fracture toughness and related parameters of fiber composites given a prescribed damage (Murthy and Chamis, 1985; Murthy and Chamis, 1986). The general-purpose finite element code MSC/NASTRAN is used to simulate the interlaminar fracture and the associated individual as well as mixed-mode strain energy release rates in modes I, II, and III in fiber composites. Those methods can be conveniently embedded into CODSTRAN to develop a unique computational capability to analyze and design progressive damage and crack growth in fiber composites.

---

\*Senior Research Associate.

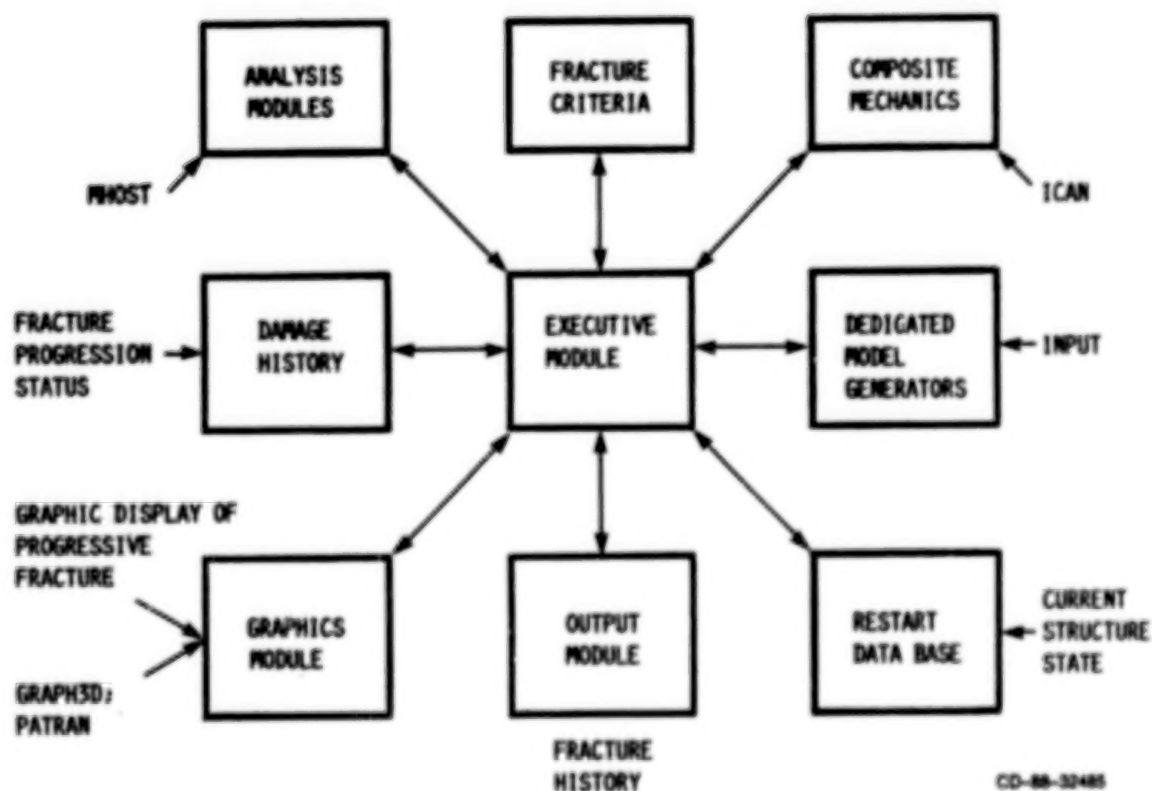
# CODSTRAN: COMPOSITE PROGRESSIVE DAMAGE ANALYZER

The computer code CODSTRAN follows an "upward-integrated and topdown-traced" architecture as depicted in the viewgraph. In this, CODSTRAN follows very closely all the steps that are involved in manufacturing a component, starting from constituents (fiber and matrix). The code starts with fiber and matrix properties, forms a laminate by using classical lamination theory, and arrives at a finite element representation. After the finite element analysis is completed, the loads at each node are used in the progressive decomposition to arrive at the constituent-level response. The response is reviewed, and either the properties are updated or the load step is increased or decreased. All this is automatically done by the code with minimal user intervention.



# CODSTRAN COMPUTER CODE DESCRIPTION

This flowchart shows some of the important analysis modules that are embedded in CODSTRAN. Many of these modules are constructed in such a way that user updates are possible with a minimum effort. The code is open ended and stand alone except for the graphics module, which may need to be modified depending on the system facilities available at the user station. The code comes with a dynamic storage allocation scheme for optimal usage of computer storage. Restart facilities are provided within the code to take care of abnormal termination or system failures. Dedicated model generators can be easily updated by the user to take care of specific requirements.

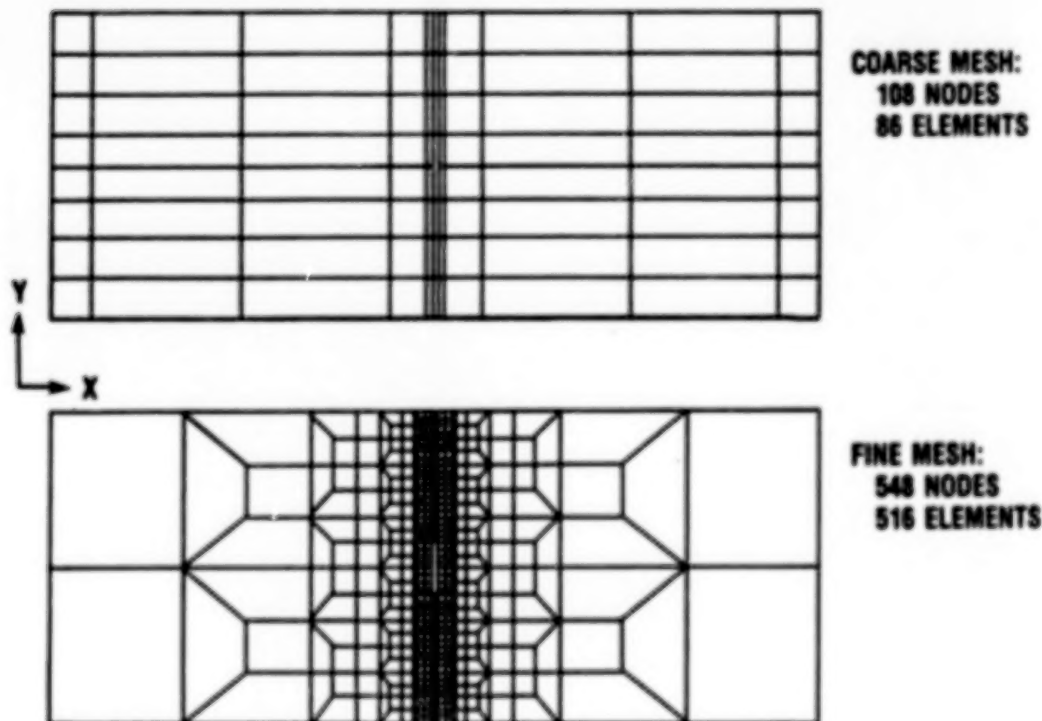


CD-88-32485

# DEDICATED MESH GENERATOR OUTPUT

Two finite element representations as generated by the dedicated model generator modules in CODSTRAN are shown below for a  $(0^\circ/30^\circ/0^\circ/-30^\circ/0^\circ)_{2s}$  graphite/epoxy laminate with a notch in the center. The coarse mesh provides quick estimates. The fine-mesh representation may have to be used to obtain a more accurate description of the damage progression.

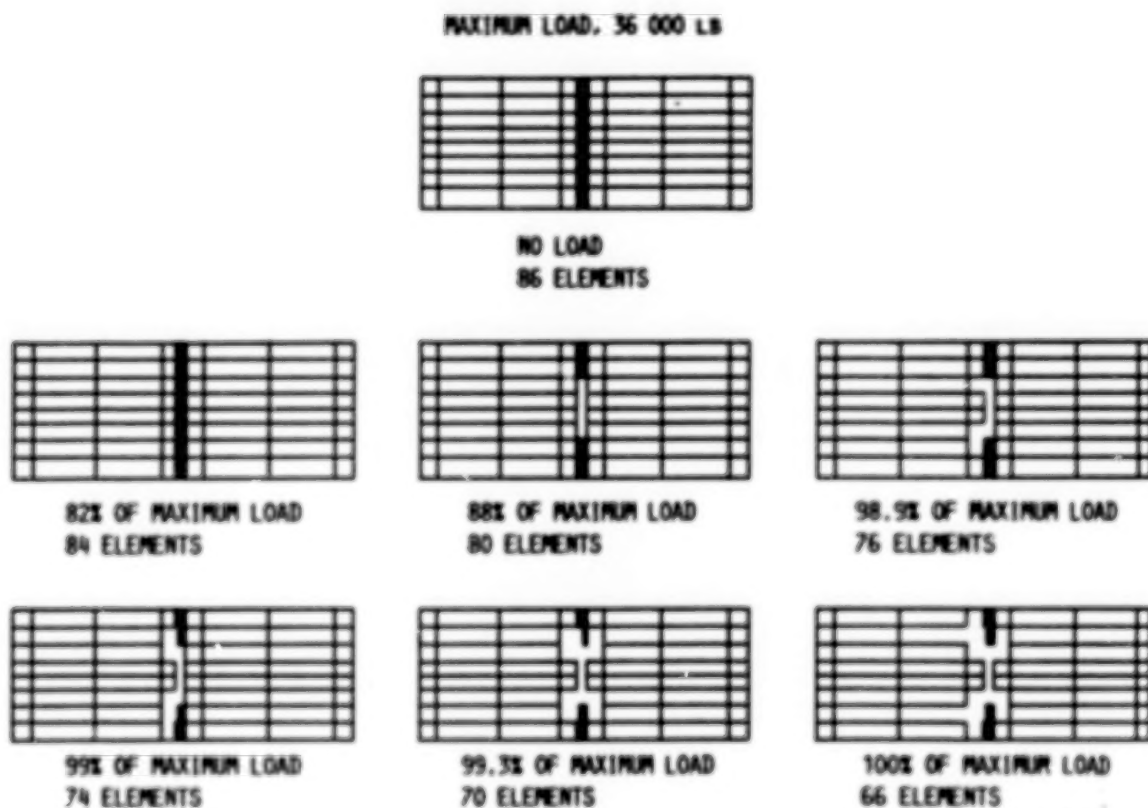
## LAMINATE CONFIGURATION, $(0^\circ/30^\circ/0^\circ/-30^\circ/0^\circ)_{2s}$ GRAPHITE/EPOXY



CO-88-32486

# CODSTRAN-PREDICTED SEQUENCE OF PROGRESSIVE FRACTURE

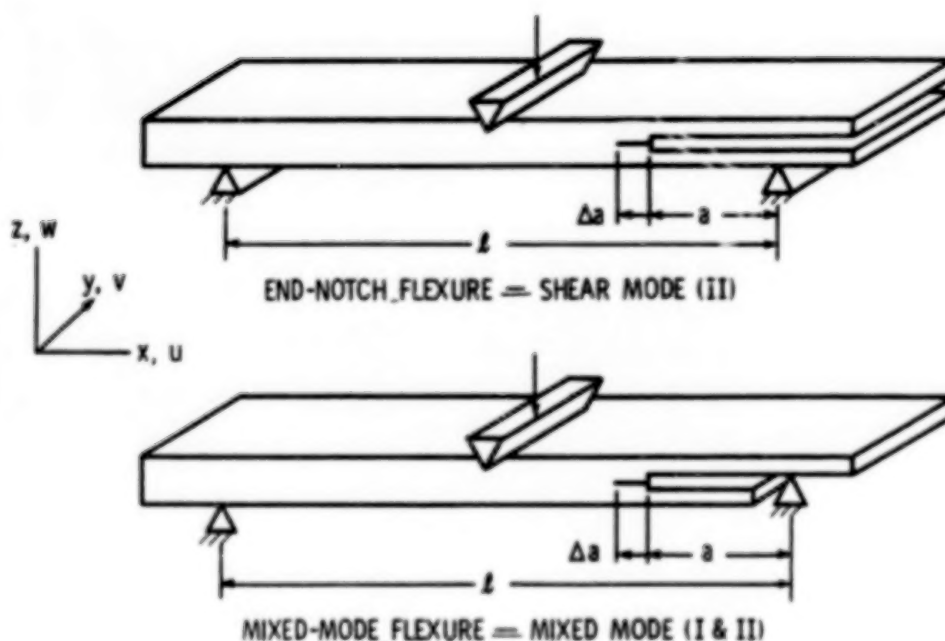
The laminate in the previous figure is subjected to a tensile load applied in small increments. Damage is tracked down at various load steps, as shown, until a complete global failure occurs. The plots are made with the aid of an in-house-developed graphics package, GRAPH3D. Also, at any stage the user may obtain ply, laminate stress, or displacement contours with PATRAN. Special translators are built in the code to generate PATRAN-compatible output.



CO-88-32487

# SCHEMATIC OF FLEXURE TEST FOR INTERLAMINAR FRACTURE MODE TOUGHNESS

This figure shows two proposed ASTM standard specimens - end-notch flexure (ENF) and mixed-mode flexure (MMF). They are essentially modifications of the standard three-point bend test specimens with end notches. The ENF specimen simulates pure shear-mode fracture (mode II). The MMF specimen simulates mixed-mode (modes I and II) fracture. These specimens are modeled with three-dimensional finite elements and are analyzed by using MSC/NASTRAN to obtain mode II and mixed-mode I and II strain energy release rates for a variety of laminate configurations (Murthy and Chamis, 1985 and 1986).

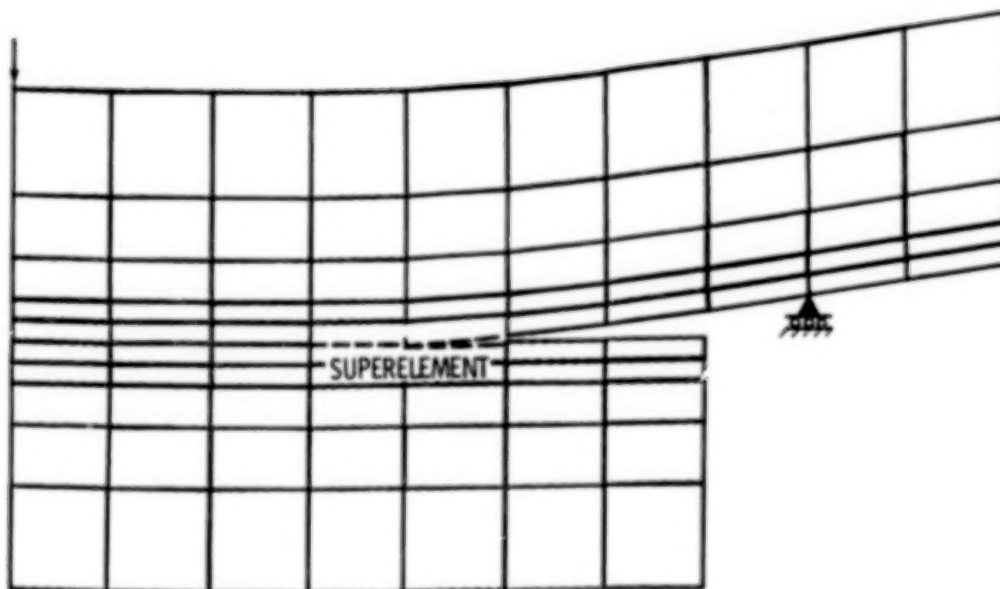


CD-88-32488



FINITE ELEMENT DEFORMED MODEL RIGHT-HALF-SPAN MIXED-MODE  
FLEXURE (GRAPHITE/EPOXY)

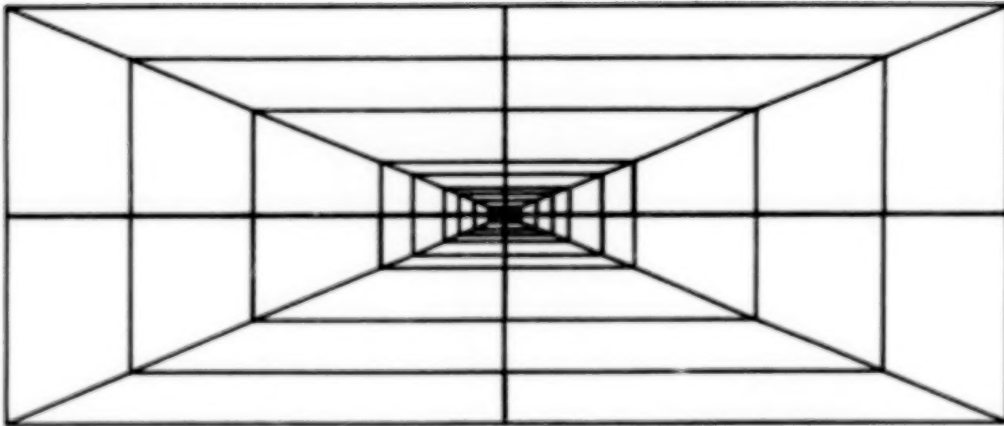
The finite element discretization for the right half span of the MMF specimen is shown in the figure. The elements used were eight-node three-dimensional bricks. The crack tip region was further substructured into a fine mesh as shown in the following figures. Increasing crack lengths were obtained by removing elements from the interply region ahead of the crack tip, and several finite element analyses were run. By using a special "single-point constraint" approach and the virtual crack closure technique, the energy release rates associated with the individual modes I and II were obtained. For details refer to Murthy and Chamis (1985 and 1986).



CD-86-32489

#### CRACK REGION SUPERELEMENT MODEL DETAILS - FRONT VIEW

The crack tip region was modeled as shown. It contains a total of 360 brick elements of which 32 are six-node pentahedrons and 328 are eight-node hexahedrons. The eight-node bricks in the interply layer ahead of the crack tip were removed progressively one by one to simulate extended crack length.

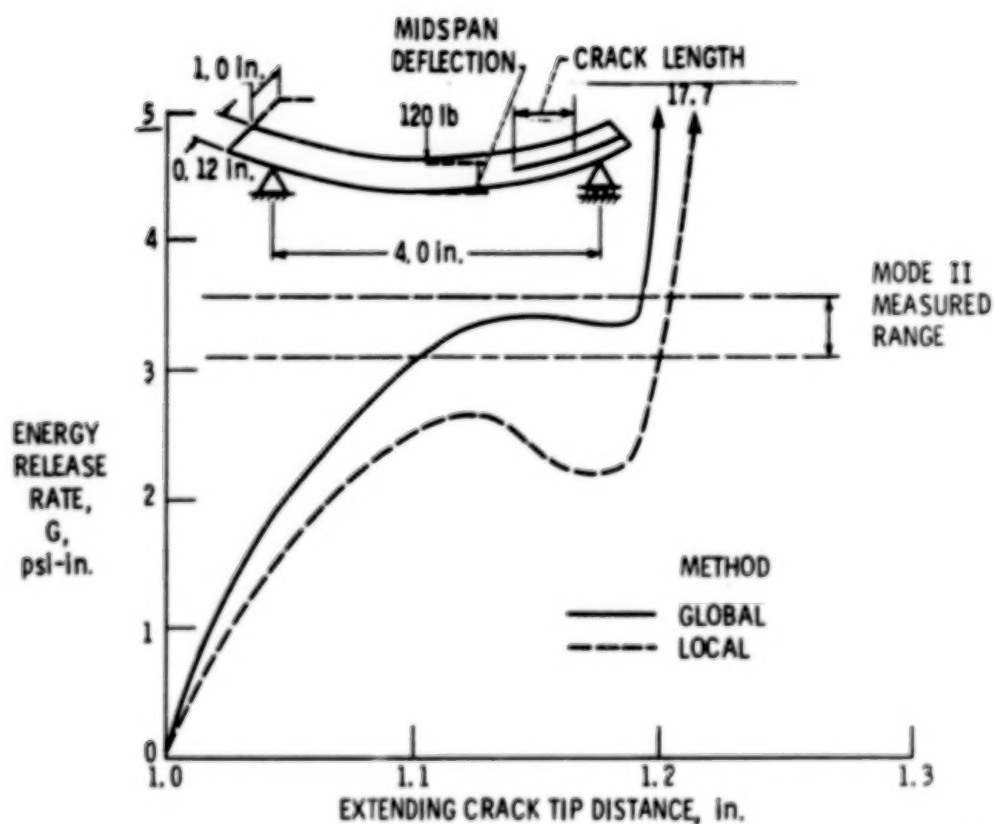


- 360 BRICKS
- 32 SIX-NODE PENTAHEDRONS
- 328 EIGHT-NODE HEXAHEDRONS

CD-88-32490

# END-NOTCH-FLEXURE ENERGY RELEASE RATE COMPARISONS

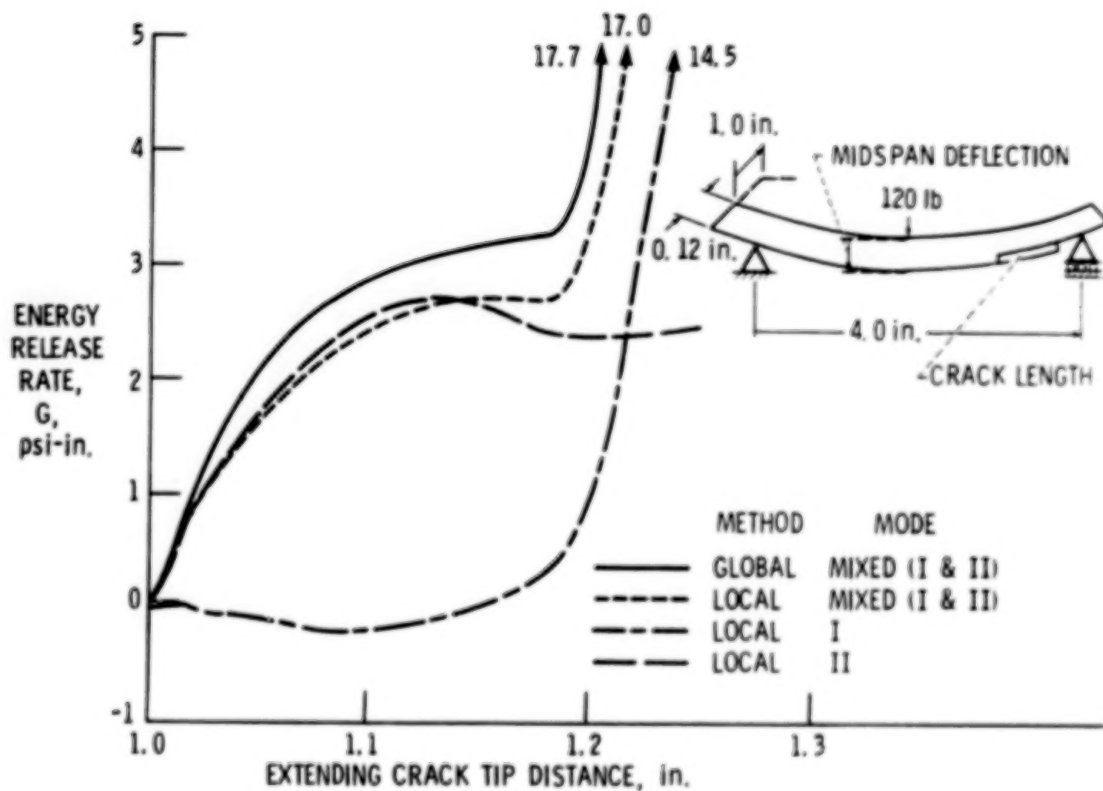
The global strain energy release rate  $G$  based on the measurement of deflections at the midspan and the local energy release rate computed by using the virtual crack closure technique are compared in the figure. Also the measured critical strain energy release rates for this specimen are shown by horizontal dashed lines.



CD-88-32491

# MIXED-MODE-FLEXURE ENERGY RELEASE RATE COMPARISONS

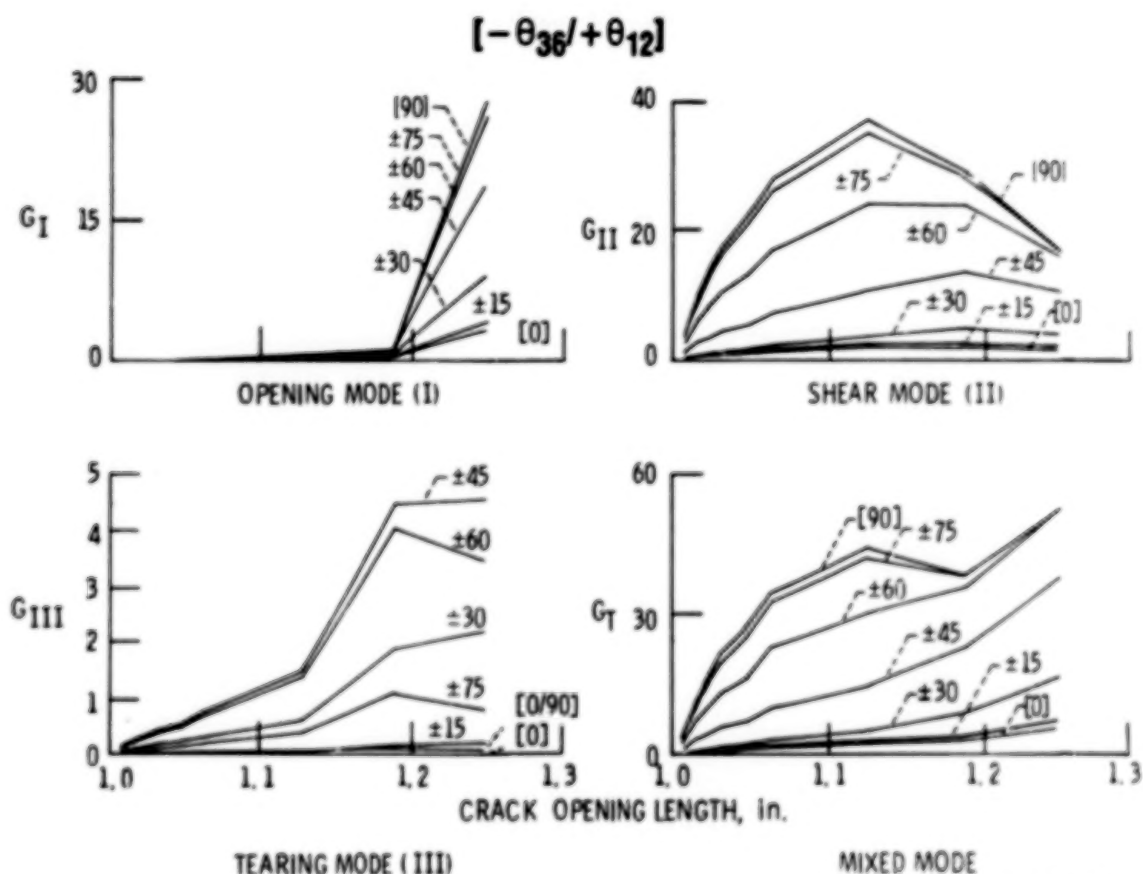
The global and local strain energy release rates are compared for the MMF specimen. From observing the local individual strain energy release rates it can be concluded that the crack growth is initiated by a mode II fracture, only to be dominated later by mode I growth. Also the sum of individual strain energy release rates  $G_I$  and  $G_{II}$  appears to be smaller than the total strain energy release rate  $G$  computed by global means.



CD-88-32492

# EFFECTS OF CRACK LENGTH AND PLY ORIENTATION ON STRAIN ENERGY RELEASE RATES

The mixed-mode-flexure specimen is modified by placing the crack plane off center and also by having all the  $+\theta$  plies on one side of the crack plane and all the  $-\theta$  plies on the other side. This ensures a component of the tearing mode (III) as well as the usual mode I and II components that are normally present in an MMF specimen. Results are presented for a family of laminate configurations. The tearing mode (III) content appears to have the smallest value of all the energy release rates attendant in this type of setup. In the figure below all release rates are in inch pounds per square inch.



CD-88-32493

## CONCLUSIONS

The important conclusions from the present study are listed below.

- COMPUTATIONAL SIMULATION METHODS ARE PRESENTED TO ASSESS PROGRESSIVE DAMAGE, CRACK GROWTH, AND FRACTURE TOUGHNESS CHARACTERISTICS.
- CODSTRAN PREDICTS AND PROVIDES QUANTITATIVE INFORMATION ON
  - FAILURE INITIATION
  - DEFECT GROWTH
  - DAMAGE AND THE VARIOUS SCALES IN WHICH IT OCCURS
- MSC/NASTRAN IS USED TO PREDICT
  - FRACTURE TOUGHNESS IN MODES I, II, AND III
  - GLOBAL AND LOCAL STRAIN ENERGY RELEASE RATES (SERR)
  - CRITICAL SERR AND THE ASSOCIATED CRACK LENGTH
- ALL THIS INFORMATION CAN BE USED IN DESIGNING COMPOSITE STRUCTURES. IT PROVIDES THE NECESSARY CONFIDENCE IN THEIR STRUCTURAL INTEGRITY, DURABILITY, AND DAMAGE TOLERANCE.

CD-88-32494

#### REFERENCES

- Chamis, C.C., and Smith, G.T., 1978, "CODSTRAN: Composite Durability Structural Analysis," NASA TM-79010.
- Chamis, C.C., 1986, "Computational Simulation of Progressive Fracture in Fiber Composites," NASA TM-87341.
- Ginty, C.A., 1985, "Progressive Damage, Fracture Predictions, and Postmortem Correlations for Fiber Composites," NASA TM-87101.
- Murthy, P.L.N., and Chamis, C.C., 1985, "Interlaminar Fracture Toughness: Three Dimensional Finite-Element Modeling for End-Notch and Mixed-Mode Flexure," NASA TM-87138.
- Murthy, P.L.N., and Chamis, C.C., 1986, "Composite Interlaminar Fracture Toughness: 3-D Finite Element Modeling for Mixed Mode I, II, and III Fracture," NASA TM-88872.



BLANK PAGE

## STRUCTURAL OPTIMIZATION

### SESSION OVERVIEW

Robert H. Johns  
Structural Mechanics Branch  
NASA Lewis Research Center

Aerospace propulsion and power systems are inherently very complex and require the technology and expertise of several technical disciplines for their conception, design, analysis, and manufacture. The technology areas most critical to these systems include aerodynamics, fluid mechanics, thermodynamics, mechanics of materials, and several areas of structural mechanics. The usual approach to developing these systems is to sequentially address the technical disciplines in the design process, which results in many time-consuming and costly iterations to arrive at a final design. Frequently, schedules and development costs result in the acceptance of a final design which may not be the "best" one for the purpose intended.

The papers in this session address the design problem as an integrated, interdisciplinary process to arrive at a structurally tailored or optimized design. In fact it is more than a "structurally" tailored or optimized design since aerodynamic performance, weight, manufacturing costs, operating costs, return on investment, and other life cycle and performance factors can be included in arriving at a final design. Some papers in this session discuss how these other factors are incorporated in arriving at the objective function and final design.

Some of the aerospace systems and component hardware discussed in this session is very advanced. For example, the very thin, highly swept and twisted composite propfan blades and the space shuttle main engine turbopump blades require new analysis methods. Key to some of these analyses is the development and application of probabilistic analysis methods to loads, material properties, and structural analysis methods. The loads, material properties, and geometry can all have an unknown amount of variation which cannot be accurately predicted and the results of which may not be measurable because of limitations on instrumentation, severe thermomechanical environments, inaccessibility, etc. Variations in one parameter can affect another parameter because these systems are interactive and interdependent. For example, variations in thickness or material properties in a propfan blade can affect the amount of untwist and, thus, the blade loading, stress magnitude, and consequent blade life.

All these interdependent analyses and system responses can be systematically and simultaneously related in one computer program. An example of this is given in the paper describing the engine structures computational simulator.

#### SESSION OVERVIEW

- R.H. JOHNS, STRUCTURAL MECHANICS BRANCH, NASA

#### PROBABILISTIC STRUCTURAL ANALYSIS COMPUTER CODE (NESSUS)

- M.C. SHIAO, STRUCTURAL MECHANICS BRANCH, SVERDRUP

#### STRUCTURAL TAILORING OF HIGH-SPEED TURBINE BLADES (SSME/STAEBL)

- R. RUBINSTEIN, STRUCTURAL MECHANICS BRANCH, SVERDRUP

#### COMPUTATIONAL STRUCTURAL MECHANICS FOR ENGINE STRUCTURES

- C.C. CHAMIS, STRUCTURES DIVISION, NASA

#### STRUCTURAL TAILORING OF ADVANCED TURBOPROPS

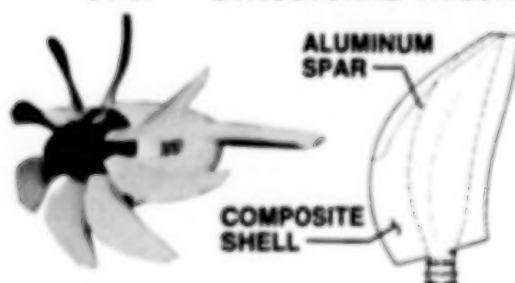
- K.W. BROWN, PRATT & WHITNEY, EAST HARTFORD, CT
- D.A. HOPKINS, STRUCTURAL MECHANICS BRANCH, NASA

#### ADVANCED PROBABILISTIC METHODS FOR QUANTIFYING THE EFFECTS OF VARIOUS UNCERTAINTIES IN STRUCTURAL RESPONSE

- V.K. NAGPAL, STRUCTURAL MECHANICS BRANCH, SVERDRUP

CD-88-33217

### STAT - - STRUCTURAL TAILORING OF TURBOPROP BLADES



#### BLADE INTERNAL STRUCTURE



#### TURBOPROP STAGE AND PROPELLER

#### MULTI-DISCIPLINARY ANALYSIS MODULES

- ADS OPTIMIZER
- BLADE MODEL GENERATION
- AERODYNAMIC ANALYSIS
- ACOUSTIC ANALYSIS
- STRESS AND VIBRATIONS ANALYSIS
- FLUTTER ANALYSIS
- 1 P FORCED RESPONSE

#### TYPICAL ANALYSIS RESULTS

|                      | <u>INITIAL</u> | <u>FINAL</u> |
|----------------------|----------------|--------------|
| EFFICIENCY, %        | 82.86          | 83.17        |
| NEAR FIELD NOISE, DB | 143.8          | 137.3        |
| WEIGHT, LB           | 41.1           | 41.2         |
| DOC                  | -0.853         | -4.201       |

CD-88-33218

## PROBABILISTIC STRUCTURAL ANALYSIS COMPUTER CODE (NESSUS)\*

Michael C. Shiao  
Sverdrup Technology, Inc.  
(Lewis Research Center Group)  
NASA Lewis Research Center

### ABSTRACT

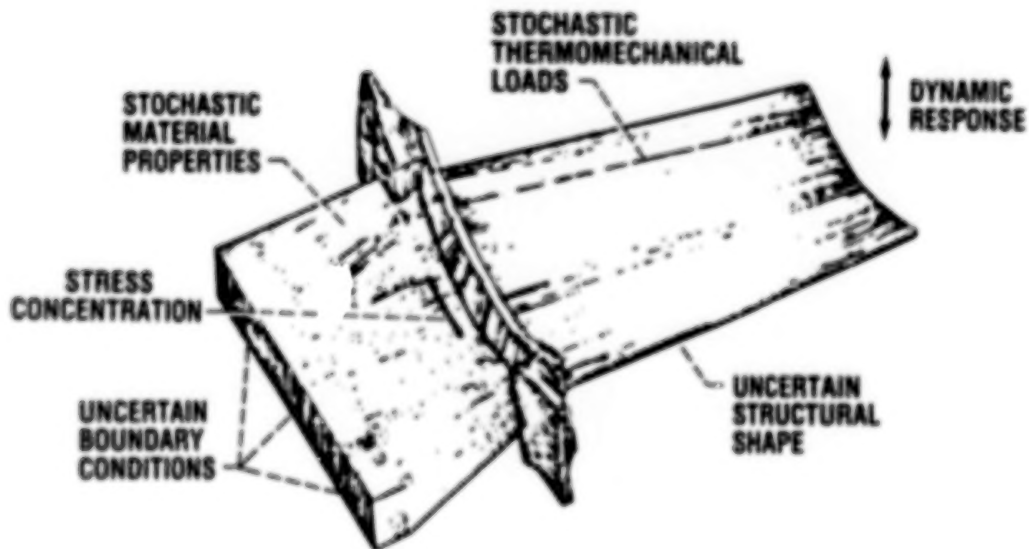
In the past, structural design was based on deterministic analysis using known geometry, material properties, loads, and boundary conditions. A safety factor was then used to ensure structural reliability. More recently, probabilistic structural analysis has been developed to analyze the effects of fluctuating loads, variable material properties, and uncertain analytical models especially for high performance structures such as SSME turbopump blades. In the deterministic approach, uncertainties in the response were not quantified and actual safety margin in the design remained unknown. Probabilistic structural analysis provides a systematic method to evaluate structural performance and durability. Probabilistic Structural Analysis Method (PSAM) for Select Space Propulsion System Components is a research and technology program sponsored by NASA Lewis. The objective of this program is to characterize the probabilistic structural response due to the stochastic environments by statistical descriptions. The computer code NESSUS (Numerical Evaluation of Stochastic Structure Under Stress) has been developed by Southwest Research Institute (SWRI) to serve as a primary computation tool for this purpose. The current code consists of three major modules NESSUS/PRE, NESSUS/FEM, and NESSUS/FPI. NESSUS/PRE is a preprocessor which decomposes the spatially correlated random variables into a set of uncorrelated random variables using a modal analysis method. NESSUS/FEM is a finite element module which provides structural sensitivities to all the random variables considered. NESSUS/FPI is Fast Probability Integration method by which a cumulative distribution function (CDF) or a probability density function (PDF) is calculated. Further risk assessment can be continued once the probability distribution function is known.

---

Work performed on-site at the Lewis Research Center for the Structural Mechanics Branch under contract NAG3-24105.

## UNCERTAINTIES IN THE PROBABILISTIC STRUCTURAL ANALYSIS

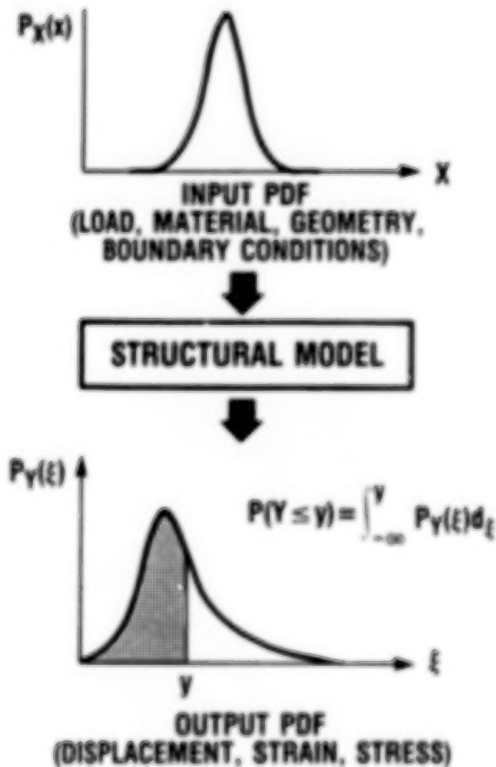
Probabilistic structural analysis requires the uncertainties involved be recognized and quantified. An SSME turbopump blade is subjected to complex mechanical and thermal loads and will be used to illustrate the randomness concerned in the analysis. The dominant loads on the turbine blade are centrifugal force, thermal load, and the differential pressure across the airfoil. Centrifugal force is induced by the rotational blade speed. Since it is difficult to maintain constant rotational speed, the centrifugal force should be defined as a random variable. Random thermal load is due to combustion irregularities which cause a random temperature distribution in the blade. Differential pressure should also be random. Uncertainties in the blade geometry arise during the manufacturing process. The stochastic material properties are caused by the imperfections in the material developed during process. Uncertainty in the temperature distribution also gives another level of material property variation. For the cantilever structure of the SSME blade shown, the boundary is modeled as fully constrained for simplicity. In real structures, flexibility is exhibited at the support due to assembly procedure which should be quantified statistically.



CD-88-32599

## CONCEPT OF PROBABILISTIC STRUCTURAL ANALYSIS BY NESSUS

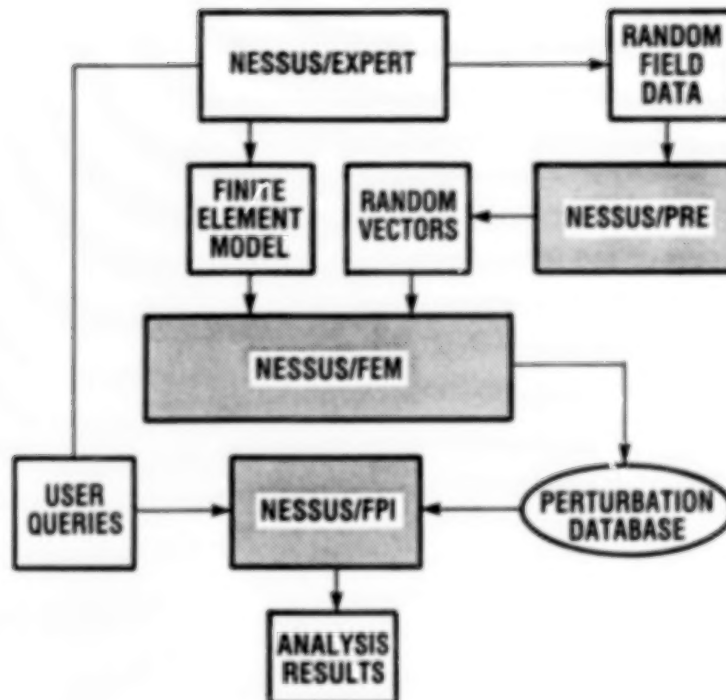
With the loading, material properties, geometry, and boundary conditions defined as random variables, the probabilistic structural analysis is then computed by NESSUS. The structure can be considered as a filter. The response variables, which can be static deflection, strains and stress at one or several locations, or natural frequencies, will also be random and will be described by a cumulative distribution function (CDF) or a probability density function (PDF). For most structures, the analytical distribution function of response can not be obtained and will be evaluated numerically by NESSUS.



CD-68-32600

## STRUCTURE OF NESSUS

NESSUS (Numerical Evaluation of Stochastic Structure Under Stress) integrates finite element methods technology with probabilistic methods. The code consists of the three major modules shown by the shaded blocks below. NESSUS/PRE analyzes the correlation model. NESSUS/FEM computes sensitivity data. NESSUS/FPI calculates probabilistic results.



CD-66-32601



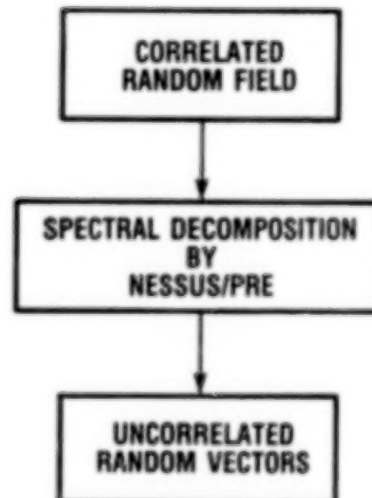
## NESSUS/PRE

NESSUS/PRE is a pre-processor used for the preparation of the statistical data needed to perform the probabilistic finite element analysis. It allows the user to describe a spatial domain defined by a set of discrete points, typically corresponding to the nodal points of a finite element mesh. One or more random variable fields may then be specified over this spatial domain by defining the mean value and standard deviation of the random variable at each point, together with an appropriate form of correlation. The current version of NESSUS/PRE limits the treatment of partially correlated fields to fields of Gaussian variables with equal correlation strength in all directions (isotropic correlation). Correlated random variables are decomposed into a set of uncorrelated vectors by a modal analysis. For strong correlation problems, the number of dominant random variables in the set of uncorrelated vectors will be much less than that of correlated random variables. The reduction of the number of random variables will also decrease the computational time required for the analysis. One other reason to have this module developed is that the current FPI code can treat uncorrelated problems only.

### ALLOWABLE RANDOM FIELDS

NODAL COORDINATE DATA  
NODAL SHELL THICKNESS  
NODAL SHELL OR BEAM NORMALS  
THICKNESS OF PLANE STRESS ELEMENTS  
MODULUS OF ELASTICITY  
POISSON'S RATIO  
THERMAL EXPANSION COEFFICIENT  
MATERIAL DENSITY  
ROTATIONAL SPEED  
NODAL FORCE VECTORS  
ELEMENT PRESSURES/EDGE TRACTION  
NODAL TEMPERATURES  
ELASTIC BEAM SECTION PROPERTIES  
BASE SPRING STIFFNESS  
ORIENTATION OF ANISO AXES

### NESSUS/PRE

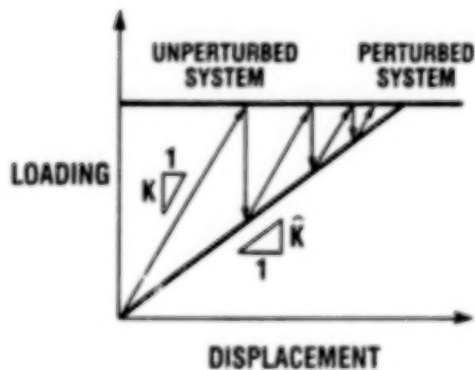


CD-88-32602

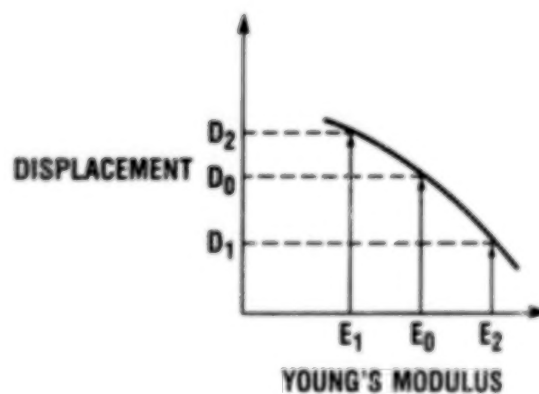
## NESSUS/FEM

NESSUS/FEM is a finite element code used for structural analysis and parameter sensitivity evaluation. It also generates a database containing all the response information corresponding to a small variation of each independent random variable. The algorithm used in NESSUS/FPI requires an explicit response function in terms of uncorrelated random variables in order to perform a reliability analysis. In complicated structural analysis problems, response can only be available implicitly through a finite element model. To overcome this difficulty, the response function is estimated numerically. In the figure shown below, the response considered is the displacement  $D$ , the uncertainty involved is the Young's modulus  $E$ . NESSUS/FEM calculated the displacement  $D_0$ ,  $D_1$ ,  $D_2$  corresponding to the Young's modulus at  $E_0$ ,  $E_1$ ,  $E_2$ .  $D_1$  and  $D_2$  are computed by a method akin to the modified Newton nonlinear algorithm. A curve is found to approximate the desired response.

MODIFIED NEWTON ITERATION



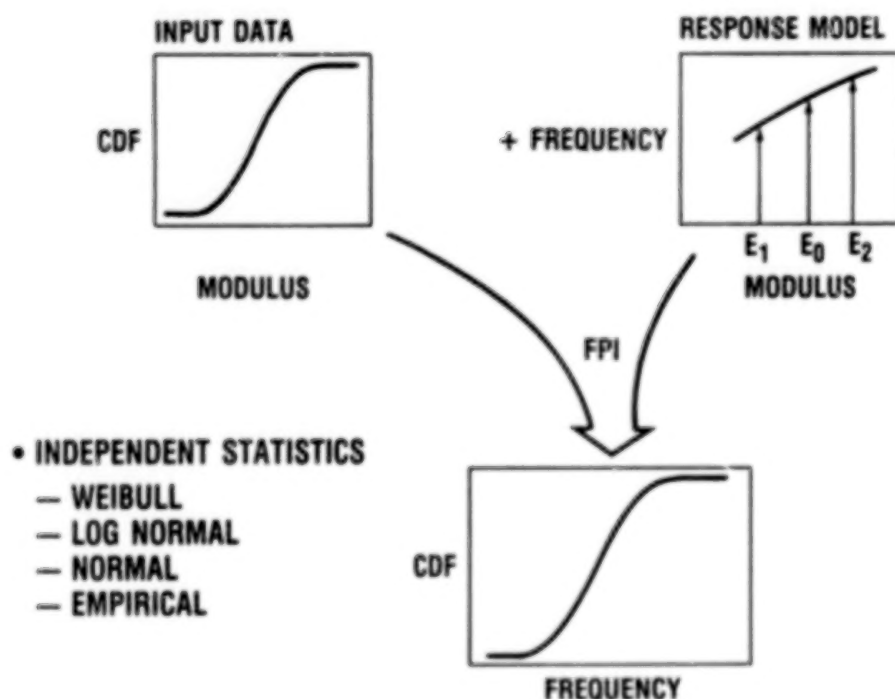
RESPONSE MODEL



CD-88-32603

# NESSUS/FPI

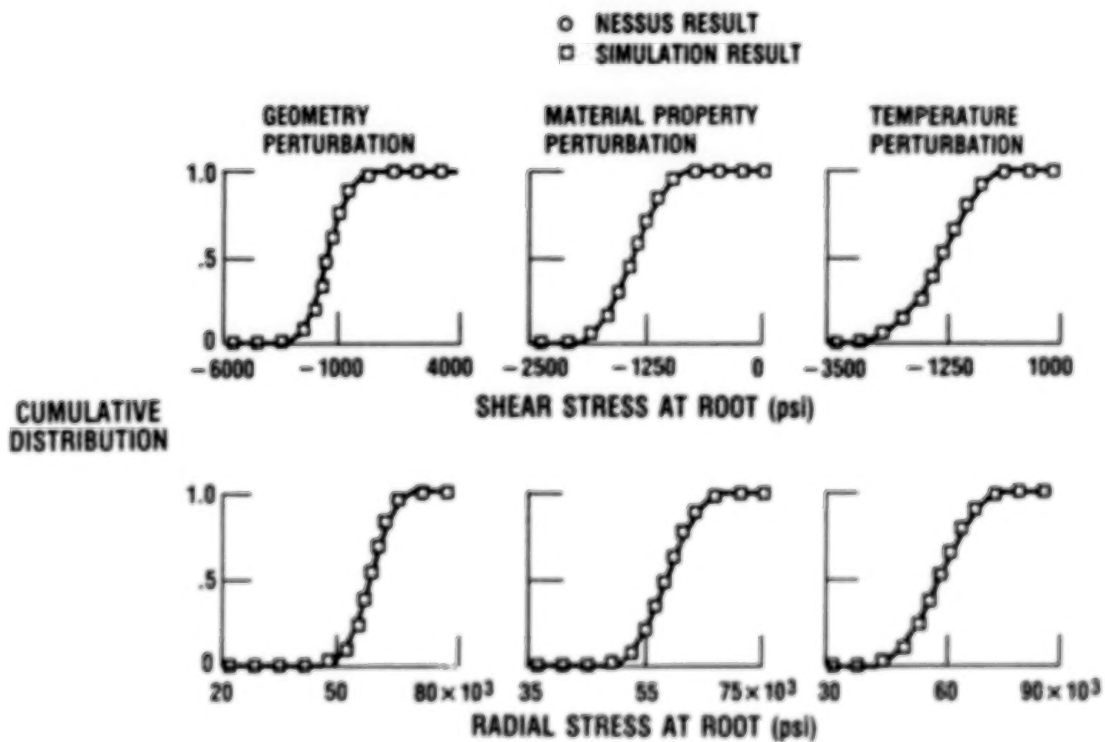
NESSUS/FPI (Fast Probability Integrator) implements an advanced reliability method. This method plays an important role in risk assessment of civil engineering structures. This module extracts data from the database generated by NESSUS/FEM to develop a response or performance model in terms of uncorrelated random variables. The probabilistic structural response is calculated from the performance model. For a given response value, the probability of exceedance at this value is estimated by a reliability method, which treats the problems as a constrained minimization. This step is called a point probability estimate. The cumulative distribution function can be obtained numerically by running FPI at several response values. One alternative for generating the distribution function for any given response is by a Monte Carlo simulation study. However in general, it is very costly. NESSUS/FPI provides a method which not only produces a reliable distribution, but also requires less computing time than that for Monte Carlo simulation, especially in the low probability region.



CD-88-32604

## NESSUS VALIDATION

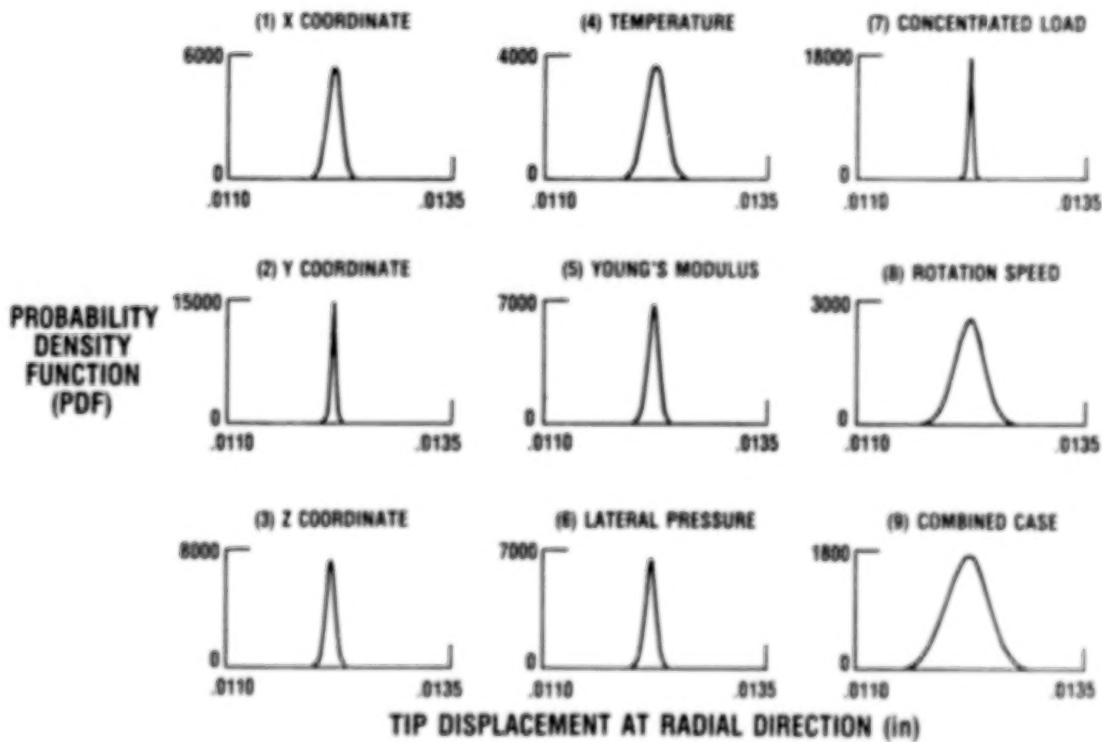
A SSME turbopump blade has been modeled by four node shell elements. NESSUS and Monte Carlo simulation are used to calculate the cumulative distribution (CDF) function. In principal, given an extremely large random sample, the Monte Carlo results will be exact. However, large computing time will be necessary to achieve convergence especially in the low probability region. NESSUS implements an approximation scheme requiring less computing effort. Three validation studies are presented. Nodal coordinates in the radial direction, Young's modulus in each element, and nodal temperatures are assumed to be random for each case. Three hundred sample points are generated by Monte Carlo simulation. In general, the results from two methods agree with each other.



CD-88-32605

# TURBINE BLADE STUDY BY NESSUS

Because of the severely stochastic launch environment for SSME components, such as a turbopump blade, deterministic analyses cannot be realistic. Examples of probabilistic analyses of a SSME blade using NESSUS are presented. The nodal coordinates, nodal temperatures, lateral pressure, Young's modulus, concentrated loads, and blade speed are modeled as random fields. The response analyzed is the radial tip displacement. Probability density functions for displacement are presented. In the first eight cases, the PDF is generated assuming one random field. The ninth example is the PDF due to the combined effect of these eight random fields. From this study, it can be concluded that rotation speed, nodal temperature, and material properties have more effect on the distribution of radial tip displacement than concentrated loads or y-coordinate perturbation. In the combined case study, NESSUS/FPI also provides sensitivity information on the response for each random variable.



BLANK PAGE

## STRUCTURAL TAILORING OF HIGH-SPEED TURBINE BLADES (SSME/STAEBL)\*

Robert Rubinstein  
Sverdrup Technology, Inc.  
(Lewis Research Center Group)  
NASA Lewis Research Center

### ABSTRACT

Space shuttle main engine (SSME) blades are subject to severe thermal, pressure, and forced vibration environments. An SSME blade design must meet tight clearance, fatigue life, and stress limit constraints. Because of the large number of potentially conflicting constraints, a "manual" design procedure may require many time-consuming iterations. Structural optimization provides an automated alternative. Any number of analyses, design variables, and constraints can be incorporated in a structural optimization computer code. This idea has been applied to develop the code SSME/STAEBL, which is a stand-alone code suitable for automated design of SSME turbopump blades.

Additions and modifications of STAEBL included in SSME/STAEBL include the following: (1) thermal stress analysis, (2) gas dynamic (pressure) loads, (3) temperature-dependent material and thermal properties, (4) forced vibrations, (5) tip displacement constraints, (6) single crystal material analysis, (7) blade cross-section stacking offsets, and (8) direct time integration algorithm for transient dynamic response. Capabilities are also included which permit data transfer from finite element models and stand-alone analysis. Descriptions of preliminary probabilistic enhancements of SSME/STAEBL will be given.

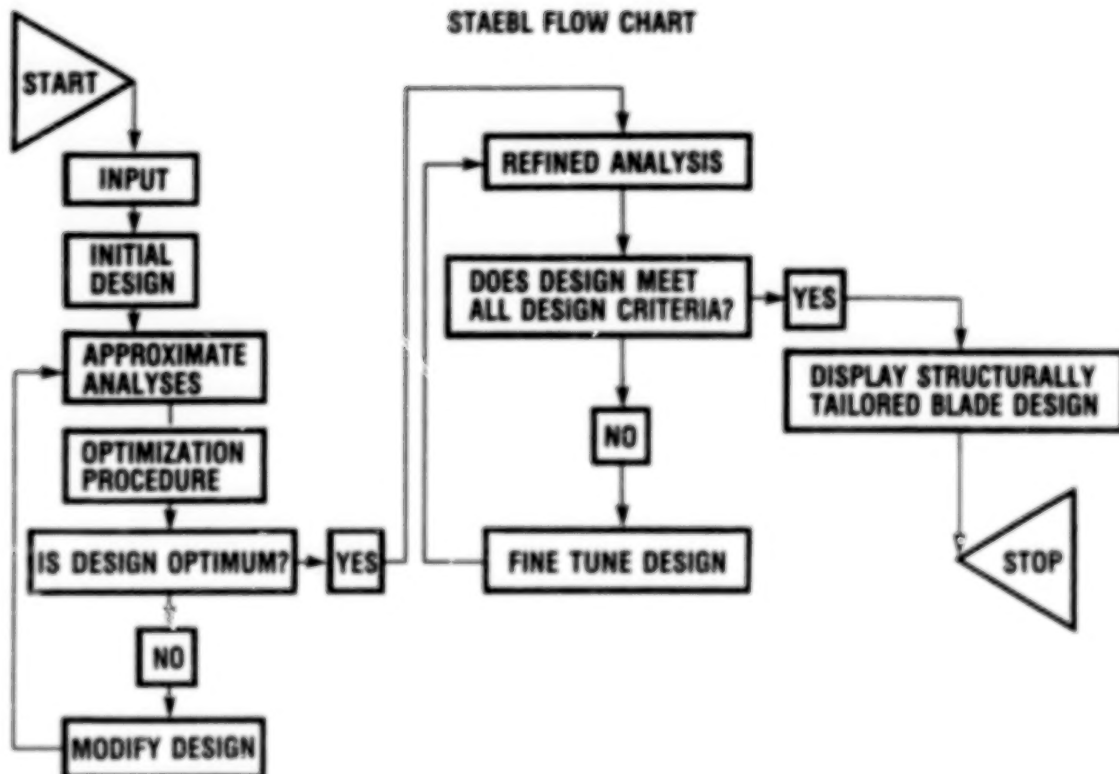
---

\*Work performed on-site at the Lewis Research Center for the Structural Mechanics Branch.



## STRUCTURAL TAILORING OF ENGINE BLADES (STAEBL)

SSME/STAEBL was developed by systematically modifying and enhancing the STAEBL (Structural Tailoring of Engine Blades) code developed by Pratt and Whitney under contract to NASA Lewis Research Center. STAEBL was designed for application to gas turbine blade design. Typical design variables include blade thickness distribution and root chord. Typical constraints include resonance margins, root stress, and root-to-chord ratios. In this program, the blade is loaded by centrifugal forces only.



CD-88-31837

# OPTIMIZATION STUDIES FOR SSME BLADE

Several design optimization studies have been completed by using an SSME blade design to test these various capabilities. Optimization studies have been completed to test the influence of thermal and pressure loads and temperature-dependent properties on optimal blade design. Comparison between designs optimized under centrifugal loads only and under centrifugal, thermal, and pressure loads with temperature-dependent blade properties shows that the additional loads require additional weight to meet all design constraints. The difference between the designs can be attributed to material property temperature dependence which, in this case, forces a much tighter root stress constraint.

## CENTRIFUGAL LOADS ONLY; TEMPERATURE-INDEPENDENT PROPERTIES

| SPAN,<br>percent | THICKNESS,<br>in | CHORD,<br>in |
|------------------|------------------|--------------|
| 0                | .224             | .890         |
| 50               | .052             | .681         |
| 100              | .065             | .650         |

## CENTRIFUGAL LOADS ONLY; TEMPERATURE-INDEPENDENT PROPERTIES

### NATURAL FREQUENCY, cps:

|        |      |
|--------|------|
| MODE 1 | 3454 |
| MODE 2 | 4868 |
| MODE 3 | 7969 |

ROOT STRESS, ksi: 108

### TIP DISPLACEMENTS:

|               |        |
|---------------|--------|
| UNTWIST, deg  | 2.8    |
| UNCAMBER, deg | 0.7    |
| TIP EXT, in   | 0.0027 |

### FORCED RESPONSE MARGINS:

|        |      |
|--------|------|
| MODE 1 | .000 |
| MODE 2 | .000 |
| MODE 3 | .000 |

BLADE WEIGHT, lb: .043

NUMBER OF BLADES: 73

STAGE WEIGHT, lb: 3.14

## REPRESENTATIVE THERMAL AND PRESSURE LOADS; TEMPERATURE-DEPENDENT PROPERTIES

| SPAN,<br>percent | THICKNESS,<br>in | CHORD,<br>in |
|------------------|------------------|--------------|
| 0                | .228             | .890         |
| 50               | .082             | .681         |
| 100              | .077             | .650         |

## REPRESENTATIVE THERMAL AND PRESSURE LOADS; TEMPERATURE-DEPENDENT PROPERTIES

3174

4438

8835

65

2.9

1.5

0.0209

.592

.557

.010

.044

73

3.18

CD-88-31838

# OPTIMIZATION STUDY INCLUDING BLADE-STACKING DESIGN VARIABLES

Optimization studies were undertaken to assess the influence of blade cross-section offsets on optimal design. These offsets are defined as the differences between the blade cross-section centers of gravity and a straight line perpendicular to the engine axis. Blade designers use these variables to balance centrifugal and pressure loads. In a typical optimization study, the initial design violated the root stress constraint. Root stress is extremely sensitive to offset variables, and the optimized design recommended a significant change in stacking.

| INITIAL DESIGN    |                  |              | FINAL DESIGN     |                  |              |
|-------------------|------------------|--------------|------------------|------------------|--------------|
| SPAN,<br>percent  | THICKNESS,<br>in | CHORD,<br>in | SPAN,<br>percent | THICKNESS,<br>in | CHORD,<br>in |
| 0.                | .233             | 1.041        | 0.               | .226             | .890         |
| -50.              | .138             | .804         | 50.              | .134             | .688         |
| 100.              | .092             | .761         | 100.             | .091             | .650         |
| BLADE STACKING:   |                  |              |                  |                  |              |
| A = 0.            |                  | B = 0.       | A = -.0012       |                  | B = .0078    |
| C = 0.            |                  | D = 0.       | C = .0013        |                  | D = .0095    |
| ROOT STRESS, ksi: |                  |              |                  |                  |              |
| 82                |                  |              | 74               |                  |              |

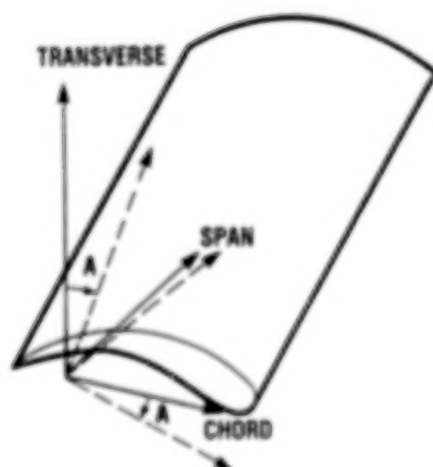
(z AXIS ALONG SPAN, BLADE LENGTH = L; x = x DISPLACEMENT FROM CENTER OF GRAVITY; AND y = y DISPLACEMENT FROM CENTER OF GRAVITY.)

$$x = A (z/L) + B (z/L)^2$$

$$y = C (z/L) + D (z/L)^2$$

# SINGLE CRYSTAL BLADE OPTIMIZATION STUDY

Design optimization studies for a blade made of a typical single crystal material showed relatively little effect on crystal axis orientation. This study was dominated by a root stress constraint which was violated by the initial design. It was found that root stress is influenced much less by crystal orientation than by the geometric design variables. The result is that the optimized design is found by adjusting the blade geometry significantly, but the crystal axis orientation insignificantly. Of course, in blade designs dominated by natural frequency constraints in particular, a different conclusion could be obtained.



—→ COORDINATE AXIS  
 - - -→ CRYSTAL AXIS

| CRYSTAL ALIGNED WITH ROOT CHORD |               |           |
|---------------------------------|---------------|-----------|
| SPAN, percent                   | THICKNESS, in | CHORD, in |
| 0                               | .23           | .89       |
| 50                              | .11           | .69       |
| 100                             | .06           | .65       |

| CRYSTAL ALIGNED WITH ROOT CHORD   |      |
|-----------------------------------|------|
| FREQUENCY, cps:                   |      |
| 5110.                             |      |
| 6851.                             |      |
| 13540.                            |      |
| ROOT STRESS, ksi:                 | 63.  |
| STAGE WEIGHT, lb:                 | 3.26 |
| CRYSTAL ORIENTATION EULER ANGLES: |      |
| .89 E-3                           |      |
| .57 E-2                           |      |
| -.51 E-3                          |      |

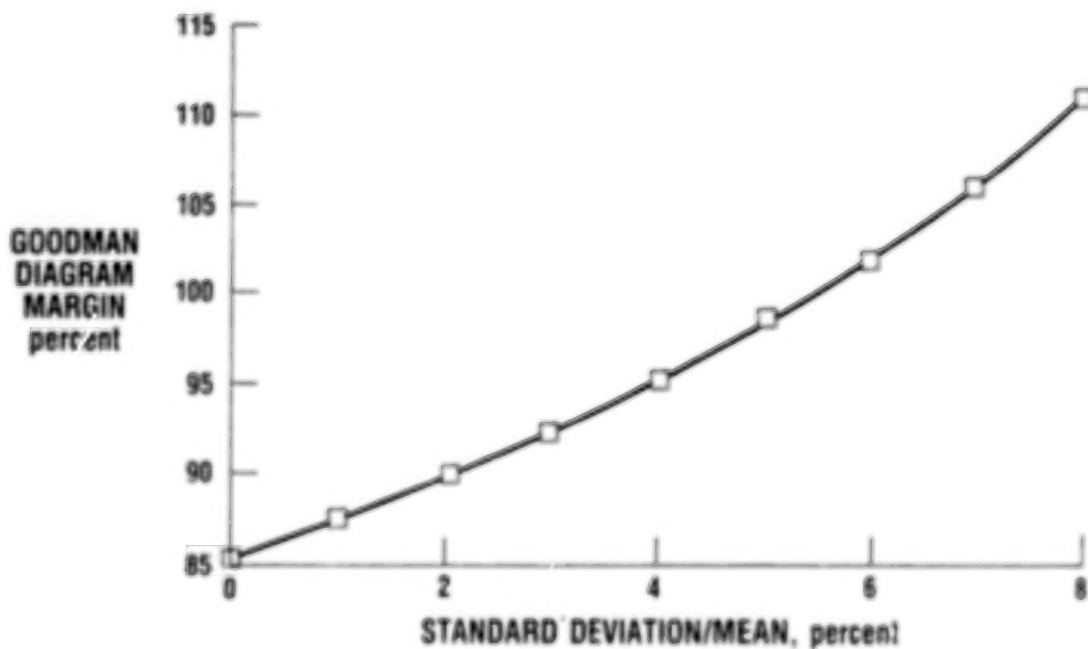
| CRYSTAL ALIGNED TO ROOT CHORD 45° |           |
|-----------------------------------|-----------|
| THICKNESS, in                     | CHORD, in |
| .23                               | .89       |
| .08                               | .69       |
| .06                               | .65       |

| CRYSTAL ALIGNED TO ROOT CHORD 45° |  |
|-----------------------------------|--|
| 5079.                             |  |
| 6847.                             |  |
| 13870.                            |  |
| 65.                               |  |
| 3.15                              |  |
| 45.00                             |  |
| -.20 E-1                          |  |
| .45 E-2                           |  |

CD-88-31840

## PROBABILISTIC ENHANCEMENTS

Preliminary capabilities have been developed to compute resonance margins, fatigue life, and stress levels probabilistically. Simple models are assumed for geometric imperfections to incorporate effects of imperfect offset stacking and twist on blade response. Probabilistic models are also assumed for strength as a function of number of cycles, stress level, and temperature. The graph shows the effect of uncertainties in material properties on Goodman fatigue strength diagram margins. As these uncertainties increase, the probability increases that the Goodman diagram margin will exceed 100 percent despite the fact that a deterministic calculation will indicate that the margin is about 85 percent.



CD-88-31841

## COMPUTATIONAL STRUCTURAL MECHANICS FOR ENGINE STRUCTURES

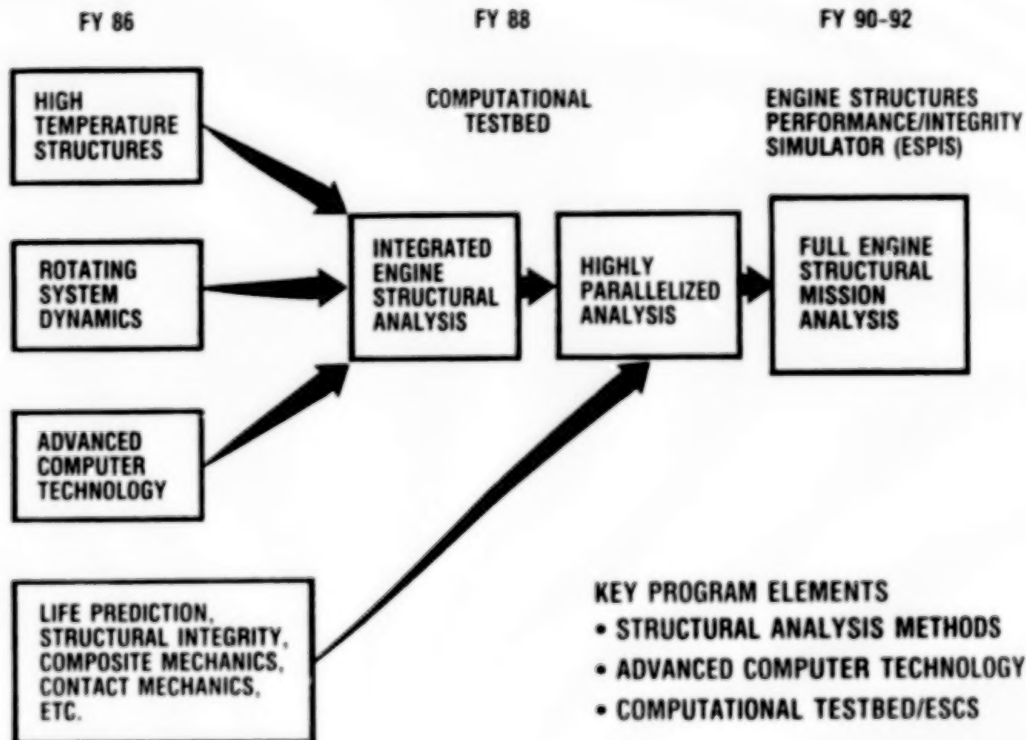
Christos C. Chamis  
Structures Division  
NASA Lewis Research Center

### ABSTRACT

The computational structural mechanics (CSM) program at Lewis encompasses the formulation and solution of structural mechanics problems and the development of integrated software systems to computationally simulate the performance, durability, and life of engine structures. It is structured to supplement, complement, and, whenever possible, replace costly experimental efforts. Specific objectives are to investigate unique advantages of parallel and multiprocesses for reformulating and solving structural mechanics and formulating and solving multidisciplinary mechanics and to develop integrated structural system computational simulators for predicting structural performance, evaluating newly developed methods, and identifying and prioritizing improved or missing methods.

COMPUTATIONAL STRUCTURAL MECHANICS LEADS TO ENGINE STRUCTURES  
COMPUTATIONAL SIMULATOR (ESCS)

The general content of the Lewis CSM program plan is summarized in the accompanying block diagram. The long-range objective of the program is the full engine structural simulation. It draws on methodology developed under research and development programs and the HOST Program over the past 10 years. This methodology is multidisciplinary and includes high temperature structures specialty analysis methods, rotating system dynamics, advanced structures specialty analysis methods, rotating system dynamics, advanced components, and durability and life.



CD-88-32972



COMPUTATIONAL STRUCTURAL METHODS IDENTIFIED  
METHODOLOGY - IMPROVED OR MISSING

An important part of the CSM for engine structures program is the identification of methodology which needs improvement or is missing. This methodology includes several key elements as listed in the accompanying chart. For example, boundary elements for hot fluid and structure interaction is natural since the boundary elements are formulated to match specified surface conditions and satisfy the interior field equations exactly.

- BOUNDARY ELEMENTS FOR 3-D INELASTIC ANALYSIS
- BOUNDARY ELEMENTS FOR HOT FLUID AND STRUCTURE INTERACTION
- EFFICIENT HYBRID ELEMENTS
- ADAPTIVE TRANSITIONAL FINITE ELEMENTS
- COMPUTATIONAL COMPOSITE MECHANICS
- COMPUTATIONAL CONTACT MECHANICS
- COUPLE COMPUTATIONAL SIMULATION WITH OPTIMIZATION

CD-88-32973

## COMPUTATIONAL STRUCTURAL MECHANICS IDENTIFIED METHODOLOGY - ALTERNATIVE

Another important part of the CSM program is to identify alternative methodology for computational simulation such as (1) the probabilistic approach for quantifying the uncertainties with all variables of structural analysis and design and (2) alternative methods for formulating structural mechanics problems. Some of the them have already been identified and are listed below

- **PROBABALISTIC OR STOCHASTIC:**

- VARIATIONAL PRINCIPLES FOR PROBABILISTIC FINITE ELEMENT
- PROBABILISTIC STRUCTURAL ANALYSIS METHODS
- PROBABILISTIC FRACTURE MECHANICS

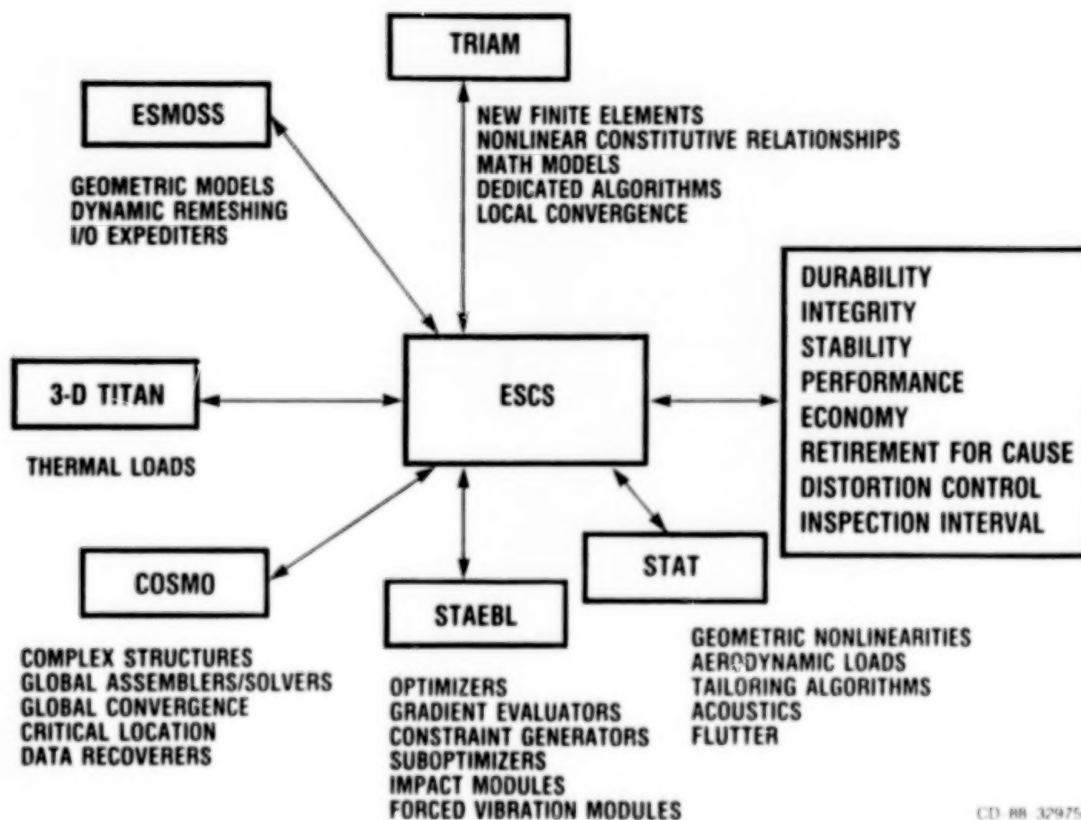
- **ALTERNATIVE FORMULATIONS:**

- MULTIPARALLEL PROCESSORS FOR MULTIDISCIPLINARY MECHANICS PROBLEMS
- SPECIALTY FUNCTIONS FOR SINGULAR MECHANICS PROBLEMS
- COUPLED CONSTITUTIVE RELATIONSHIPS
- DEDICATED EXPERT SYSTEMS

CD-88-32974

## ENGINE STRUCTURES COMPUTATIONAL SIMULATOR (ESCS)

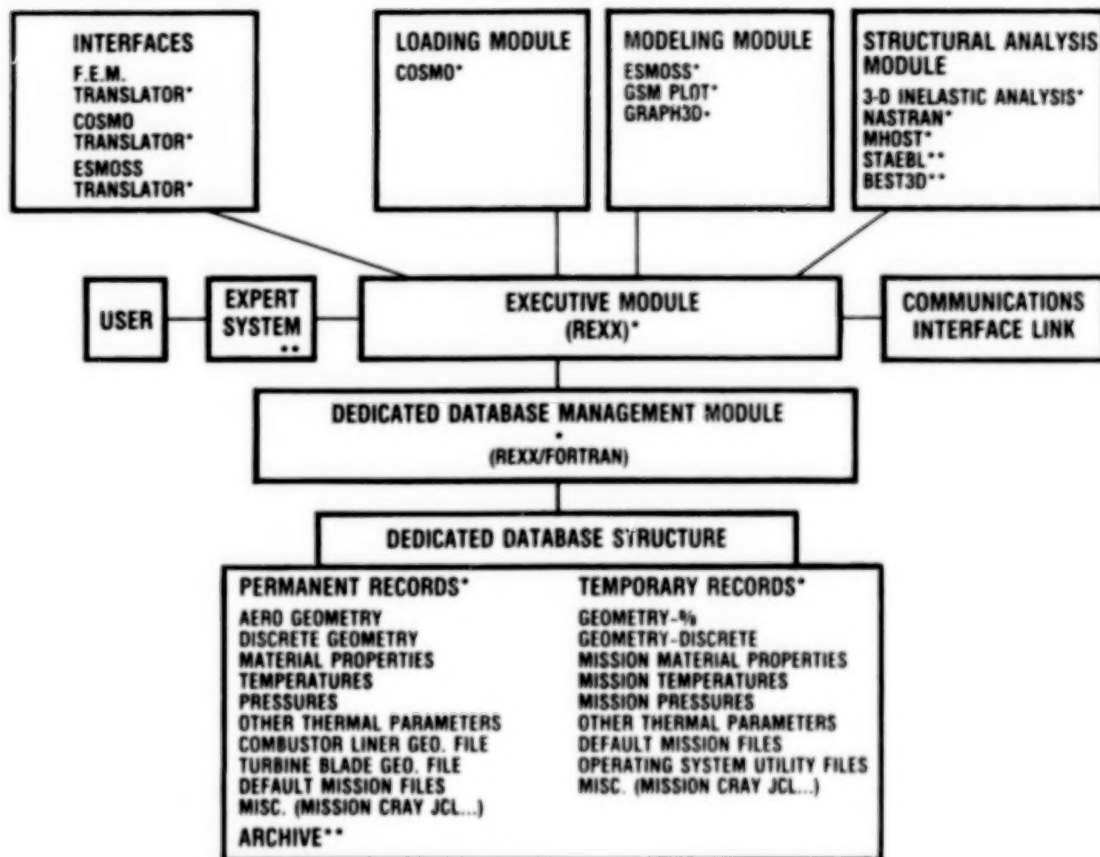
A major part of the Lewis CSM program is the development of engine structures computational simulator (ESCS). ESCS integrates discipline specific methodology and computer codes developed under research and technology programs as indicated below. ESCS-predicted results will be postprocessed to make assessment of engine structural performance in terms of the items listed in the block at the right.



CD 88 32975

# ESCS SOFTWARE SYSTEM ARCHITECTURE

ESCS is modular with an expert-system-driven executive module. It includes interfacing modules, a database, and its manager. A schematic of the ESCS present status configuration is shown in the accompanying chart. The interface module provides the logic to merge different analysis models as well as loading conditions to the analysis models. The analysis module includes advanced analysis methods such as specialty finite elements (three-dimensional inelastic analysis), mixed elements (MHOST), and boundary elements (BEST3-D). It also includes NASTRAN and structures optimization (STAEBL).



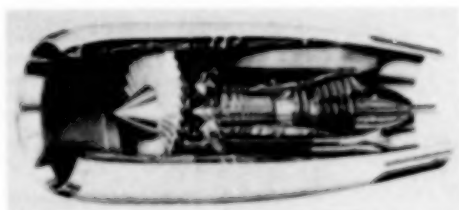
\*—PRELIMINARY VERSION AVAILABLE

\*\*—TO BE INSTALLED

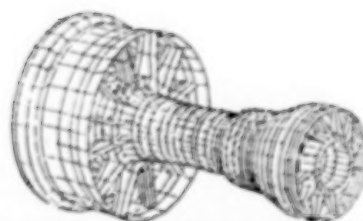
CD 88 32976

## ESCS CONFIGURED FOR ENGINE STRUCTURES FROM COMPONENT TO ENGINE

ESCS is configured to computationally simulate the structural performance of engine structures: (1) subcomponents, (2) components, (3) subassemblies, (4) assemblies, and (5) integrated systems for mission specified requirements. These are shown below from bottom left to top right, respectively.



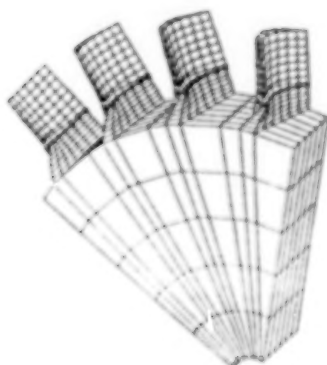
**ENGINE**



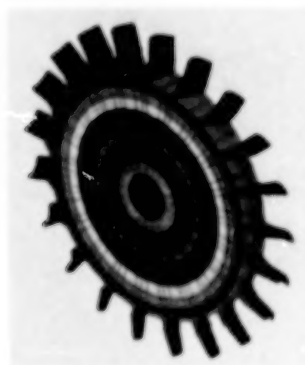
**FINITE ELEMENT MODEL**



**BLADE**



**ROTOR SECTOR**

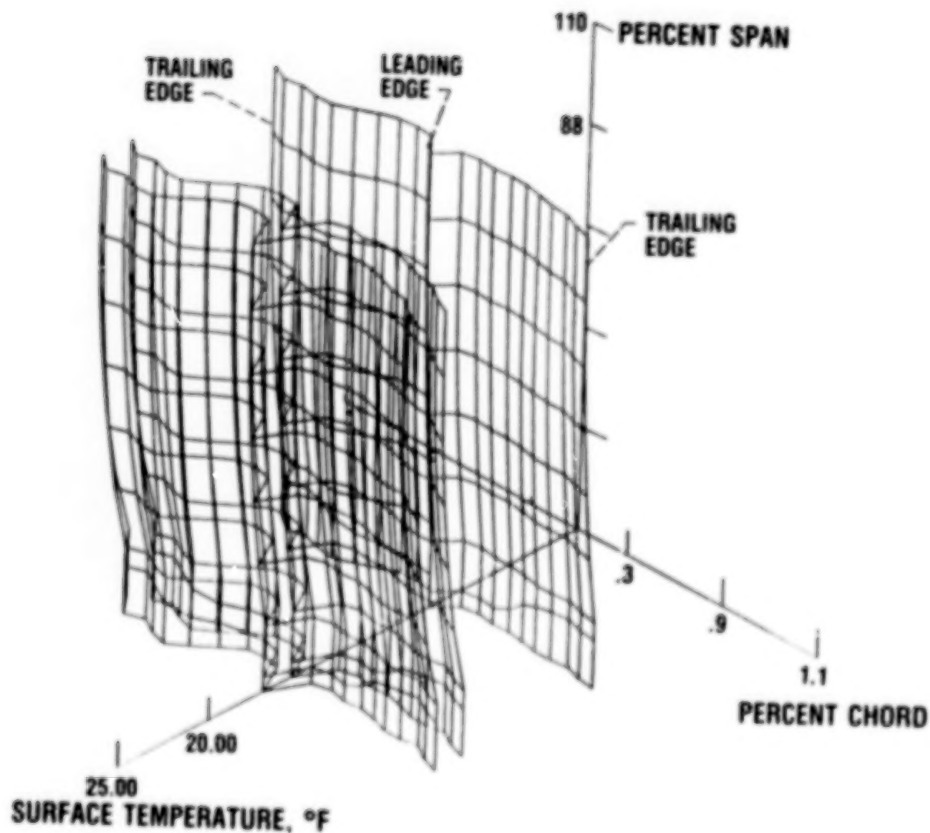


**ROTOR STAGE**

CD 88-32977

## ESCS HAS MODULE FOR LOADS

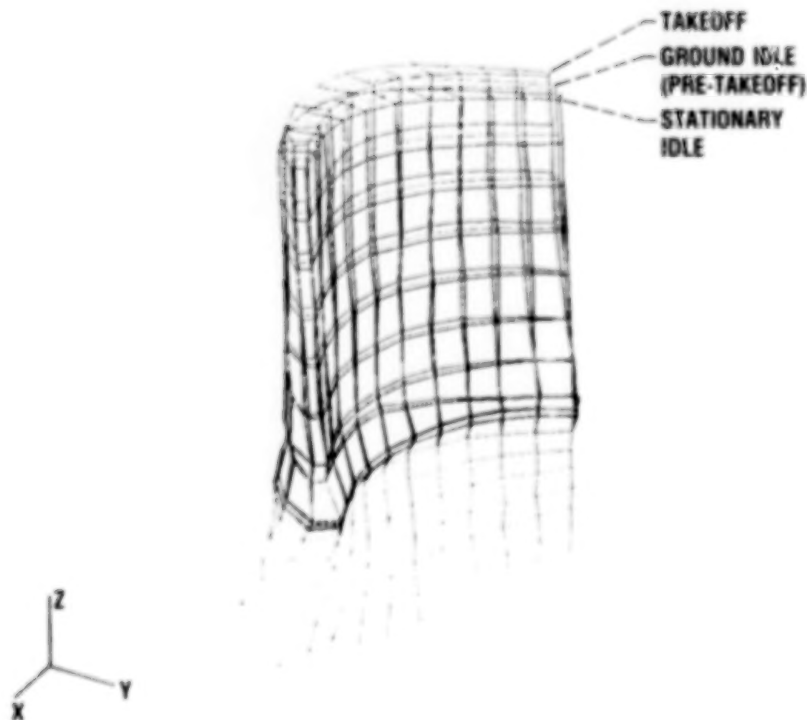
The loads on the blades (temperatures, pressures, and rotating speeds) are determined by an engine loads module (COSMO in the ESCS schematic). This module is based on engine thermodynamics. The temperatures and pressures are predicted on the surface at user-selected span stations. The accompanying chart is a typical example for temperatures. The blade has been unfolded for 3-D plotting presentation. Pressures and speeds can be similarly represented.



CD-88-32978

# DEFORMATION OF TURBINE BLADE UNDER FLIGHT CONDITIONS - A SAMPLE ESCS CASE

The ESCS executive module couples the loads module with the analysis-modeling module and with the analysis module through module-communication links and proceeds to determine the blade structural response at the preselected times during the mission. Results from such an analysis for the displacements of a turbine blade are shown below for three mission conditions.

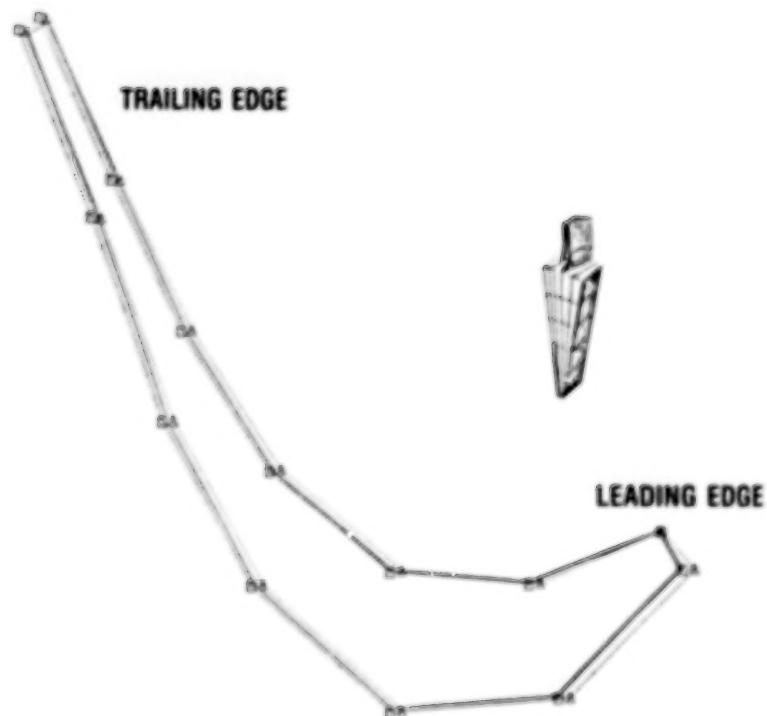


CD-88-32979



### ESCS ANALYSIS MODULES - PREDICTION COMPARISONS

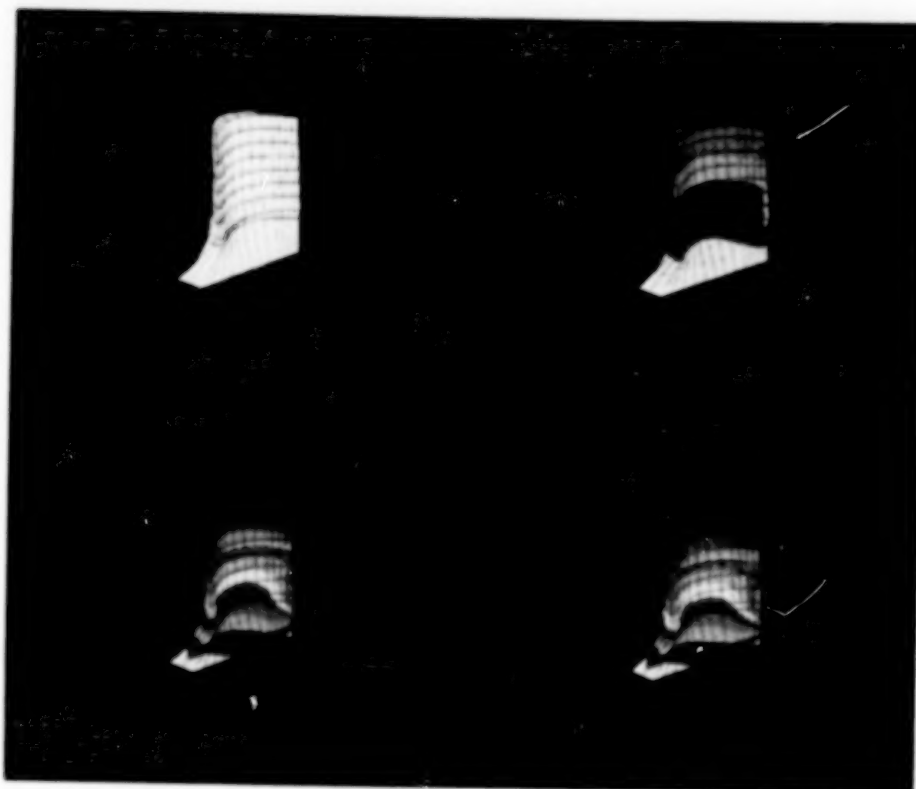
ESCS has two finite-element analysis modules at its present status - MSC/NASTRAN and MHOST. Results predicted by these two analysis modules are compared in the accompanying chart. The predicted results for the blade airfoil displacements from the two analysis modules for combined mechanical and thermal loads are indistinguishable.



CD-88-32980

### ESCS SAMPLE RESULTS - SINGLE COMPONENT

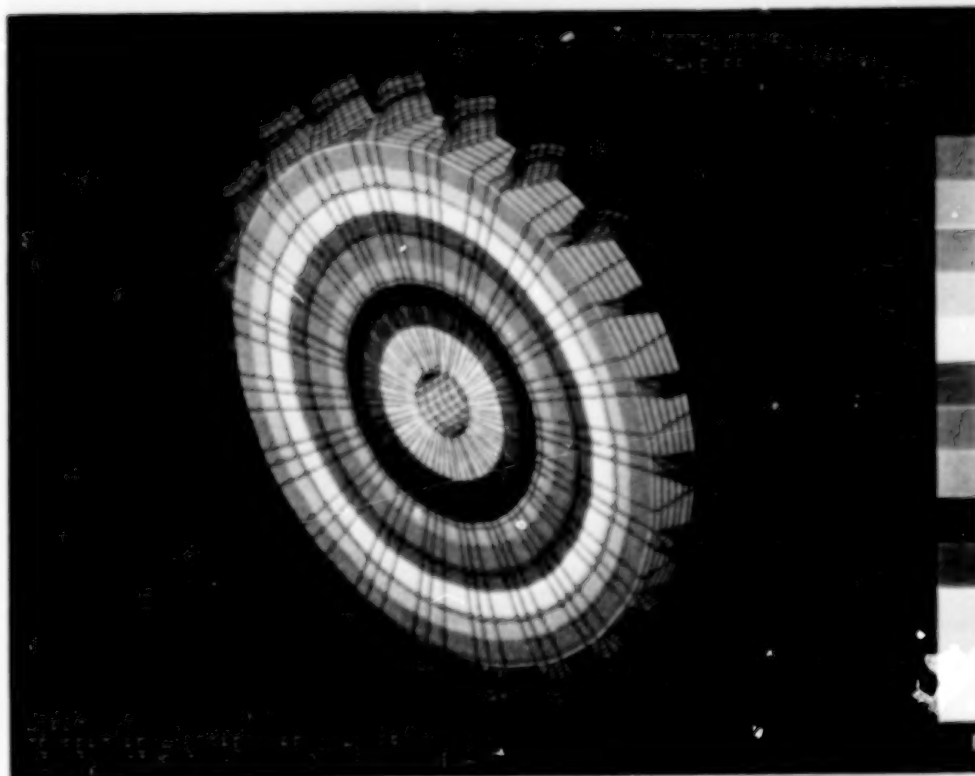
ESCS postprocesses analysis results for computer graphics display. Examples include a single component in this chart at three stages during the mission: ground idle, takeoff, and cruise. The dynamic motion of the blade is assessed by comparing it with the reference state (stationary position in the figure).



CD-88-32981

# ESCS SAMPLE RESULTS - BLADED ROTOR ASSEMBLY

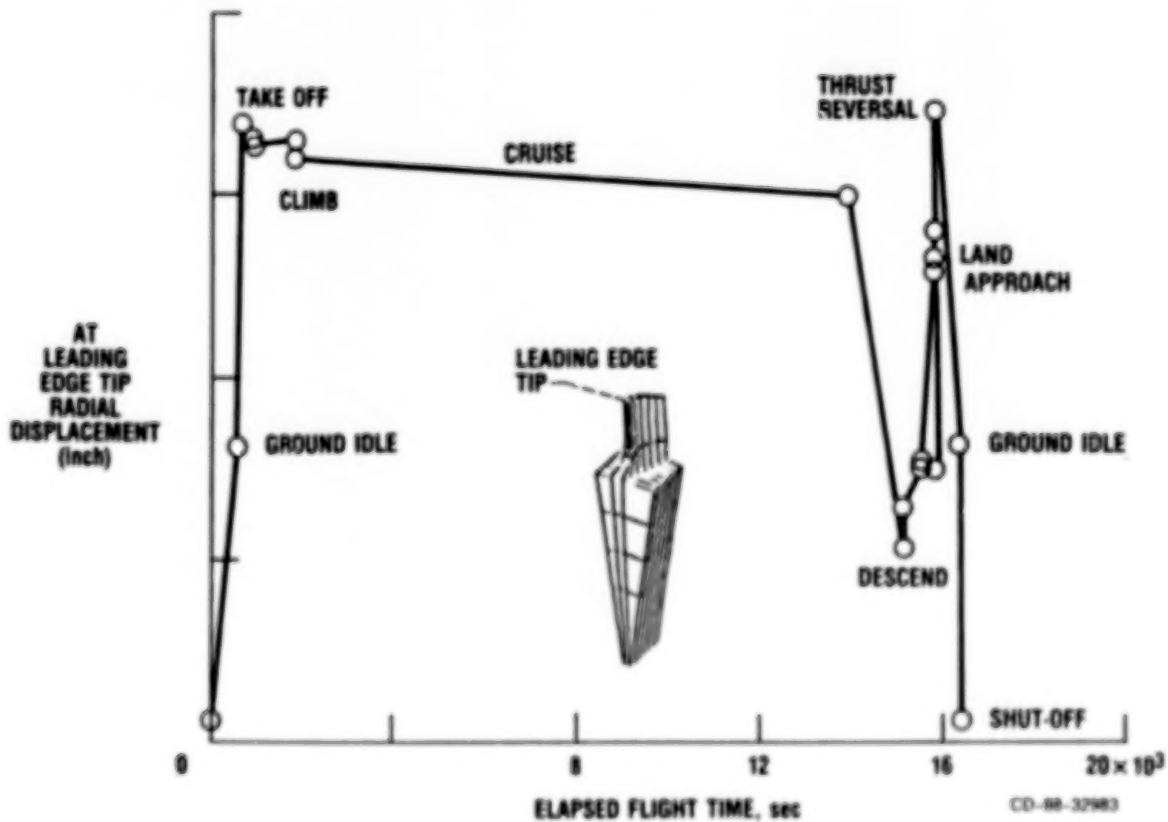
The structural dynamic response of blades assembled in a bladed rotor is different from that of an individually simulated blade. The dynamic motion of a bladed rotor determined using ESCS is shown below at the takeoff conditions.



CD-88-32982

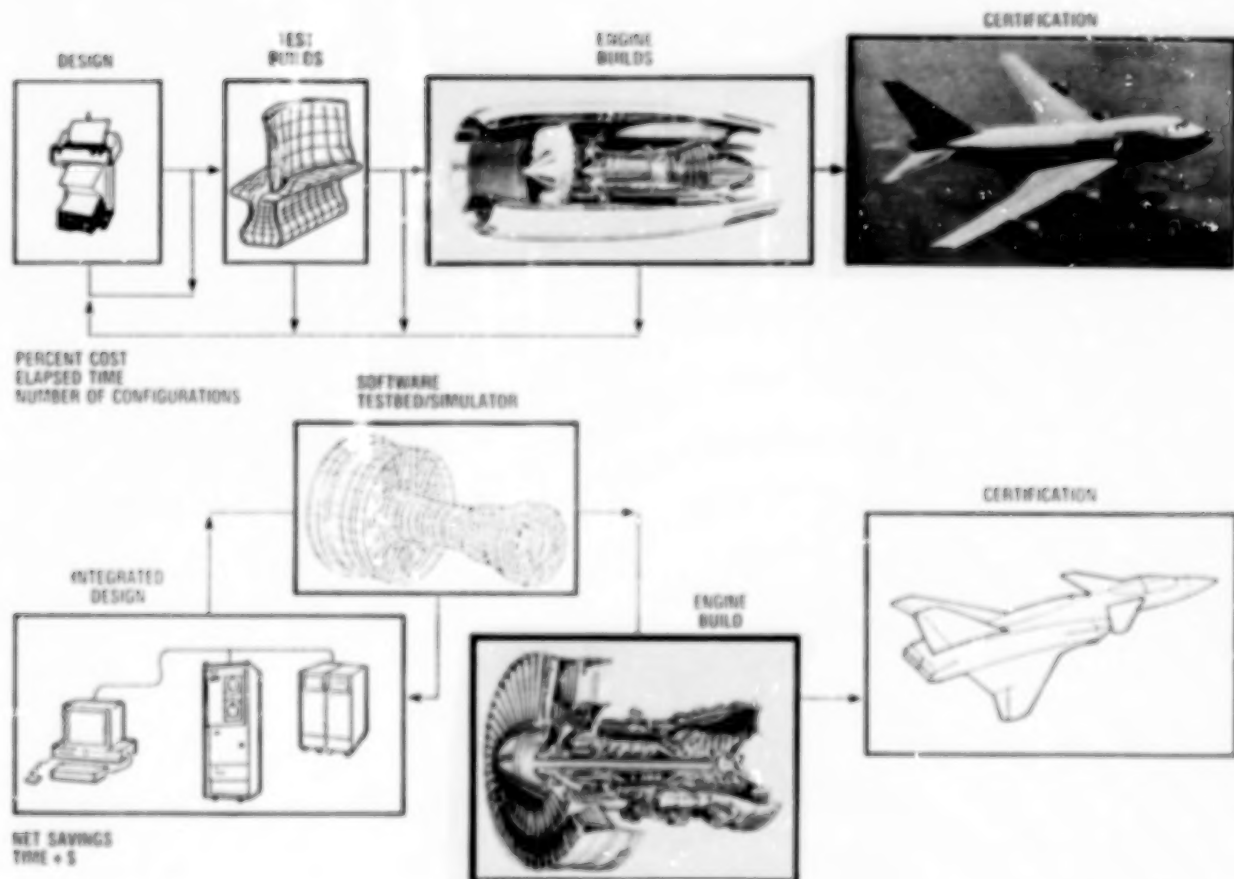
# ESCS SAMPLE RESULTS FOR FLIGHT MISSION SIMULATION

The structural response can be predicted throughout the mission. Representative results for blade-tip radial displacement are shown graphically at identifiable stages during the flight for corresponding pressures, temperatures, and centrifugal loadings. These types of results can be obtained for any point in the component included in the simulation. The significance of having structured response throughout the mission is that all dynamic interactions are properly accounted for, and the stress-strain results are suitable for life assessments.



## ESCS LONG RANGE OBJECTIVE REVISITED

The long range objective of the ESCS is to provide a computational simulation that parallels and replaces, in part, the current development methods which make extensive use of experimental procedures. The parallel between the current development procedures and ESCS are depicted below. ESCS will minimize the effort expended from initial design to engine builds and will often result in more cost effective engine builds for the same engine performance.



ESD-44 1/1984

## ESCS ANTICIPATED BENEFITS

The anticipated benefits to aerospace industry of having and exercising ESCS are summarized in the accompanying chart using qualitative terms. Engine manufacturers have cost estimates for each of the items in the chart based on their own development experience. Suffice it to say that each item runs into multimillions of dollars

- REDUCED DEVELOPMENT TIME AND COSTS
- FEWER DEVELOPMENT ENGINE BUILDS
- LONGER LIFE COMPONENTS
- REDUCED LIFE CYCLE COSTS ON COMPONENTS
- REDUCED COMPONENT AND ENGINE WEIGHT
- IMPROVED ENGINEERING PRODUCTIVITY
- INCREASED PERFORMANCE

CD-88-34030

DEAN PAGE



## STRUCTURAL TAILORING OF ADVANCED TURBOPROPS\*

K.W. Brown\* and Dale A. Hopkins  
Structural Mechanics Branch  
NASA Lewis Research Center

### ABSTRACT

The Structural Tailoring of Advanced Turboprops (STAT) computer program was developed to perform numerical optimizations on highly swept propfan blades. The optimization procedure seeks to minimize an objective function defined as either; (1) direct operating cost of full-scale blade or, (2) aeroelastic differences between a blade and its scaled model, by tuning internal and external geometry variables that must satisfy realistic blade design constraints.

The STAT analysis system includes an aerodynamic efficiency evaluation, a finite element stress and vibration analysis, an acoustic analysis, a flutter analysis, and a once-per-revolution forced response life prediction capability. STAT includes all relevant propfan design constraints.

The STAT system has been applied to three large scale advanced propfan applications. The STAT program made significant improvements in all three cases and demonstrated the great potential for design enhancements through the application of numerical optimization to turboprop fan blades of composite construction.

---

\*Pratt & Whitney Aircraft, East Hartford, CT. Work performed under NASA contract NAS-23941.

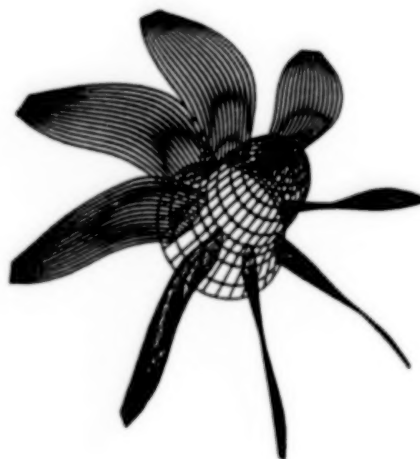
## THE HIGHLY COMPLICATED PROCESS OF THE SWEPT PROPFAN DESIGN

The swept turboprop design process involves the application of state-of-the-art interdisciplinary engineering technologies. Numerous design iterations are required between several work disciplines, including aerodynamics, acoustics, structures, and aeroelastic analysis groups. Using these current design procedures, it is very difficult to arrive at a satisfactory turboprop design, much less an optimum one, because of multi-iterative, manual intergroup design process that is required.

The penalties of this process include less than optimum designs, long design times, low performance, and high noise and weight levels.

### MANY DISCIPLINES MUST BE TIED TOGETHER

- AERODYNAMICS
- ACOUSTICS
- STRUCTURES
- AEROELASTIC (FLUTTER)



CD-88-32924

## SR-7 PROPFAN DESIGN HISTORY -- CONFLICTS BETWEEN FLUTTER AND STRESS CONSTRAINTS

In the design process for the SR-7 Propfan, a satisfactory aerodynamic configuration was reached by design iteration number 40. The final, acceptable design, however, was not reached until design number 100. Thus, 60 configuration changes were required before all structural design constraints could be met. The cost and labor required to complete this process is obviously very high.

For the SR-7, the increased sweep tended to improve the flutter stability margin, at the expense of higher foil stresses. The final 20 iterations in the design process proved to be little more than a fine-tuning of the blade sweep.

- HIGHER SWEEP IMPROVES FLUTTER MARGIN.
- INCREASED SWEEP INCREASED AIRFOIL STRESS.
- THE FINAL SR-7 BLADE IS DESIGN ITERATION NUMBER 100.



CD-88-32925

## MULTIDISCIPLINARY ANALYSIS CAPABILITIES OF STAT

STAT is a highly modular software package, consisting of an executive system, an optimizer, a design preprocessor, a set of approximate analyses, and a set of refined analyses. Currently, STAT uses the ADS optimization package, which is quite versatile, and also publicly available.

STAT's design preprocessor uses design curves to define both geometric and construction blade properties. Based on input from the optimizer, a new geometry is defined, and appropriate numerical models constructed.

STAT's approximate and refined analyses include aerodynamic, acoustic, flutter, finite element stress and vibrations, and 1-P forced response analyses.

- **OPTIMIZER:**

- ADS**

- **DESIGN PROCESSING:**

- BASELINE DESIGN CURVES**

- DESIGN CURVE PERTURBATIONS**

- **MODULAR APPROXIMATE, REFINED ANALYSES:**

- AERODYNAMICS**

- ACOUSTICS**

- FLUTTER**

- STRESS**

- VIBRATIONS**

- FORCED RESPONSE**

CD-88-32926

### THREE PROPFAN APPLICATIONS OF STAT

The STAT program has successfully demonstrated the potential of design optimization when applied to turboprop fan blades of composite construction. STAT produced improved designs for both the SR-7 and 18-E LAP blades. Additionally, the optimizer proved to be capable of constructing an improved aeroelastic scaled model propfan.

The final SR-7 blade was design number 100 in a long, expensive development process. STAT was able to demonstrate further improvements available from this finely tuned design. The 18-E Propfan was an early infeasible design candidate in the SR-7 development program. STAT showed the capability to take an early configuration and significantly improve it, thus greatly reducing the expense of the design process.

By applying STAT to an aeroelastic scaled model blade, STAT shows the potential for increasing the relevance of wind tunnel testing, while aiding design of these test configurations.

- **SR-7 PROPFAN—CAN WE IMPROVE ON THIS DESIGN (100th ITERATION)?**
  
- **PROPFAN 18-E—CAN WE GET TO A FEASIBLE PROPFAN FASTER THAN HSD'S ENGINEERS DID?**
  
- **AEROELASTIC SCALE MODEL—CAN STAT BE USED TO DESIGN AEROELASTICALLY SIMILAR SCALE MODELS FOR WIND TUNNEL TEST?**

#### DEMONSTRATIONS OF STAT UTILIZED TWO DIFFERENT OBJECTIVE FUNCTIONS

For conventional swept propfans, STAT uses aircraft direct operating cost as the objective function. Thus, a weighted function including aircraft fuselage noise level, propeller efficiency, and propeller weight is minimized, subject to appropriate design constraints.

For economical evaluation of candidate propfan designs, wind tunnel tests of scaled models are conducted. For effective wind tunnel testing, it is necessary to have aerodynamic, aeroelastic, and modal similarities between the full scale blade and the scaled model. In STAT, a weighted overall measure of full scale to scaled model configurations is minimized. A properly scaled blade will have similar flutter, resonance, efficiency, acoustic, and static and modal deflection characteristics.

- FOR FULL SIZE PROPFANS, DIRECT OPERATING COST IS MINIMIZED.
- FOR THE AEROELASTIC SCALE MODEL, A WEIGHTED SIMILARITY FUNCTION MEASURES DIFFERENCES IN VIBRATORY, MASS, MODE SHAPES AND UNTWIST DEFLECTIONS.

CD-88-32928

## STANDARD PROPFAN DESIGN CONSTRAINTS USED BY STAT

STAT includes all design constraints normally considered in the propfan design process. Side constraints limit the movement available on the various components of geometry. Vibratory frequencies are limited according to prescribed resonance margins. Stresses are limited via a Goodman diagram construction including both steady stress and once per revolution forced response stresses. Both classical unstalled and stalled flutter are constrained. Finally, rotor power is held constant through an equality constraint.

### BLADE GEOMETRY

- THICKNESS/CHORD
- ROOT STACKING POSITION

### FLUTTER

- CLASSICAL FLUTTER
- STALL FLUTTER

### POWER

### RESONANCE MARGINS

- 1st MODE 2E
- 2nd MODE 4E
- 2nd MODE 5E
- 3rd MODE 5E

### STRESSES

- STEADY STRESS
- 1-P FORCED RESPONSE

CD-88-32929



#### STAT IMPROVES DOC FOR SR-7 PROPFAN BY 3.0 PERCENT

The SR-7 Propfan utilizes a complex composite construction. A nickel sheath edge layer protects a fiberglass outer shell. Also utilized are an internal aluminum spar, and foam to fill the gaps between the spar and the shell.

The initial optimization pass, using 38 design variables, reduced DOC by 5.0 percent. When design space was unscaled, however, the 1-P life was found to be unacceptable.

Using just 12 design variables to optimize the blade stacking, an improvement of 5.3 percent over the base blade was found. Subsequent refined analysis found that all constraints were satisfied, but that the actual DOC reduction was 3.0 percent.

- INITIAL OPTIMIZATION PASS, USING 38 DESIGN VARIABLES, REDUCED DOC BY 5.0 PERCENT, BUT THE 1-P FORCED RESPONSE LIFE CONSTRAINT WAS VIOLATED.
- USING TWELVE STACKING VARIABLES, STAT IMPROVED APPROXIMATE DOC BY 5.3 PERCENT
- REFINED ANALYSIS INDICATED:  
ALL CONSTRAINTS WERE SATISFIED.  
ACTUAL DOC IMPROVEMENT WAS 3.0 PERCENT.

CD-88-32930

THE 18-E LAB DESIGN WAS AN EARLY, INFEASIBLE  
DESIGN IN THE SR-7 HISTORY

The 18-E Propfan design was a candidate in the SR-7 design evolution that was unacceptable because of stress considerations. An interesting study performed with STAT was to see how this design would evolve relative to the manually designed SR-7.

Using 12 stacking and twist variables, STAT was able to improve the approximate DOC by 5.3 percent, which is a 4.4 percent improvement over the final SR-7 configuration.

- STEADY, 1-P STRESSES OF THE 18-E DESIGN ARE UNACCEPTABLE.
- BY ALTERING THE BLADE STACKING AND STAGGER, STAT WAS ABLE TO FIND AN IMPROVED DESIGN.
- TWELVE DESIGN VARIABLES EMPLOYED.
- ALL CONSTRAINTS SATISFIED.
- DOC REDUCED BY 5.3 PERCENT (OR, 4.4 PERCENT IMPROVED OVER FINAL SR-7 DESIGN).

CD-86-32931

## THE SR-7A IS AN AEROELASTIC PROPFAN SCALE MODEL

The SR-7A is a 2/9 size aerodynamic scaled model of the SR-7 LAP blade design.

The blade is composite in construction, made up with 12 layers. For the STAT optimization, the exterior shape was fixed to the scaled SR-7. The composite construction was tailored using 37 design variables to better match the aerostuctural performance of the blades, including: scaled frequencies, mode shapes, untwist static deflections, and mass distribution.

As the objective function, a summation of squared differences for all the above parameters was minimized. STAT was successful at reducing this objective function by 32 percent over the existing scaled model configuration.

- 2/9 SIZE SCALE MODEL, LAMINATED COMPOSITE CONSTRUCTION.
- EXTERIOR GEOMETRY IS FIXED BY THE SR-7, BUT COMPOSITE CONSTRUCTION WAS TAILORED TO BETTER MATCH AEROSTRUCTURAL SCALING REQUIREMENTS (37 DESIGN VARIABLES).
  - FREQUENCIES
  - MODE SHAPES
  - DEFLECTIONS
  - MASS DISTRIBUTION
- COMPONENT STRESSES WERE THE ONLY DESIGN CONSTRAINT.
- DIFFERENCES SQUARED OBJECTIVE FUNCTION WAS REDUCED BY 32 PERCENT

CD-88-32932

#### WORK IN PROGRESS

Currently, STAT is being expanded to allow the tailoring of counter rotation propfans. This effort involves extensive improvements to the aerodynamic and acoustic modules, including an upgrade of the approximate acoustic analysis, to improve correlations with refined analysis.

Enhancements to STAT include an improved optimization scaling algorithm, and also improved flexibility in initial design selection.

- APPLICATION TO COUNTER ROTATION PROPFANS.  
AERODYNAMICS  
ACOUSTICS
- INCREASED AIRFOIL DEFINITION FLEXIBILITY.
- IMPROVED OPTIMIZATION SCALING ALGORITHMS

CD-88-32933

## CONCLUSIONS

The STAT propfan optimization system has shown that design tailoring can be effectively applied to large, multidisciplinary systems, showing great potential for manpower requirement reductions, relative to present, manual design procedures.

STAT has been successfully applied to the optimization of two full scale propfans, and also to an aerostructural scaled model. With the exception of the approximate acoustic analysis, all approximate analysis modules have shown very good accuracy.

- DESIGN OPTIMIZATION HAS BEEN SUCCESSFULLY APPLIED TO THE COMPLEX PROPFAN DESIGN PROCESS.
- STAT HAS BEEN SUCCESSFULLY APPLIED TO THE OPTIMIZATION OF TWO PROPFANS, AND ALSO TO AN AEROSTRUCTURAL SCALE MODEL.
- THE APPROXIMATE ACOUSTIC ANALYSIS NEEDS IMPROVEMENT.

#### REFERENCES

- Brown, et al., 1987, "Structural Tailoring of Advanced Turboprops," AIAA/ASME/ASCE/AHS 28th Structures, Structural Dynamics, and Materials Conference, Monterey, CA, April, 1987.
- Sullivan, et al., "Large-Scale Advanced Prop-Fan SR-7 Blade," NASA Contract NAS3-23051 (to be published).
- Vanderplaats, et al., 1983, "ADS-1: A New General Purpose Optimization Program," AIAA 24th Structures, Structural Dynamics and Materials Conference, Lake Tahoe, NV, May 1983.

BLANK PAGE



## ADVANCED PROBABILISTIC METHODS FOR QUANTIFYING THE EFFECTS OF VARIOUS UNCERTAINTIES IN STRUCTURAL RESPONSE\*

Vinod K. Nagpal  
Sverdrup Technology, Inc.  
(Lewis Research Center Group)  
Lewis Research Center

A probabilistic structural analysis of a space shuttle main engine (SSME) turbopump blade has been underway at the Lewis Research Center for the last 3 years. The immediate objectives of this study are to evaluate the effects of actual variations, also called uncertainties, in geometry and material properties on the structural response of the turbopump blades. In this study a normal distribution has been assumed to represent the uncertainties statistically. Uncertainties were assumed to be totally random, partially correlated, and fully correlated. The magnitudes of these uncertainties have been represented in terms of mean and variance. These two quantities were selected such that the absolute magnitudes of uncertainty at any point were either less than or equal to 10 percent of their original values.

Many studies have demonstrated that probabilistic analysis methods for components under random loading are more reliable than deterministic approaches. Probabilistic methods have been predominantly used in fatigue, fracture mechanics, and structural reliability analyses under random vibrations (e.g., studies reported by Dover, 1979; Yang, 1981; Wirshing, 1981; Kawamoto, 1982; and Huang and Nagpal, 1984). Particularly in fatigue, improvements in estimating fatigue life ranged up to several hundred percent in comparison with a widely used deterministic approach developed by Miner (1945). Because of the potential, the application of probabilistic methods has been accepted in the other fields of engineering in recent years. These fields include input loading, finite elements, and metallurgy. A probabilistic approach to develop a composite loading for SSME components is underway at the Battelle Laboratories under the technical guidance of R. Kurth (1985) and has been discussed by Shinozuka and Lin (1981). Other studies using probabilistic finite-element methods have been briefly reviewed by DasGupta (1986). A variational approach for developing the probabilistic finite elements is under development by Belytschko and Liu (1985). The usefulness and importance of the probabilistic approach, especially for turbopump blades, has been summarized by Chamis (1986).

Blade response, recorded in terms of displacements, natural frequencies, and maximum stress, was evaluated and plotted in the form of probabilistic distributions under combined uncertainties. These distributions provide an estimate of the range of magnitudes of the response and probability of occurrence of a given response. Most importantly, these distributions provide the information needed to estimate quantitatively the risk in a structural design.

---

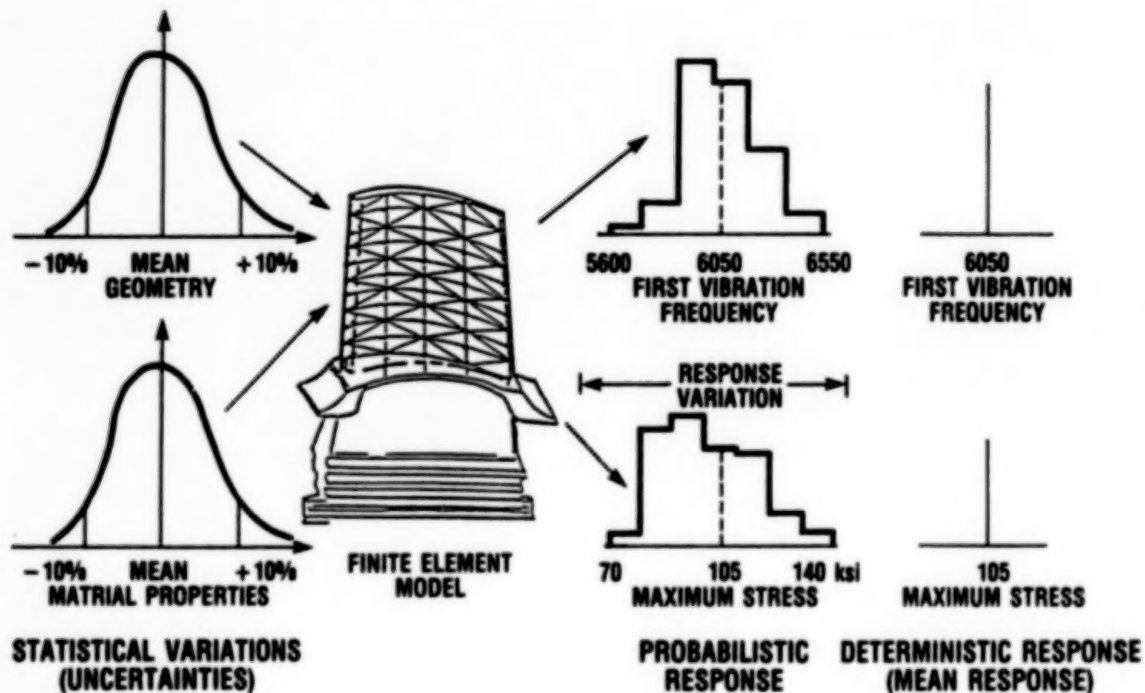
\*Work performed for the Structural Mechanics Branch under contract NAS3.

A wide range of response, such as a maximum stress distribution, implies that small natural uncertainties in the geometry and material properties can cause a large variation in the response. Consequently, designs based on deterministic methods will not be as safe as probability-based designs. Higher stresses, which have low but certain probability of occurrence, are not included in the deterministic designs. In most cases available experimental results are insufficient to provide an entire range of stresses and their probabilities of occurrence. Limited experimental results as well as deterministic methods provide estimates of the mean response but do not cover the scatter. Consequently, the risk in design even after using the factor of safety may or may not be within acceptable limits.

The results of the study indicate that an uncertainty up to 10 percent in the material properties had no significant effect on the response. However, uncertainty up to 10 percent in geometry, only through the thickness, has significant effect on the structural response. Based on the results, a number of probabilistic models has also been developed using regression analysis. These models predict the response for given uncertainties in the geometry and material property parameters. The models for uncertainties in temperature combined with those in geometry and material properties are under development.

## PROBABILISTIC STRUCTURAL ANALYSIS ESTIMATES OF RESPONSE

The probabilistic approach provides the scatter in the response and also provides the probability of occurrence. This information helps assess the risk quantitatively for all levels of response. Contrarily, the deterministic response provides an estimate of mean value and does not cover the scatter. Consequently, the risk even after using a safety factor may or may not be within the acceptable range.



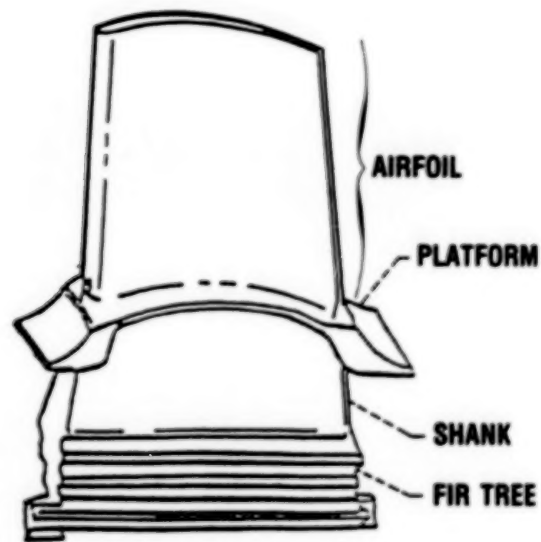
CD-88-32631

## OBJECTIVE

The analysis was performed on the airfoil of a typical SSME turbine blade. Nominal dimensions of the airfoil are 1 to 1½ inches long, about 1 inch wide, and a ⅛ inch thick. Generally, these blades are made of anisotropic materials. The number of blades per turbine stage is about 65. The other parts of the blade are the platform, shank, and fir tree.

### QUANTIFY UNCERTAINTIES ASSOCIATED WITH PROBABILISTIC RESPONSE

- GEOMETRY
  - UNCORRELATED
  - CORRELATED
- MATERIAL PROPERTIES
- LOADING
- TEMPERATURE



A TYPICAL TURBINE BLADE

CD-88-32632

## PROBABILISTIC STRUCTURAL RESPONSE

The probabilistic structural response of the blade was recorded in terms of first three natural frequencies, root stress, which is also the maximum stress, and blade tip displacements. The root stress is the stress at the junction of the airfoil and the platform. Since the blade airfoil is considered fixed at this junction for this analysis, stress at that location becomes the maximum. The tip displacements were estimated in three directions. Two displacements were in the plane of the airfoil, and one was perpendicular to the plane of the airfoil.

- **NATURAL FREQUENCIES**

- FIRST**

- SECOND**

- THIRD**

- **ROOT (MAXIMUM) STRESS**

- **TIP DISPLACEMENTS**

CD-88-32633

## METHODOLOGY

The developed methodology is generic and can be used to analyze other structural components which may or may not be related to this problem. This chart describes the major steps used for performing this analysis. The first step is the generation of random numbers. Correlated or uncorrelated random numbers are used for perturbation of the geometry, spatial location, and/or material properties. Uncorrelated numbers indicate no bearing of the perturbation of one point on any other point on the airfoil.

The second step is modeling the blade with a finite-element model. Eighty triangular shell elements with 55 nodes were used to model the airfoil.

The third step involves setting up of the design to run simulations. Full factorial design was used because it is considered more economical than other available approaches.

The fourth step involved analyzing the response and developing its probabilistic distribution and models to predict the response for given uncertainties.

- **SELECTED RANDOM DISTRIBUTION TO SIMULATE UNCERTAINTIES IN GEOMETRY, SPATIAL LOCATION, AND MATERIAL PROPERTIES**

- NORMAL**

- **MODELED BLADE WITH FINITE-ELEMENT MODEL**

- 80 ELEMENTS**

- 55 NODES**

- **USED NUMERICAL EXPERIMENT DESIGN TO PERFORM SIMULATION**

- FULL FACTORIAL DESIGN**

- **ANALYZED RESPONSE**

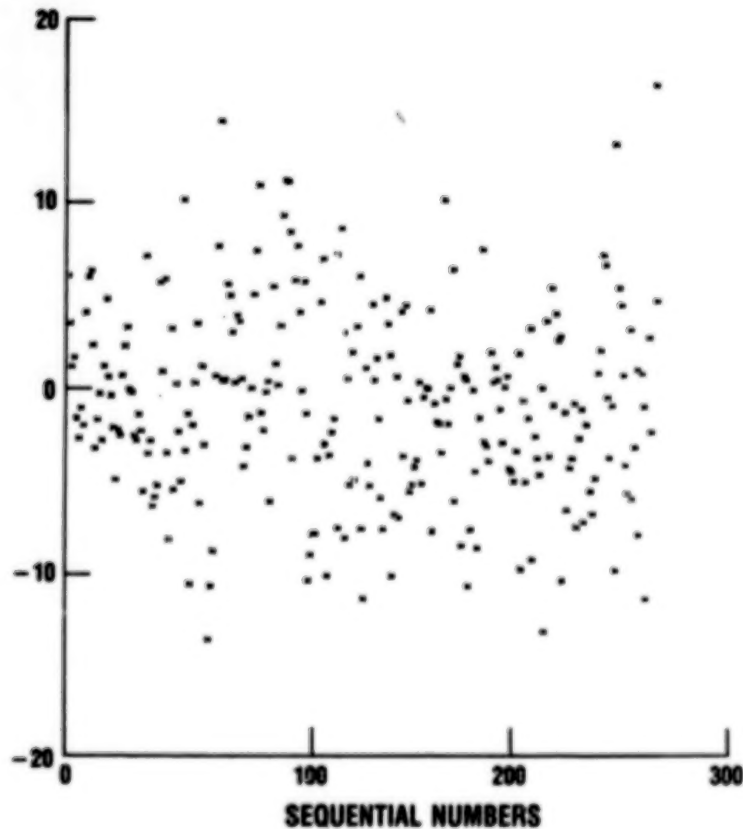
- PROBABILISTIC MODELS**

- PROBABILISTIC DISTRIBUTIONS**

- STATISTICAL TESTS**

### SAMPLE RANDOMNESS USED IN PERTURBATIONS

Both uncorrelated and correlated random numbers are generated by the computer. They can be generated using any distribution and with preselected statistical properties such as mean, standard deviation, etc. In the present study a normal distribution with selected mean and variance was used. The random numbers have the property that they can be multiplied by any constant without losing their randomness. A plot of random numbers is shown.



CD-88-36235

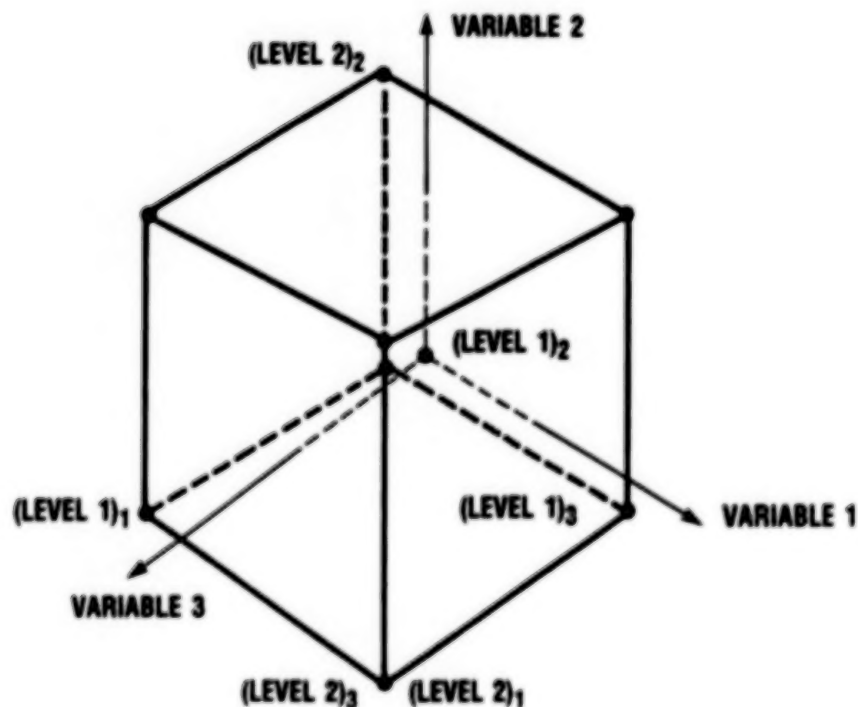


### FACTORIAL DESIGN FOR THREE VARIABLES

A factorial design is an economical method for performing real experiments or computational simulations. Unlike a parametric approach, the influence of individual variables and their interactions can be estimated discretely. Another advantage of the factorial design is that the range of the variables can be extended by amending the design scientifically.

There are two limitations with the factorial design: it can be used only for the independent variables, and the results of the study are only applicable within the range studied.

A representation of the factorial design for three variables is shown in the attached figure. The solid circles at the corners or in the center of the box represent the experiment or simulation points. A range of variables is defined as the difference between its two extreme levels.



CD-88-32636



## RANDOM COORDINATE PERTURBATION OF SSME BLADE

A geometric perturbation is done by perturbing the nodal coordinates in all three dimensions. The figure shows an exaggeration of perturbation of nodal coordinates in the  $x$  direction only. Perturbation in all three directions is difficult to show in graphical form. The geometric perturbation in this study is intended to simulate realistic geometric variation due to manufacturing tolerances and the errors in finite-element modeling. The variations in geometry at any point were limited to less than 10 percent.

Perturbations were created using random numbers. Uncorrelated and partially correlated random numbers were used to simulate truly uncorrelated or patterned variations in the geometry.



CD-88-32637

## RANDOM YOUNG'S MODULUS DISTRIBUTIONS IN SSME BLADE

Material properties perturbation is done by perturbing the properties of each finite element. The attached figure is a demonstration of the variation of modulus of elasticity for a blade that is made of an isotropic material. For a blade made of anisotropic material the entire material property matrix is perturbed at the same time. Material properties, like geometry, were perturbed using uncorrelated and partially correlated random numbers.

These perturbations are to represent realistic variation in the material properties. The maximum variation at any location was limited to 10 percent. The "10 percent" number was selected based on expert opinion.



CD-88-32638

# PROBABILISTIC MODELS

Probabilistic models were developed using regression analysis. The general form of the model is represented at the top of the following figure. The left side of the model represents dependent variables, which can be any variable in the response. The right side of the model consists of means and standard deviations of uncertainties and their coefficients. Over 20 models were developed. For demonstration purposes coefficients of only one of the models are plotted. This model is for estimating the variation first natural frequency due to combined effect of uncertainties in geometric and material properties.

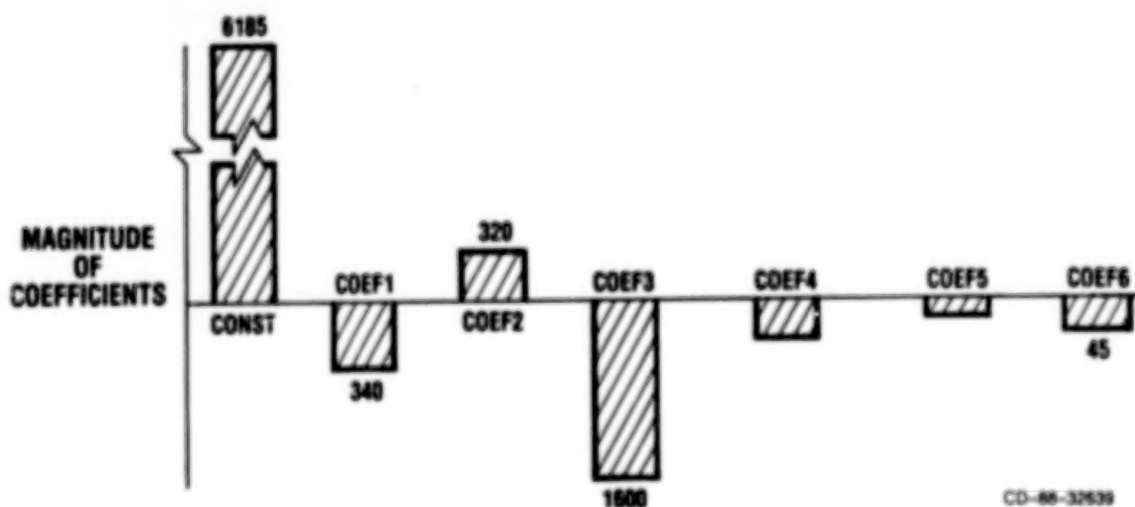
## MODEL

$$\hat{Y} = (\text{CONST}) + (\text{COEF})_1 \sigma_1 + \dots + (\text{COEF})_6 \sigma_{C_{33}} + \dots + (\text{COEF})_{21} \sigma_3 \sigma_{C_{33}}$$

## WHERE

$\sigma_1$  STANDARD DEVIATION OF PERTURBATION IN I DIRECTION

$\sigma_{C_{ij}}$  STANDARD DEVIATION OF PERTURBATIONS OF MATERIAL PROPERTY MATRIX ELEMENT  $C_{ij}$

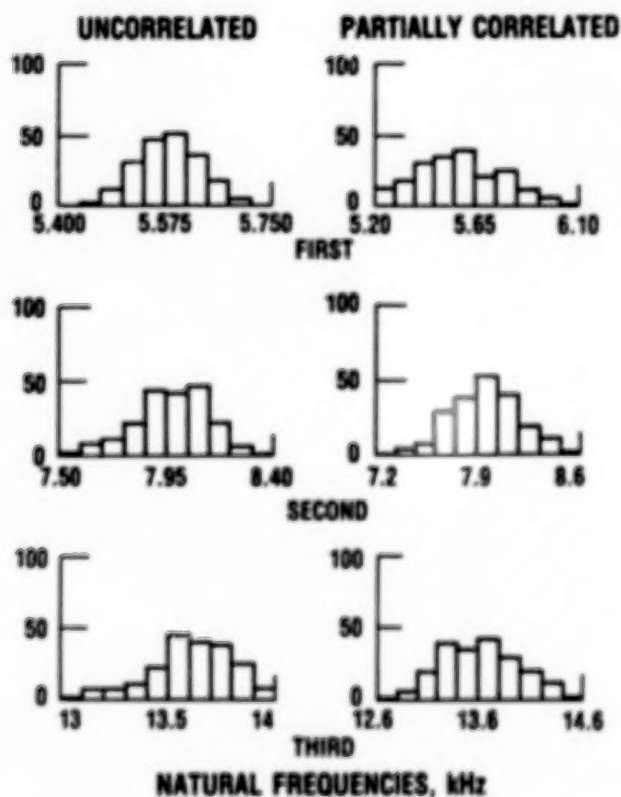


CD-86-32639

## INFLUENCE OF MATERIAL PERTURBATIONS ON NATURAL-FREQUENCY DISTRIBUTION

The response variables were evaluated for both uncorrelated and correlated random variations in geometry and material properties. The variation in the natural frequencies for partially correlated variations in material properties was slightly wider than for uncorrelated variations. However, the increment in variations was not significant. The response for variation in geometry alone and combined variation in geometry and material properties was studied.

Sample histograms of variations in the first three natural frequencies are shown.



CD-68-32640

- **METHODOLOGY TO QUANTIFY UNCERTAINTIES IN THE DESCRIPTORS OF SSME BLADES HAS BEEN DEVELOPED AND APPLIED.**
- **METHODOLOGY IS GENERIC AND EXTENDABLE TO ANY STRUCTURAL COMPONENT AND ALL ASPECTS OF STRUCTURAL ANALYSIS AND DESIGN.**
- **GEOMETRIC UNCERTAINTIES SHOWED SIGNIFICANT EFFECT ON COMPONENT STRUCTURAL RESPONSE.**
- **MATERIAL PROPERTIES UNCERTAINTIES AND THEIR INTERACTIONS HAVE INSIGNIFICANT EFFECTS ON COMPONENT STRUCTURAL RESPONSE.**
- **RANGE OF VARIATION IN STRUCTURAL RESPONSE QUANTIFIED AND EXPLICIT PROBABILISTIC MODELS HAVE BEEN DEVELOPED.**
- **INFLUENCE OF UNCORRELATED AND PARTIALLY CORRELATED VARIATIONS IN GEOMETRY AND MATERIAL PROPERTIES ON THE RESPONSE HAVE BEEN STUDIED.**

CD-88-32641

## REFERENCES

- Belytschko, T., and Liu, W.K., 1985, "Probabilistic Finite Elements: Variational Theory," Structural Integrity and Durability of Reusable Space Propulsion Systems, NASA Report CP-2381.
- Box, G.E.P., Hunter, W.G., and Hunter, J.S., 1982, An Introduction to Design, Data Analysis, and Model Building, John Wiley and Sons.
- Chamis, Christos C., 1986, "Probabilistic Structural Analysis Methods for Space Propulsion System Components," presented in 3rd Space System Technology AIAA Conference, San Diego, California.
- DasGupta, G., 1986, "Literature Review on Probabilistic Structural Analysis and Stochastic Finite Element Methods," Probabilistic Structural Analysis Methods for Select Space Propulsion System Components, Southwest Research Institute, Annual Report.
- Dover, W.D., 1979, "Fatigue Crack Growth in Tubular Welded Connections," Second International Conference on Behavior of Offshore Structures, held at Imperial College, London, England.
- Huang, T.C., and Nagpal, Vinod K., 1984, "Probabilistic Factors, Experimental Design and Statistical and Variance Analyses for Fatigue Under Random Vibrations," edited by T.C. Huang and P.D. Spanos, New Orleans.
- Kawamoto, James, et al., 1982, "An Assessment of Uncertainties in Fatigue Analysis of Steel Jacket Offshore Platform," Applied Ocean Research, Vol. 4, No. 1.
- Kurth, R., 1985, "Composite Load Spectra For Select Space Propulsion Structural Components, Structural Integrity and Durability of Reusable Space Propulsion Systems," NASA Report CP-2381.
- Lin, Y.K., 1981, "Random Vibrations of Civil Engineering Structures," Proceedings of Symposium on Probabilistic Methods in Structural Engineering, HSCE, St. Louis, Missouri.
- Miner, M.A., 1945, "Cumulative Damage in Fatigue," Journal of Applied Mechanics, Vol. 12.
- Shirozuka, M., and Tan, R., 1981, "Probabilistic Load Combinations and Crossing Rate," Proceedings of Symposium Probabilistic Methods in Structural Engineering, ASCE, St. Louis, Missouri.
- Wirshing, Paul H., 1981, "Fatigue Reliability Analysis in Offshore Structures," Proceedings of Symposium on Probabilistic Methods in Structural Engineering, ASCE, St. Louis, Missouri.
- Yang, J.N., 1981, "Reliability Analysis of Aircraft Structures," Proceedings of Symposium on Probabilistic Methods in Structural Engineering, ASCE, St. Louis, Missouri.

## STRUCTURAL MECHANICS CODE APPLICATIONS

### SESSION OVERVIEW

Robert H. Johns  
Structural Mechanics Branch  
NASA Lewis Research Center

The papers in previous sessions described recent developments in structural mechanics codes made in-house at Lewis and under contract. Prominent among the specific technical problems addressed are the prediction of mechanical and thermal properties of resin matrix and metal matrix composites, and the structural response of components made from these materials. The codes include unique, nonlinear, three-dimensional finite element analysis methods, inelastic anisotropic material behavior, and the effects of defects, cracks, and other damage on composite and component behavior. In addition, a code to predict the effect of impact loads on damage and dynamic structural response will be described.

In this session, examples are presented of the application of these codes to various aerospace hardware. One paper shows the results of a new thermostructural analysis of space shuttle main engine turbopump blades. Another paper shows some interesting results and quantifies the problem of the severe heat load and associated thermal stresses and strains in a cooled cowl leading edge for a hypersonic airplane engine inlet. Another hypersonic engine application for which the results of a thermomechanical structural analysis are presented is that of actively cooled engine walls. Finally, the analysis and results of a structural assessment of a space station solar dynamic heat receiver thermal energy storage canister are described.



#### SESSION OVERVIEW

- R.H. JOHNS, STRUCTURAL MECHANICS BRANCH, NASA

#### IMPACT DAMAGE IN COMPOSITE LAMINATES

- J.E. GRADY, STRUCTURAL MECHANICS BRANCH, NASA

#### THERMOSTRUCTURAL ANALYSIS OF SIMULATED COWL LIPS

- M.E. MELIS, STRUCTURAL MECHANICS BRANCH, NASA

#### THERMAL-STRUCTURAL ANALYSES OF SPACE SHUTTLE MAIN ENGINE (SSME)

##### HOT SECTION COMPONENTS

- A. ABDUL-AZIZ, STRUCTURAL MECHANICS BRANCH, SVERDRUP

- R.L. THOMPSON, STRUCTURAL MECHANICS BRANCH, NASA

#### STRUCTURAL ANALYSES OF ENGINE WALL COOLING CONCEPTS AND MATERIALS

- A. KAUFMAN, STRUCTURAL MECHANICS BRANCH, SVERDRUP

#### STRUCTURAL ASSESSMENT OF A SPACE STATION SOLAR DYNAMIC HEAT RECEIVER

##### THERMAL ENERGY STORAGE CANISTER

- R.L. THOMPSON, STRUCTURAL MECHANICS BRANCH, NASA

- T.W. KERSLAKE, SOLAR DYNAMIC POWER MODULE DIVISION, NASA

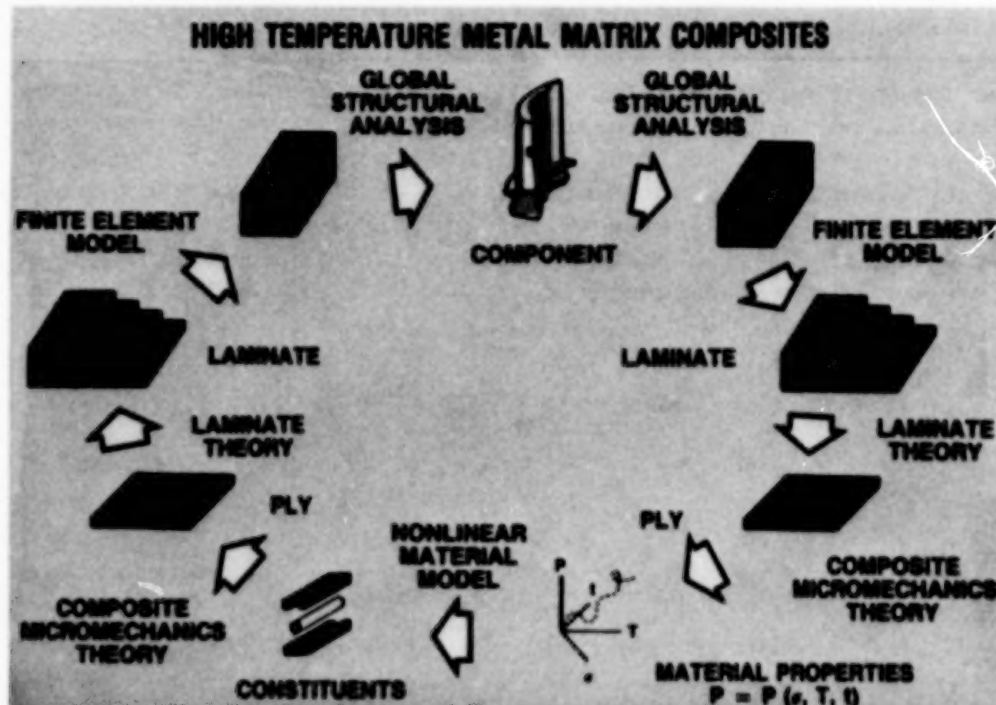
- M.T. TONG, STRUCTURAL MECHANICS BRANCH, SVERDRUP

#### AN EFFICIENT MINDLIN FINITE STRIP PLATE ELEMENT BASED ON ASSUMED STRAIN DISTRIBUTION

- A. CHULYA, STRUCTURAL MECHANICS BRANCH, ICOMP

- R.L. THOMPSON, STRUCTURAL MECHANICS BRANCH, NASA

CD-88-33220





## IMPACT DAMAGE IN COMPOSITE LAMINATES

Joseph E. Grady  
Structural Mechanics Branch  
NASA Lewis Research Center

### ABSTRACT

Damage tolerance requirements have become an important consideration in the design and fabrication of composite structural components for modern aircraft. The ability of a component to contain a flaw of a given size without serious loss of its structural integrity is of prime concern. Composite laminates are particularly susceptible to damage caused by transverse impact loading.

The ongoing research program described herein is aimed, therefore, at developing experimental and analytical methods that can be used to assess damage tolerance capabilities in composite structures subjected to impulsive loading. The objective of this presentation is to outline some significant results of this work and the methodology used to obtain them, including

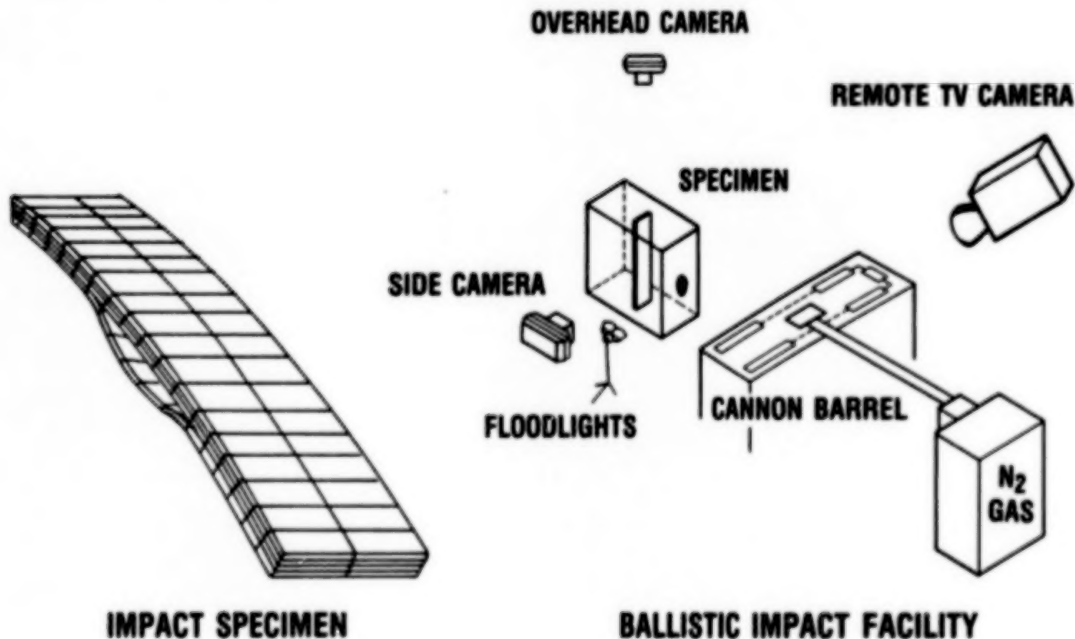
- (1) Identification of the mechanisms that cause delamination damage initiation and growth under impact loading (Grady and Sun, 1986)
- (2) Calculation of the dynamic delamination "fracture toughness" in composite laminates (Sun and Grady, 1987)
- (3) Computational simulation of dynamic response and damage initiation in composite laminates (Grady, Chamis, and Aiello, 1987)
- (4) Measurement of the effect that impact damage has on the structural integrity of a laminate (Grady and Chamis, 1988)

## LEWIS BALLISTIC IMPACT RESEARCH

The unique ballistic impact test facility at the Lewis Research Center is used for performing a variety of instrumented impact tests. In addition to multiple channel high-speed digital data acquisition capabilities, a series of high-speed cameras can be used to record the impact event photographically. The impact cannon itself is able to accommodate impactors ranging in size from 1/2 to 6 inches in diameter. It has been used to simulate the impact of birds on engine components and is currently being used to investigate dynamic crack propagation in composite materials.

Post-impact inspections of damaged specimens can be conducted with any of the available supporting experimental facilities, which include:

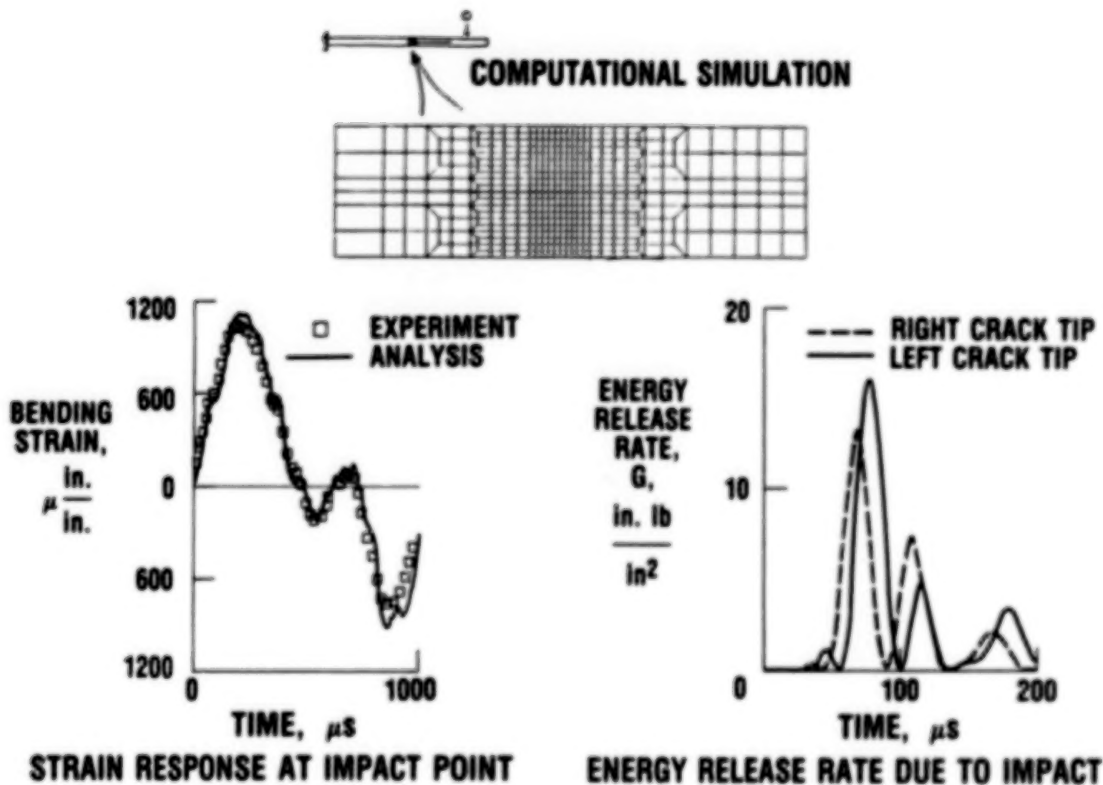
- Ultrasonic C-scan and x-ray inspection facilities, which are used to detect the type and location of impact damage
- A vibration testing facility used to measure natural frequencies and mode shapes of damaged specimens
- Static and fatigue load frames to measure the reduction in strength, stiffness, and durability of test specimens caused by impact



CD-88-31801

# DYNAMIC FRACTURE TOUGHNESS IN COMPOSITES

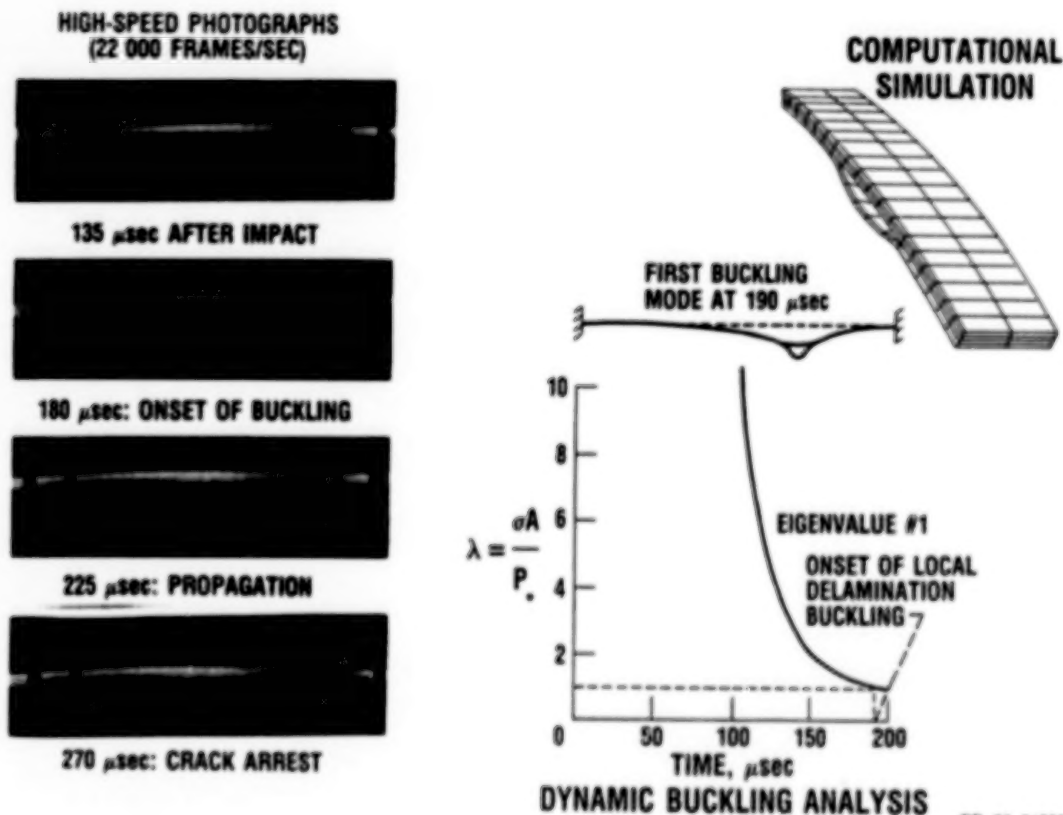
A combined experimental and analytical approach was used (Grady and Sun, 1986, 1988) to predict both the dynamic response measured in a simulated engine blade and the dynamic delamination fracture toughness of the composite material. Impact tests were conducted on cantilevered graphite/epoxy laminates, and a two-dimensional finite element model was developed to computationally simulate the post-impact dynamic response. Correlations between calculated crack-tip strain energy release rates and high-speed photographs of crack initiation and propagation were used to estimate the dynamic fracture toughness of the composite material.



CD-88-31802

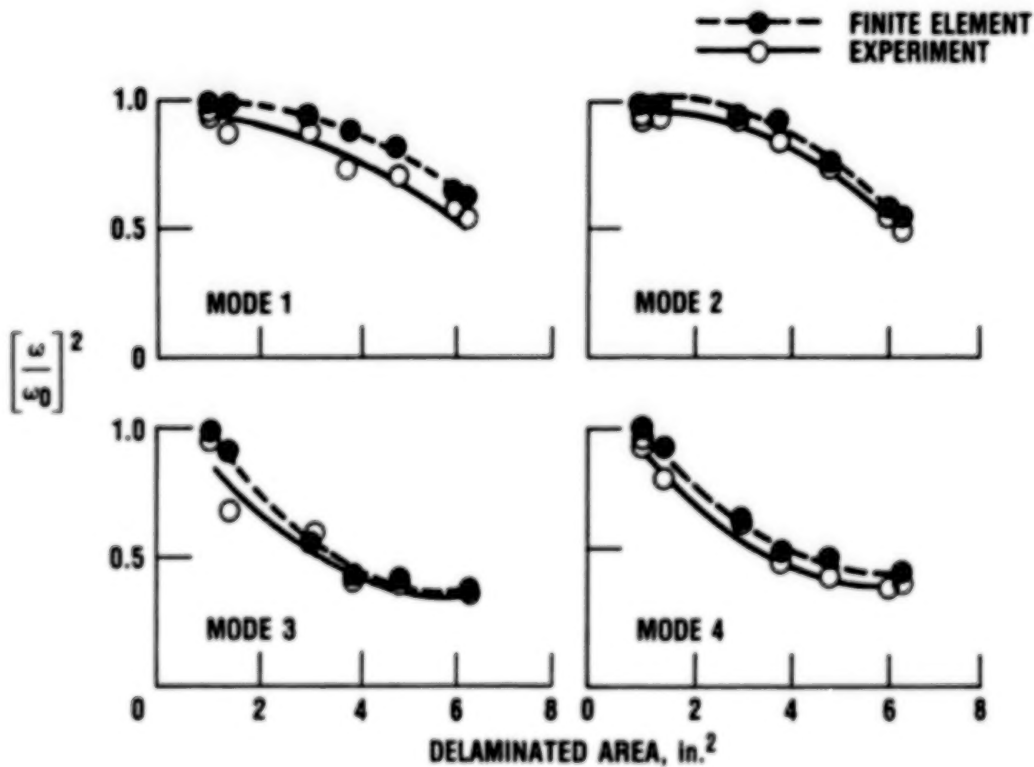
## DYNAMIC DELAMINATION BUCKLING: COMPUTATIONAL SIMULATION

A unique dynamic delamination buckling and delamination propagation analysis capability has been developed and incorporated into the MSC/NASTRAN finite element analysis computer program. This capability consists of (1) a modification of the direct time integration solution sequence which provides a new analysis algorithm that can be used to predict delamination buckling in a laminate subjected to dynamic loading, and (2) a new method of modeling the composite laminate using plate-bending elements and multipoint constraints. With these modifications, NASTRAN is used to predict both impact-induced buckling in composite laminates with initial delaminations and the strain energy release rate due to extension of the delamination (Grady et al., 1987). It is shown that delaminations near the outer surface of a laminate are susceptible to local buckling and buckling-induced delamination propagation when the laminate is subjected to transverse impact loading. The capability now exists to predict the time at which the onset of dynamic delamination buckling occurs, the dynamic buckling mode shape, and the dynamic delamination strain energy release rate.



# STIFFNESS LOSS DUE TO IMPACT DAMAGE

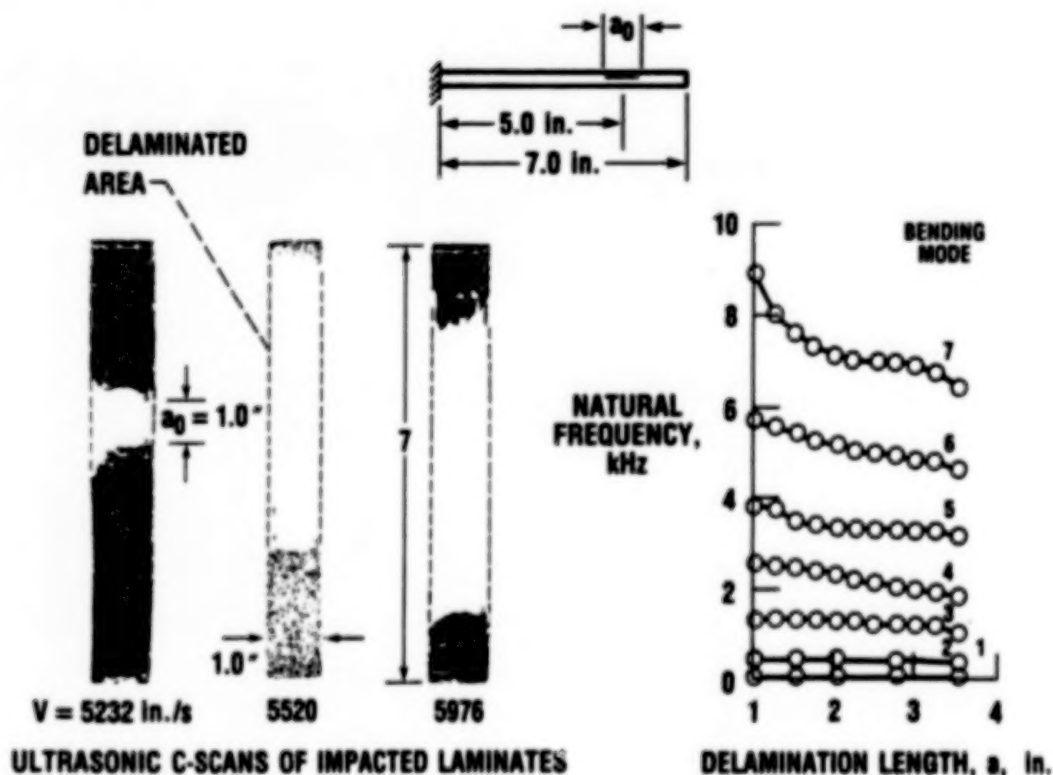
A series of additional post-impact tests were conducted on the composite impact specimens to measure the effect of impact damage on the structural integrity of the laminates. A decrease in stiffness, such as that caused by impact damage, results in a corresponding decrease in the natural frequencies of a damaged composite structure. To quantify this effect for the case of impact-induced delamination, the first four natural frequencies of a series of cantilevered composite specimens with initial embedded delaminations were measured before and after impact. The measured reduction in the natural frequencies of the first four bending modes for varying amounts of impact damage are compared with the results of a two-dimensional plane strain finite element simulation of the damaged specimens in the figures below. The difference between the two curves represents the extent to which damage other than delamination has occurred in the laminates.



CD-88-31804

# DETECTING IMPACT DAMAGE

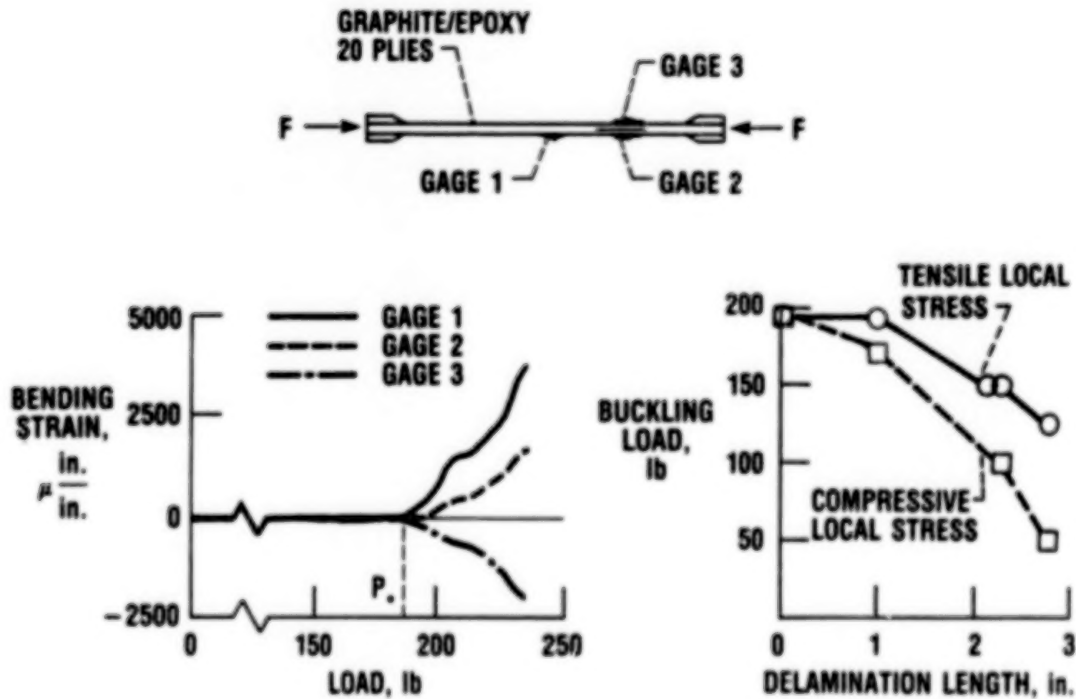
Composite laminates are particularly susceptible to damage caused by transverse impact. Ply debonding, or delamination, is the most serious type of impact damage. One method of detecting delamination in composites is by non-destructive ultrasonic C-Scan. Shown below are C-Scans of composite laminates that have been impacted at various energy levels, causing different amounts and distributions of damage. The corresponding effects of this damage on the natural frequencies of vibration are shown below. The loss of stiffness caused by delamination is most apparent in the reduction of natural frequencies for the higher modes of vibration. Since impact damage such as delamination is often undetectable visually, either of these methods can serve as a practical means of field-testing a composite structure to determine if significant amounts of internal damage exist.



CD-88-31805

# EFFECT OF DELAMINATION ON BUCKLING LOADS

Instrumented composite impact specimens were tested in compression after being impacted at velocities up to 1000 ft/s with a soft rubber projectile. Longitudinal strain measurements at three gage locations were used to identify the buckling loads. Small amounts of impact-induced delamination damage were found to cause a significant drop in the critical buckling loads, as shown in the last figure. Compressive longitudinal stress near the delaminated area can cause a secondary "local" buckling of the delamination and an increased drop in the effective load-carrying capability of the laminate.



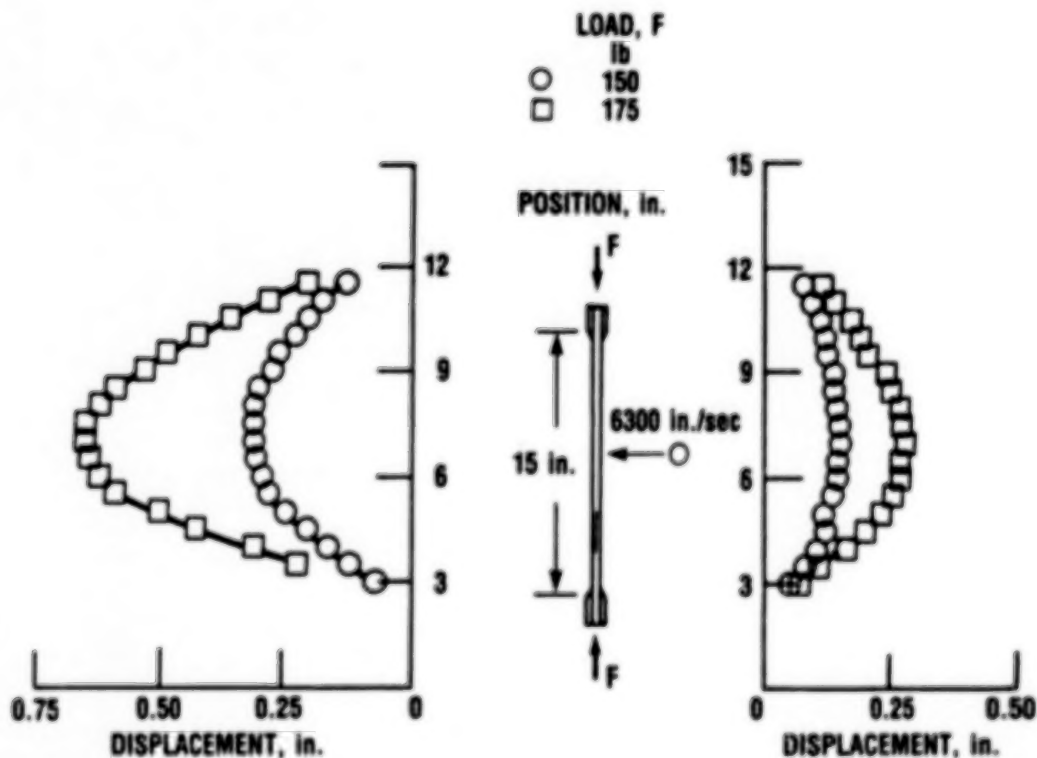
CD-88-31806



# EFFECT OF IMPACT DAMAGE ON POST-BUCKLING DISPLACEMENTS

Impact damage which is not detectable by visual inspection may cause a significant loss in the structural integrity of a composite laminate. This is illustrated below, using post-impact compression tests of damaged graphite/epoxy laminates. Experimentally measured post-buckling configurations at several load levels show that internal damage caused by transverse impact can cause a large "direction-dependent" stiffness loss in composite laminates.

Under uniform compression loading, the laminate buckles in the direction of the prior impact load, as shown on the left. The measured displacement shape shows that the effective bending stiffness is significantly reduced from that of the original undamaged laminate. If lateral restraints are used to support the laminate in this direction, buckling occurs in the opposite direction, and the laminate shows a much higher post-buckling stiffness at all load levels.



CO-88-31807



## REFERENCES

- Avva, V.S., 1983, "Effect of Specimen Size on the Buckling Behavior of Laminated Composites Subjected to Low-Velocity Impact." *Compression Testing of Homogeneous Materials and Composites*, ASTM STP 808, Richard Cait and Ralph Papirno, eds., American Society for Testing and Materials, pp. 140-154.
- Grady, J.E., and Chamis, C.C., 1988, "Effect of Impact Damage on Structural Response of Composite Laminates." To be presented at the Fourth Japan-U.S. Conference on Composite Materials, Washington, D.C.
- Grady, J.E., Chamis, C.C., and Aiello, R.A., 1987, "Dynamic Delamination Buckling in Composite Laminates Under Impact Loading: Computational Simulation." *Composite Materials: Fatigue and Fracture*, ASTM STP, P.O. Lagace, ed., American Society for Testing and Materials. Also published as NASA TM 100192.
- Grady, J.E., and DePaola, K.J., 1987, "Measurement of Impact-Induced Delamination Buckling in Composite Laminates." *Proceedings of the 1987 SEM Fall Conference on Dynamic Failure*, Society for Experimental Mechanics.
- Grady, J.E., and Sun, C.T., 1986, "Dynamic Delamination Crack Propagation in a Graphite/Epoxy Laminate." *Composite Materials: Fatigue and Fracture*, ASTM STP 907, H.T. Hahn, ed., American Society for Testing and Materials, Philadelphia, pp. 5-31.
- Joshi, S.P., and Sun, C.T., 1987, "Impact-Induced Fracture in a Quasi-Isotropic Laminate." *Journal of Composites Technology and Research*, Vol. 9, No. 2, pp. 40-46.
- Sierakowski, R.L., Ross, C.A., and Malvern, L.E., 1981, "Studies on the Fracture Mechanisms in Partially Penetrated Filament Reinforced Laminate Plates." Final Report DAAG29-79-G-0007, U. S. Army Research Office.
- Sun, C.T., and Grady, J.E., 1988, "Dynamic Delamination Fracture Toughness of a Graphite/Epoxy Laminate Under Impact." To appear in *ASTM Journal of Composites Technology and Research*.
- Whitcomb, J.D., and Shivakumar, K.N., 1987, "Strain-Energy Release Rate Analysis of a Laminate with a Post-Buckled Delamination." NASA TM 89091.

BLANK PAGE

## THERMOSTRUCTURAL ANALYSIS OF SIMULATED COWL LIPS

Matthew E. Melis  
Structural Mechanics Branch  
NASA Lewis Research Center

### ABSTRACT

With the most recent efforts to develop state-of-the-art hypersonic technologies, a significant number of challenging problems have surfaced. One of the major concerns is the development of an aeropropulsion system capable of handling the high heat fluxes during hypersonic flight. On the leading edges of such systems, not only must the maximum heating rates be tolerated, but also distortions to the flow field due to excessive blunting and/or thermal warping of the compression surface must be held to a minimum if high inlet performance is to be achieved. Active cooling schemes are required to maintain acceptable temperatures in the leading edge regions as well as in the relatively large flat panels located in the combustion zone. To assess these problems, an interdisciplinary cowl lip technology team (COLT) has been formed at NASA Lewis. COLT comprises a completely integrated loop of the design, analysis, and experimental verification process in developing actively cooled cowl lip concepts for use on a propulsion system for the proposed National Aerospace Plane (NASP).

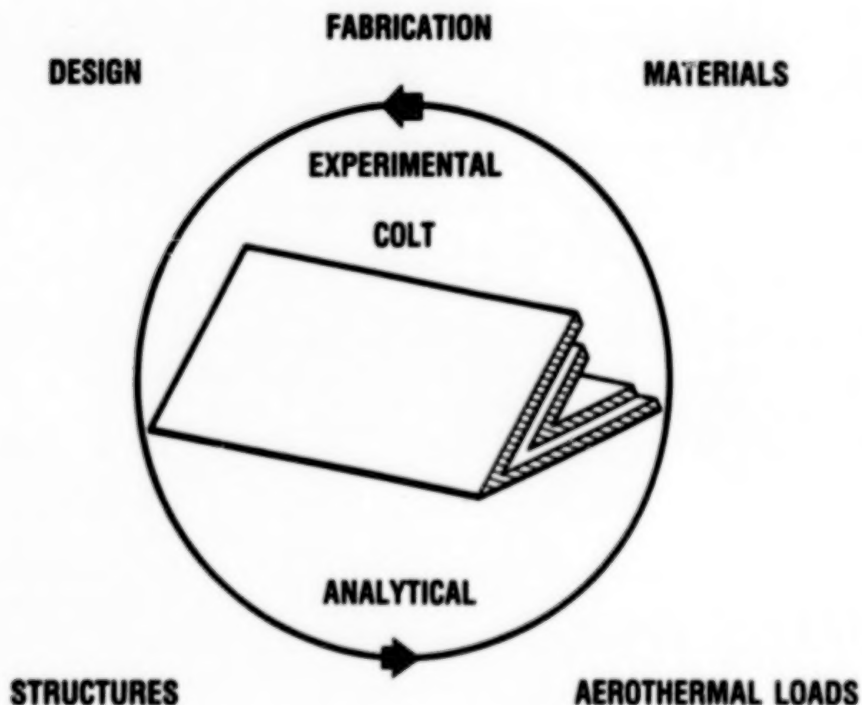
Three-dimensional finite element analyses using MSC/NASTRAN and MARC are performed to predict the thermal and structural response of the various cooling schemes under high heat loads. Steady state heat-transfer analyses and elastic stress analyses are performed using MSC/NASTRAN. Elastic/plastic stress analyses are done using MARC.

To help verify these analyses experimentally, a hydrogen-oxygen rocket engine has been modified to use the exhaust stream as a high-enthalpy, high-heat-flux source to evaluate various actively cooled, simulated cowl lip segments as well as flat structural segments. The facility is capable of providing heat flux levels from about 200 (Btu/ft<sup>2</sup>)/sec up to 10 000 (Btu/ft<sup>2</sup>)/sec. Crossflow and parallel flow cooling configurations have been tested and analyzed using cooling fluids of water and gaseous hydrogen. In addition, various material types have been tested and compared. These material types include high-conductivity copper, nickel, and a copper and graphite metal matrix composite.

## METHODOLOGY OF LEADING EDGE CONCEPT EVALUATION

Engine inlet leading edge surfaces and their associated high heating rates during flight on hypersonic vehicles are one of the major concerns in the development of the proposed National Aerospace Plane (NASP). Ongoing work by an inlet cowl lip technology team (COLT) at the Lewis Research Center has been to analyze, fabricate, and test, in a hot gas facility, generic, actively cooled cowl lip concepts made of both homogeneous and metal matrix composite materials in order to develop analytical, experimental, and material technologies to support the research and development of hypersonic inlet configurations for NASP propulsion.

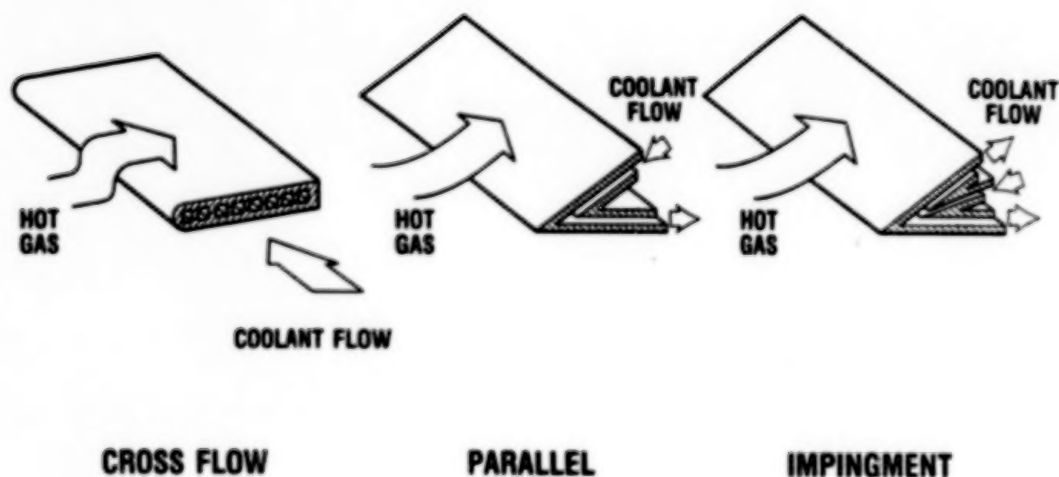
The approach is an iterative one through analysis, design fabrication, and testing of the actively cooled cowl lip concepts. Integrated thermal and structural analysis codes are used to evaluate the various concepts. Concepts analyzed and tested are made from pure metals, including copper, nickel, and titanium sheets, and a metal matrix composite material, copper/graphite. Configurations are tested in a hot gas test facility at Lewis with the test data acquired used for calibration and verification of the analysis tools as well as for evaluation of the cowl lip concept itself.



CD-88-32364

### COWL LIP COOLING CONCEPTS

The figure shows three actively cooled cowl lip concepts which will be analyzed and tested in the hot gas facility at Lewis. Included is a generic crossflow cooling concept, a parallel-flow cooled concept, and an impingement-flow concept. To date, crossflow-cooled specimens have been fabricated from copper, nickel, and titanium. A crossflow specimen with a copper/graphite leading edge is very close to completion. The copper and nickel specimens have been tested using both water and gaseous hydrogen as coolants. Several copper parallel-flow test pieces have been fabricated and await testing pending the completion of some modifications to the test cell.



CO-88-32365

## HOT GAS TEST FACILITY

The high heat flux generated in the test facility is obtained from the combustion of a hydrogen-oxygen rocket engine. The rocket engine, on the right in the figure, fires horizontally across a test specimen fixed at the exit of the nozzle. Tests have been conducted for a wide latitude of conditions providing gas temperatures from 1800 to 5000 °F and stagnation point heat fluxes of up to 2000 (Btu/ft<sup>2</sup>)/sec.

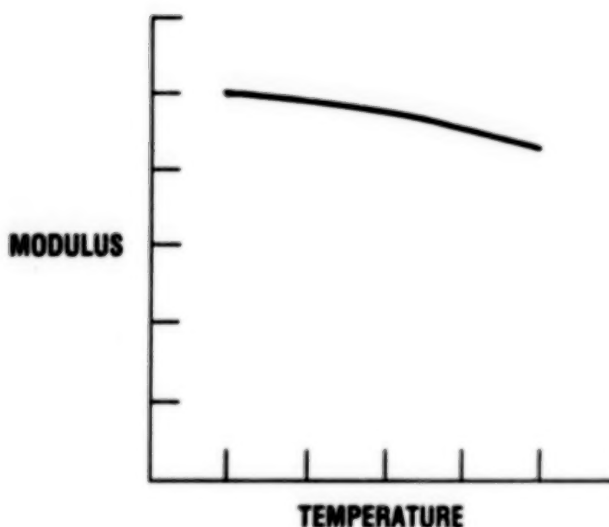


CD-88-32366

## METCAN-GENERATED MATERIAL PROPERTIES FOR METAL MATRIX COMPOSITES

METCAN, a code developed at NASA Lewis, is used to predict the thermal and structural material properties required for the analysis of a metal matrix composite structure. METCAN also predicts composite structural response and composite stress results with detail on failure. Shown in the figure are examples of typical METCAN-generated material properties plotted as a function of temperature. METCAN is discussed in more detail in another presentation at this conference.

ELASTIC MODULI  
SHEAR MODULI  
POISSON RATIOS  
EXPANSION COEFFICIENTS  
DENSITY  
HEAT CAPACITY  
HEAT CONDUCTIVITIES  
STRENGTHS  
FLEXURAL MODULI  
FAILURE ANALYSIS  
LOCAL STRESSES



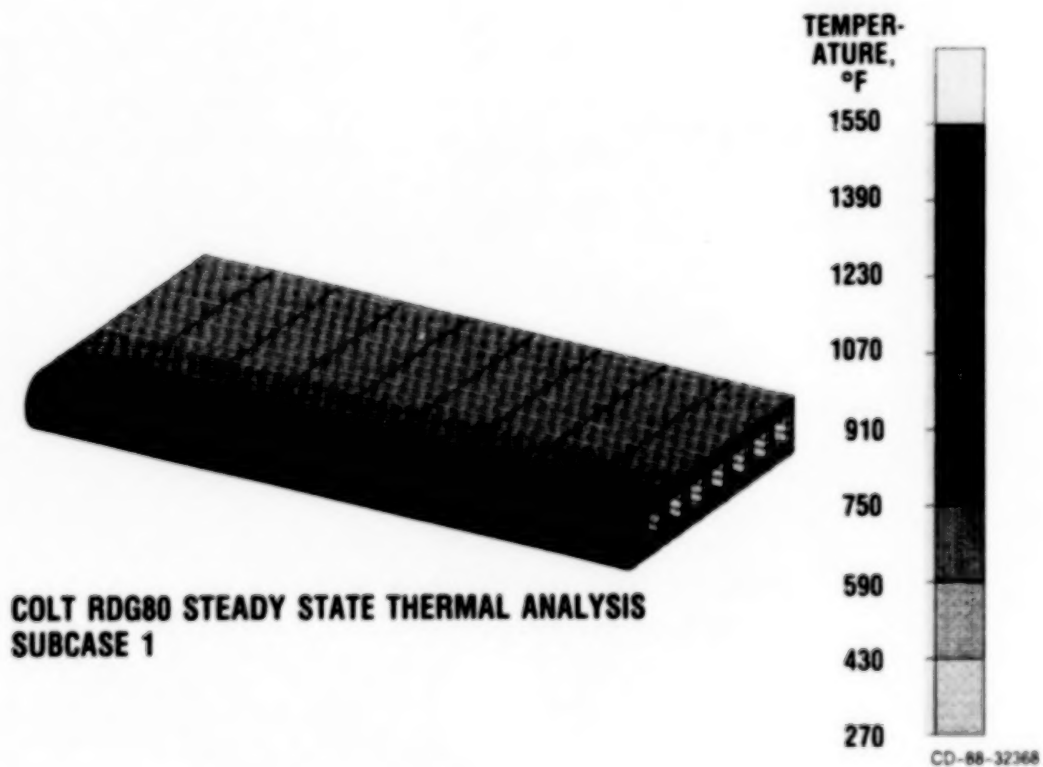
ICAN—POLYMER MATRIX COMPOSITE ANALYZER  
METCAN—METAL MATRIX COMPOSITES ANALYZER

CD-88-32367



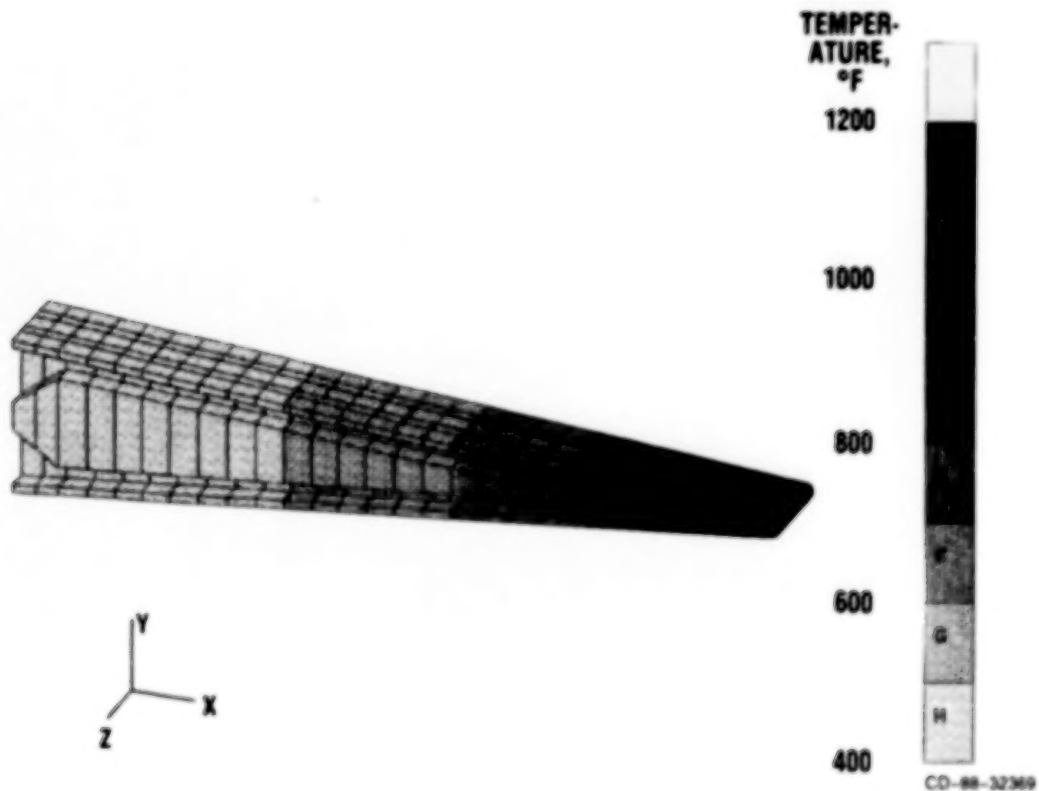
# THERMAL FINITE ELEMENT ANALYSIS OF COPPER CROSSFLOW CONFIGURATION

Three-dimensional thermal and structural finite element analyses are performed on copper, nickel, and copper and graphite composite crossflow configurations using MSC/NASTRAN. The model, used for both thermal and stress analysis, consists of 4760 nodes and 3294 eight-node brick elements (HEXA). The PATRAN code is used to generate the mesh and to process the results. The figure shows a thermal profile predicted from a steady state heat-transfer analysis of a copper crossflow specimen with gaseous hydrogen coolant. The hot gas temperature was 2800 °F, and the coolant was 50 °F. The nonsymmetric temperature distribution is due to a pressure differential between the top and bottom surfaces. The predicted nodal temperatures are used as input (thermal loads) for a linear stress analysis with NASTRAN.



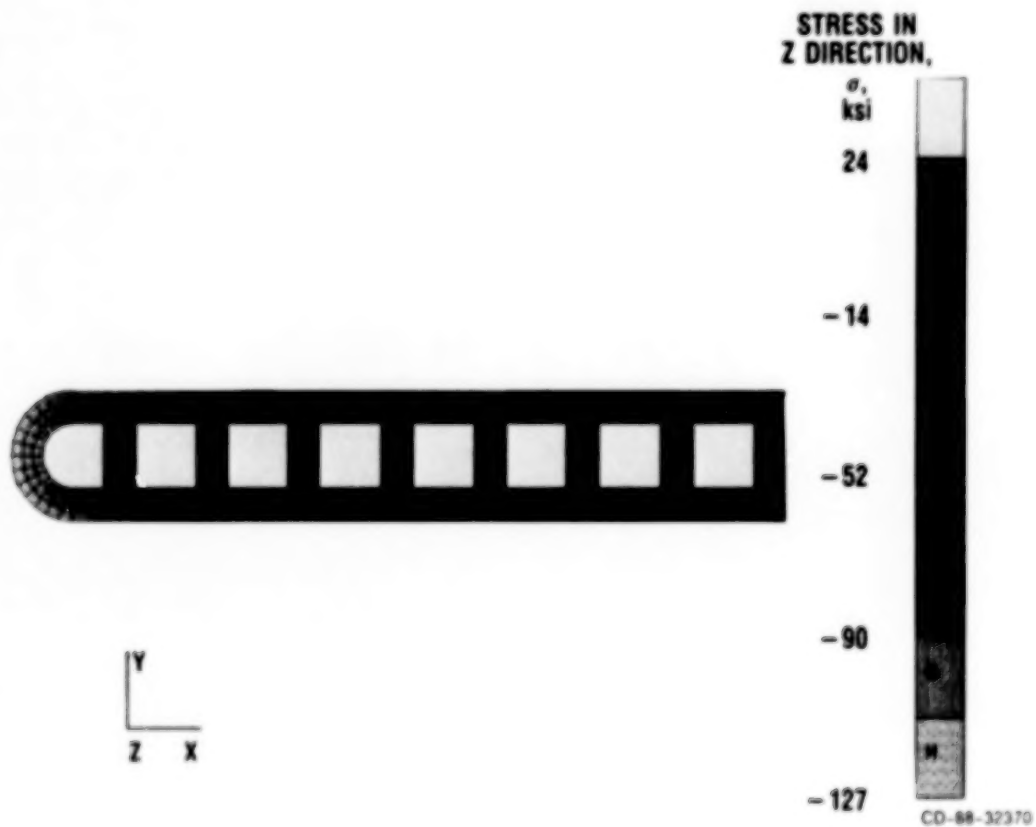
# THERMAL FINITE ELEMENT ANALYSIS OF PARALLEL-FLOW CONFIGURATION

The parallel-flow cowl lip concept is evaluated in the same fashion as the crossflow concept. The model, representing a slice of the actual test piece, consists of 532 solid brick elements and 1010 nodes. Analytical thermal boundary conditions are under development for this model; however, a representative temperature profile has been predicted using assumed heat fluxes (see figure). Testing of the copper parallel-flow specimen is in progress.



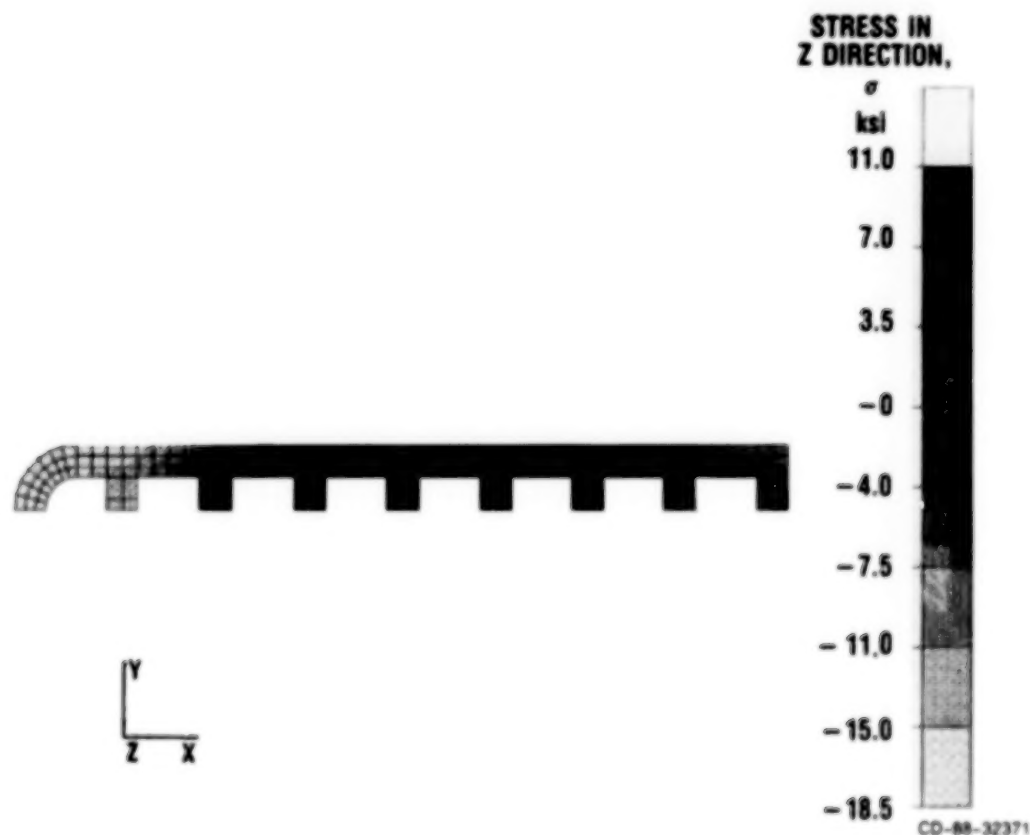
# THERMAL STRESS DISTRIBUTION IN COPPER CROSSFLOW CONFIGURATION

Nodal temperature data from the thermal analyses previously described are applied to the same finite element models in order to predict stresses resulting from the constrained thermal expansion. Shown in the figure is an elastic thermal stress profile on a small section of the copper crossflow model. Material properties were input as temperature dependent in this NASTRAN analysis. The stresses plotted are along the Z direction of the axes shown. Stresses in the other directions were calculated but are not shown here. The high compressive stresses along the Z axis, seen analytically to be the most significant in the structure, are due to the high differential of expansion in this direction. The leading edge, at very high temperatures, is trying to expand with the bulk of the material aft of the leading edge at much cooler temperatures restraining it. The elastic analysis indicates yielding at the leading edge and warrants a nonlinear analysis to accurately predict the material behavior in this problem.



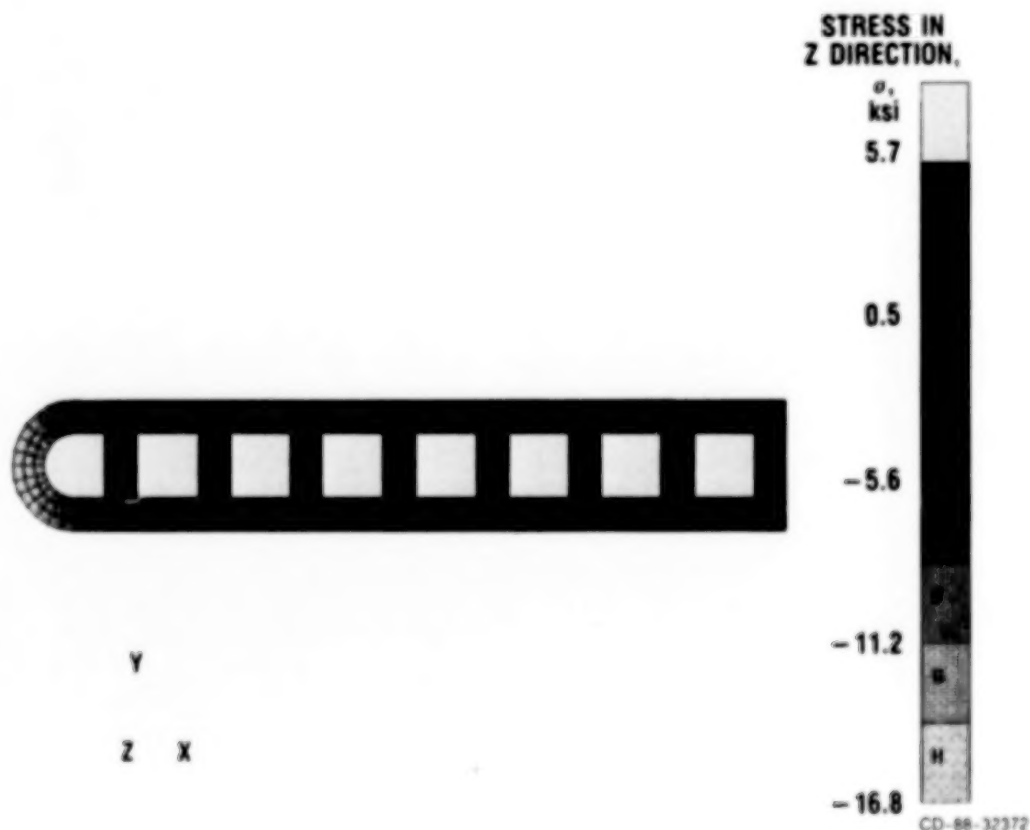
## NONLINEAR STRESS DISTRIBUTION IN COPPER CROSSFLOW CONFIGURATION

A nonlinear finite element analysis was performed on the crossflow configuration using the MARC analysis code. The model used with MARC made use of symmetry and was half the size of the NASTRAN model. This was necessary due to the intensive CPU time required for a nonlinear analysis. The analysis was a transient one, utilizing a combined isotropic-kinematic hardening rule and temperature-dependent material properties. Shown in the figure is the steady-state resultant stress profile for the stresses along the Z axis shown in the figure. Time-dependent effects will be incorporated into the analysis at a later date, as well as some life-prediction methods.



# ELASTIC STRESS ANALYSIS OF CROSSFLOW CONFIGURATION MADE OF COPPER AND GRAPHITE COMPOSITE

A linear, steady state heat-transfer analysis of a crossflow configuration is run using material properties for copper/graphite predicted from METCAN. The model is assumed to be made of a unidirectional (50% P100 fiber) composite with fibers running parallel to the leading edge of the model (Z direction). Resultant nodal temperatures are input for an elastic stress analysis and the stresses in the Z direction are plotted as before. Because of a significantly lower coefficient of thermal expansion and a high modulus in the fiber direction, the global structural stresses are much lower in the leading edge for the copper and graphite composite than for pure copper; however, microstresses within the material itself must also be taken into consideration as they may limit the material's performance at high temperatures. The METCAN code will predict these stresses. This still suggests that the copper and graphite composite and other metal matrix composites might offer realistic solutions to the cowl lip problem. Reduction of the thermal expansion coefficient is the key to controlling stresses in areas of high thermal gradients, and this can be done with metal matrix composites if the fabrication hurdles can be overcome.



## THERMAL-STRUCTURAL ANALYSES OF SPACE SHUTTLE

### MAIN ENGINE (SSME) HOT SECTION COMPONENTS

Ali Abdul-Aziz\* and Robert L. Thompson  
Structural Mechanics Branch  
NASA Lewis Research Center

#### ABSTRACT

Three-dimensional nonlinear finite-element heat transfer and structural analyses were performed for the first-stage high-pressure fuel turbopump (HPFTP) blade of the space shuttle main engine (SSME). Directionally solidified (DS) MAR-M 246 and single crystal (SC) PWA-1480 material properties were used for the analyses. Analytical conditions were based on a typical test stand engine cycle. Blade temperature and stress-strain histories were calculated by using the MARC finite-element computer code (MARC Analysis Research Corporation, 1980).

This study was undertaken to assess the structural response of an SSME turbine blade and to gain greater understanding of blade damage mechanisms, convective cooling effects, and thermal-mechanical effects (Kaufman, 1984). Other objectives are also to address problems of calculating the thermal response of high-temperature gas-path components, such as turbopump blades in space power propulsion systems, and to evaluate the stress-strain response at the blade critical location for life prediction purposes. Another purpose is to exercise nonlinear finite-element computer codes on anisotropic SSME components for a typical mission cycle.

Thermal environment on the airfoil was predicted by running a boundary layer analysis using STAN5 code (Gaugler, 1981) to generate the film coefficients needed for the heat transfer analysis. For the complete blade, the heat transfer conditions around the platform and shank regions were provided by Lockheed Missiles & Space Company, Huntsville Research and Engineering Center (1983). Additional assumptions also had to be made to complete the boundary conditions. Transient results were obtained by scaling steady-state heat transfer coefficients based on transient flow and temperature. More details regarding the heat transfer analysis are given by Abdul-Aziz (1987).

Elastoplastic analyses have been conducted for the HPFTP blade with the MARC code. Plastic strains calculations were based on incremental plasticity theory using von Mises yield criterion, the normality rule, and a kinematic hardening model. The material elastoplastic behavior was specified by the yield strength and work hardening properties in the longitudinal direction; transverse properties were not available. Approximately 2 million words of core storage on the

---

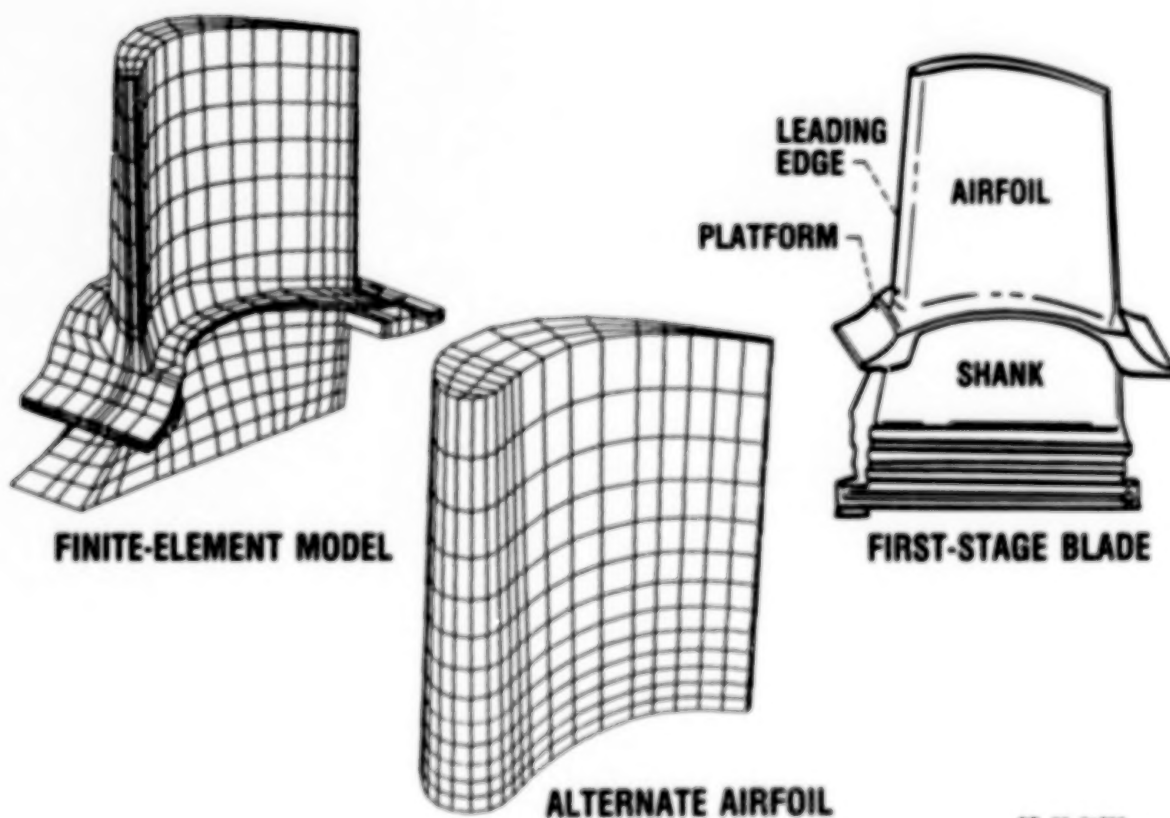
\*Sverdrup Technology, Inc., Lewis Research Center Group, NASA Lewis Research Center.

Cray XMP computer were needed to run the problem. Analysis required about 4 hours of Cray XMP central processor unit (CPU) time. About half of that was needed for the airfoil problem.



## TURBINE BLADE FINITE-ELEMENT MODEL

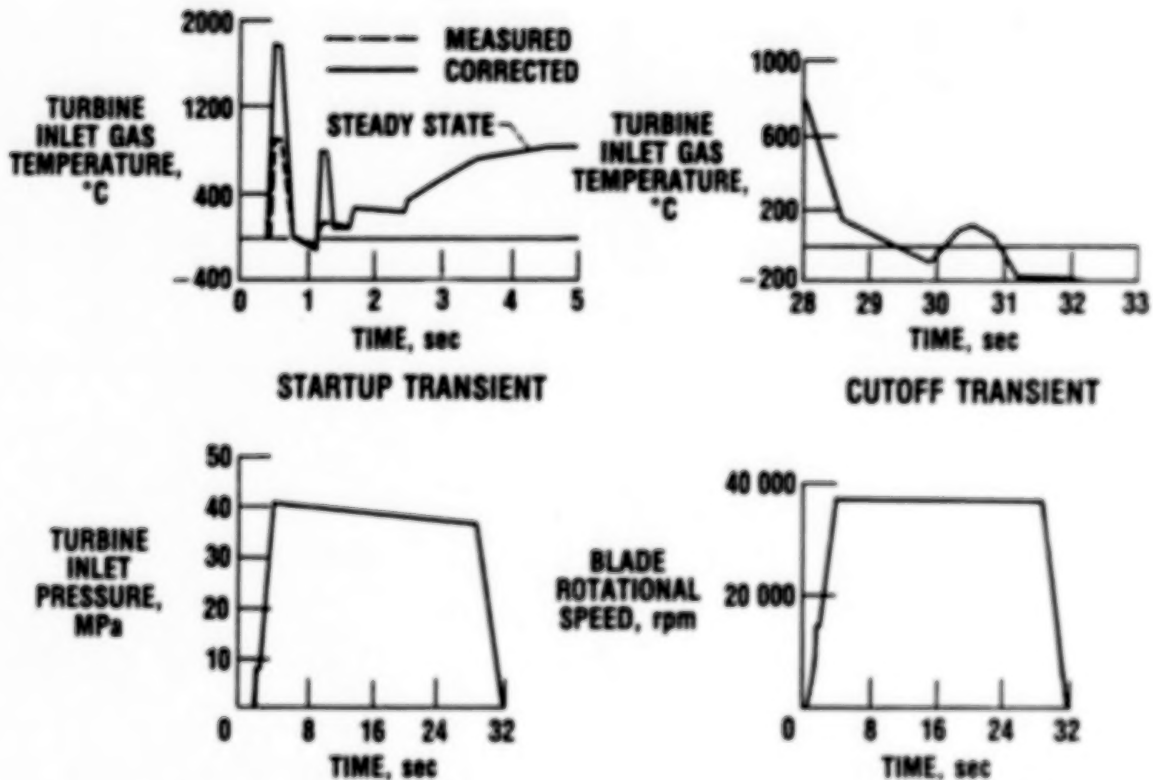
In the past, first-stage turbine blades in the high-pressure fuel turbopump (HPFTP) of the space shuttle main engine have suffered cracking in the blade shank region and at the leading edge of the airfoil immediately above the platform. A finite-element model for a complete blade has been constructed with eight-node, solid, isoparametric elements. Another model is shown for an alternate airfoil design which is also undergoing thermal-structural analyses. The complete-blade finite-element model consists of 1025 elements and 1575 nodes. The airfoil portion contains 360 elements and 576 nodes, while the alternate airfoil design includes 546 elements and 840 nodes. The MARC code and PATRAN-G graphic package were used to construct these finite-element models.



CD-88-31703

# MISSION CYCLE FOR ANALYSIS

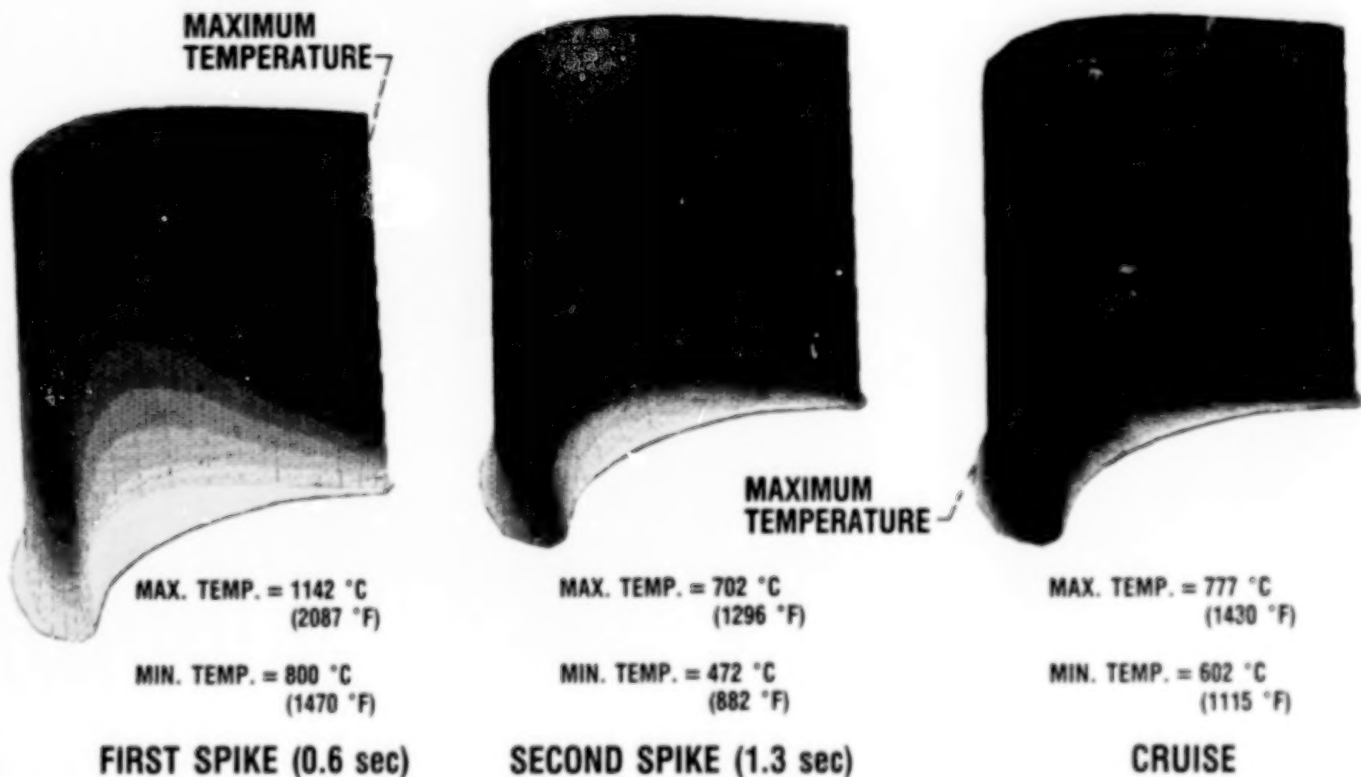
The mission cycle used for the analyses in terms of measured and corrected turbine inlet gas temperature, gas pressure, and blade rotational speed is shown below. This cycle is typical of a factory test of the engine; it is also reasonably representative of a flight mission except for the fore-shortened steady-state operating time. Since the major factor inducing cracking is the transient thermal stresses caused by the sharp ignition and shutoff transients, deletion of the steady-state portion is acceptable.



CD-68-31704

## AIRFOIL TEMPERATURE DISTRIBUTION

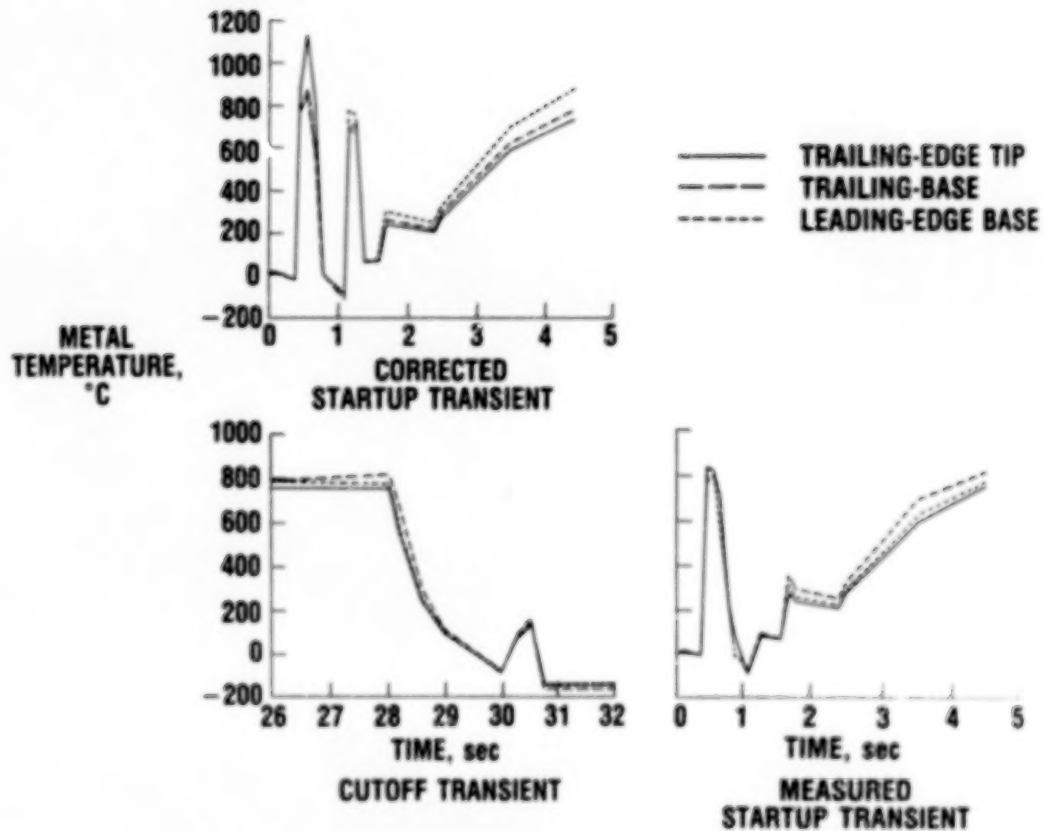
Metal temperatures obtained from MARC heat transfer analysis for the two startup transient spikes are shown below. For the first ignition spike, the highest temperature occurred at the trailing edge near the tip where the airfoil is the thinnest. For the second ignition spike, the maximum temperature was at both the leading and trailing edges. During cruise the airfoil experienced a uniform temperature distribution except near the base because of colder boundary conditions in the region. The maximum temperature location was at the leading and trailing edges and was due to high gas-path pressures, which resulted in high heat transfer coefficients in those areas. The temperature reached 1142 °C during the first spike and 777 °C at cruise.



CD-88-31771

# AIRFOIL TRANSIENT TEMPERATURE RESPONSE

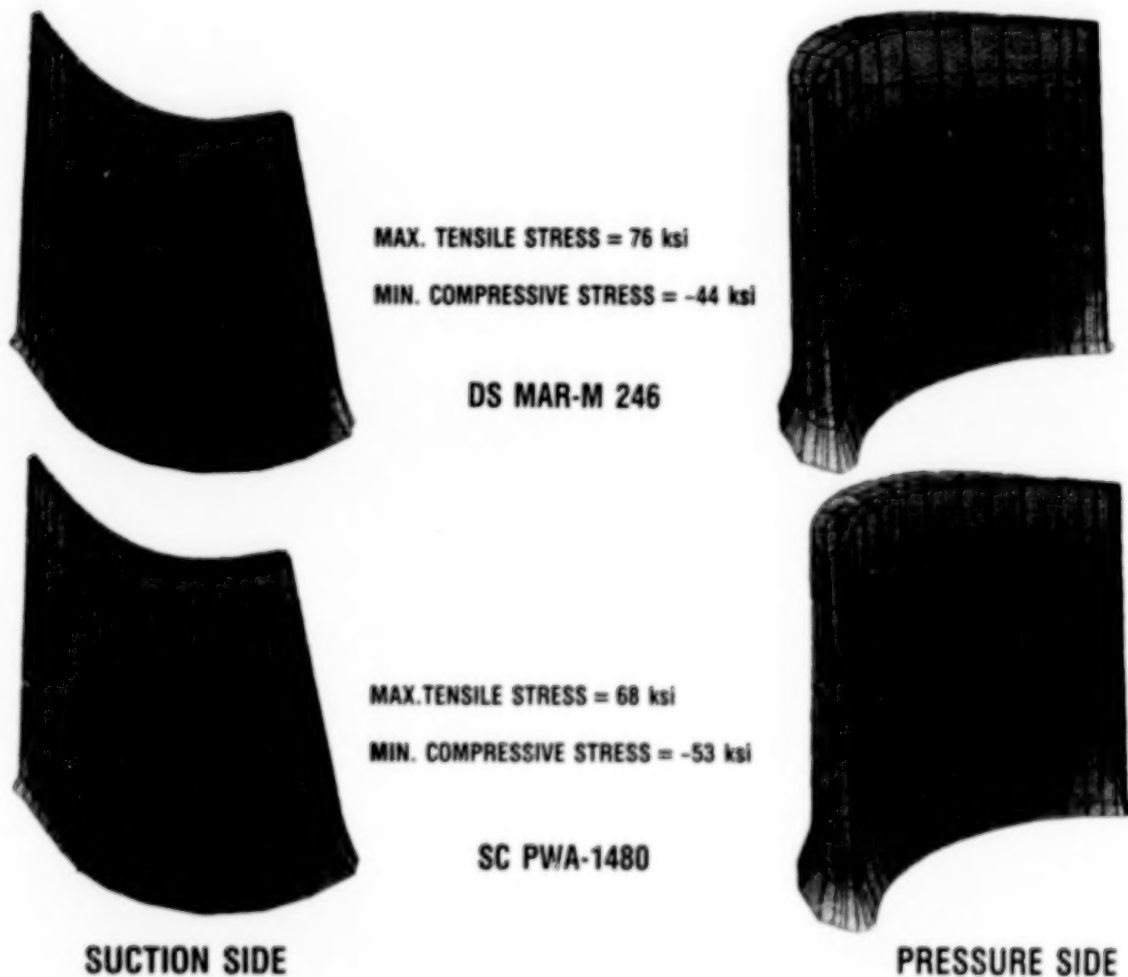
The thermal response predicted from the finite-element analysis shown below revealed that the leading and trailing-edge bases of the airfoil are the hottest locations. This was expected because of the presence of high heat transfer coefficients in the region. However, the corrected temperatures (which are higher than those measured by the poor thermocouple response) gave rise to 28 percent higher leading-edge temperatures and a 100 percent higher temperature between the midspan surface and the leading-edge base. The coldest spot was always at the airfoil base because of colder boundary conditions.



CD-88-31705

## AIRFOIL RADIAL STRESS DISTRIBUTION AT CRUISE

The radial stress components (i.e., along the span) are shown for the elastoplastic MARC airfoil analyses of directionally solidified (DS) MAR-M 246 and single crystal (SC) PWA-1480. Incremental loading included centrifugal and gas-pressure loads and metal temperature distributions as calculated from the heat transfer analysis. Maximum stresses reached 119 ksi for the SC material and 110 ksi for the DS material during the cruise portion of the mission cycle. The radial component of the strain ranges were 2.1 percent for the MAR-M 246 and 1.57 percent for the PWA-1480.



CD-88-317X

## COMPLETE-BLADE TEMPERATURE CONTOURS

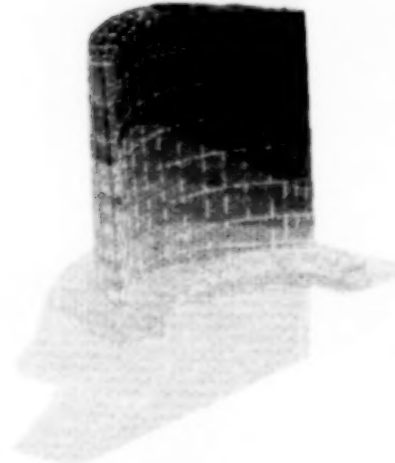
Temperature contours on the surface of the blade are shown for the first temperature spike and at cruise. As expected, the hottest spot of about 1110 °C occurred at the trailing-edge tip of the airfoil during the first temperature overshoot. Uniform temperature dominated most of the airfoil except at the junction of the airfoil, platform, and shank, where a steep temperature gradient is clearly shown. This is because of the effects of the cold and hot gas mixture in the region. A lack of reliable data on the thermal environment in the platform and shank regions may have affected the local heat transfer predictions.



MAX. TEMP. = 772 °C  
(1422 °F)

MIN. TEMP. = 472 °C  
(882 °F)

**CRUISE**



MAX. TEMP. = 1179 °C  
(2150 °F)

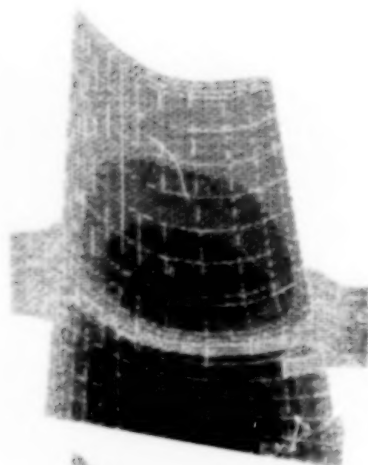
MIN. TEMP. = 589 °C  
(1092 °F)

**FIRST SPIKE**

CD-88-31707

## COMPLETE-BLADE RADIAL STRESS DISTRIBUTION AT CRUISE

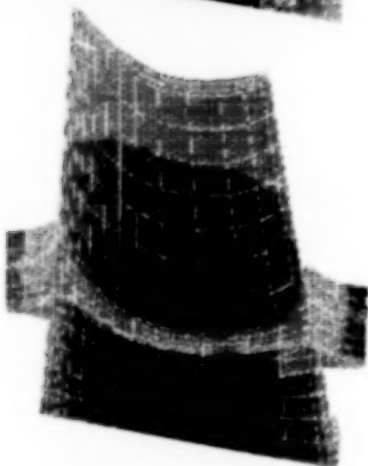
The results of elastoplastic analyses with the MARC code are shown below for the radial components of stress on the complete-blade structure for both DS MAR-M 246 and SC PWA-1480. Considerable difference in structural response has been observed in analyzing the complete blade rather than the airfoil alone. This is mainly due to the uncertainties in the prescribed boundary conditions and assumptions made at the shank-platform interface. However, any difference in life for the two materials would come from their fatigue characteristics. While the fatigue resistances are not well defined, results indicate thermal low-cycle fatigue lives of several thousand cycles.



MAX. TENSILE STRESS = 118 ksi

MIN. COMPRESSIVE STRESS = -40 ksi

DS MAR-M 246



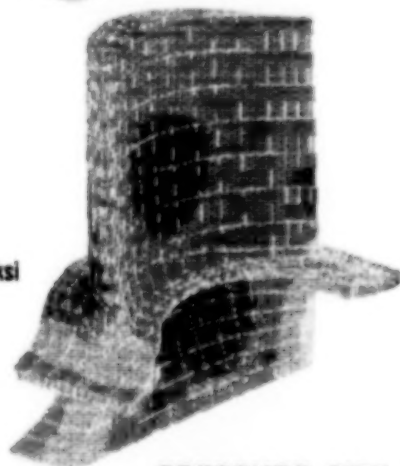
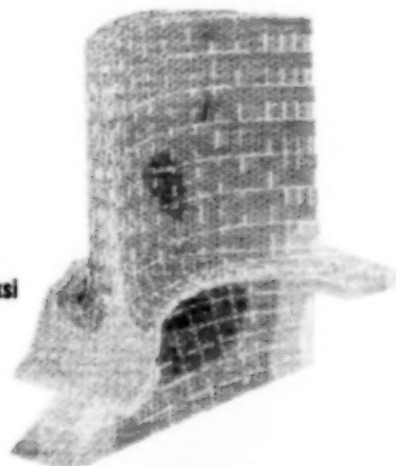
MAX. TENSILE STRESS = 110 ksi

MIN. COMPRESSIVE STRESS = -40 ksi

SC PWA-1480

SUCTION SIDE

LST '88



PRESSURE SIDE

CD-88-31708



#### REFERENCES

- Abdul-Aziz, A., Tong, M., and Kaufman, A., 1987, "Thermal Finite-Element Analysis of an SSME Turbine Blade," NASA TM-100117.
- Gaugler, R.E., 1981, "Some Modification to, and Operational Experiences With, The Two-Dimensional, Finite-Difference, Boundary-Layer Code, STAN5," NASA TM-81631.
- Kaufman, A., 1984, "Development of a Simplified Procedure for Cyclic Structural Analysis," NASA TP-2243.
- Lekhnitskii, S.G., and Brandstatter, J.J., eds., 1963, Theory of Elasticity of an Anisotropic Elastic Body, Holden-Day, Inc., pp. 24-25.
- Lockheed Missiles & Space Company, Huntsville Research and Engineering Center, 1983, "Space Shuttle Main Engine, Powerhead Structural Modeling, Stress and Fatigue Life Analysis," NASA Contract NAS8-34978, NASA CR-170999.
- MARC Analysis Research Corporation, 1980, MARC General Purpose Finite Element Analysis Program, Vol. A: User Information Manual; Vol. B: MARC Element Library; Vol. F: Theoretical Manual, Palo Alto, CA.
- Milligan, W. Walter, Jr, 1986, "Yielding and Deformation Behavior of The Single Crystal Nickel-Base Superalloy PWA 1480," NASA CR-175100.

## STRUCTURAL ANALYSES OF ENGINE WALL COOLING CONCEPTS AND MATERIALS

Albert Kaufman\*  
Sverdrup Technology, Inc.  
(Lewis Research Center Group)  
NASA Lewis Research Center

### ABSTRACT

The severe thermal environments under which hypersonic aircraft such as the National AeroSpace Plane (NASP) will operate require cooling of the engine walls, especially in the combustor. The NASA Lewis Research Center is undertaking an extensive in-house effort to investigate composite materials and cooling concepts for their applicability to NASP engine walls. In this study a preliminary assessment is made of some candidate materials based on structural analyses for a number of convective cooling configurations. Three materials are currently under consideration; graphite/copper (Gr/Cu) and tungsten/copper (W/Cu) composite alloys with 50 percent fiber volume fractions and a wrought cobalt-base superalloy, Haynes 188. Anisotropic mechanical and thermal properties for the composites were obtained from a computer code developed at NASA Lewis. The code, called ICAN, determines the composite material properties from the individual properties of the fiber and matrix materials. The Haynes 188 material properties were obtained from an International Nickel Company brochure. The structural analyses were performed by using the MARC nonlinear finite-element code. The analyses were based on steady-state operation at an inlet ramp condition. Heat transfer analyses were conducted to calculate the metal temperature distributions. Elastic-plastic analyses were performed for the Haynes 188 and W/Cu materials. The Gr/Cu composite was treated as an elastic material because of the lack of adequate material property information. The analyses demonstrate the applicability of nonlinear structural analysis technology to complex real-world problems.

---

\*Work performed on-site at the Lewis Research Center for the Structural Mechanics Branch; subcontract number, 5215-80; technical monitor, Robert L. Thompson.

## ANALYTICAL INPUT CONDITIONS

A preliminary assessment is made of some candidate materials based on heat transfer and structural analyses for several cooling configurations. Three materials were considered: Gr/C and W/Cu composite alloys with 50 percent fiber volume fractions and a wrought cobalt-base superalloy, Haynes 188. Anisotropic mechanical and thermal properties for the composites were obtained from the ICAN computer code developed at NASA Lewis. The heat transfer analyses were based on the gas and coolant temperatures and pressures shown below. The heat flux was 500 Btu/ft<sup>2</sup> sec, which would be characteristic of the engine inlet region.

### CONFIGURATIONS

- RECTANGULAR PASSAGES
- CURVED (D-SHAPED) PASSAGES
- CIRCULAR PASSAGES

### MATERIALS

- HAYNES 188
- Gr/Cu
- W/Cu

### CONDITIONS

- GAS TEMPERATURE, 4000 °F; GAS PRESSURE, 50 psi  
COOLANT TEMPERATURE, 100 °F; COOLANT PRESSURE, 1200 psi
- HEAT FLUX, 500 Btu/ft<sup>2</sup> sec

CD-68-31773

## FINITE-ELEMENT MODELS

Finite-element models were created for cooling configurations involving rectangular, curved (D-shaped), and circular passages. The configurations had wall and fin thicknesses of 0.015 in. Passage spacings were 0.150 in. for the rectangular and curved geometries and 0.075 in. for the circular geometry. The models were constructed of 110 twenty-node, three-dimensional elements. The three-dimensional elements were needed to impose the directional properties of the composite materials. Five passages were modeled for each configuration in order to avoid temperature and stress distortions from the boundary conditions applied at the end surfaces. The shape of the structures was maintained by applying the boundary conditions so that all nodes on the end surfaces were tied together and had the same displacements perpendicular to the initial position of these faces. Only the central passages were considered in evaluating the analytical results. Elastic-plastic analyses were performed for the Haynes 188 and W/Cu materials by using the MARC nonlinear finite-element code. Only elastic analyses were performed for the Gr/Cu material because of the lack of inelastic stress-strain properties.

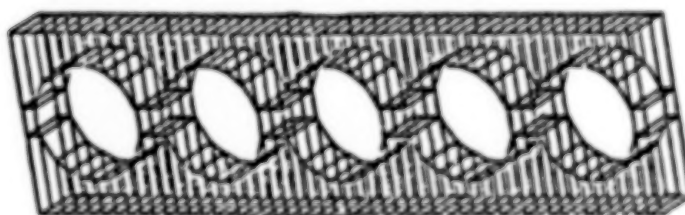
### RECTANGULAR PASSAGES



### CURVED PASSAGES



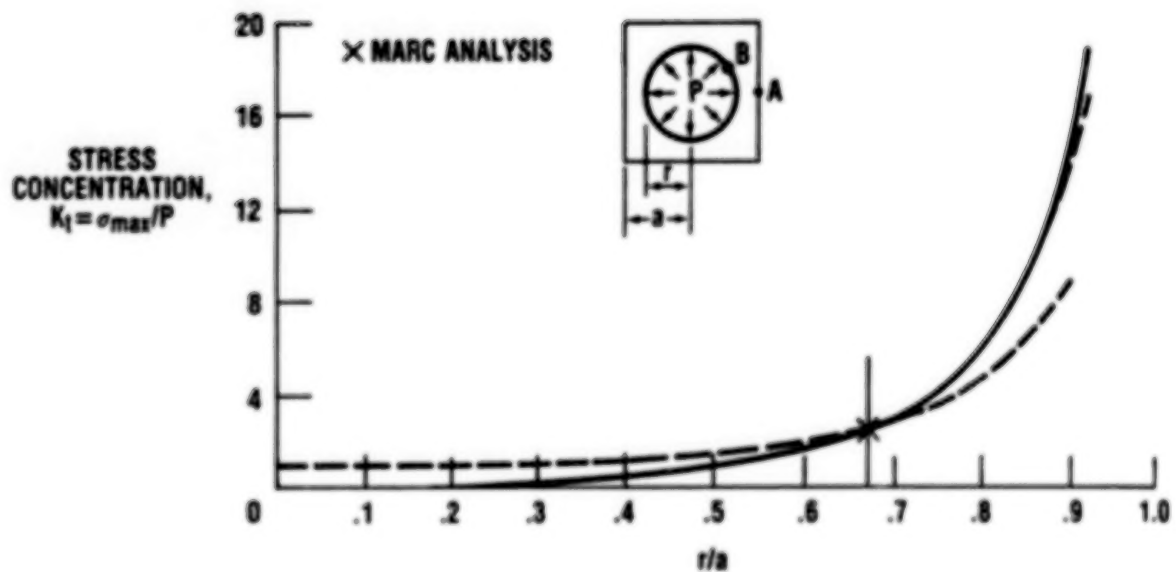
### CIRCULAR PASSAGES



CD-88-311/4

# VERIFICATION OF STRUCTURAL ANALYSIS ACCURACY

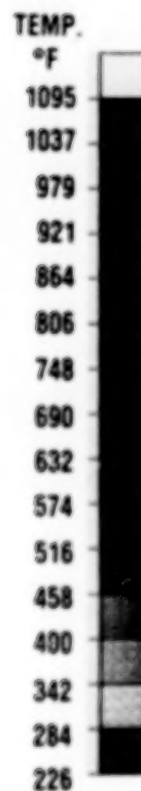
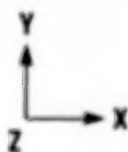
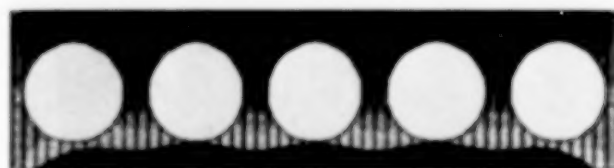
So that the accuracy of the structural analyses could be verified with finite-element models, an isolated circular passage was analyzed as a flat plate with a central hole. Internal pressure loading was applied around the rim of the hole. Calculated stresses at the horizontal and vertical diametral points were compared with photoelastically determined elastic stress concentration factors from Peterson (1974). Agreement between the analytical and experimental results was within 4 percent.



CD-68-31775

# TEMPERATURE DISTRIBUTION IN HAYNES 188 CIRCULAR CONFIGURATION

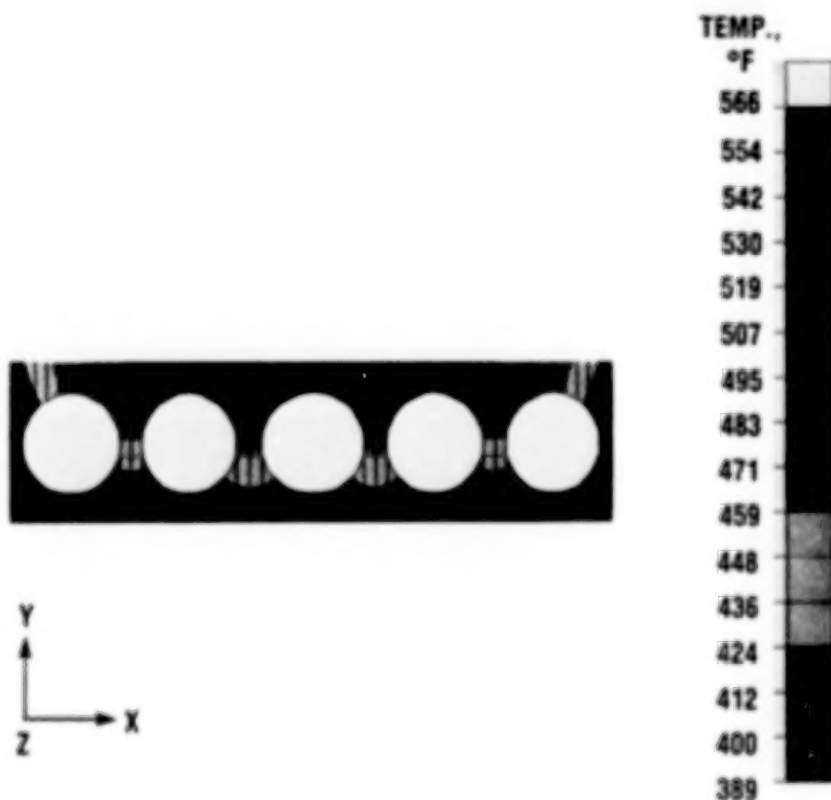
The temperature distribution in a Haynes 188 circular configuration is shown. The maximum metal temperature was above 1000 °F, in contrast to about 900 and 1300 °F for the rectangular and curved configurations, respectively.



CD-88-3111

# TEMPERATURE DISTRIBUTION IN W/Cu CIRCULAR CONFIGURATION

The temperature distribution for a W/Cu circular configuration is shown. The maximum metal temperatures were about 600 °F. The metal temperatures in the composite material structures were lower than those for Haynes 188 structures because their thermal conductivities were much higher. The maximum temperatures for the composite structures were not significantly affected by the passage geometry. This figure illustrates the temperature nonuniformity due to the end boundary conditions and shows why the analyses had to be conducted for a number of passages.

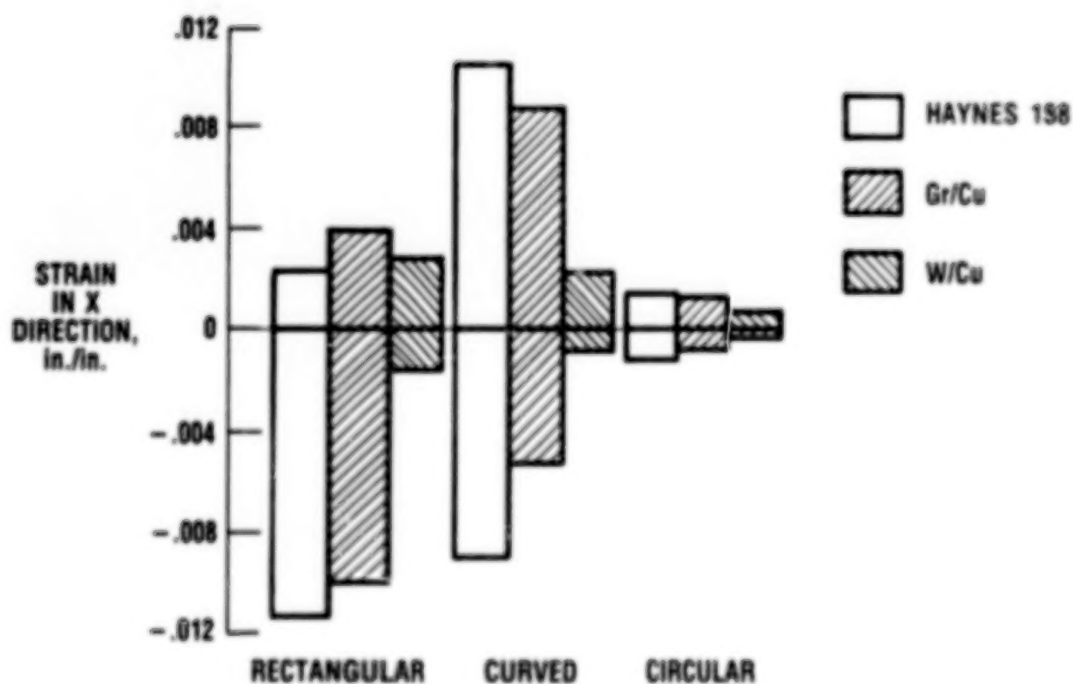


CD-68-31777



### PEAK STRAINS IN COOLING CONFIGURATIONS

The bar graph shows the peak tensile and compressive strains for each material for the three passage geometries. The Haynes 188 alloy had the largest strains because it has the highest temperatures and thermal gradients; the W/Cu composite had the smallest strains because it has the lowest temperatures and thermal gradients. Of the three cooling configurations the curved geometry was the worst and the circular geometry the best in terms of the maximum strain levels.



CD-68-31778

# INELASTIC STRAINS IN HAYNES 188 CURVED CONFIGURATION

The inelastic strain distributions in the central passage region for the curved configuration are shown for the Haynes 188 alloy. Compressive plastic strains of almost 1 percent occurred at the hot upper surface. Smaller tensile plastic strains are evident adjacent to the passage corners and on the cold bottom surface. The creep strain distribution after 2500 seconds of dwell time is also shown. An equivalent creep strain (which is always positive) of 0.75 percent was reached at the hot upper surface.

## STRAIN, in./in.

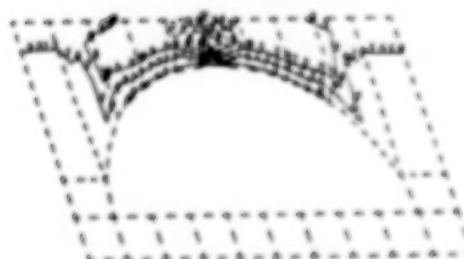
|      |            |
|------|------------|
| 1 =  | -0.876E-02 |
| 2 =  | -0.767E-02 |
| 3 =  | -0.639E-02 |
| 4 =  | -0.621E-02 |
| 5 =  | -0.404E-02 |
| 6 =  | -0.286E-02 |
| 7 =  | -0.168E-02 |
| 8 =  | -0.602E-03 |
| 9 =  | 0.676E-03  |
| 10 = | 0.186E-02  |



PLASTIC STRAIN

## STRAIN, in./in.

|      |            |
|------|------------|
| 1 =  | -0.343E-03 |
| 2 =  | 0.629E-03  |
| 3 =  | 0.140E-02  |
| 4 =  | 0.227E-02  |
| 5 =  | 0.314E-02  |
| 6 =  | 0.402E-02  |
| 7 =  | 0.489E-02  |
| 8 =  | 0.676E-02  |
| 9 =  | 0.663E-02  |
| 10 = | 0.760E-02  |

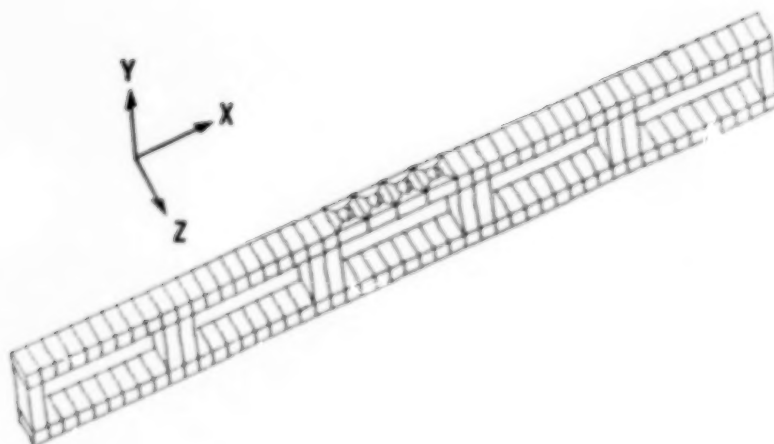


EQUIVALENT CREEP STRAIN  
(2500 SEC)

CD-88-31779

#### FINITE-ELEMENT MODEL OF SIMULATED FILM-COOLING CONFIGURATION

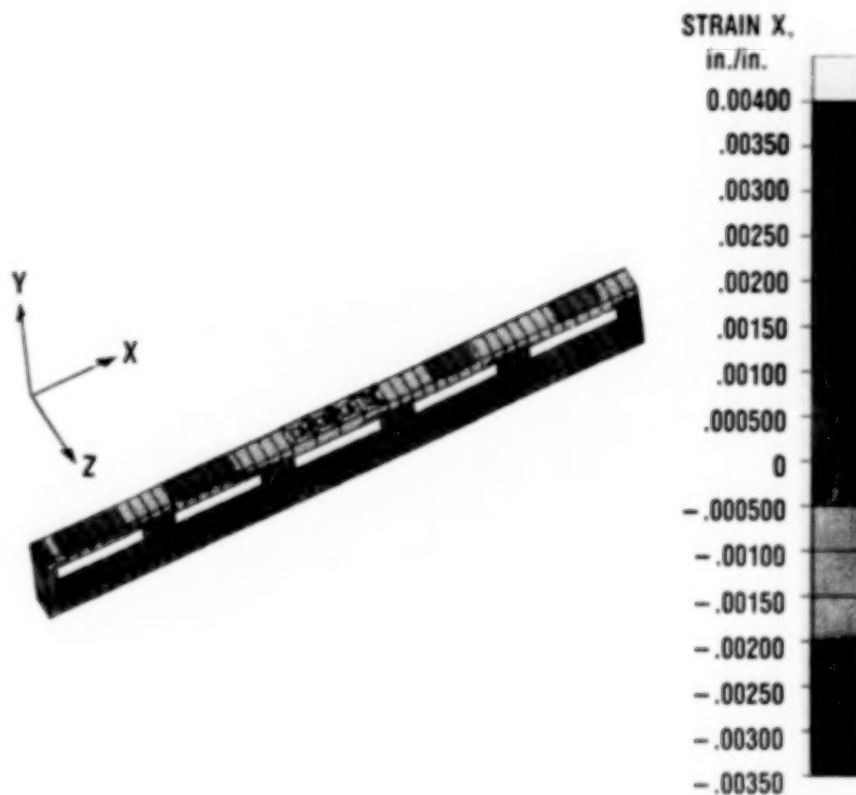
Film cooling was studied by modeling cooling holes in the upper surface of the rectangular central passage region, as shown in the finite-element model below. This increased the number of 20-node, three-dimensional elements to 118. The effects of film cooling on the upper surface were simulated by reducing the gas-side heat transfer coefficient by 10 percent. This decreased the maximum temperatures by several hundred degrees. The simulated film cooling reduced the maximum metal temperature in the central passage region from 900 °F to about 300 °F.



CD-88-31780

## STRAIN DISTRIBUTION IN HAYNES 188 FILM-COOLING CONFIGURATION

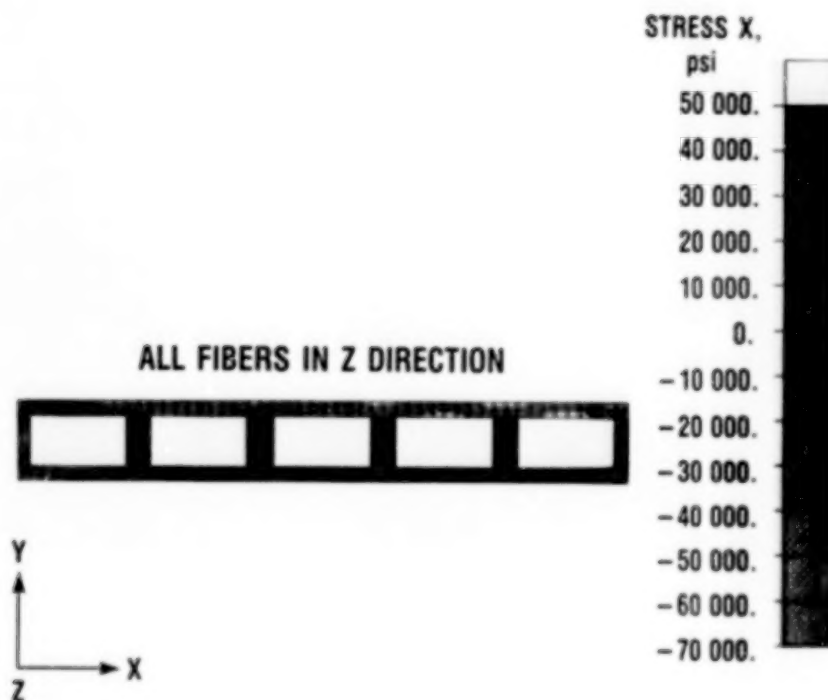
The strain distribution is shown for the Haynes 188 film-cooling configuration. High local strains are evident near the end surfaces. In the central passage region the highest strains occurred adjacent to the passage corners. There was a significant reduction in the maximum compressive strain at the hot upper surface, from 0.0050 in the rectangular geometry to 0.0025 in the film-cooling geometry. Also, the plastic flow previously encountered at the upper surface was eliminated because of the lower metal temperatures, improved material properties, and decreased strain levels.



CD-66-31781

# STRESS DISTRIBUTION IN W/Cu CONFIGURATION - ALL FIBERS IN Z DIRECTION

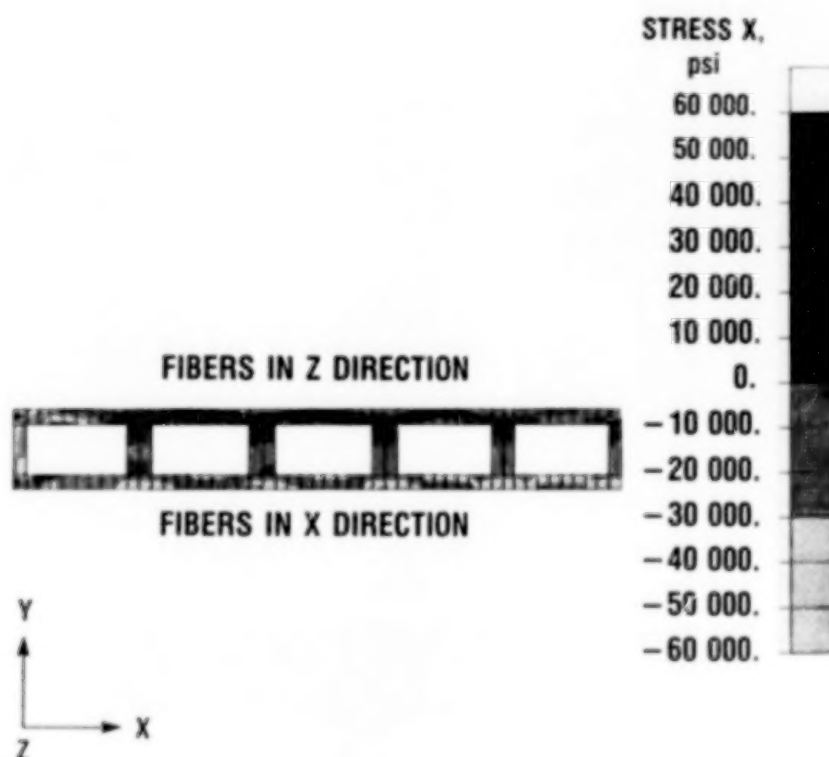
The W/Cu structures were initially analyzed for fibers oriented parallel with the direction of the fins (z direction). This orientation would be required in the thin-fin region and would be most convenient for the whole structure from a fabrication standpoint. However, it places the weak transverse properties in the x direction, where the stresses are the most severe. Small plastic strains (under 0.1 percent) were induced at the hot upper surface.



CD-88-31782

# STRESS DISTRIBUTION IN W/Cu CONFIGURATION - FIBERS IN X AND Z DIRECTIONS

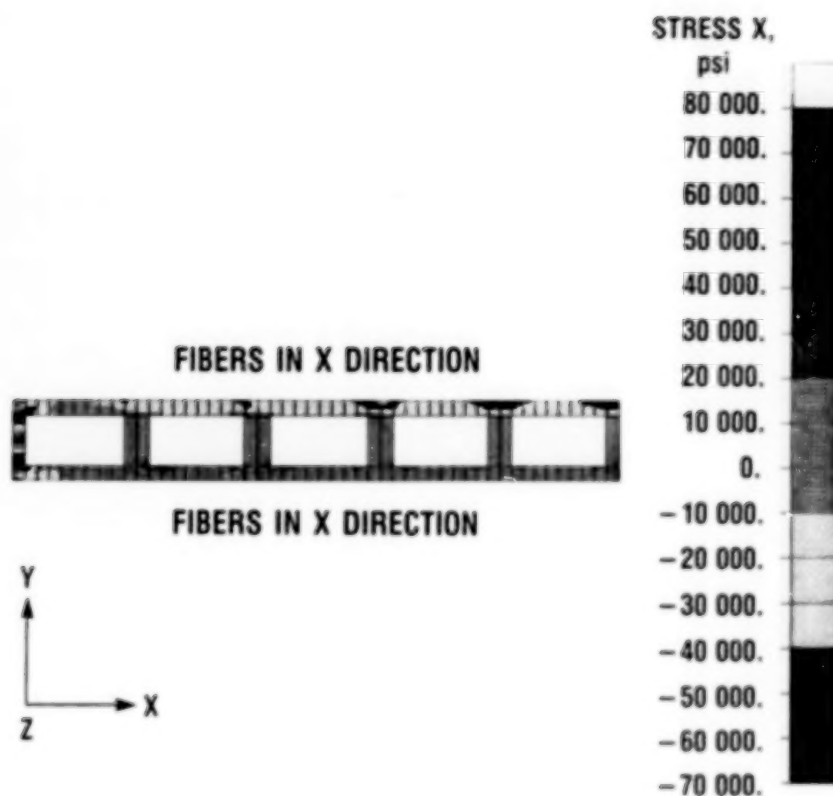
The fiber orientation was changed analytically so that the fibers were in the x direction, transverse to the fins, in the bottom or cold wall. The fibers at the top wall remained in the z direction. In doing this, essentially two different materials were being joined because of the significant differences in material properties between the longitudinal and transverse directions in the material. These differences are even greater in the Gr/Cu composite. From a structural analysis standpoint the stress-free temperature is that at which the structure is cured. The curing temperature of the W/Cu composite was assumed to be 1800 °F. This assumption resulted in reversing the signs of the stresses in the walls so that tensile stresses were induced in the hot upper wall and compressive stresses in the cold bottom wall.



CD 88-31783

# STRESS DISTRIBUTION IN W/Cu CONFIGURATION - ALL FIBERS IN X DIRECTION

In this configuration the fibers were oriented in the x direction everywhere except in the fin region. This gave the structure the strongest properties in the most severe direction and temperature region. No plastic straining occurred with this orientation.

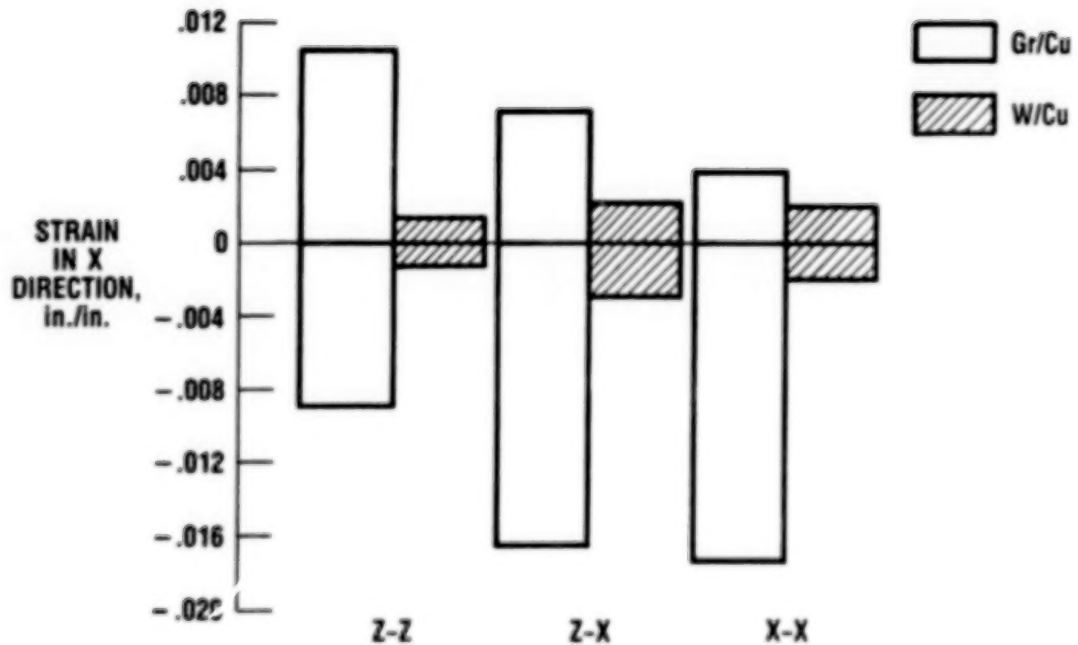


CD-68-31784



# EFFECT OF FIBER ORIENTATION ON STRAINS IN W/Cu CONFIGURATION

This bargraph summarizes the effects of fiber orientation on the strain levels. For the Gr/Cu composite the effect of changing the fiber orientation to the x direction was to reduce the tensile strain and increase the compressive strain. The W/Cu configuration with both the fin and transverse fiber orientations exhibited the smallest strains of the three candidate materials.



CD-88-31785

## CONCLUSIONS

- HIGHEST STRESS COMPONENT WAS IN TRANSVERSE DIRECTION TO FINS
- CIRCULAR PASSAGES GAVE LOWEST AND CURVED PASSAGES HIGHEST STRAINS
- W/Cu WITH TRANSVERSE FIBERS GAVE LOW TEMPERATURES AND STRAINS WITHOUT PLASTIC FLOW
- HAYNES 188 WAS ACCEPTABLE WITH CIRCULAR AND FILM-COOLED GEOMETRIES; HIGH CREEP STRAIN IN CURVED GEOMETRY

CD-68-31786

#### REFERENCES

Peterson, R.E., 1974, "Stress Concentration Factors." John Wiley & Sons.

# STRUCTURAL ASSESSMENT OF A SPACE STATION SOLAR DYNAMIC HEAT RECEIVER THERMAL ENERGY STORAGE CANISTER

R.L. Thompson, T.W. Kerslake,\* and M.T. Tong†  
Structural Mechanics Branch  
NASA Lewis Research Center

## ABSTRACT

Advanced analytical tools and experimental techniques were recently developed in the Structural Mechanics Branch to assess the structural performance of a space station thermal energy storage (TES) canister subjected to orbital solar flux variation and cold startup operating conditions. Included in the assessment were the impact of working fluid temperature and salt-void distribution on the canister structure. Both analytical and experimental studies were conducted to determine the temperature distribution in the canister. Subsequent three-dimensional, nonlinear, finite-element, structural analyses of the canister were performed using both analytically and experimentally obtained temperatures. For the lack of a better material constitutive model, the Arrhenius creep law was incorporated into the procedure, using secondary creep data for the canister material, Haynes-188 alloy. The predicted cyclic creep-strain accumulations at the hot spot were used to assess the structural performance of the canister. Structural tests on a canister were also conducted. This was a cooperative program with the Space Station Solar Dynamic Power Module Division, Power Conversion and Heat Receiver Branch.

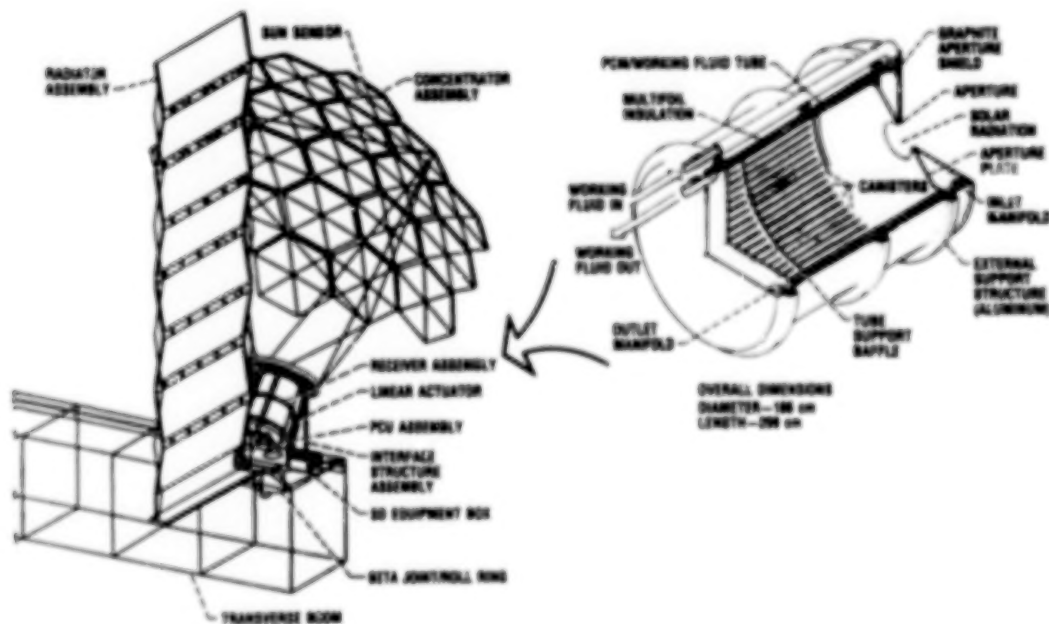
---

\*Solar Dynamic Power Module Division, NASA Lewis Research Center.

†Sverdrup Technology, Inc., Lewis Research Center Group, NASA Lewis Research Center.

## SPACE STATION CLOSED BRAYTON CYCLE SOLAR DYNAMIC POWER MODULE

As part of the Phase II option of the space station, an additional power requirement of 50 kilowatts will be met by two high-efficiency solar dynamic (SD) power modules. NASA Lewis Research Center has chosen the Closed Brayton Cycle (CBC) for the Space Station SD power modules. The solar dynamic modules employ a concentrator to collect and focus incident solar flux onto the wall of a cylindrical cavity-type heat receiver where it is converted to thermal energy. A fraction of the thermal energy is transferred to a circulating working fluid to operate the heat engine and produce electrical power. The remaining thermal energy melts a eutectic composition  $\text{LiF-CaF}_2$  salt in thermal energy storage (TES) canisters integral with the receiver cavity. The salt stores and releases thermal energy by undergoing phase changes at its melting point of  $767^\circ\text{C}$  ( $1413^\circ\text{F}$ ). This permits continuous operation of the Brayton heat engine during insolation and eclipse periods of the orbit. Shown are the solar dynamic power module and a cutaway of the solar receiver assembly.

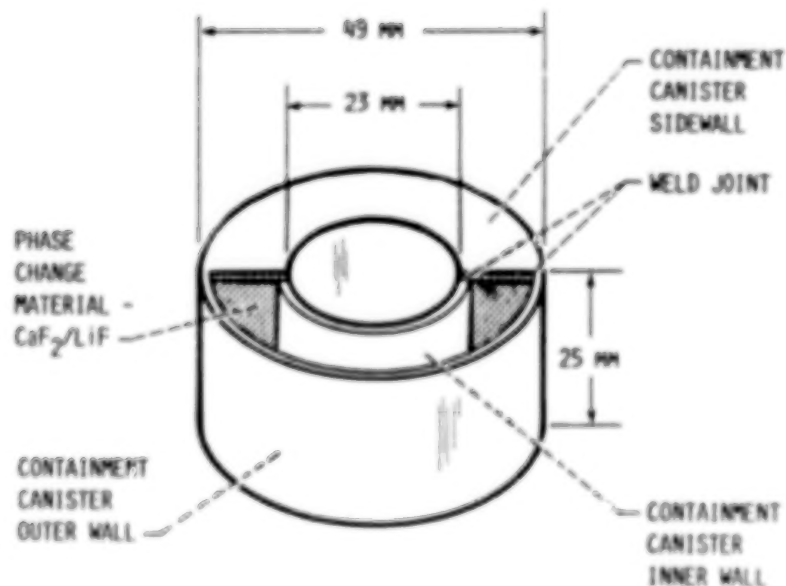


CO-65-32496

## SPACE STATION THERMAL ENERGY STORAGE CANISTER

The space station orbit under consideration is a minimum insulation orbit. It has a period of 91 minutes, with 37 minutes eclipse and a solar constant of  $1323 \text{ W/m}^2$  ( $420 \text{ Btu/hr/ft}^2$ ). During each orbital cycle, the canister is subjected to appreciable transient thermal loads. Inelastic deformation can be induced in localized regions leading to potential structural failure. Assessment of durability requires reasonably accurate calculation of the structural response under cyclic loading. This problem is an ideal case in which to apply the recently developed analytical tools and procedures developed at NASA Lewis.

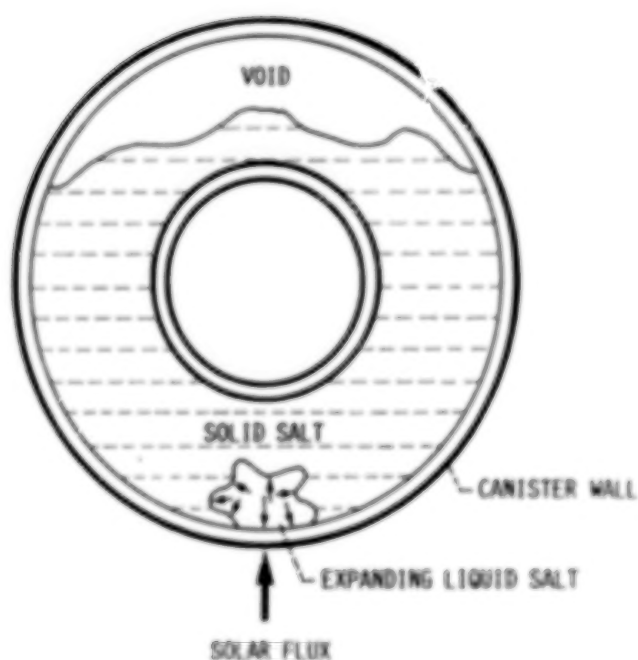
The canister under consideration was located 1143 mm (3.75 ft) behind the receiver focal plane - the location believed to have the most severe thermal environment. It is made of Haynes-188 alloy, and was designed by the NASA Lewis Phase B Space Station contractor team of Rockwell International Rocketdyne Division and Garrett Corporation-AiResearch (Anon., 1986). The canister under study is shown here.



CO-88-32497

## THERMAL ENERGY STORAGE CANISTER

A canister with the  $\text{LiF-CaF}_2$  salt in its solidified state is shown here. The void is approximately 25 percent of the total volume. As the solar flux heats the salt, the salt liquefies and fills the canister volume. The liquefaction process is extremely complex, particularly in a microgravity environment where the surface tension induced flow phenomenon is the driving mechanism for convection. Because the liquefaction process is not predictable, several worst-case conditions were assumed in order to determine the structural performance of the canister.



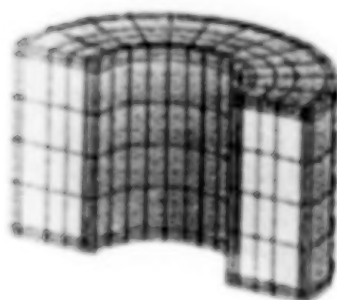
CD-4 1-32498



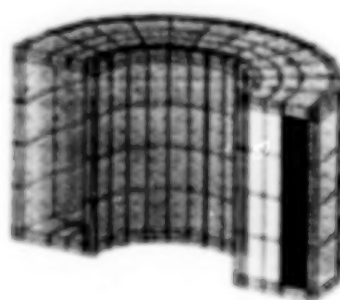
## CANISTER-SALT CONFIGURATIONS FOR STEADY-STATE ANALYSES

Because the exact salt formation in the canister under microgravity is not quantified, several different canister-salt configurations were analyzed to determine the effect of salt-void distribution on the canister structure. The configurations evaluated for the steady-state analyses are (a) canister filled with salt, (b) canister with an entrapped liquid pocket, (c) canister with circumferential void at the canister outer-diameter wall, and (d) canister with void at the sidewall. These configurations are shown below. Three-dimensional finite-element thermal and structural analyses of the canister were performed using the MARC finite-element program (Anon., 1984).

Subsequent nonlinear transient analyses were performed to obtain the cyclic stress-strain history for structural assessment of the canister. A canister-salt configuration with circumferential void at the outer-diameter wall was chosen for the transient analyses because steady-state analyses showed it to be the most severe case. A total of four transient analytical cases were studied to determine how the structural performance of the canister was affected by void in the canister, working fluid temperature, and cold startup operating condition.

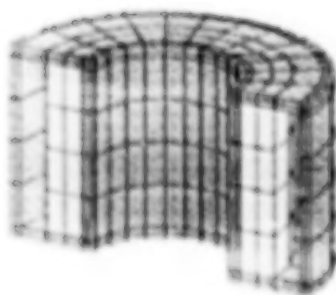


CANISTER FILLED WITH SALT

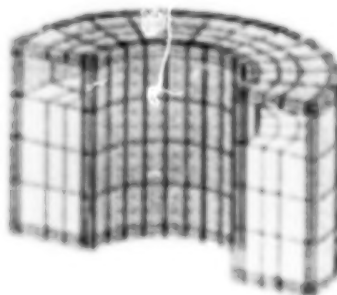


CANISTER WITH LIQUID POCKET

- 672 8-NODE SOLID ELEMENTS
- 936 NODES



CANISTER WITH CIRCUMFERENTIAL VOID

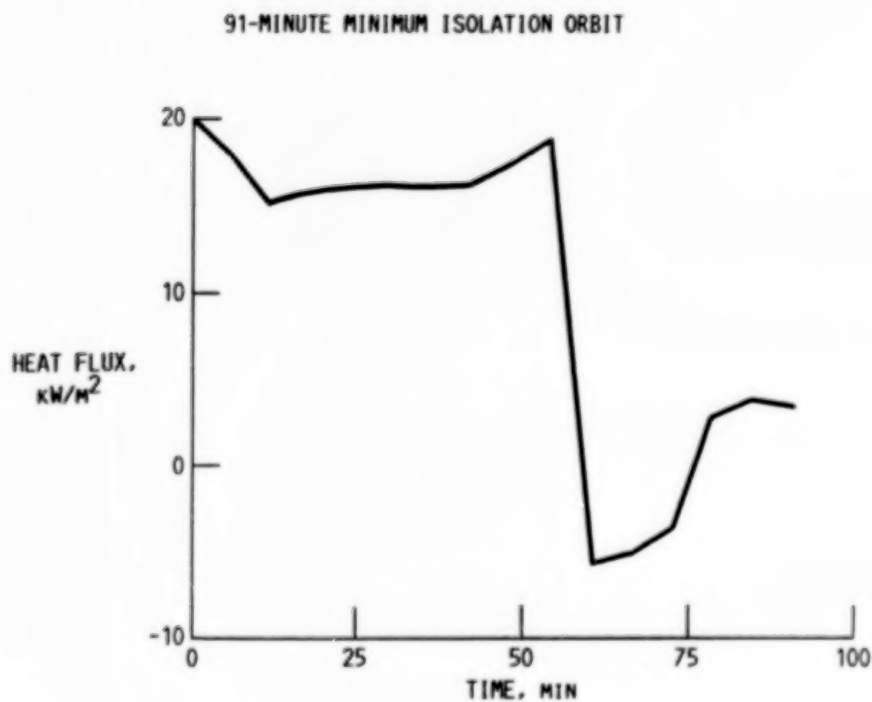


CANISTER WITH VOID AT SIDEWALL

CD-86-30499

## ORBITAL SOLAR FLUX HISTORY FOR CANISTER TRANSIENT ANALYSES

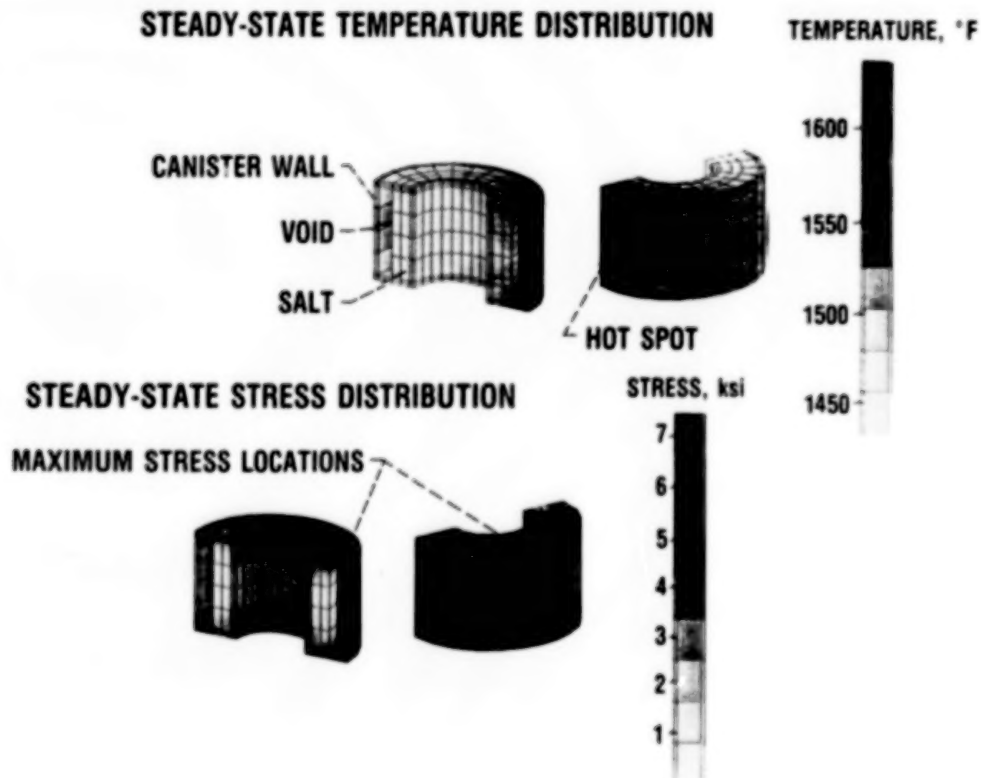
Steady-state thermal boundary conditions were the maximum solar heat flux of  $19.9 \text{ kW/m}^2$  ( $6300 \text{ Btu/hr/ft}^2$ ) distributed according to the canister projected surface area, working fluid temperature of  $704^\circ\text{C}$  ( $1300^\circ\text{F}$ ), and thermal radiation at the backwall. Based on these boundary conditions, metal temperatures were predicted by using MARC and were then used in the structural analyses. Determination of transient thermal loads was based on the transient orbital heat flux shown below. Other transient thermal boundary conditions were the working fluid temperature histories and backwall temperature histories. The phase change of  $\text{LiF-CaF}_2$  salt was also considered in the analyses. The calculated canister temperature histories were then used in the structural analyses of the canister.



CD-88-32500

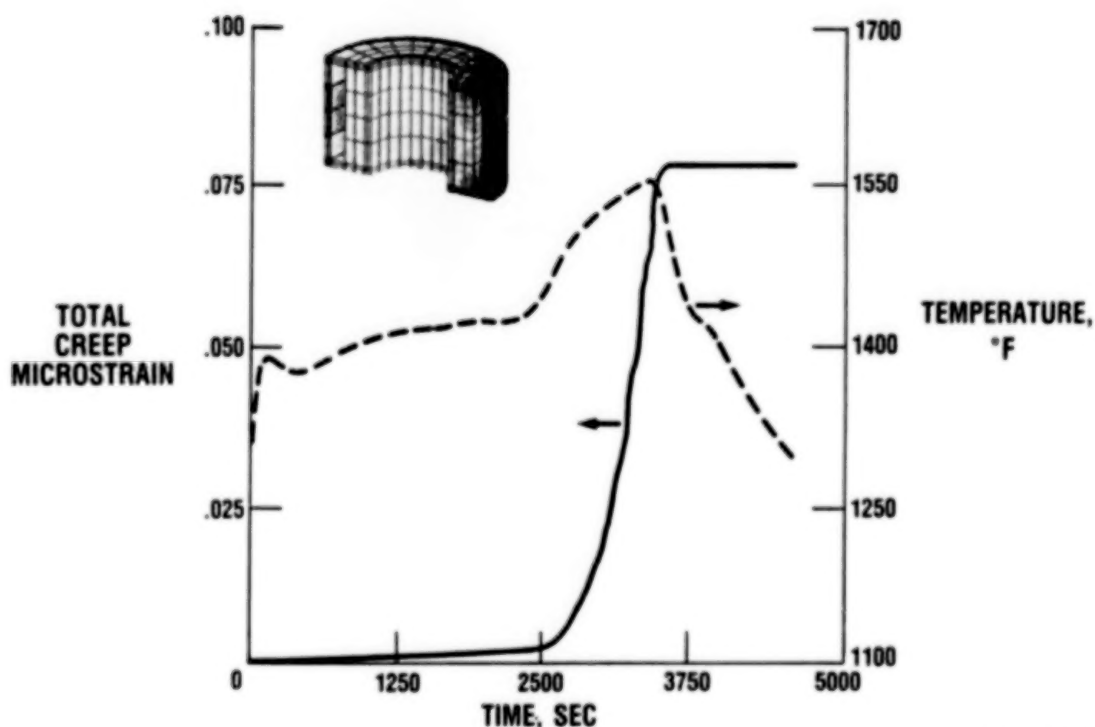
## TYPICAL STEADY-STATE CANISTER TEMPERATURES AND STRESSES

Typical steady-state temperatures and resulting stress distributions are shown for the case of a circumferential void at the canister outer diameter wall. The hot spot is at the point of maximum solar flux. The temperature at this location is 891 °C (1630 °F). The maximum Von Mises stress of 52 MPa (7568 psi) occurs at the corners of the canister, as indicated in the figure. Since steady-state analyses showed that creep would be the predominant damage mode (ignoring oxidation and hot corrosion), an Arrhenius creep law was incorporated into the MARC code by means of a user subroutine.



# ORBITAL VARIATION OF MAXIMUM TEMPERATURE AND TOTAL CREEP STRAIN IN CANISTER

Typical transient temperatures and resulting creep strains are shown for the case of a circumferential void at the canister outer-diameter wall. The temperatures and creep strains for the minimum insulation orbit are plotted at the location indicated on the figure. The working fluid temperature ranged from 980 to 1280 °F. Using the predicted temperatures and strains, thermomechanical tests on Haynes-188 specimens have been conducted to determine if the stress predictions are accurate and also to determine the effects of thermomechanical cycling and possible ratcheting of the material. These tests, conducted in the NASA Lewis High Temperature Fatigue and Structures Facility, are unique to this effort.

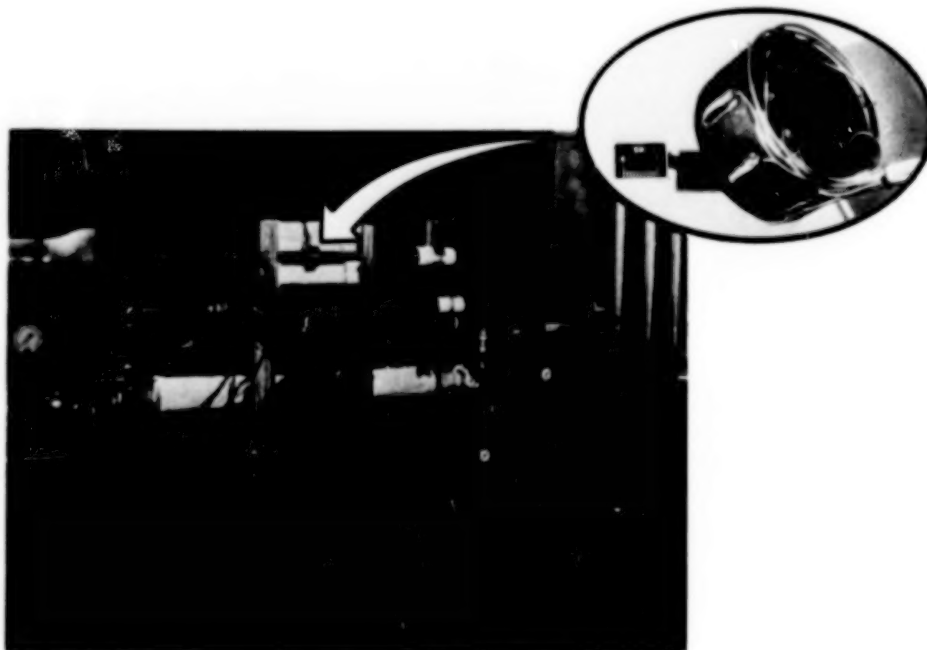


CD-88-32502

## TEST APPARATUS AND INSTRUMENTED CANISTER

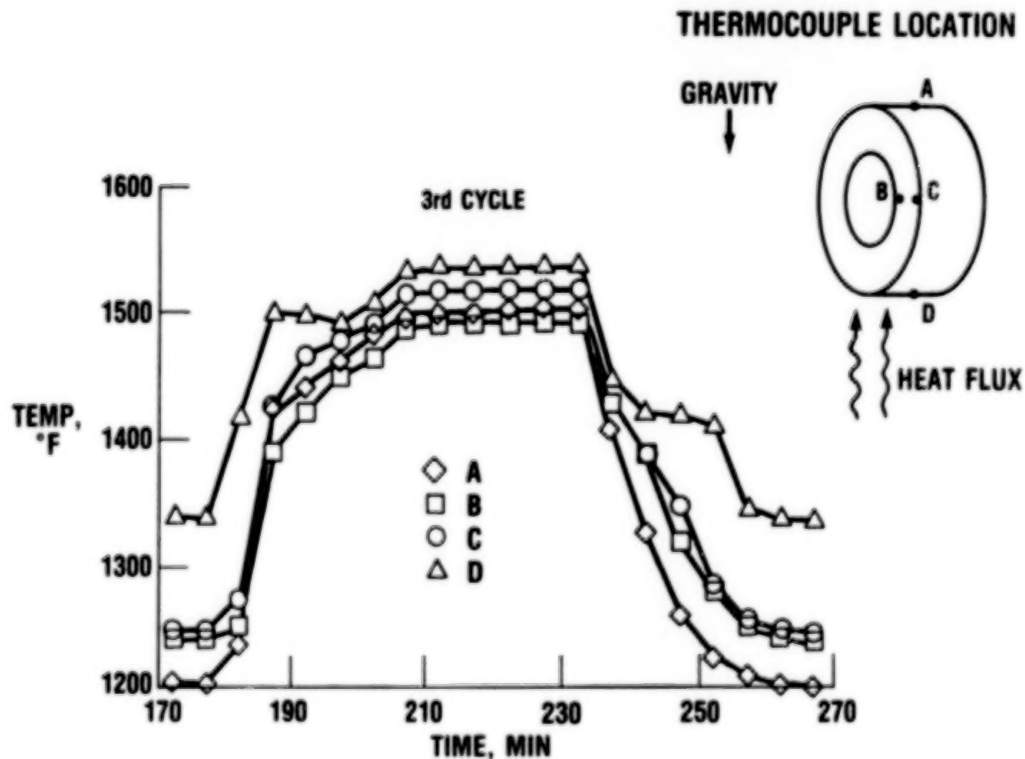
Three canister test articles were used in the testing program. Each canister was instrumented with chromel-alumel thermocouples and radiation shields. The canisters were tested individually using a bench-top rig. The test article was slip-fitted onto a Haynes-188 pipe and was enclosed in an insulated test chamber that provided a high-temperature environment representative of the heat receiver cavity. A solar simulator, consisting of high flux quartz lamps, was also enclosed in the test chamber to irradiate the bottom half of the canister exterior surface. The dual loop power controller was programmed to automatically produce the expected orbital heat flux variation for the minimum insulation orbit described above. Preheated air flow, which simulated the engine working fluid, provided the convective cooling to the canister interior surface. The experimental objectives were twofold:

1. to demonstrate the structural adequacy of the TES canister under several worst-case heating and salt configuration conditions.
2. to determine canister temperature distributions in sufficient detail to support finite-element structural analyses for several known canister salt configurations.



## CYCLIC THERMAL RESULTS

Cold startup and cyclic tests were conducted to simulate the operation of the canister under on-orbit receiver startup and orbital cyclic heat flux conditions, respectively. The effect of salt distribution on canister temperature profiles was evaluated by testing canisters with three different salt configurations. Cold startup canister tests were conducted by subjecting the test article (at ambient temperature) to a step-input of maximum heat flux without internal cooling airflow. This procedure was developed to simulate only the first 15 to 30 minutes of the receiver startup cycle - the time period believed to have the highest canister temperature gradients and highest canister salt traction forces. Canister temperature response was measured until steady-state conditions were approached (about 20 minutes). Cyclic canister tests were conducted by subjecting the test article to a series of high-low step heat fluxes. Cooling airflow rate and temperature were established at the beginning of each test and held constant throughout the testing period (10 simulated orbits or about 15 hours). All three canisters were inspected before and after each test for signs of deformation, cracks, or leaks. Inspection was performed nondestructively through the use of dye penetrant tests, x-ray radiography, and visual inspection. Canister dimensions were also measured to quantify deformation. Typical measured temperatures for a cyclic run are shown for four thermocouple locations. These temperatures are in reasonably good agreement with predicted temperatures.



CD-88-32504

# SUMMARY OF STEADY-STATE ANALYSIS RESULTS

Results of steady-state thermal and elastic structural analyses for the four canister/salt configurations are summarized below. Typical canister hot spot and maximum stress locations were shown in an earlier figure. As expected, the canister wall hot spot was located in the region of maximum heat input. The maximum stress location was at the canister side wall outer diameter. Among the four cases studied, the canister-salt configuration with circumferential void at the outer-diameter wall had the highest stress level, 52 MPa at 891 °C (7568 psi at 1635 °F). In all cases, however, the maximum stress level was well below the yield strength of the Haynes-188 alloy, 262 MPa at 871 °C (38000 psi at 1600 °F). This indicates an insignificant amount of material plasticity. However, creep deformation could occur because of long-time exposure to the receiver environment.

| Analytical case                                 | Maximum temperature |      | Maximum von Mises stress |      |
|---|---------------------|------|--------------------------|------|
|   | °C                  | °F   | MPa                      | psi  |
| Canister filled with salt                       | 862                 | 1583 | 40                       | 5823 |
| Canister with circumferential void at O.D. wall | 891                 | 1635 | 52                       | 7568 |
| Canister with entrapped liquid salt pocket      | 862                 | 1583 | 41                       | 5976 |
| Canister with void at sidewall                  | 868                 | 1594 | 42                       | 6164 |



# SUMMARY OF TRANSIENT ANALYSIS RESULTS

Results from the transient analyses are summarized below. The accumulated creep strain per cycle at the critical location (the hot spot, as noted earlier) is the most crucial parameter to consider. This value is tabulated for several different configurations of salt-void within the canister. For lack of better knowledge of the constitutive material properties of the Haynes-188 alloy, an Arrhenius steady-state creep law was used. As seen from the table, the calculated creep strain is highly dependent upon the void configuration. This dependency arises because the void affects the heat conducted from the canister wall to the salt and onto the working fluid. A void interferes with the heat path, thus causing an increased thermal stress. This higher thermal stress increases the resultant creep strain dramatically. Higher working fluid temperatures also increase the calculated amount of creep strain per cycle. The time required to accumulate one percent creep strain is also indicated in the table.

| Case   | Total accumulated creep microstrain per cycle | Amount of time to accumulate 1 percent creep |
|--|---|--|
| Canister filled with salt, 527 to 693 °C working fluid temperature                       | 0.0018  | 960 years                                    |
| Canister with circumferential void at O.D. wall, 527 to 693 °C working fluid temperature | .0760   | 23 years                                     |
| Canister with circumferential void at O.D. wall, 613 to 697 °C working fluid temperature | .1300   | 13 years                                     |
| Canister with circumferential void at O.D. wall, engine cold startup                     | 7.2500  | 0.24 years<br>or<br>1400 cycles              |

## SUMMARY OF RESULTS AND CONCLUSIONS

The creep-failure criteria had not been defined for the canister. Preliminary NASA Lewis in-house testing of the Haynes-188 alloy has shown that it behaved in a significantly different manner under thermal cyclic loading than under isothermal loading. The design data available for the Haynes-188 alloy are based on monotonic and isothermal loadings. Because of this, further tests and analyses are in progress at NASA Lewis to determine the behavior of the Haynes-188 alloy under thermal cyclic loading. In addition, long-term testing of the canister is being planned. The results from these programs should enable more refined analyses and further improve the design of the canister that will be subjected to repetitive orbital thermal loadings.

The structural performance of a space station TES canister was evaluated analytically and experimentally at various operating conditions. Creep-strain results from structural analyses were used for the structural assessment. The major results of this study are as follows:

1. Creep rupture will most likely be the predominant failure mode for the TES canister (ignoring oxidation and hot corrosion), according to the canister operating thermal environment information provided.
2. Structural performance of the TES canister is sensitive to the salt-void distribution inside the canister. This is because of the higher peak temperature and stress levels caused by the exact location of the void.
3. Structural performance of the TES canister is sensitive to the thermal environment because creep depends strongly on temperature. Working fluid temperature also has a significant effect on the structural performance of the canister.
4. The existence of a liquid salt pocket inside the canister has no significant effect on the structural performance of the canister because the  $\text{LiF-CaF}_2$  salt has a much lower modulus than the Haynes-188 alloy.
5. Additional thermal cyclic testing of Haynes-188 specimens and canisters must be conducted before creep-failure criteria can be defined for the canister.
6. Advanced analytical tools and experimental techniques have been successfully demonstrated for this application.

#### REFERENCES

- Anon., 1986, MARC General Purpose Finite Element Program, MARC Analysis Research Corporation, Palo Alto, California.
- Anon., 1984, Space Station WP-04 Power System Preliminary Analysis and Design Document, DR02.NAS 3-24666, June 1986, Vol. 1, Section 2, pp. 240-267.
- Ellis, J.R., Bartolotta, P.A., and Mladsi, S.W., 1987, "Preliminary Study of Creep Thresholds and Thermomechanical Response in Haynes 188 at Temperatures in the Range 649 C to 871 C," Proceedings of the Conference on Turbine Engine Hot Section Technology, NASA CP-2493, pp. 317-334 (FEDD document, available to general public after October 1989).

**AN EFFICIENT MINDLIN FINITE STRIP PLATE ELEMENT  
BASED ON ASSUMED STRAIN DISTRIBUTION**

**Abhisak Chulya\* and Robert L. Thompson  
Structural Mechanics Branch  
NASA Lewis Research Center**

**ABSTRACT**

A simple two-node, linear, finite strip plate bending element based on Mindlin-Reissner plate theory for the analysis of very thin to thick bridges, plates, and axisymmetric shells is presented. The new transverse shear strains are assumed for constant distribution in the two-node linear strip. The important aspect is the choice of the points that relate the nodal displacements and rotations through the locking transverse shear strains. The element stiffness matrix is explicitly formulated for efficient computation and ease in computer implementation. Numerical results showing the efficiency and predictive capability of the element for analyzing plates with different supports, loading conditions, and a wide range of thicknesses are given. The results show no sign of the shear locking phenomenon.

---

\*Institute for Computational Mechanics in Propulsion; work funded under Space Act Agreement C99066G; affiliated with Case Western Reserve University.

## FINITE STRIP VERSUS FINITE ELEMENT

The finite strip method was first introduced by Cheung (1968a) for the analysis of elastic plates. It became well known because of its advantages over the conventional finite element method in the simplicity of the formulation and the reduction in size as well as bandwidth of the assembled stiffness matrix. The combined use of finite elements in one direction and Fourier-series expansions in another direction makes it simple and computationally efficient for analyzing a wide variety of structures (i.e., bridges, curved plates, sandwich plates, composite plates, and axisymmetric shells).

In the early stage classical Kirchhoff thin-plate theory, which does not account for shear deformation, was used (Cheung, 1968a and 1968b) and obviously restricted to "thin" situations only. Later the transverse shear effect based on Mindlin-Reissner plate theory (Mindlin, 1951) was included by Mawenya and Davies (1974), and this was applicable to modeling thin plates as well as moderately thick plates. However, despite its mathematical elegance over stiff numerical results, often called "shear locking" effect, were detected when using lower-order elements for analyzing thin and very thin structures. In this presentation the emphasis is on developing a simple, low-order element for general-purpose usage in thin and thick structures that will not produce the shear locking phenomenon.

### FINITE ELEMENT METHOD (CONVENTIONAL)

### FINITE STRIP METHOD

#### FORMULATION

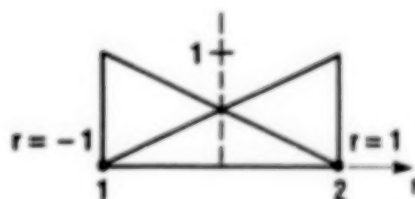
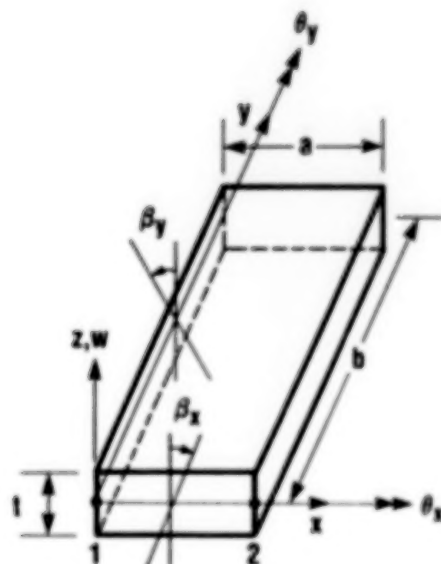
- |                                   |  |
|-----------------------------------|--|
| • TOTAL POTENTIAL ENERGY          | • TOTAL POTENTIAL ENERGY   |
| • MINDLIN-REISSNER PLATE THEORY   | • MINDLIN-REISSNER PLATE THEORY                                  |
| • DISPLACEMENT BASE               | • DISPLACEMENT BASE  |
| • INTERPOLATION IN ALL DIRECTIONS | • INTERPOLATION IN X-DIRECTION;<br>FOURIER SERIES IN Y-DIRECTION |

#### PERFORMANCE

- |  |   |
|--|---|
| • ALMOST ALL TYPES OF BOUNDARY CONDITIONS                | • LIMITED TO SOME PARTICULAR BOUNDARY CONDITION               |
| • LARGE OVERALL MATRIX                                   | • MUCH SMALLER OVERALL MATRIX                                 |
| • LARGE BANDWIDTH  | • MUCH SMALLER BANDWIDTH                                      |
| • NORMALLY REQUIRES VERY FINE MESH FOR LOW-ORDER ELEMENT | • EXCELLENT PERFORMANCE FOR LOW-ORDER ELEMENT AND COARSE MESH |
| • LOCKING IN THIN SITUATION                              | • LOCKING IN THIN SITUATION                                   |

# MINDLIN-REISSNER STRIP ELEMENT FORMULATION

A two-node, linear strip element is formulated for static analysis of plate structures. The midplane deflection and rotations are interpolated separately as the products of the sum of the Fourier series in the y-direction and the polynomial functions in the x-direction. The positive direction is shown below. Only the simply supported case is considered. The loads are also resolved into a sine series in the y-direction similar to the deflection. By using the orthogonality properties of the harmonic series (Cheung, 1976), the stiffness matrix is uncoupled. Note that the shear term of this stiffness matrix is derived by using the troublesome transverse shear strains. Next these strains will be replaced by the new assumed shear strains.



$$N_1 = \frac{1-r}{2}$$

$$N_2 = \frac{1+r}{2}$$

CD-88-32471

$$w = \sum_{r=1}^n \sum_{i=1}^2 N_i w_i^r \sin \frac{r\pi y}{b}$$

$$\beta_x = \sum_{r=1}^n \sum_{i=1}^2 N_i \beta_{x,i}^r \sin \frac{r\pi y}{b}$$

$$\beta_y = \sum_{r=1}^n \sum_{i=1}^2 N_i \beta_{y,i}^r \cos \frac{r\pi y}{b}$$

$$\epsilon_x = \frac{\partial w}{\partial x} + \beta_x = \sum_{r=1}^n \sum_{i=1}^2 [B_1^r]_x U_i^r$$

$$\epsilon_y = 2\kappa$$

$$\kappa = \begin{bmatrix} \beta_{x,y} \\ -\beta_{y,y} \\ \beta_{x,y} - \beta_{y,x} \end{bmatrix} = \sum_{r=1}^n \sum_{i=1}^2 [B_1^r]_y U_i^r$$

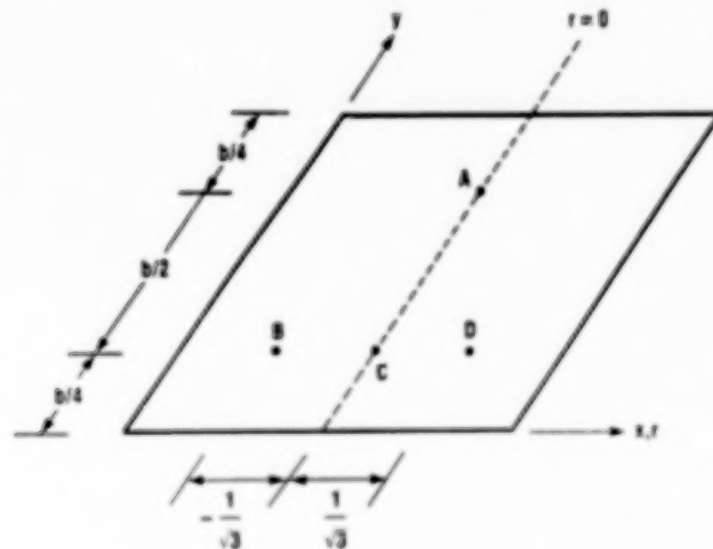
$$\sum_{r=1}^n \sum_{i,j} [K_0^r] U_i^r = \sum_{r=1}^n R_i^r$$

$$\begin{bmatrix} [K^1] \\ [K^2] \\ \vdots \\ [K^n] \end{bmatrix} \begin{bmatrix} U^1 \\ U^2 \\ \vdots \\ U^n \end{bmatrix} = \begin{bmatrix} R^1 \\ R^2 \\ \vdots \\ R^n \end{bmatrix}$$

CD-88-32472

## ASSUMED STRAIN DISTRIBUTIONS

The finite strip formulation has some drawbacks. The element locks when the structure is thin because it uses two-point Gauss quadrature integration for both bending and shear stiffness. The shear stiffness terms overwhelm the bending stiffness terms, and this leads to the over stiff element even though a very fine mesh is used. Although selective and reduced integration is a well-established approach, new assumed strain distributions are introduced to circumvent this locking phenomenon for transverse shear effects (MacNeal, 1982). Note that these assumed shear strains are evenly distributed across the cross sections and constrained to equal the troublesome shear strains at prespecified points. The choice of these points is of paramount importance in evaluating the predictive capability of the element even though the new assumed strains are an integral part of the overall performance.



CD-88-32473

$$\gamma_{xz}^i = \frac{1}{2} (\gamma_{xz}^A + \gamma_{xz}^C)$$

$$\gamma_{yz}^i = \frac{1}{2} (\gamma_{yz}^B + \gamma_{yz}^D)$$

$$\gamma_{xz}^A = \frac{1}{2} S_1^A [-w_1^i/J + \theta_1^i + w_2^i/J + \theta_2^i]$$

$$\gamma_{xz}^C = \frac{1}{2} S_1^C [-w_1^i/J + \theta_1^i + w_2^i/J + \theta_2^i]$$

$$S_1^A = \sin(3\pi/4), \quad S_1^C = \sin(\pi/4), \quad \text{AND} \quad J = h/2$$

$$\gamma_{yz}^B = C_1^B [(0.7887)(\pi/h)w_1^i - (0.7887)\theta_1^i + (0.2113)(\pi/h)w_2^i - (0.2113)\theta_2^i]$$

$$\gamma_{yz}^D = C_1^D [(0.2113)(\pi/h)w_1^i - (0.2113)\theta_1^i + (0.7887)(\pi/h)w_2^i - (0.7887)\theta_2^i]$$

$$C_1^B = C_1^D = \cos(\pi/4)$$

$$[B^s]_h = \begin{bmatrix} -(S_1^A + S_1^C)/4J & 0 & (S_1^A + S_1^C)/4 \\ (\pi/h)C_1^B & -C_1^B/2 & 0 \\ (S_1^A + S_1^C)/4J & 0 & (S_1^A + S_1^C)/4J \\ (\pi/h)C_1^D & -C_1^D/2 & 0 \end{bmatrix}$$

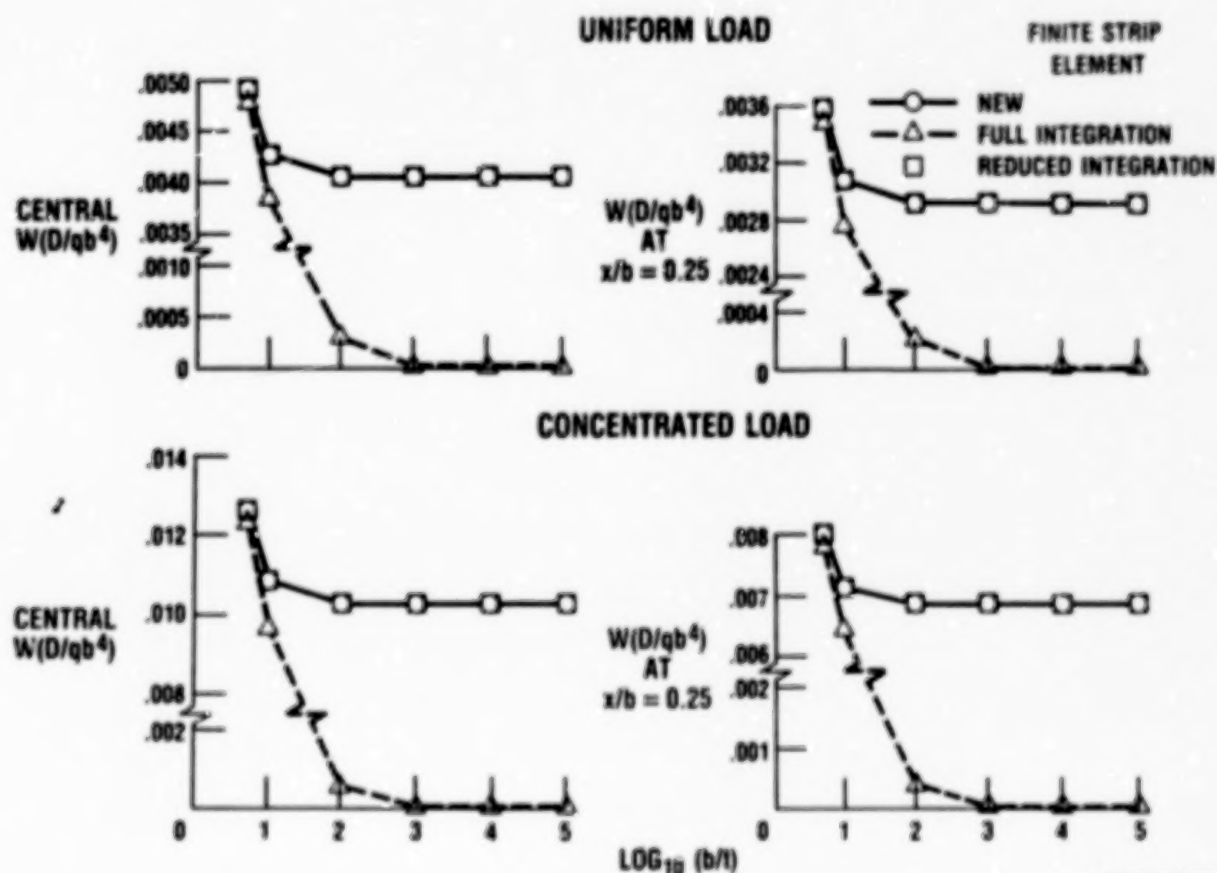
CD-88-32474



# CASE STUDIES - SHEAR LOCKING INVESTIGATION

The new finite strip element has been implemented into the finite element computer program FEAP (Zienkiewicz, 1982) with relative ease. The subroutines written in Fortran 77 for the formulation of the element stiffness matrix consist of approximately 200 lines. Results of numerical benchmark problems are presented to evaluate the performance of the element in different aspects: mesh size and harmonic term convergence characteristics, shear locking phenomenon as the thickness decreases, and shear force and bending moment prediction. The "full" numerical integration is employed.

A benchmark problem is used to detect the shear locking effects. Using eight strip elements with four nonzero harmonic terms and a Poisson's ratio  $\nu$  of 0.3, a simply supported square plate subjected to two loading conditions, uniform and concentrated loads, is investigated for a range of aspect (span to thickness) ratios from 5 to  $10^5$ . The resulting central deflections of the plate are normalized by the classical thin-plate solution (Timoshenko and Woinowsky-Krieger, 1959) and plotted below for both uniform and concentrated loads. For the entire range of aspect ratios shear locking was not detected. Note that the range of aspect ratios investigated varies from relatively thick to very thin situations; therefore this strip element would be useful for a wide range of applications, including the analysis of bridges, curved plates, and axisymmetric shells.



CD-88-32475



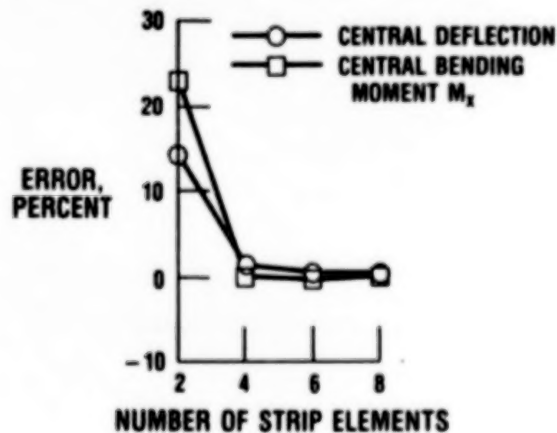
# CASE STUDIES - CONVERGENCE OF MESH SIZE

To assess the convergence characteristics predicted by the new element, we consider here again the analysis of a simply supported, uniformly loaded square plate with aspect ratio equal to 100 and  $\nu = 0.3$ . For mesh convergence the central deflections and central bending moments in the x- and y-directions are tabulated for the four meshes as well as for the exact solution. The number of available degrees of freedom for each mesh is shown as well. This gives a more realistic view of the numerical computation cost. Graphical representation is presented by plotting the percentage error of the central deflections and the central bending moment in the x-direction versus mesh size. The rate of convergence is rapid for both displacement and moment, with no sign of shear locking. As illustrated below, satisfactory convergence is reached by using four strips.

$$b/t = 100$$

| DEGREES OF FREEDOM | NUMBER OF STRIP ELEMENTS | CENTRAL DEFLECTION  | CENTRAL BENDING MOMENTS* |                  |
|--------------------|--------------------------|---------------------|--------------------------|------------------|
|                    |                          |                     | $M_x$                    | $M_y$            |
| 5                  | 2                        | 0.00348             | 0.03691                  | 0.03865          |
| 11                 | 4                        | .00401              | .04785                   | .04699           |
| 17                 | 6                        | .00404              | .04799                   | .04753           |
| 23                 | 8                        | .00405              | .04794                   | .04766           |
| EXACT MULTIPLIER   |                          | 0.00406<br>$qb^4/D$ | 0.0479<br>$qb^2$         | 0.0479<br>$qb^2$ |

\*LINEARLY EXTRAPOLATED FROM GAUSS POINTS.



CD-88-32476

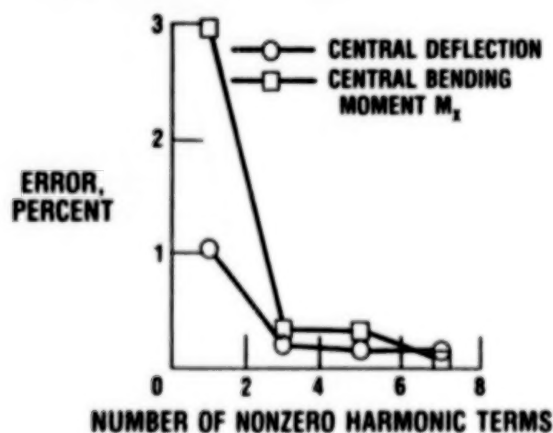
# CASE STUDIES - CONVERGENCE OF HARMONIC TERM

For the convergence of the harmonic term an eight-strip element mesh is used. The numerical results, tabulated with four nonzero harmonic terms, result in fairly good convergence once again. Errors are less than 0.4 percent when the third nonzero harmonic term is specified for both quantities. Note that this element is a low-order, two-node strip. The numerical computation is minimal but the convergence rate is relatively high.

## $b/l = 100$ ; EIGHT STRIP ELEMENTS

| HARMONIC TERM | CENTRAL DEFLECTION | CENTRAL BENDING MOMENTS* |          |
|---------------|--------------------|--------------------------|----------|
|               |                    | $M_x$                    | $M_y$    |
| $i = 1$       | -0.004101          | -0.04930                 | -0.05162 |
| $i = 3$       | .000051            | .00158                   | .00461   |
| $i = 5$       | -.000004           | -.00032                  | -.00103  |
| $i = 7$       | .000001            | .00011                   | .00038   |
| SUM           | -.004054           | -.04794                  | -.04766  |
| EXACT         | -0.00406           | -0.0479                  | -0.0479  |
| MULTIPLIER    | $qb^4/D$           | $qb^2$                   | $qb^2$   |

\*LINEARLY EXTRAPOLATED FROM GAUSS POINTS.



CD-88-32477

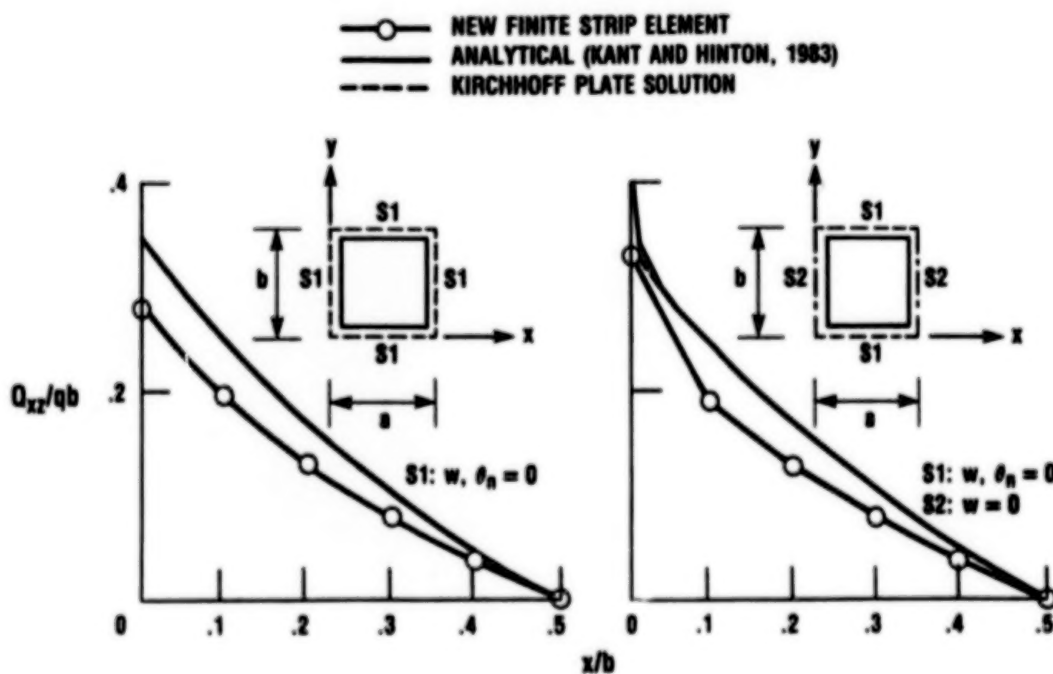
## CASE STUDIES - PREDICTIONS OF SHEAR FORCE AND BENDING MOMENT

For a low-order element the standard finite strip formulation based on Mindlin-Reissner plate theory is well recognized to predict accurate displacements and fairly good bending moments when using the selective and reduced integration technique (Onate and Suarez, 1983b). However, the shear force predictions are poor and rarely found in the finite strip literature even though they are desperately needed in designing structures such as bridges and slabs. Therefore the shear force predictive capability of this new finite strip element is presented here. Because of the limited number of cases of the analytical solution, only four cases for shear forces and one case for bending moment are compared.

The uniformly loaded square plates involving a variety of support conditions in the x-direction are investigated. In order to capture the steep gradient of the dependent variables near the plate edge, a rather fine mesh is used in the analysis with the new strip element. The resulting variations of shear forces and bending moments across the center of the plate in the various cases are plotted along with analytical solutions by Kant and Hinton (1983) and by Kirchhoff plate theory. These analytical solutions based on Mindlin plate theory assume transverse displacement and sectional rotations similar to those for a standard finite strip element. Kant and Hinton (1983) claimed that the analytical results compared favorably well with the finite strip method.

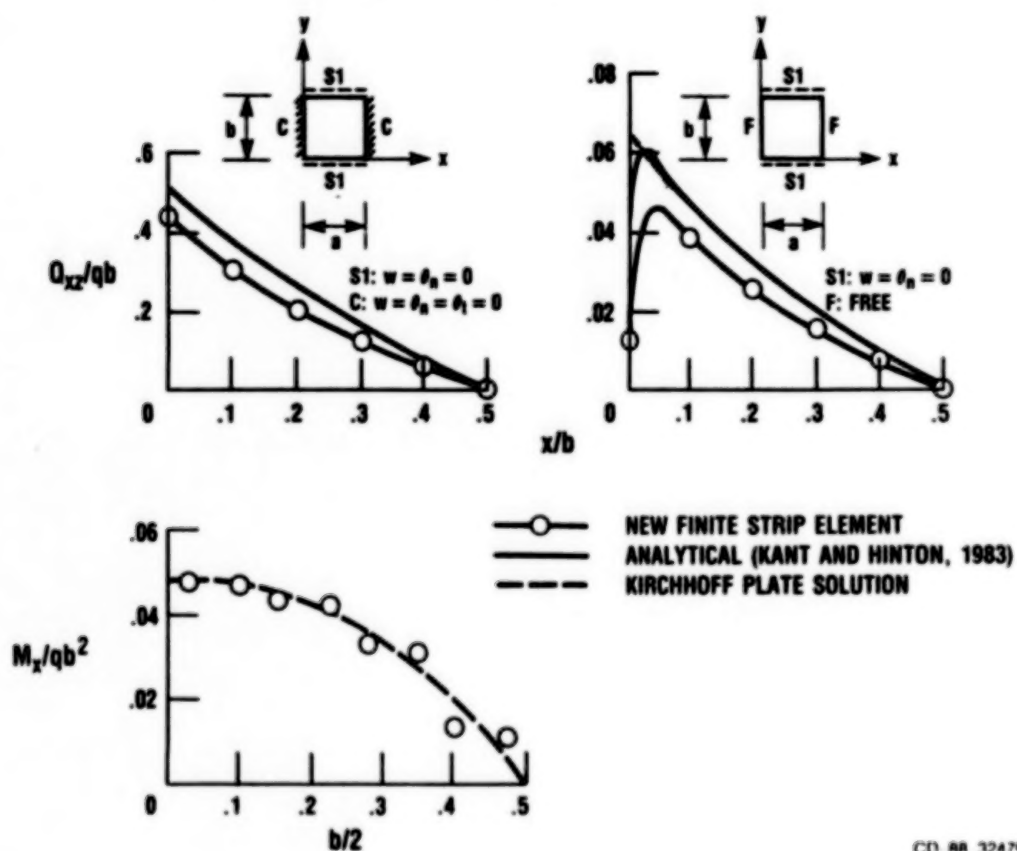
The results of shear force and bending moment, shown with the pertinent data and boundary conditions, are in good agreement near the center of the plates. In the regions further away from the center the differences start to magnify and are average at 15 percent near the edge of the plate. However, the curves for both solutions seem to follow the same pattern. Note that this new strip element is only a simple, two-node linear element and its predictive capabilities are shown to exceed its expectation.

**$y/b = 0.5$ ;  $b/t = 50$ ;  $\nu = 0.3$ ; UNIFORM LOAD; FOUR NONZERO HARMONIC TERMS**



CD-88-32478

$y/b = 0.5$ ;  $b/t = 50$ ;  $\nu = 0.3$ ; UNIFORM LOAD; FOUR NONZERO HARMONIC TERMS



CEI RR 32479

# PROPERTIES OF NEW FINITE STRIP ELEMENT

A two-node linear strip element based on Mindlin-Reissner plate theory is presented for the static analysis of bending plates. The new shear strain distributions are assumed and connected to the standard shear strains at the preselected points. These points are chosen by following the guideline of removing the shear locking phenomenon without the need for the "reduced integration" technique. Because of the uncoupling nature of the finite strip method the element stiffness matrix can be explicitly formulated for efficient computations and computer implementation. On the basis of the results obtained, the following properties can be stated:

- SIMPLE AND RELIABLE
- COMPUTATIONALLY EFFICIENT
- EASY FOR COMPUTER IMPLEMENTATION
- GOOD CONVERGENCE CHARACTERISTICS
- NO SHEAR LOCKING EFFECT FOR THIN SITUATION
- FAIRLY ACCURATE MOMENT AND SHEAR FORCE PREDICTIONS

$$D_1 = Et^3/12(1 - \nu^2) \quad D_2 = Et^3\nu/12(1 - \nu^2) \quad C = \cos^2(r\pi/4) \quad F = r\pi/b$$

$$D_3 = Et^3/24(1 + \nu) \quad D_4 = Et\nu/2(1 + \nu) \quad H = 0.25 \left( \sin 3r\frac{\pi}{4} + \sin r\frac{\pi}{4} \right)$$

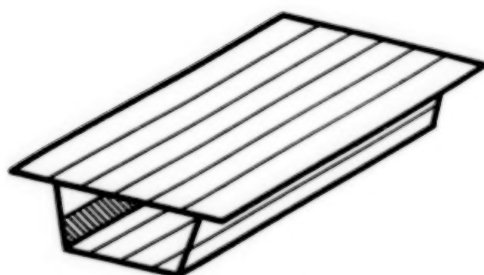
WHERE  $E$  IS YOUNG'S MODULUS AND  $\nu$  IS POISSON'S RATIO

$$[K] = \begin{bmatrix} D_1 \left( 4 \frac{b}{a} H^2 + a \frac{b}{4} F^2 C \right) & -D_2 a \frac{b}{4} \cdot FC & -2bH^2 D_4 & -D_1 \left( 4 \frac{b}{a} H^2 + a \frac{b}{4} F^2 C \right) & -D_2 a \frac{b}{4} \cdot FC & -2bH^2 D_4 \\ \frac{b}{2} \left( D_1 F^2 \frac{a}{3} + \frac{D_3}{a} + D_4 \frac{a}{2} C \right) & \frac{b}{4} F(D_3 - D_2) & -D_2 a \frac{b}{4} \cdot FC & \frac{b}{2} \left( D_1 F^2 \frac{a}{3} + \frac{D_3}{a} + D_4 \frac{a}{2} C \right) & \frac{b}{4} F(D_3 - D_2) \\ b \left( \frac{D_1}{2a} + D_2 F^2 \frac{a}{6} + D_4 a H^2 \right) & 2D_4 b H^2 & -\frac{b}{4} F(D_3 + D_2) & b \left( -\frac{D_1}{2a} + D_2 F^2 \frac{a}{12} + D_4 a H^2 \right) \\ D_1 \left( 4 \frac{b}{a} H^2 + a \frac{b}{4} F^2 C \right) & -D_2 a \frac{b}{4} \cdot FC & 2bH^2 D_4 \\ \frac{b}{2} \left( D_1 F^2 \frac{a}{3} + \frac{D_3}{a} + D_4 \frac{a}{2} C \right) & \frac{b}{4} F(D_3 - D_2) \\ \text{SYMMETRIC} & b \left( \frac{D_1}{2a} + D_2 F^2 \frac{a}{6} + D_4 a H^2 \right) \end{bmatrix}$$

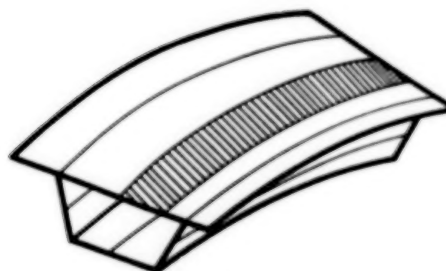
CD 88 32480

## APPLICATIONS AND FUTURE DEVELOPMENT

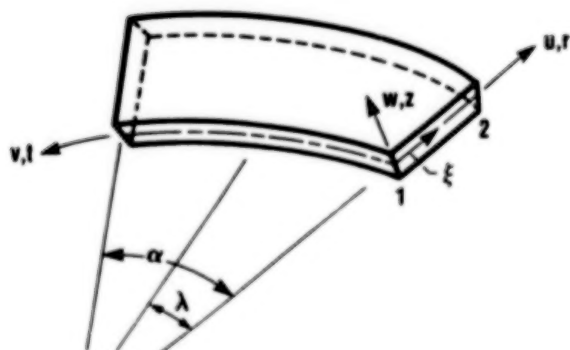
Because of the simplicity of its formulation the application of the finite strip method to the analysis of bridges, curved plates, and axisymmetric shells is straightforward. Onate and Suarez (1983a) demonstrated this in detail. Since the element stiffness matrix can be explicitly formulated, it is very convenient for practical engineers to implement this element into existing conventional finite element computer programs such as NFAP, developed by Chang (1987). NFAP is available to general users here at the NASA Lewis Research Center. Future research will involve extending the concept of this strip element for geometrically nonlinear analysis.



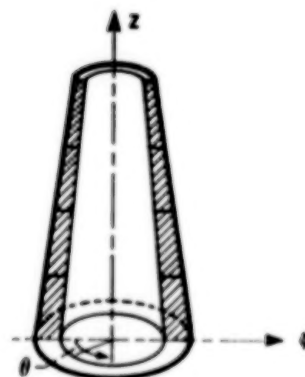
**STRAIGHT BRIDGE**



**CURVED BRIDGE**



**CURVED PLATE**



**AXISYMMETRIC SHELL**

CD-88-32481

## REFERENCES

- Chang, T.Y., 1987, NFAP - A General Purpose Non-linear Finite Element Program, Department of Civil Engineering, University of Akron.
- Cheung, Y.K., 1968a, "The Finite Strip Method in the Analysis of Elastic Plates With Two Opposite Simply Supported Ends," Proc. Inst. Civ. Engs., Vol 40, pp. 1-7.
- Cheung, Y.K., 1968b, "Finite Strip Method of Analysis of Elastic Slabs," Proc. Am. Soc. Civ. Engs., Vol. 94, EM6, pp. 1365-1378.
- Cheung, Y.K., 1976, The Finite Strip Method in Structural Analysis, Pergamon Press, Oxford.
- Kant, T., and Hinton, E., 1983, "Mindlin Plate Analysis by Segmentation Method," Journal of Engineering Mechanics, ASCE, Vol. 109(2), pp. 537-556.
- MacNeal, R.H., 1982, "Derivation of Element Stiffness Matrices by Assumed Strain Distribution," Nucl. Eng. Design., Vol. 70, pp. 3-12.
- Mawenya, A.S., and Davies, J.D., 1974, "Finite Element Analysis of Plate Bending Including Transverse Shear Effects," Building Sci., Vol. 9, pp. 175-180.
- Mindlin, R.D., 1951, "Influence of Rotatory Inertia and Shear on Flexural Notion of Isotropic Elastic Plates," J. Appl. Mech., Vol. 18, pp. 31-38.
- Onate, E., and Suarez, B., 1983a, "A Unified Approach for the Analysis of Bridges, Plates and Axisymmetric Shells Using the Linear Mindlin Strip Element," Comput. Structures, Vol. 17, pp. 407-426.
- Onate, E., and Suarez, B., 1983b, "A Comparison of the Linear Quadratic and Cubic Mindlin Strip Elements for the Analysis of Thick and Thin Plates," Comput. Structures, Vol. 17, pp. 427-439.
- Timoshenko, S., and Woinowsky-Krieyer, S., 1959, Theory of Plates and Shells, 2nd Edition, McGraw Hill, New York.
- Zienkiewicz, O. C., 1982, The Finite Element Method, McGraw Hill, New York.

**APPENDIX**  
**CONTENTS TO VOLUMES 1 AND 3**



## CONTENTS TO VOLUME 1

### VIBRATION CONTROL

|  |      |
|--|------|
| Session Overview . . . . .   | 1-1  |
| Louis J. Kiraly, NASA Lewis Research Center  |      |
| Survey of Impact Damper Performance . . . . .  | 1-3  |
| Gerald V. Brown, NASA Lewis Research Center  |      |
| Periodic Response of Nonlinear Systems . . . . .   | 1-13 |
| C. Nataraj, Trumpler Associates, Inc., and H.D. Nelson,<br>Arizona State University  |      |
| Piezoelectric Pushers for Active Vibration Control of Rotating<br>Machinery . . . . .  | 1-29 |
| Alan B. Palazzolo, Texas A&M University, and Albert F. Kascak,<br>U.S. Army Aviation Research and Technology Activity - AVSCOM |      |
| Active Control and System Identification of Rotordynamic Structures . .  | 1-47 |
| M.L. Adams, Case Western Reserve University  |      |
| Electromagnetic Dampers for Cryogenic Applications . . . . .   | 1-53 |
| Gerald V. Brown and Eliseo DiRusso, NASA Lewis Research Center   |      |

### PARALLEL COMPUTING

|  |       |
|--|-------|
| Session Overview . . . . .   | 1-65  |
| Louis J. Kiraly, NASA Lewis Research Center  |       |
| Multigrid for Structures Analysis . . . . .  | 1-67  |
| Albert F. Kascak, U.S. Army Aviation Research and Technology<br>Activity - AVSCOM          |       |
| Parallel Computer Methods for Eigenvalue Extraction . . . . .                              | 1-91  |
| Fred Akl, Ohio University  |       |
| Adapting High-Level Language Programs for Parallel Processing<br>Using Data Flow . . . . . | 1-103 |
| Hilda M. Standley, University of Toledo  |       |
| Iterative Finite Element Solver on Transputer Networks . . . . .                           | 1-113 |
| Albert Danial and James Watson, Sparta, Inc.   |       |
| Multiprocessor Graphics Computation and Display Using Transputers . . .                    | 1-125 |
| Graham K. Ellis, Institute for Computational Mechanics in<br>Propulsion                    |       |

### DYNAMIC SYSTEMS

|   |       |
|---|-------|
| Session Overview . . . . .  | 1-141 |
| Louis J. Kiraly, NASA Lewis Research Center                                       |       |
| Microgravity Mechanisms and Robotics Program . . . . .                            | 1-143 |
| Douglas A. Rohn, NASA Lewis Research Center                                       |       |
| Base Reaction Optimization of Manipulators with Redundant<br>Kinematics . . . . . | 1-157 |
| C.L. Chung and S. Desa, Carnegie Mellon University                                |       |

|  |              |
|--|--------------|
| <b>Evaluation of a High-Torque Backlash-Free Roller Actuator . . . . .</b> | <b>1-175</b> |
| Bruce M. Steinetz, NASA Lewis Research Center                              |              |
| <b>Low-Cost Optical Data Acquisition System for Blade</b>                  |              |
| <b>Vibration Measurement . . . . .</b>                                     | <b>1-191</b> |
| Stephen J. Posta, NASA Lewis Research Center                               |              |
| <b>Roller Drive Materials Performance . . . . .</b>                        | <b>1-203</b> |
| Douglas A. Rohn, NASA Lewis Research Center                                |              |
| <b>Microgravity Manipulator Demonstration . . . . .</b>                    | <b>1-217</b> |
| Andrew S. Brush, Sverdrup Technology, Inc., Lewis Research<br>Center Group |              |
| <b>Accurate Positioning of Long, Flexible ARM's . . . . .</b>              | <b>1-229</b> |
| Michael J. Malachowski, CCE - Robotics                                     |              |

## AEROELASTICITY

|  |              |
|--|--------------|
| <b>Session Overview . . . . .</b>  | <b>1-245</b> |
| Louis J. Kiraly, NASA Lewis Research Center                                  |              |
| <b>Development of Aeroelastic Analysis Methods for Turborotors</b>           |              |
| <b>and Propfans - Including Mistuning . . . . .</b>                          | <b>1-247</b> |
| Krishna Rao V. Kaza, NASA Lewis Research Center                              |              |
| <b>2-D and 3-D Time Marching Transonic Potential Flow Method</b>             |              |
| <b>for Propfans . . . . .</b>  | <b>1-263</b> |
| Marc H. Williams, Purdue University  |              |
| <b>Propfan Model Wind Tunnel Aeroelastic Research Results . . . . .</b>      | <b>1-273</b> |
| Oral Mehmed, NASA Lewis Research Center                                      |              |
| <b>Aeroelastic Forced Response Analysis of Turbomachinery . . . . .</b>      | <b>1-287</b> |
| Todd E. Smith, Sverdrup Technology, Inc., Lewis Research<br>Center Group     |              |
| <b>Reduced Order Models for Nonlinear Aerodynamics . . . . .</b>             | <b>1-299</b> |
| Aparajit J. Mahajan, Earl H. Dowell, and Donald B. Bliss,<br>Duke University |              |
| <b>Application of Navier-Stokes Analysis to Stall Flutter . . . . .</b>      | <b>1-309</b> |
| J.C. Wu, R. Srivastava, and L.N. Sanker, Georgia Institute<br>of Technology  |              |

## COMPUTATIONAL METHODS FOR DYNAMICS

|  |              |
|--|--------------|
| <b>Session Overview . . . . .</b>  | <b>1-321</b> |
| Louis J. Kiraly, NASA Lewis Research Center  |              |
| <b>A Computational Procedure for Automated Flutter Analysis . . . . .</b>                                    | <b>1-323</b> |
| Durbha V. Murthy, University of Toledo   |              |
| <b>Characterization of Structural Connections for Multicomponent</b>   |              |
| <b>Systems . . . . .</b>   | <b>1-337</b> |
| Charles Lawrence, NASA Lewis Research Center, and<br>Arthur A. Huckelbridge, Case Western Reserve University |              |
| <b>Mixed Finite Element Formulation Applied to Shape Optimization . . . . .</b>                              | <b>1-353</b> |
| Helder Rodrigues, John E. Taylor, and Noboru Kikuchi,<br>The University of Michigan                          |              |
| <b>Modal Forced Response of Propfans in Yawed . . . . .</b>  | <b>1-367</b> |
| G.V. Narayanan, Sverdrup Technology, Inc., Lewis Research<br>Center Group                                    |              |

## STRUCTURAL DYNAMICS CODE APPLICATIONS

|  |       |
|--|-------|
| <b>Session Overview</b> . . . . .  | 1-377 |
| Krishna Rao V. Kaza, NASA Lewis Research Center                                |       |
| <b>Vibration and Flutter Analysis of the SR-7L Large-Scale Propfan</b> . . . . | 1-379 |
| Richard August, Sverdrup Technology, Inc., Lewis Research<br>Center Group      |       |
| <b>Supersonic Axial-Flow Fan Flutter</b> . . . . .                             | 1-393 |
| John K. Ramsey, NASA Lewis Research Center                                     |       |
| <b>Stall Flutter Analysis of Propfans</b> . . . . .                            | 1-405 |
| T.S.R. Reddy, University of Toledo   |       |
| <b>SSME Single-Crystal Turbine Blade Dynamics</b> . . . . .                    | 1-421 |
| Larry A. Moss, Sverdrup Technology, Inc., Lewis Research<br>Center Group       |       |
| <b>PADAFRASE Restructuring of FORTRAN Code for Parallel Processing</b> . . . . | 1-431 |
| Atul Wadhwa, Sverdrup Technology, Inc., Lewis Research<br>Center Group         |       |
| <b>Analysis of Rotating Flexible Blades Using MSC/NASTRAN</b> . . . . .        | 1-449 |
| Michael A. Ernst, NASA Lewis Research Center                                   |       |

## CONTENTS TO VOLUME 3

### CERAMIC COMPONENT RELIABILITY

|  |      |
|--|------|
| <b>Session Overview</b> . . . . .  | 3-1  |
| John P. Gyekenyesi, NASA Lewis Research Center   |      |
| <b>Monolithic Ceramic Analysis Using the SCARE Program</b> . . . . .                   | 3-5  |
| Jane M. Manderscheid, NASA Lewis Research Center                                       |      |
| <b>Whisker-Reinforced Ceramic Composites for Heat Engine Components</b> . . . .        | 3-21 |
| Stephen F. Duffy, Cleveland State University   |      |
| <b>Continuous Fiber Ceramic Matrix Composites for Heat Engine Components</b> . . . . . | 3-41 |
| David E. Tripp, Cleveland State University   |      |

### NONDESTRUCTIVE EVALUATION

|  |       |
|--|-------|
| <b>Session Overview</b> . . . . .  | 3-63  |
| Alex Vary, NASA Lewis Research Center  |       |
| <b>Nondestructive Evaluation by Acousto-Ultrasonics</b> . . . . .  | 3-67  |
| Harold E. Kautz, NASA Lewis Research Center  |       |
| <b>Characterization of Sintered SiC by Using NDE</b> . . . . .   | 3-79  |
| George Y. Baaklini, NASA Lewis Research Center   |       |
| <b>Systems for Ultrasonic Scanning, Analysis, and Imagery</b> . . . . .  | 3-93  |
| David B. Stang, Sverdrup Technology, Inc., Lewis Research Center Group, Edward R. Generazio, NASA Lewis Research Center, and Steve Abe, Cleveland State University |       |
| <b>Flaw Characterization in Structural Ceramics Using Scanning Laser Acoustic Microscopy</b> . . . . .   | 3-107 |
| Don J. Roth, NASA Lewis Research Center  |       |
| <b>Nondestructive Evaluation of Sintered Ceramics</b> . . . . .  | 3-123 |
| George Y. Baaklini, Stanley J. Klima, and William A. Sanders, NASA Lewis Research Center   |       |

### FRACTURE MECHANICS

|   |       |
|---|-------|
| <b>Session Overview</b> . . . . .   | 3-135 |
| John L. Shannon, Jr., NASA Lewis Research Center  |       |
| <b>Fracture Technology for Brittle Materials</b> . . . . .  | 3-141 |
| Jonathan A. Salem, NASA Lewis Research Center   |       |
| <b>Mode II Fracture Mechanics</b> . . . . .   | 3-149 |
| Robert J. Buzzard, NASA Lewis Research Center, and Louis Ghosn, Cleveland State University  |       |
| <b>In Situ Fatigue Loading Stage Inside Scanning Electron Microscope</b> . . .  | 3-161 |
| Jack A. Telesman, NASA Lewis Research Center, Peter Kantzos, Case Western Reserve University, and David N. Brewer, U.S. Army Aviation Research and Technology Activity - AVSCOM |       |

|  |       |
|--|-------|
| <b>Grain Boundary Oxidation and Low-Cycle Fatigue at Elevated Temperatures</b> . . . . . | 3-173 |
| H.W. Liu and Y. Oshida, Syracuse University  |       |
| <b>Elevated Temperature Crack Growth</b> . . . . .                                       | 3-187 |
| K.S. Kim, R.H. Van Stone, S.N. Malik, and J.H. Laflen,<br>General Electric Co.           |       |

## FATIGUE AND DAMAGE

|   |       |
|---|-------|
| <b>Session Overview</b> . . . . .   | 3-199 |
| Marvin H. Hirschberg, NASA Lewis Research Center  |       |
| <b>Cumulative Fatigue Damage Models</b> . . . . .   | 3-201 |
| Michael A. McGaw, NASA Lewis Research Center  |       |
| <b>Fatigue Damage Mapping</b> . . . . .   | 3-213 |
| Darrell Socie, University of Illinois at Urbana-Champaign   |       |
| <b>Bithermal Fatigue: A Simplified Alternative to Thermomechanical Fatigue</b> . . . . .  | 3-221 |
| Michael J. Verrilli, NASA Lewis Research Center   |       |
| <b>Life Prediction Modeling Based on Strainrange Partitioning</b> . . . . .   | 3-231 |
| Gary R. Halford, NASA Lewis Research Center   |       |
| <b>Life Prediction Modeling Based on Cyclic Damage Accumulation</b> . . . . .   | 3-245 |
| Richard S. Nelson, Pratt & Whitney  |       |
| <b>Fatigue Damage Modeling for Coated Single Crystal Superalloys</b> . . . . .  | 3-259 |
| David M. Nissley, Pratt & Whitney   |       |
| <b>Life and Reliability of Rotating Disks</b> . . . . .   | 3-271 |
| Erwin V. Zaretsky, NASA Lewis Research Center, and<br>Todd E. Smith and Richard August, Sverdrup Technology,<br>Inc., Lewis Research Center Group |       |

## WIND TURBINES

|  |       |
|--|-------|
| <b>Large-Scale Wind Turbine Structures</b> . . . . . | 3-285 |
| David A. Spera, NASA Lewis Research Center           |       |

## HOST

|   |       |
|---|-------|
| <b>Aircraft Engine Hot Section Technology - An Overview of the HOST Project</b> . . . . . | 3-299 |
| Daniel E. Sokolowski, NASA Lewis Research Center  |       |
| <b>Research Sensors</b> . . . . .   | 3-323 |
| David R. Englund, NASA Lewis Research Center  |       |
| <b>HOST Combustion R&amp;T Overview</b> . . . . .   | 3-337 |
| Raymond E. Gaugler and James D. Holdeman, NASA Lewis<br>Research Center                   |       |
| <b>Review and Assessment of the HOST Turbine Heat Transfer Program</b> . . . .            | 3-349 |
| Herbert J. Gladden, NASA Lewis Research Center  |       |



|   |  |                             |   |   |  |
|---|--|-----------------------------|---|---|--|
| 1. Report No.<br>NASA CP-3003—Vol. 2  |  | 2. Government Accession No. |   | 3. Recipient's Catalog No.                                      |  |
| 4. Title and Subtitle<br>Lewis Structures Technology—1988<br>Volume 2—Structural Mechanics  |  |                             |   | 5. Report Date<br>December 1988                                 |  |
|   |  |                             |   | 6. Performing Organization Code                                 |  |
| 7. Author(s)  |  |                             |   | 8. Performing Organization Report No.<br>E-3970                 |  |
|   |  |                             |   | 10. Work Unit No.<br>505-63-1B                                  |  |
| 9. Performing Organization Name and Address<br>National Aeronautics and Space Administration<br>Lewis Research Center<br>Cleveland, Ohio 44135-3191   |  |                             |   | 11. Contract or Grant No.                                       |  |
|   |  |                             |   | 13. Type of Report and Period Covered<br>Conference Publication |  |
| 12. Sponsoring Agency Name and Address<br>National Aeronautics and Space Administration<br>Washington, D.C. 20546-0001  |  |                             |   | 14. Sponsoring Agency Code                                      |  |
|   |  |                             |   |   |  |
| 15. Supplementary Notes   |  |                             |   |   |  |
| 16. Abstract<br><br>A Symposium and Exposition entitled Lewis Structures Technology—1988 (LST '88), sponsored by the Structures Division of the NASA Lewis Research Center, was held May 24 and 25, 1988, in Cleveland, Ohio. The charter of the Structures Division is to perform and disseminate results of research conducted in support of aerospace engine structures. These results have a wide range of applicability to practitioners of structural engineering mechanics beyond the aerospace arena. The specific purpose of the symposium was to familiarize the engineering structures community with the depth and range of research performed by the division and its academic and industrial partners. The more significant results of the division's research efforts were presented in 14 overviews and 83 technical presentations. The complete text of each presentation is included in this volume. Sessions covered vibration control, fracture mechanics, ceramic component reliability, parallel computing, nondestructive evaluation, constitutive models and experimental capabilities, dynamic systems, fatigue and damage, wind turbines, hot section technology (HOST), aeroelasticity, structural mechanics codes, computational methods for dynamics, structural optimization, and applications of structural dynamics, and structural mechanics computer codes. |  |                             |   |   |  |
| 17. Key Words (Suggested by Author(s))<br>Engine structures, Structures mechanics, Structural dynamics, Structural optimization, Structural durability, Fatigue (metals), Fracture mechanics, Nondestructive evaluation, Aeroelasticity, Parallel computing, Cyclic constitutive models, Wind turbines, HOST  |  |                             | 18. Distribution Statement<br>Unclassified—Unlimited<br>Subject Category 39 |   |  |
| 19. Security Classif. (of this report)<br>Unclassified  | 20. Security Classif. (of this page)<br>Unclassified | 21. No of pages<br>312      | 22. Price*<br>A14   |   |  |



END

11—14—91